Influence des perturbations fluvioglacielles sur la biogéomorphologie des rivières froides : analyse de la végétation riveraine et des ajustements géomorphologiques dans deux cours d'eau gaspésiens soumis aux embâcles de glace

Thèse présentée

dans le cadre du programme de doctorat en sciences de l'environnement

en vue de l'obtention du grade de philosophiæ doctor (Ph.D)

PAR

© Matthieu Prugne

Mai 2026

Composition du jury :

Daniel Germain, président du jury, Université du Québec à Montréal

Thomas Buffin-Bélanger, directeur de recherche, Université du Québec à Rimouski

Maxime Boivin, codirecteur de recherche, Université du Québec à Chicoutimi

Dov Corenblit, codirecteur de recherche, Université de Toulouse, France

Lovisa Lind, examinatrice externe, Sweden Environmental Court, Suède

Lina Polvi, examinatrice externe, Umeå University, Suède

Dépôt initial le 17 décembre 2025 Dépôt final le 21 mai 2026

UNIVERSITÉ DU QUÉBEC À RIMOUSKI
Service de la bibliothèque

Avertissement

La diffusion de ce mémoire ou de cette thèse se fait dans le respect des droits de son auteur, qui a signé le formulaire « *Autorisation de reproduire et de diffuser un rapport, un mémoire ou une thèse* ». En signant ce formulaire, l'auteur concède à l'Université du Québec à Rimouski une licence non exclusive d'utilisation et de publication de la totalité ou d'une partie importante de son travail de recherche pour des fins pédagogiques et non commerciales. Plus précisément, l'auteur autorise l'Université du Québec à Rimouski à reproduire, diffuser, prêter, distribuer ou vendre des copies de son travail de recherche à des fins non commerciales sur quelque support que ce soit, y compris Internet. Cette licence et cette autorisation n'entraînent pas une renonciation de la part de l'auteur à ses droits moraux ni à ses droits de propriété intellectuelle. Sauf entente contraire, l'auteur conserve la liberté de diffuser et de commercialiser ou non ce travail dont il possède un exemplaire.

J’M…

REMERCIEMENTS

Le temps passe vite. Déjà cinq années écoulées depuis le début de cette aventure qui commença par une simple curiosité intellectuelle m'entraînant vers la maîtrise, pour finalement aboutir au dépôt d'une thèse de doctorat. Je profiterai de cette section de remerciements pour écrire au gré des pensées qui viennent, sans contraintes de style cancé dans un langage technique et académique. Ce texte risque donc d'être pas mal décousu, mais, je l'espère, ressenti. Il y aurait tant de personnes à remercier qui ont contribué, de près ou de loin, directement ou indirectement, pratiquement ou émotionnellement, à l'aboutissement de ce travail. Un travail qui demande de se plonger dans l'inconnu, un peu naïf, et qui nous fait traverser une gamme d'émotions, allant de la fierté aux remises en question. Sur cette finalité, qui représente aussi (et surtout) le début d'un nouveau chapitre de vie, je n'éprouve aucun regret et, à devoir recommencer, je recommencerais. Entre les apprentissages, les campagnes de terrain, les nouvelles rencontres, les voyages, les heures de lecture et les mois à traiter, analyser et interpréter des jeux de données complexes, j'ai grandi, évolué. Tant sur le plan personnel que professionnel, ce fut une expérience plus qu'enrichissante et elle n'aurait pu être possible sans la contribution de tant de gens. Je souhaite donc, ici, prendre le temps. Prendre le temps de partager mes sincères remerciements à vous toustes, vous qui m'avez accompagné dans ce périple.

Je souhaite avant tout mettre de l'avant l'importance que mon trio de directeurs a eue dans l'accomplissement de cette thèse. Tom, Max et Dov, le trio des trois-lettres, votre accompagnement était inestimable, je n'aurais sans doute pas pu tomber sur une meilleure équipe pour me rendre où je me suis rendu. Tom! Je pourrais possiblement écrire trois pages de remerciements dédiées à toi seulement, mais il faut garder de la place pour tout le monde. Tu m'as pris sous ton aile, m'as offert d'inestimables opportunités et m'as fait découvrir le monde de la géographie et de l'hydrogéomorphologie. Tu as été un modèle marquant et je

me compte chanceux d'avoir été formé au LGDF, au sein d'une équipe passionnée et passionnante. Tes précieux conseils et ta passion contagieuse ont rendu ces années de recherches exceptionnelles. Toujours les bons mots et les bonnes réflexions au bon moment, ta maturité scientifique et ton excellente pédagogie représentent à mes yeux l'un des éléments qui m'ont le plus inspiré. Je te dis merci pour toutes ces riches discussions et pour ton soutien tout au long de ces années. Max, le deuxième mousquetaire! Tu es présent depuis le tout début, depuis mes premières tentatives à faire du sens des différentes théories issues de la biogéomorphologie. Merci d'avoir rejoint l'équipe, de t'être lancé dans un sujet certes intéressant mais pas évident, et de ta présence soutenue lors des rencontres Zoom, toujours prêt à sortir des informations en un quart de tour lorsqu'on se questionne et discute d'aspects techniques. Dov, le troisième mousquetaire d'outre-mer! Je suis heureux de t'avoir contacté, il y a maintenant quatre ans, pour de simples petites questions sur différentes méthodes qui, à cette époque, m'étaient perçues comme une langue étrangère. Ce petit geste aura donné toute une tournure à la thèse! Merci de nous avoir partagé ton expertise en biogéomorphologie, ce qui a donné tout un élan au projet! Puis merci pour ton accueil chaleureux lors de mon séjour en France, pour tous ces moments à discuter de biogéomorphologie et de plein d'autres sujets, soit à l'heure du midi au labo, au bar de la Concorde avec un café ou une bière à la main, ou encore dans un resto autour d'un bon tajine. Je garderai bons souvenirs de nos rencontres au Portugal, en France et en Italie. Bref, merci à vous trois, sans qui cette thèse n'aurait pas vu le jour dans sa forme actuelle ; vous y avez joué un rôle majeur et je vous en remercie. En espérant pouvoir collaborer sur d'autres projets dans l'avenir!

Je tiens aussi à remercier tous les membres du LGDF avec qui j'ai passé beaucoup de temps au cours des dernières années. Même si, au cours des deux dernières années, je me suis un peu plus transformé en fantôme de laboratoire et que le télétravail a pris beaucoup de place depuis l'arrivée de mon petit Éli, sachez que ce fut un plaisir d'être votre collègue! Que ce soit pendant les diners, les midis-fluviaux, les bières du jeudi ou des rencontres imprévues dans différentes soirées, les discussions qui s'y créaient autour de notre vécu dans le parcours académique permettaient de se sentir moins isolé et d'avoir des gens significatifs avec qui

relate. Vous étiez un moteur de motivation ! Je souhaite davantage étendre ces remerciements, particulièrement à tous ceux et celles qui ont activement participé à mon projet de thèse, tant sur le terrain qu'en laboratoire de dendrochronologie, que sur les ordinateurs, à tracer des polygones de végétation. Merci notamment à Étienne GG, Étienne GD, Alex D, Sam L, Zoé M et Félix L pour votre aide sur le terrain. Alex et Sam, merci particulièrement pour votre aide considérable pour la récolte des rondelles d'arbres, et surtout sur la Petite-Cascapédia, où vous avez dû faire vos récoltes sous une température de -8000°C. Tout ça, pour que Zoé puisse ensuite passer des heures à sabler et scanner des rondelles d'arbre. Et pour ça, un gros merci Zoé! Je souhaite aussi particulièrement remercier Kassandra Croteau, ma chère amie du Bac, pour ton aide botanique. Sans toi, on aurait probablement obtenu la moitié des données que nous avons réussi à récolter. Ton aide pour l'identification des plantes fut plus qu'utile!

Je tiens aussi à souligner la contribution de collaborateurs externes qui ont soit participé de près, soit de loin aux travaux de ma thèse. Je pense notamment à André Évette, collaborateur sur une publication découlant de mon examen doctoral. André, que ce soit par les discussions qu'on a eues sur le génie végétal ou par ton invitation à faire une présentation au colloque de la SQP, j'aurai pu ajouter une corde à mon arc quant à la gestion des cours d'eau. Merci également à Aziz Syammach et Eduardo González pour votre précieuse aide concernant les analyses statistiques des communautés de plantes et des traits fonctionnels. Finalement, je tiens à remercier Luc Sirois et Étienne Boucher, qui, de l'élaboration de mon projet de thèse jusqu'à l'examen doctoral, ont stimulé les réflexions pratiques et théoriques de mon projet.

Sortons maintenant un peu du cadre universitaire. Je veux remercier de tout mon cœur mes amis proches qui m'ont soutenu tout au long du projet. Louis, Louis, Louis (oui ça fait beaucoup de Louis dans mon cercle), Yan, Dan, Anis, Alex, Félix, Sara, Sarah, Patoue et j'en passe… C'est grâce aux moments passés avec vous autres que je pouvais décrocher, créer des souvenirs et nourrir ma vie personnelle. Merci d'être vous et de m'avoir encouragé tout au long de ces cinq années. Que ce soit par de simples, ou parfois profondes, discussions

(même au téléphone, ça comptait), par des moments partagés lors de concerts, de soirées ou de soupers, c'est grâce à ces petits moments-là que j'avance et que je me sens bien.

Je tiens surtout à remercier toute ma famille immédiate, sans qui je ne me serais jamais rendu là où je suis actuellement. Maman, Papa, Romain, Chloé… sans la vie que j'ai vécue avec vous, sans les conseils et le support que vous m'avez apportés, je n'aurais pas eu toutes ces opportunités. Vous avez toujours été là pour moi, et ça, c'est un méchant privilège. Merci d'être vous et merci pour tout ce qu'on a vécu depuis mes courtes 32 années de vie. Même dans des moments plus difficiles, vous vous pliiez en quatre pour m'aider, peu importe la situation. Je vous en suis plus que reconnaissant pour la vie que j'ai eue, et sachez que si j'arrive à déposer cette thèse, c'est en très grande partie grâce à vous! Je vous aime.

Et finalement… Merci à vous, Julianne et Éli. Julianne, toi que je peux maintenant officiellement présenter comme ma « femme », je ne te remercierai jamais assez pour le soutien constant que tu m'as apporté. Dans les bons moments comme dans les plus difficiles, tu as toujours eu les mots justes et une profonde considération pour ce que je vivais. Tu étais aux premières loges lors des creux de motivation et tu as toujours été là pour m'encourager, me remonter le moral. Merci de m'avoir accompagné dans ce projet de longue haleine, incertain, et d'avoir toujours été présente. Je t'aime. Merci aussi à toi, Éli, le petit coconut qui est entré dans nos vies depuis maintenant deux ans déjà. Ton arrivée aura été le plus beau des cadeaux. Oui, par moments, ce n'était pas évident d'être jeune parent en plus de devoir terminer une thèse de doctorat… disons que les nuits étaient moins reposantes. Mais c'est aussi toi qui arrivais le plus facilement à me changer les idées lorsque les journées étaient empreintes de démotivation et de diverses difficultés. Je t'aime, mon petit Éli. Et toi qui n'as pas encore de nom, on t'attend avec impatience… sache que je t'aime déjà et que tu mérites aussi ta place dans ce court texte. Tu as été une source de motivation supplémentaire au cours du dernier sprint de cette thèse. Bref, ma petite famille, sans vous, cette aventure n'aurait jamais abouti. Je vous aime.

RÉSUMÉ

Depuis deux décennies, la biogéomorphologie fluviale émerge comme discipline clé afin de comprendre les ajustements spatiotemporels et l'évolution des rivières. En intégrant des outils d'analyse issus de l'hydrogéomorphologie et de l'écologie végétale, elle a permis de décrire les influences réciproques entre dynamiques végétales et processus hydrogéomorphologiques. Les nombreux modèles conceptuels, statistiques et numériques qui en ont émergé ont apporté un éclairage sur le rôle actif de la végétation dans l'évolution des cours d'eau. Toutefois, les bases fondamentales de cette science proviennent majoritairement d'études en milieux tempérés, où les crues représentent le principal régime de perturbations. Les rivières des régions froides ont fait l'objet de moins d'études, bien qu'elles subissent l'action d'une perturbation singulière, la glace, qui impose des contraintes mécaniques et physiologiques majeures. Les formes et processus fluvioglaciels, particulièrement les embâcles, peuvent augmenter les forces de cisaillement, moduler les dynamiques sédimentaires et exacerber les inondations. Comprendre l'influence de la glace sur les dynamiques biogéomorphologiques s'avère essentiel pour enrichir les fondements théoriques de la biogéomorphologie fluviale et les adapter à la diversité des contextes climatiques.

Cette thèse définit le rôle des perturbations fluvioglacielles, notamment les embâcles, dans les dynamiques biogéomorphologiques des rivières froides. La réponse biogéomorphologique aux embâcles est d'abord examinée à différentes échelles spatio-temporelles : à l'échelle du corridor fluvial sur une période pluri-décennale (Chapitre 1), puis à l'échelle des communautés végétales riveraines d'un point de vue taxonomique (Chapitre 2) et fonctionnel (Chapitre 3). Ces analyses sont ensuite synthétisées dans une réflexion conceptuelle sur les implications biogéomorphologiques des processus fluvioglaciels dans les rivières froides (Chapitre 4). Nous avons combiné des analyses diachroniques de photographies aériennes pour quantifier les changements hydrogéomorphologiques et végétaux (1963-2016), et des analyses statistiques multivariées pour examiner la composition de la végétation. Des régimes d'embâcle ont été caractérisés à l'aide de données historiques et d'analyses dendrochronologiques, afin d'établir des relations entre le régime de perturbation et les réponses biogéomorphologiques. Afin d'explorer la variabilité des réponses selon le contexte hydrogéomorphologique, les chapitres présentent une comparaison entre une rivière confinée (Matapédia) et mobile (Petite-Cascapédia), toutes deux située en Gaspésie.

Les résultats de cette thèse révèlent que les embâcles de glace constituent un régime de perturbations structurant pour les dynamiques biogéomorphologiques des rivières froides, bien que leurs effets varient selon le contexte hydrogéomorphologique. À l'échelle du

corridor fluvial, les analyses diachroniques ont révélé que les embâcles affectent principalement la végétation en provoquant des renouvellements récurrents, alors que les ajustements morphologiques des chenaux demeurent principalement dictés par le régime de crue. À l'échelle des communautés riveraines, les analyses taxonomiques et fonctionnelles ont révélé que les caractéristiques hydrogéomorphologiques constituent les facteurs principaux qui structurent la végétation, sur lesquels se superposent les effets des embâcles. Le régime d'embâcle exerce néanmoins un filtrage écologique significatif en sélectionnant des traits fonctionnels spécifiques, tels que la propagation végétative et la flexibilité (associée aux perturbations mécaniques), ou la tolérance à la submersion (associée aux inondations). Alors que la rivière confinée (Matapédia) illustre une résistance plus importante aux glaces par la dominance d'espèces plus tolérantes à l'abrasion, la rivière non-confinée exhibe une résilience axée sur le réajustement spatial des mosaïques végétales et une dynamique de succession biogéomorphologique plus importante. Ces résultats suggèrent que les embâcles influencent indirectement les trajectoires biogéomorphologiques soit en modulant la composition fonctionnelle des communautés et, par conséquent, leur potentiel à agir comme ingénieurs d'écosystème, soit en contrôlant les cycles de renouvellements de la végétation.

En somme, cette thèse suggère que les processus fluvioglaciels ne se limitent pas qu'à des agents d'érosion, mais constituent des facteurs structurants qui influencent l'organisation spatiale et temporelle des systèmes fluviaux. Elle marque un premier apport pour l'intégration explicite de la glace dans les cadres théoriques de la biogéomorphologie fluviale et ouvre des perspectives prometteuses pour de futures recherches. Dans un contexte de changements climatiques où les régimes fluvioglaciels sont appelés à se transformer, une compréhension approfondie de ces interactions devient d'autant plus pertinente pour anticiper les futures trajectoires d'évolution des cours d'eau avec plus de précision.

Mots-clefs : biogéomorphologie fluviale, embâcles de glace, fluvioglaciel, traits fonctionnels, rivières froides, co-ajustement, régime de perturbation, trajectoires d'ajustement, ripisylve, composition

ABSTRACT

In the last two decades, fluvial biogeomorphology has emerged as a key discipline for understanding the spatiotemporal adjustments and evolution of rivers. By integrating analytical tools from hydrogeomorphology and plant ecology, it has enabled the description of reciprocal influences between vegetation dynamics and hydrogeomorphological processes. The numerous conceptual, statistical, and numerical models that have emerged from this approach have shed light on the active role of vegetation in river evolution. However, the fundamental bases of this science come mainly from studies in temperate environments, where floods represent the primary disturbance regime. Rivers in cold regions have been the subject of fewer studies, although they experience the action of a unique disturbance, which imposes major mechanical and physiological constraints: Ice. Fluvioglacial forms and processes, particularly ice jams, can increase shear forces, modulate sedimentary dynamics, and exacerbate flooding. Understanding the influence of ice on biogeomorphological dynamics is therefore essential to enrich the theoretical foundations of fluvial biogeomorphology and adapt them to the diversity of climatic contexts.

This thesis defines the role of fluvioglacial disturbances, particularly ice jams, in the biogeomorphological dynamics of cold rivers. The biogeomorphological response to ice jams is first examined at different spatiotemporal scales: at the river corridor scale over a multi-decadal period (Chapter 1), then at the scale of riparian plant communities from a taxonomic (Chapter 2) and functional (Chapter 3) perspective. These analyses are then synthesized in a conceptual reflection on the biogeomorphological implications of fluvioglacial processes in cold rivers (Chapter 4). We combined diachronic analyses of aerial photographs to quantify hydrogeomorphological and vegetation changes (1963-2016), and multivariate statistical analyses to examine vegetation composition. Ice jam regimes were characterized using historical data and dendrochronological analyses to establish relationships between the disturbance regime and biogeomorphological responses. To explore the variability of responses according to hydrogeomorphological context, the chapters present a comparison between a confined river (Matapédia) and a mobile river (Petite-Cascapédia), both located in Gaspésie.

The results of this thesis reveal that ice jams constitute a structuring disturbance regime for the biogeomorphological dynamics of cold rivers, although their effects vary according to hydrogeomorphological context. At the river corridor scale, diachronic analyses revealed that ice jams primarily affect vegetation by causing recurrent renewals, whereas morphological channel adjustments remain mainly dictated by the flood regime. At the riparian community scale, taxonomic and functional analyses revealed that hydrogeomorphological characteristics constitute the primary factors structuring vegetation,

upon which the effects of ice jams are superimposed. The ice jam regime nevertheless exerts significant ecological filtering by selecting specific functional traits, such as vegetative propagation and flexibility (associated with mechanical disturbances), or submersion tolerance (associated with flooding). While the confined river (Matapédia) demonstrates greater resistance to ice through the dominance of species more tolerant to abrasion, the unconfined river exhibits resilience focused on spatial readjustment of vegetation mosaics and greater biogeomorphological succession dynamics. These results suggest that ice jams indirectly influence biogeomorphological trajectories either by modulating the functional composition of communities and, consequently, their potential to act as ecosystem engineers, or by controlling vegetation renewal cycles.

In summary, this thesis suggests that fluvioglacial processes are not limited to erosion agents but constitute structuring factors that condition the spatial and temporal organization of fluvial systems. It represents a first contribution toward the explicit integration of ice into the theoretical frameworks of fluvial biogeomorphology and opens promising perspectives for future research. In a context of climate change where fluvioglacial regimes are expected to transform, a thorough understanding of these interactions becomes all the more relevant to anticipate future trajectories of river evolution with greater precision.

Keywords: fluvial biogeomorphology, ice jams, ice processes, functional traits, cold rivers, co-adjustment, disturbance regime, adjustment trajectories, riparian, composition

TABLE DES MATIÈRES

REMERCIEMENTS ix

RÉSUMÉ xiv

ABSTRACT xvii

TABLE DES MATIÈRES xx

LISTE DES TABLEAUX xxv

LISTE DES FIGURES xxxi

LISTE DES ABRÉVIATIONS, DES SIGLES ET DES ACRONYMES xlii

INTRODUCTION GÉNÉRALE 1

1. MISE EN CONTEXTE ET MOTIVATIONS 1

2. LES PRINCIPES DE LA BIOGÉOMORPHOLOGIE FLUVIALE 4

2.1 Les interactions fondamentales entre la végétation et l'hydrogéomorphologie 4
2.2 L'importance des échelles spatio-temporelles 8
2.3 Une approche interdisciplinaire sur la taxonomie et les traits fonctionnels 13

3. LA PARTICULARITÉ DES RIVIÈRES FROIDES 16

3.1 Processus fluvioglaciels 16
3.2 Le cas des embâcles de glace 19
3.3 Les embâcles : décrire un régime de perturbation 20

4. OBJECTIFS DE RECHERCHE 23

5. APPROCHE MÉTHODOLOGIQUE ET SITES D'ÉTUDE 24

6. ORGANISATION DE LA THESE 28

CHAPITRE 1 Trajectoires d'ajustements des communautés riveraines et des chenaux en régions froides : les effets des perturbations fluvioglacielles dans deux cours d'eau gaspésiens 32

1.1 RESUME EN FRANÇAIS DU DEUXIEME ARTICLE 32

1.2 VEGETATION AND CHANNEL ADJUSTMENT TRAJECTORIES IN COLD REGIONS: THE EFFECTS OF ICE DISTURBANCES IN TWO GASPESIAN RIVERS 34

1.3 INTRODUCTION 35

1.4 STUDY RIVERS 37

1.5 METHODOLOGY 38

1.5.1 GIS imagery 38
1.5.2 Characterization of ice jam and flood chronologies 39
1.5.3 Analysis of geomorphological trajectories 41
1.5.4 Analysis of vegetation succession processes 43

1.6 RESULTS 46

1.6.1 Disturbance regime 46
1.6.2 Geomorphological planform adjustments 50
1.6.3 Vegetation trajectory of change 58

1.7 DISCUSSION 65

1.7.1 Role of ice-jams and floods on channel planform and vegetation trajectories 65
1.7.2 Biogeomorphological behavior interpretation 69

1.8 CONCLUSION 73

1.9 ACKNOWLEDGEMENTS 75

1.10 AUTHOR CONTRIBUTIONS 75

CHAPITRE 2 L'effet du régime d'embâcles de glace sur la diversité et la composition des communautés végétales riveraines diffère entre deux rivières géomorphologiquement contrastées 76

2.1 RESUME EN FRANÇAIS DU DEUXIEME ARTICLE 76

2.2 THE EFFECTS OF ICE-JAM REGIME ON RIPARIAN PLANT DIVERSITY AND COMMUNITY COMPOSITION DIFFER BETWEEN GEOMORPHOLOGICALLY CONTRASTED RIVERS 79

2.3 INTRODUCTION 81

2.4 METHODOLOGY 84

2.4.1 Study area 84
2.4.2 Sampling design and field campaigns 85
2.4.3 Data 86
2.4.4 Statistical analysis 87

2.5 RESULTS 91

2.5.1 Vegetation patterns between rivers and main hydrogeomorphological driving factors 91
2.5.2 Ice-jam regime effects on community composition and diversity 95

2.6 DISCUSSION 101

2.6.1 Differences in vegetation composition between hydrogeomorphological settings 101
2.6.2 Ice-jam regime effects on riparian vegetation composition and diversity 103
2.6.3 Challenges in studying ice dynamics in rivers and future research 106

2.7 CONCLUSION 107

2.8 ACKNOWLEDGEMENTS 109

2.9 AUTHOR CONTRIBUTIONS 109

CHAPITRE 3 Le contexte hydrogéomorphologique module la réponse fonctionnelle de la végétation riveraine aux perturbations liées aux embâcles de glace 110

3.1 RESUME EN FRANÇAIS DU DEUXIEME ARTICLE 110

3.2 HYDROGEOMORPHOLOGICAL CONTEXT MEDIATES THE FUNCTIONAL RESPONSE OF RIPARIAN VEGETATION TO ICE-JAM DISTURBANCES 113

3.3 INTRODUCTION 115

3.4 MATERIALS AND METHODS 117

3.4.1 Study area and sampling design 117
3.4.2 Data 119
3.4.3 Data processing 123
3.4.4 Statistical analysis 125

3.5 RESULTS 128

3.5.1 Functional guilds 128
3.5.2 Community-weighted mean 135

3.6 DISCUSSION 141

3.6.1 The hydrogeomorphological context explains most of plant community functional structure....142
3.6.2 Ice-jam disturbances affect plant community functional structure....143
3.6.3 Functional responses to ice disturbances are mediated by fluvial behaviour....144

3.7 IMPLICATIONS AND CONCLUDING REMARKS....147

3.8 ACKNOWLEDGEMENTS....148

3.9 AUTHOR CONTRIBUTIONS....148

CHAPITRE 4 La biogéomorphologie des rivières froides : L'intégration des dynamiques fluvioglacielles....149

4.1 RESUME EN FRANÇAIS DU DEUXIEME ARTICLE....149

4.2 THE BIOGEOMORPHOLOGY OF COLD RIVERS: INTEGRATION OF FLUVIAL ICE DYNAMICS....152

4.3 INTRODUCTION....154

4.4 ICE DYNAMICS AS A DISTURBANCE REGIME....158

4.5 KNOWN EFFECTS OF ICE DYNAMICS ON RIVERSCAPES....161

4.5.1 Active channels....163
4.5.2 Riverbanks....164
4.5.3 Floodplains....166

4.6 FROM TRAITS TO LANDSCAPES: HOW ICE DYNAMICS MAY MODULATE THE EXPRESSION OF BIOGEOMORPHOLOGICAL DYNAMICS AND ADJUSTMENTS....167

4.6.1 Plants: establishment, growth and dispersion....168
4.6.2 Communities: linking functional traits to feedbacks....172
4.6.3 Biogeomorphological landforms: biotic-abiotic co-construction and succession dynamics....175
4.6.4 Reach scale: Spatial organization and adjustment....181

4.7 CHALLENGES AND PERSPECTIVES....185

4.7.1 Developing techniques and tools to characterize ice dynamics....185
4.7.2 Quantitative assessments and threshold identification....186
4.7.3 Long-term monitoring....187
4.7.4 Comparative studies....188
4.7.5 Modeling integration....189

4.8 CONCLUDING REMARKS....189

4.9 AUTHOR CONTRIBUTIONS 190

CONCLUSION GÉNÉRALE 191

Les défis pour l'étude des processus fluvioglaciels 192
Ajustements biogéomorphologiques face aux perturbations par embâcle 194
Le régime d'embâcle comme facteur structurant de la végétation 197
La biogéomorphologie : Une science fondamentale et appliquée à approfondir 202

ANNEXE I : Chapter 1 supplementary materials 206

ANNEXE II : Chapter 2 supplementary materials 210

ANNEXE III : Chapter 3 supplementary materials 221

ANNEXE IV : Measurements of site geomorphological characteristics 228

ANNEXE V : Ice-Jam disturbance regime gradient 229

ANNEXE VI : Habitat classification 231

ANNEXE VII : Functional trait data 234

RÉFÉRENCES BIBLIOGRAPHIQUES 242

LISTE DES TABLEAUX

Table 1. Aerial photographs and their characteristics used to analyze planform and vegetation trajectories 40

Table 2. Description of each surface cover and their visual characteristics used for photointerpretation 44

Table 3. Change classes used to calculate the different indices. For example, the progression value for I_{BS} came from the sum of BS-SV (bare surface to sparse vegetation), BS-DV (bare surface to dense vegetation), and BS-FO (bare surface to forest)..... 45

Table 4. Years in which ice jams occurred based on dendrochronological analysis, historical newspapers, watershed organizations databases, and government databases and reaches in which they occurred. 48

Table 5. Mean and ± 1 SE of geomorphological and ice jam regime variables for each river. 87

Table 6 List of variables used in the multivariate statistical analyses, with abbreviations, descriptions and relevance as environmental variables. The family represents the defined groups of variables used in Variation Partitioning, and each variable is associated with the model(s) to which it was retained after forward selection..... 90

Table 7 Mean and ± 1 SE of geomorphological and ice jam regime variables for each river. 120

Table 8 Functional traits selected for the analyses, grouped by trait category. For each trait, the variable type, unit of measurement (or modalities), and the abbreviation used in subsequent analyses are provided. See Table 33 (ANNEXE VII) for trait values and references used to retrieve them. 122

Table 9 List of the variables used in the multivariate statistical analyses, their description and relevance as environmental variables. The family represents the defined groups of variables used in Variation Partitioning, and each variable is associated with the model(s) for which it was retained after forward selection. This table was reproduced from Prugne et al. (2025, *In Prep.*)..... 126

Table 10 Functional guilds identified from clustering of species. Each guild is described by its main representative characteristic trait combination, along with the number of species included and representative examples. The first six rows correspond to woody guilds, and the remaining rows to non-woody guilds. 130

Table 11 Results of partial redundancy analysis models testing the effects of ice-jam regime on community-weighted means of plant traits in each river (Matapédia and Petite-Cascapédia). For each trait group (morphological, life-history, and ecological), the overall model effect is reported by its F-statistics and p-value from the anova.cca () function, along with the adjusted R^2 calculated with the RsquareAdj() function in the vegan R package (Oksanen et al., 2025). Marginal effects for ice-jam frequency (PC1_freq) and magnitude (Havg) are also reported, along with F statistics and associated p-values. P <0.050 in bold. 139

Table 12 Main ice-related processes and their known effects on hydraulics, geomorphology and vegetation. 158

Table 13. Summary of the dendrochronological results, presenting both the total number of jams identified in each site (total jams) and the number of confirmed jams. 206

Table 14. Summary of discharge characterization and ice jam analysis. QMmax, QMmean, and QMmin are descriptive statistics of the annual maximum discharge (m3/s) by period. The flood interval and jams indicate the number of events that occurred in the given period, followed by the calculated frequency (in bold). Missing years from the discharge database were not counted in the frequency calculation. 207

Table 15. Descriptive table of mean width and mean area of subreaches. 208

Table 16. Surface area (ha) for each cover classes, rivers and years. WA = Water, BS = Barren surface, SV = Sparse Vegetation, DV = Dense vegetation 209

Table 17. List of the 115 species identified and used for this study in the Matapédia River and the Petite-Cascapédia River. Codes of the species are derived from the U.S. Department of Agriculture (USDA) Plants Database and codes for species identified at the genus level (n = 27) were coded with the three first letters of the genus followed by “sp”. Abundance was calculated as the mean estimated cover ± 1 SE when present in each river. and the frequency of occurrences was measured as the number of plots where the species occurred divided by the total number of plots for each river. 210

Table 18. Pairwise PERMANOVA (adonis2) results comparing Hellinger-transformed species composition between all combinations of habitat–river

groups. The table reports the proportion of explained variance (R^2), F-values, and Bonferroni-adjusted p-values (adj.p) for each pairwise comparison. All tests were based on Bray-Curtis's dissimilarity and 999 permutations. Mata - Matapédia River, PC - Petit-Cascapédia River.....214

Table 19. Pairwise PERMANOVA (adonis2) results comparing presence-absence species composition between all combinations of habitat–river groups. The table reports the proportion of explained variance (R^2), F-values, and Bonferroni-adjusted p-values (adj.p) for each pairwise comparison. All tests were based on Jaccard's dissimilarity and 999 permutations. Mata - Matapédia River, PC - Petit-Cascapédia River 215

Table 20. Pairwise Wilcoxon rank-sum test results comparing community richness, Shannon's diversity and Piélou's Evenness across River–Habitat combinations. Reported are the test statistic (W), raw p-values, and adjusted p-values (Benjamini–Hochberg correction) for each pairwise comparison. Mata - Matapédia River, PC - Petit-Cascapédia River.....216

Table 21. Kendall's tau correlation matrix between community-aggregated metrics and ice-jam regime variables. Values underlined with asterisks shows significant p-values prior to post-hoc corrections (*pval < 0.05; **pval < 0.01, *pval < 0.001). Benjamini-Hochberg procedure was applied but adjusted p-values were all non-significant. 217

Table 22. Results of variation partitioning analysis on Hellinger-transformed plant community composition for the Matapédia and Petite-Cascapédia rivers. The three defined groups are: ice-jam regime variables ("Ice"), plot-scale hydrogeomorphological variables ("Plot"), and reach-scale hydrogeomorphological variables ("Reach"). Values represent the percentage of variance explained uniquely by each variable group (controlling for the others), along with F-statistics and associated p-values from permutation tests (rda with anova.cca). 218

Table 23. Results of partial redundancy analysis (partial RDA) assessing the contribution of ice regime variables (PC1_freq, Havg) to species composition (Hellinger-transformed) after accounting for reach-scale and plot-scale hydrogeomorphological variables in the Matapédia and Petite-Cascapédia rivers. Plant composition = f (ice regime | hydrogeomorphology). 218

Table 24. Results of variation partitioning analysis on presence-absence plant community composition for the Matapédia and Petite-Cascapédia rivers. The three defined groups are: ice-jam regime variables ("Ice"), plot-scale hydrogeomorphological variables ("Plot"), and reach-scale hydrogeomorphological variables ("Reach"). Values represent the

percentage of variance explained uniquely by each variable group (controlling for the others), along with F-statistics and associated p-values from permutation tests (cca with anova.cca). 219

Table 25. Results of partial canonical correspondence analysis (partial CCA) assessing the contribution of ice regime variables (PC1_freq, Havg) to species composition (presence-absence) after accounting for reach-scale and plot-scale hydrogeomorphological variables in the Matapédia and Petite-Cascapédia rivers. Plant composition = f (ice regime | hydrogeomorphology). 219

Table 26. Results of pairwise permutational multivariate analysis of variance (pairwise PERMANOVA) based on Bray–Curtis dissimilarities of riparian plant guild composition across habitat–river groups. Groups represent the interaction of river (Mata:Matapédia, PC:Petite-Cascapédia) and habitat type (Bar, Floodplain, Ecotone). Reported are the coefficient of determination (R^2), F statistic, and Bonferroni-adjusted p-values (adj. p) based on 999 permutations 221

Table 27. Results of pairwise Wilcoxon rank–sum tests (two-sided Mann–Whitney U) comparing guild abundances within each habitat across rivers. For each guild, the Wilcoxon W statistic is reported along with the raw p-value and the false discovery rate–adjusted p-value (Benjamini–Hochberg correction).... 222

Table 28. Results of pairwise permutational multivariate analysis of variance (pairwise PERMANOVA) based on Euclidean distances of community-weighted mean traits composition across habitat–river groups. Groups represent the interaction of river (Mata:Matapédia, PC:Petite-Cascapédia) and habitat type (Bar, Floodplain, Ecotone). Reported are the coefficient of determination (R^2), F statistic, and Bonferroni-adjusted p-values (adj. p) based on 999 permutations 223

Table 29. Results of pairwise Wilcoxon rank–sum tests (two-sided Mann–Whitney U) comparing CWM within each habitat across rivers. For each trait, the Wilcoxon W statistic is reported along with the raw p-value and the false discovery rate–adjusted p-value (Benjamini–Hochberg correction). Only the significant results are shown. See methods for the definition of each trait abbreviation. 224

Table 30. Results of permutation tests (999 permutations) on individual RDA axes for each trait group (morphological, life-history, ecological) in the Matapédia and Petite-Cascapédia rivers. For each axis, the table reports the explained variance, F-statistic, and associated P-value from anova.cca(by = "axis") using the R package vegan (Oksanen et al., 2025), indicating which axes

significantly explain variation in community-weighted means after conditioning on hydrogeomorphological covariates 225

Table 31. Data showing the number of trees sampled in each study site (see study map for localisation), the number of individuals ice-jams identified from tree rings, the year of the most recent and oldest ice-jam event, and the frequency value resulting from the three different method (freq, freq2008, freq2008old) described above. 230

Table 32. Characteristics of sediment and vegetation cover in the defined habitats. 232

Table 33. Values, by species, of the fourteen functional traits used in the Chapter 3 analyses. 237

LISTE DES FIGURES

Figure 1 Représentation schématique de l'interdisciplinarité de la biogéomorphologie intégrant des notions issues de la géomorphologie, de l'écologie et de la biologie évolutive. 2

Figure 2 Schéma conceptuel des interactions entre la structure de l'écoulement, les formes fluviales et la végétation. Modifié de Corenblit et al. (2007) 5

Figure 3 Modèle conceptuel des interactions entre la végétation, la structure d'écoulement et les dynamiques sédimentaires. Tiré de Corenblit et al. (2007). 7

Figure 4 Représentation schématique des phases de la succession biogéomorphologique intégrant les fonctions écosystémiques, les interactions HGM-végétation dominantes, la connectivité hydrogéomorphologique et la force des rétroactions biogéomorphologiques. Figure adaptée de Corenblit et al. (2015) et Corenblit et al. (2009). 11

Figure 5 Modèle conceptuel des interactions entre les composantes hydrogéomorphologiques et fluvioglaciels. Modifiée de Allard (2010)..... 16

Figure 6. Exemple des potentiels impacts d'embâcles de glace, soit (a) des poussées glacielles en haut des berges, (b) des cicatrices glacielles laissées sur les arbres de rives et (c) écorchement glaciel laissé sur les berges après le passage d'un embâcle. Les photographies ont été tirées de Prowse et Culp (2003). 21

Figure 7. Exemple d'un échantillon ligneux (rondelle) provenant d'un thuya occidental ayant subi plusieurs perturbations par embâcles. Les cercles identifient les cicatrices visibles dans la chronologie des cernes. Comme illustré sur cette image, les cernes de croissance cessent de se former là où des cicatrices se sont formées, ce qui permet d'identifier l'année de la perturbation. 23

Figure 8 Localisation des segments de rivières sélectionnés dans le cadre de la thèse. Les boîtes représentent la délimitation des bassins-versants (A), les tronçons à l'étude de la rivière Matapédia (B) et de la rivière Petite-Cascapédia (C), ainsi que des photographies aériennes d'un tronçon de la Matapédia (D) et de la Petite-Cascapédia (E). Les points rouges représentent les sites

d'échantillonnage où des données d'abondance et d'échantillons ligneux ont pu être recueillies. 27

Figure 9 Schéma conceptuel intégrant les dynamiques fluvioglacielles (représentées par l'ellipse grise pointillée et les flèches grises) au cadre théorique de la biogéomorphologie fluviale proposé par Corenblit et al. (2007), accompagné d'un schéma situant l'organisation de la thèse. Les boîtes jaunes indiquent les interactions abordées au chapitre 1, tandis que les pastilles vertes correspondent aux interactions traitées dans les chapitres 2 et 3. Le gradient en bas de la figure illustre l'échelle spatiale propre à chacun de ces chapitres. 29

Figure 10 Figure of the study sites. *(A)* Location map of the two watersheds on the Gaspesian Peninsula, Canada. (B and C) Map of the studied river segments (B for Matapédia River and C for Petite-Cascapédia River); blue polygon represents the active channel, black squared outlines the study reaches, black lines along the channel represent the limits of the 1 km subreaches and red points identify the dendrochronological sampling sites. (D and E) Oblique photographs (camera angled between 30 and 60 degrees from vertical) of the Matapédia River (D) and the Petite-Cascapédia River (E). 39

Figure 11 (A) Picture of the sampling method: cutting of wedges at two different identified scars. (B) Example of a scanned tree cross-section with visible ice scars forming a "cat's paw". (C) Graph showing results from dendrochronological analysis; tree samples are on the ordinate and dating year on the abscissa; colored bars (colors are according to river reach and tones to sampling sites) show the maximum rings counted for each sample, dark blue points indicate the dated ice jams events, and orange bars indicate the confirmed ice jams with respect to the rule of n>2. 42

Figure 12. Site locations and dated years of confirmed ice jams. Y-axis represents the site number along the rivers in which the identified ice jam happened, and x-axis represents the dated years. The color gradients correspond to the average height (cm) of the scars above the bankfull level. 46

Figure 13. Time series of available maximum discharges for both rivers. The colored horizontal lines represent the discharges associated with flood recurrences Q2, Q5, Q10, Q20, and Q50. The blue points and vertical lines represent the years with known ice jam events. The alternating grey and white colors show the periods between the available series of aerial photographs. The hatched areas identify missing data of flood discharges. 49

Figure 14. (A) Minimum, maximum, and mean discharges of the maximum discharges during periods covered with aerial photographs, where blue bars show the number of ice jams that occurred during the specified period. (B)

Spatiotemporal description of the number of jams throughout the river reaches and periods 51

Figure 15. (A) Width variation across subreaches. (B) Width variation across years. Fill colors distinguish Matapédia (red) from Petite-Cascapédia (blue). 52

Figure 16. Variation in sinuosity index, bare surface area, and river width over time and selected reaches. Types of points and lines represent reaches from 1 to 4 for the Matapédia and 1 to 3 for the Petite-Cascapédia 53

Figure 17 (A) Variation in width across periods and subreaches for both rivers. The colors of the bar distinguish narrowing (black) from widening (grey) processes. The increase/decrease in width was standardized by the mean width of each subreach and divided by the number of years in a given period. Vertical dotted lines mark the limits of each selected reach. (B) Mean changes in the standardized width change rate across the selected reaches. The line and point types distinguish the reaches. 55

Figure 18 (A) Aggregated migration rate index (AMI) across periods and subreaches for both rivers. The AMI value was standardized using the mean width of each subreach. Vertical dotted lines mark the limits of each selected reach. (B) Mean changes in AMI across the selected reaches. The line and point types distinguish the reaches. 56

Figure 19 (A) Erosion and deposition rates across periods and subreaches for both rivers. The colors of the bar distinguish erosion (orange) from deposition (blue) processes. The erosion-deposition areas were standardized by the mean area of each subreach and divided by the number of years in each period. Vertical dotted lines mark the limits of each selected reach. (B) Mean balance of erosion-deposition rate (difference between deposition and erosion) across selected reaches. The line and point types distinguish the reaches. 57

Figure 20 Classification map resulting from the photo-interpretation of the different land covers (WA: Water, BS: Bare surface, SV: Sparse vegetation, DV: Dense vegetation, FO: Forest, ANT: Anthropic). These are samples of the most downstream and dynamic reaches of both rivers 58

Figure 21 (A) Proportions of surface cover classes for each year. (B) Change rate of cover classes over time showing gain and loss between periods. Negative values represent loss surfaces and positive values represent gained surfaces between two years. 60

Figure 22 Trajectory of succession processes for each class of surface cover during different periods. The colored bars represent the area of progression (green), regression (red), and stability (blue). The progression area represents a

change from the initial cover to a later successional state, regressing the area that passed from the initial cover to an earlier successional state and the stability of the area that depicted no change. The line graph on the secondary axis shows the trajectory of the indices measuring the dominant process and its importance compared to the total area of change..... 61

Figure 23 Rate of change in succession path through specific reaches and periods. Progression changes depict all progression pathways, similar to regression. Balance is the difference between the progression and regression rates. The colors of the bars represent the path of succession (green for progression; red for regression; grey for balance), and the color gradient represents the reach number (1 to 4: light to dark). 62

Figure 24 (A) The I_{all} index value across periods and subreaches for both rivers (left y-axis), along with the progression (green) and regression (red) rates of each subreach (right y-axis). I_{all} is calculated with every succession path (see Methods for details), where positive and negative values indicate a dominance process of progression and regression, respectively. The closer the value is to -1 or 1, the more important is the dominant process. (B) Mean I_{all} values across the selected reaches. Line and point types distinguish the reaches. 64

Figure 25. Synthesis figure agglomerating both dominant vegetation progression/regression dynamics at the sub-reach scale and significant/dominant channel adjustment at the reach scale, along with a summary of the disturbances. The timeline on the top of the graphs identifies years when a certain disturbance occurred (empty circle for Q_2, empty triangle for Q_5, solid square for Q_{10}, solid triangle for Q_{20}, lozenge for Q_{50}, and star for ice jams) at the corridor scale. Ice jam years (stars) were also reported spatially in the synthesis figure to spatialize known jams throughout the reaches. Circle and arrow symbols show the dominant hydrogeomorphological processes and are based on the average value. Migration (presence or absence of a lateral arrow) and widening/narrowing (diverging grey arrows for widening and converging black arrows for narrowing) are shown when the values are larger than the RMSE. Erosion (red circle) or deposition (blue circle) is shown when one of the processes is more important than the other in a given reach. 66

Figure 26 Relationship between sparse/dense vegetation progression rate and deposition/width change rate. Horizontal lines in the width change plots delimit narrowing (negative) and widening (positive). Each point (red for Matapédia; blue for Petite-Cascapédia) corresponds to a specific subreach in a specific period. The deposition rate was normalized based on the average channel area of each sub-reach. The width change rate was

normalized based on the average channel width of each sub-reach. Regression line is based on the ordinary least squares.....72

Figure 27 Location of the two study rivers and study sites. (A) Watersheds boundaries of the two rivers, in black, and segments studied, in blue lines. (B) and (C) River segments studied and the sites (red circles and red labels for site numbers) where dendrochronological and taxonomical samples were taken on the Matapédia and Petite-Cascapédia rivers, respectively. (D) and (E) Aerial views of characteristic reach in the Matapédia and Petite-Cascapédia rivers, respectively. 85

Figure 28 Mean cover of 30 species across habitats and rivers that were identified by their high loadings in a preliminary Principal Component Analysis (PCA). The colors of the heatmap discriminate the life form of the species, and the color gradient shows the mean cover in %.....92

Figure 29 Redundancy Analysis (RDA) diagram of the 169 vegetation plots composition (Hellinger-transformed), constrained by selected environmental variables. The positions of the 20 species with the highest loading scores are indicated with red code labels (see Annexe II Table 17 for full species name). Predictors illustrated by arrows in grey and associated labels were first filtered through a Variance Inflation Factor (VIF) and then a forward selection was applied (see Methods for the name of the acronyms).....93

Figure 30 Canonical correspondence analysis (CCA) diagram of the 169 vegetation plots composition (presence-absence), constrained by selected environmental variables. The positions of the 20 species with the highest loading scores are indicated with red code labels (see Annexe II Table 17 for full species name). Predictors illustrated by arrows in grey and associated labels were first filtered through a Variance Inflation Factor (VIF) and then a forward selection was applied (see Methods for the name of the acronyms).....94

Figure 31 Mean values ± 1 SE (error bar) of (a) species richness, (b) Shannon's H diversity and (c) Piélou's evenness. Each community-aggregated metric was calculated for each habitat in each river. A pairwise Wilcox test was used to assess significant differences between river-habitat groups. The multcompLetters function (R Package MultcompView, version 0.1-1) was used to apply letters for the groupings. Different letters depict a significant difference between the means of two groups. The numbers in the graph bars represent the sample sizes for each group.....96

Figure 32 Partial Redundancy Analysis (pRDA; Ice Regime | Reach + Plot hydrogeomorphology) of vegetation abundance (Hellinger-transformed)

constrained by ice disturbance variables (Havg: ice scars height, PC1_freq: ice jam frequency gradient) and conditioned by all the other hydrogeomorphological variables in the (A) Matapédia and (B) Petite-Cascapédia rivers. The 15 species with the highest loadings are shown with red code labels, and their scores were multiplied by 5 for better visuality. Scaling: 2 scores are shown by open squares (Matapédia River — Panel A) and filled squares (Petite-Cascapédia River—Panel B). Colors of squares and ellipses represent the three habitats. Ellipses were set at a level of 0.95 to capture most of the dispersion. Ice-jam regime variables are represented as blue vectors and labels. Bar graph at the top left shows the mean dispersion of points for each habitat measured on scaling 1 scores for better emphasis on Euclidean distance, with SE + 1 represented by the tick. On the top right is a Venn diagram from the variation partitioning of plot communities (Hellinger-transformed) against the three groups of variables described in the methodology. The numbers in the circles represent the % of explained variability in plot composition. The Venn diagram is the result of plotting an “Euler” function object (Package *eulerr*; Larssen, 2021). 98

Figure 33 Partial Canonical Correspondence Analysis (pCCA; Ice Regime | Reach + Plot hydrogeomorphology) of vegetation composition (presence-absence) constrained by ice disturbance variables (Havg: ice scars height, PC1_freq: ice jam frequency gradient) conditioned by all the other hydrogeomorphological variables in the (A) Matapédia and (B) Petite-Cascapédia rivers. The 5 species with the highest loadings in the pCCA1 positive values and the 5 with the highest loadings in the pCCA1 negative values are shown as red code labels, and the scaling 2 scores of plots are shown by open squares (Matapédia River) and filled squares (Petite-Cascapédia River). Colors of squares identify the three studied habitats, and ellipses were set at a level of 0.95 to capture most of the dispersion for the three habitats (two rivers combined). Ice-jam regime variables are represented as blue vectors and labels. The bar graph at the top left shows the mean dispersion of points for each habitat, with SE + 1 represented by the tick. On the top right is a Venn diagram from the variation partitioning of plot communities (presence-absence) against the three groups of variables described in the methodology. The numbers in the circles represent the % of explained variability in plot composition. The Venn diagram is the result of plotting an “Euler” function object (Package *eulerr*; Larssen, 2021)..... 100

Figure 34 Location of the two study rivers and study sites. (A) Watershed boundaries of the two rivers, in black, and segments studied, in blue lines. (B) and (C) River segments studied and the sites (red circles and red label for site numbers) where dendrochronological and taxonomical samples were taken on the Matapédia and Petite-Cascapédia rivers, respectively. (D) and (E)

Aerial views of characteristic reach in the Matapédia and Petite-Cascapédia Rivers, respectively. 118

Figure 35 A) Principal coordinate analysis (PCoA) diagram of the 27 woody species based on a set of five functional traits (maximum height, specific leaf area, rooting depth, reproduction mode and resprout capacity), clustered into six distinct functional guilds. Labels' colors correspond to distinct guilds, and the plotted vectors with grey labels represent the significant traits after envfit () analysis. B) Dendrogram from the hierarchical clustering illustrating the functional similarity among the 27 woody species. Distances were computed using the Gower dissimilarity optimized with the gawdis algorithm, and species were grouped using Ward's minimum variance method. 129

Figure 36 Mean cover of the 14 functional guilds across habitats and rivers, where colors distinguish woody (olive greens) from non-woody (dark greens) guilds and where color intensity shows the mean cover in %. Asterisks denote significant differences between rivers within the same habitat, based on Wilcoxon tests, where the marked habitat in one river shows significantly greater cover of the corresponding guild compared to the same habitat in the other river. Statistics from the Wilcoxon tests are presented in Table 27 (Annexe III). 132

Figure 37 Redundancy Analysis (RDA) ordination of 169 vegetation plots based on the Hellinger-transformed functional guilds abundances, constrained by selected environmental predictors. Species scores (scaling 2) of the 14 guilds (multiplied by 2 for better visualization) are displayed in red code labels, and grey arrows and labels represent environmental variables. The selected environmental predictors were retained following a Variance Inflation Factor (VIF) to remove collinear variables. 133

Figure 38 Partial Redundancy Analysis (pRDA; Ice Regime | Reach + Plot hydrogeomorphology) of Hellinger-transformed functional guild abundances constrained by ice disturbance variables (Havg: ice-scar height; PC1_freq: ice-jam frequency gradient) and conditioned by hydrogeomorphological variables, in (A) the Matapédia and (B) the Petite-Cascapédia rivers. Guilds are displayed in red labels, and ice-jam vectors are displayed in blue labels and vectors. Plot scores are shown in Scaling 2 as open squares (Matapédia, Panel A) and filled squares (Petite-Cascapédia, Panel B), with colors indicating the three habitat types. The inset Venn diagram (top left) summarizes variation partitioning of functional composition (Hellinger-transformed) among three groups of predictors (see Methods). Values inside circles indicate the percentage of explained variation, and the diagram was produced using the "euler" function from the eulerr package (Larssen, 2021). 134

Figure 39 Radarcharts of the community-weighted means averaged to the scale of the habitat and river. Each row represents a group of traits (Morphological, Life history, Ecological), columns are divided by habitat, and filled/solid polygons identify the river. For better visual representation, all traits were scaled to 0–1 before averaging. Full names of the trait's abbreviations can be found in *Table 8*. Radarcharts were constructed with the *fmsb* R package (Nakazawa, 2024). 136

Figure 40 Redundancy Analysis (RDA) ordination of 169 vegetation plots based on community-weighted traits composition, constrained by selected environmental predictors. Species scores (scaling 2) of the 15 traits with the highest loadings (multiplied by 2 for better visualization) are represented in red code labels and grey arrows, and labels represent environmental variables. The selected environmental predictors were retained following a Variance Inflation Factor (VIF) to remove collinear variables 137

Figure 41 Partial Redundancy Analysis (pRDA; Ice Regime | Reach + Plot hydrogeomorphology) of Z-score scaled CWM traits constrained by ice disturbance variables (Havg: ice-scar height; PC1_freq: ice-jam frequency gradient) and conditioned by hydrogeomorphological variables. Each model was computed for each river (A-C Matapédia, D-F Petite-Cascapédia) and trait-group (A&D morphological, B&E life history, C&F ecological). Species scores (scaling = 2) of traits are displayed in red labels, and environmental scores of ice-jam vectors are displayed in blue vectors and blue labels. In each model, environmental vector scores were divided by 2 for better visualization. Convex hulls encompass the site by habitat. 140

Figure 42 Location of the regions with potential presence of ice-related dynamics, where temperatures reach values below -3 ˚C for over a month in a year. The map is based on the Köppen-Geiger climate classification, for which data were taken from Beck et al. (2023). 157

Figure 43 Schematic representation of all the ice forms and processes impacts left as visible markers within the fluvial corridor that are discussed in the following section. The illustration synthesizes the main features generated by ice dynamics across the active channel (scour holes, pavements, inner-bend erosion), riverbanks (two-level banks, Bechevniks, ice-pushed ridges), and floodplains (gullies, avulsions, overbank ice bulldozing, ice-jam flood extent). Annotations highlight the various forms and processes, while photographs provide field examples from cold-region rivers. Pictures were taken from Uunila and Church (2014), Prowse and Culp (2003), and Vandermause et al. (2021). 162

Figure 44 Conceptual models illustrating the interactions between flow structure, fluvial landforms, vegetation and ice dynamics that shape riverscapes. 169

Figure 45 Schematic representation of a pioneer tree recruitment and growth under ice abrasion constraints, illustrating (1) the inverse relation between plant growth and flexibility, (2) the requirements for successful establishment from the recruitment box to the WoO model, and (3) highlighting the need to identify thresholds associated with ice abrasion vulnerability. To note that dimensions and relative proportions are exaggerated for clarity. 171

Figure 46 Schematic representation of ice dynamics as an environmental filter shaping community functional composition and biogeomorphological feedbacks. Points represent individual traits (e.g., height, reproduction, flexibility) while colors distinguish different families of traits (e.g., ecological, morphological, biomechanical). From a pool of traits initially shaped by fluvial processes, ice dynamics select for specific response traits that confer resistance or resilience to ice-related disturbances. These selected response traits often overlap with effect traits (indicated by the ellipses' intersection) that subsequently influence hydrosedimentary processes and fluvial landform development, thereby modulating the nature and strength of biogeomorphological feedbacks. 174

Figure 47 Schematic representation of pulse-driven biogeomorphological development in ice-affected systems. The figure illustrates that ice-scouring events vary in their impact: some are insufficient to remove established vegetation, while others cause aboveground reset without eroding landforms. Following severe ice scour, rootmats densify and enhance both sediment cohesiveness and resprout capacity, while biogeomorphological feedbacks resume during subsequent ice-free periods after reaching sufficient plant development and succession (i.e., reaching the Biogeomorhpological Feedback Window). 179

Figure 48 A conceptual model of differences in floodplain aggradation between rivers affected by frequent ice-jam floods versus the absence of ice dynamics based on a theoretical common discharge. 180

Figure 49. Conceptual model illustrating the range of effects that mechanical ice breakup frequency and magnitude may have on reach-scale vegetation and landform spatial organization. The color gradient spans from flood-driven systems (lower left), where ice exerts minimal influence, to ice-driven systems (upper right), where frequent high-magnitude events maintain vegetation-free conditions. Intermediate conditions (centre) may foster ice-induced increases in mosaic heterogeneity. Along the frequency axis, high-frequency low-magnitude events may inhibit pioneer landform emergence, while along the magnitude axis, infrequent high-magnitude events may cause periodic spatial reorganization or vegetation reset. The succession inhibition zone (right) represents conditions in which early communities are maintained by frequent disturbance. 183

Figure 50. Proportion of plots with adequate trait coverage across the three trait groups (Morphological, Life history, Ecological). Bars represent the proportion of plots falling into different coverage classes: moderate (0.50–0.80), good (0.80–0.95), and excellent (>0.95). Traits are grouped by category, with coverage classes shown by color. 226

Figure 51. Principal coordinate analysis (PCoA) diagram of the 88 non-woody species based on a set of five functional traits (maximum height, specific leaf area, rooting depth, reproduction mode and morphotype), clustered into eight distinct functional guilds. Labels' colors correspond to distinct guilds and the plotted vectors with grey labels represent the significant traits after envfit(). 227

Figure 52. PCA with the three ways of measuring the ice jam frequencies. Numbers with different colors represent the site scores of the study sites across rivers (blue for Petite-Cascapédia and red for Matapédia) 230

Figure 53. Dendrograms (A: Matapédia River; B: Petite-Cascapédia River) showing clusters based on geomorphological and vegetation strata cover variable. 231

Figure 54. Geomorphological characteristics of plots in each defined habitat (bar, ecotone, floodplain) in each river (Mata = Matapédia, PC = Petite-Cascapédia). From top to bottom, the measured variables are the averaged pebble sediment size, the fine sediment depth, the relative height above the low flow water line and relative distance from the low flow water line. Top and bottom whiskers represent the maximum and minimum, respectively. The boxes limits represent the first and third quantiles and the horizontal black line represent the median. Empty circles are the mean of the samples..... 233

LISTE DES ABRÉVIATIONS, DES SIGLES ET DES ACRONYMES

AMI	Indice agrégé du taux de migration (*Aggregated Migration rate Index*)
ANT	Anthropique
BanQ	Bibliothèque et Archives nationales du Québec
BFW	Fenêtre de rétroactions biogéomorphologiques (*Biogeomorphological feedback windows)*
BS	Sol nu (*Barren surface*)
CCA	Analyse de correspondance (*Canonical Correspondence Analysis*)
CEHQ	Centre d'Expertise Hydrique du Québec
CWM	Moyenne pondérée à la communauté (*Community-weighted mean*)
DV	Végétation dense (*Dense vegetation*)
D50	Taille granulométrique médiane
FBS	Succession biogéomorphologique fluviale (*Fluvial Biogeomorphological Succession*)
FO	Forêt
LGDF	Laboratoire de recherche en Géomorphologie et Dynamique Fluviale
LW	Bois en rivière (*Large Wood*)
LWJ	Embâcle de bois en rivière (*Large Wood Jam*)

MAMH	Ministère des Affaires municipales et de l'Habitation
MELCCFP	Ministère de l'Environnement, de la Lutte contre les changements climatiques, de la Faune et des Parcs
MSP	Ministère de la Sécurité Publique
OBVMR	Organisme de bassin versant Matapédia-Restigouche
Q_{xx}	Flood recurrence intervals
RDA	Analyse de redondance
RMSE	Erreur quadratique Moyenne (*Root Mean Square Error*)
SLA	Aire foliaire spécifique (*Specific-Leaf-Area*)
SV	Végétation éparse (*Sparse Vegetation*)
UQAR	Université du Québec à Rimouski
VIF	Facteur d'inflation de la variance (*Variation Inflation Factor*)
WA	Eau (*Water*)
WoO	Fenêtre d'opportunité (*Windows of Opportunity*)

INTRODUCTION GÉNÉRALE

1. MISE EN CONTEXTE ET MOTIVATIONS

La biogéomorphologie est une science qui gagne en popularité depuis le début des années 2000 (Gurnell & Bertoldi, 2024; Viles, 2020). Considérée initialement comme une sous-discipline de la géomorphologie, elle se distingue par son aspect interdisciplinaire qui intègre des notions de géomorphologie, d'écologie et de biologie évolutive (Figure 1). Cette perspective intégrative, cherchant à relier les processus écologiques aux processus géomorphologiques (érosion, transport et déposition), a provoqué un changement de paradigme selon lequel les organismes participent activement aux dynamiques de surface et à l'évolution des paysages. Elle repose sur l'idée que dans certains contextes morphodynamiques (par. ex., côtiers, rivières et montagnes), les composantes biotiques et abiotiques s'ajustent réciproquement dans le temps et l'espace pour façonner les formes du relief (Corenblit et al., 2007a).

La biogéomorphologie s'est particulièrement développée dans l'étude des milieux fluviaux, où les recherches se sont attardées à comprendre les interactions entre les formes fluviales, le régime hydrosédimentaire et les dynamiques végétales. Initialement, les axes de recherche se concentraient sur des approches descriptives visant à établir un lien entre les communautés végétales riveraines, les formes fluviales et les contraintes hydrogéomorphologiques. Cependant, l'attention s'est rapidement portée sur les mécanismes d'interaction entre les dynamiques végétales et fluviales, avec pour objectifs d'identifier, de quantifier et de modéliser les rétroactions entre les processus écologiques et hydrosédimentaires (Gurnell & Bertoldi, 2024). Ces études ont mis en lumière (1) certains mécanismes expliquant la structuration spatiale et temporelle des unités végétales; (2) les effets des espèces et des communautés végétales herbacées, arbustives et arborées sur les

dynamiques hydrosédimentaires; et (3) les dynamiques d'ajustement réciproque entre les formes physiques et les communautés végétales.

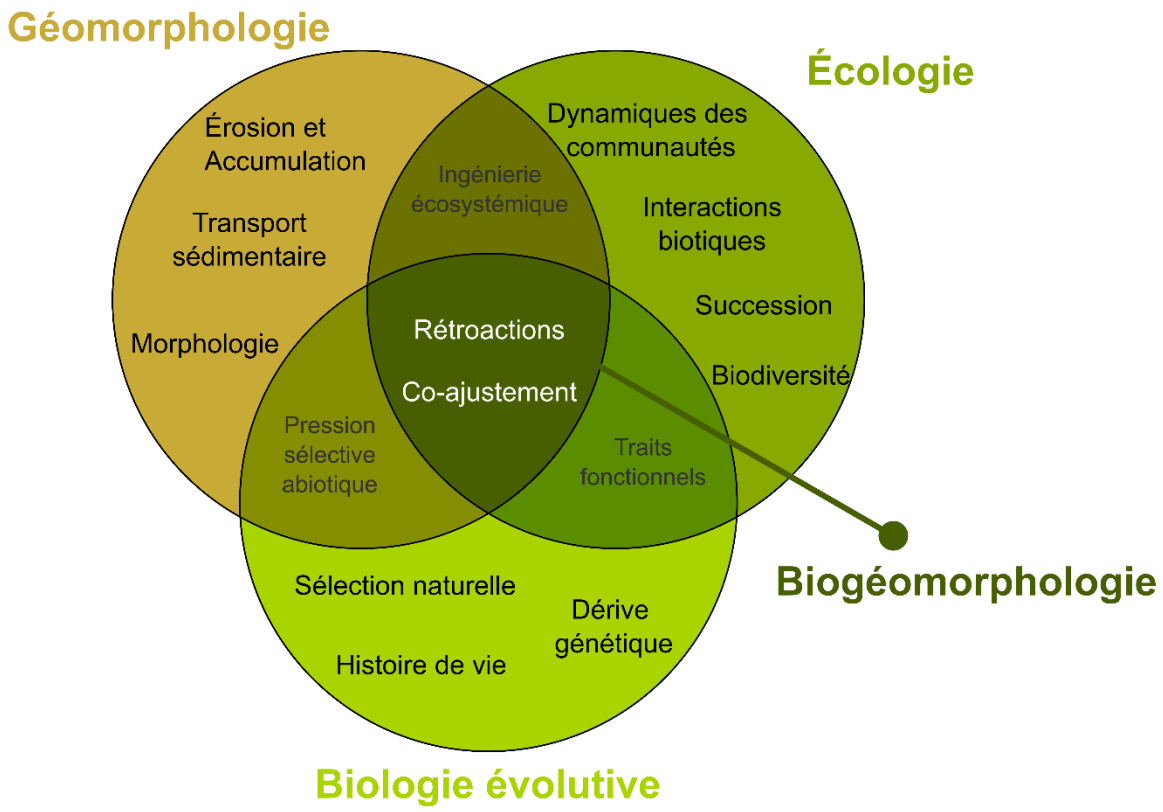


Figure 1 Représentation schématique de l'interdisciplinarité de la biogéomorphologie intégrant des notions issues de la géomorphologie, de l'écologie et de la biologie évolutive.

La végétation riveraine n'est plus considérée comme un élément passif répondant aux contraintes hydrogéomorphologiques ou comme un simple facteur de rugosité, mais bien comme un agent actif, adaptatif et plastique, qui influence les trajectoires d'évolution des cours d'eau (Corenblit et al., 2007b). Ces nouvelles perspectives sont non seulement intéressantes d'un point de vue fondamental pour comprendre les dynamiques des paysages fluviaux, mais offrent aussi des outils inestimables dans un cadre appliqué. Alors que le besoin de restauration et de gestion des cours d'eau est grandissant, l'intégration de la végétation comme facteur de contrôle des dynamiques hydrogéomorphologiques permet de mieux prédire, estimer et évaluer l'issue de divers projets (O'Briain et al., 2024). Si de

nombreux travaux ont contribué à faire progresser ces connaissances, la grande majorité d'entre eux ont été menés en milieux tempérés, alors que les rivières des régions froides demeurent sous-représentées.

Ces rivières de régions froides présentent la particularité d'être soumises à des régimes de perturbations qui se distinguent des régions tempérées, associés aux dynamiques de la glace fluviale. Il est à se questionner si les cadres théoriques issus de la biogéomorphologie, largement fondés sur les régimes de crue, s'appliquent aussi aux rivières des régions froides et par quels mécanismes les processus glaciels peuvent moduler la nature et la dynamique des interactions entre la végétation et la morphologie fluviale. Les études portant sur les processus fluvioglaciels ont permis d'exposer de leurs effets sur l'hydraulique, la géomorphologie et la végétation (Beltaos & Burrell, 2021; Chassiot et al., 2020; Lind et al., 2014a). Toutefois, il n'en demeure pas moins que les connaissances restent limitées, et ce, particulièrement quant aux interactions entre les dynamiques fluvioglacielles et la dynamique de la végétation (Poulin et al., 2019). Il persiste donc un intérêt marqué à explorer ces effets afin d'approfondir notre compréhension de ces systèmes biogéomorphologiques, mais aussi de générer des connaissances susceptibles de nourrir les réflexions sur les bonnes pratiques de gestion, de restauration et de conservation des milieux hydriques.

À la lumière de ces lacunes, ce projet de thèse a été motivé par trois ambitions. **Premièrement, intégrer les dynamiques fluvioglacielles comme régime de perturbation structurant au sein des cadres théoriques de la biogéomorphologie.** En explorant le rôle des dynamiques fluvioglacielles, nous souhaitons compléter et étendre les modèles conceptuels de la biogéomorphologie fluviale en intégrant explicitement les effets d'un régime de perturbations jusqu'ici non examiné. Les dynamiques fluvioglacielles demeurent toutefois très variées, et il serait impossible de couvrir l'ensemble des aspects essentiels à une compréhension exhaustive des dynamiques biogéomorphologiques fluviales dans les régions froides. Cette thèse met d'abord l'accent sur le rôle des **embâcles de glace** en tant que médiateurs des rétroactions entre dynamique géomorphologique et dynamique végétale. **Deuxièmement, stimuler la recherche fondamentale en biogéomorphologie fluviale au**

Québec. Bien que la biogéomorphologie tienne une place particulière au Québec, les recherches se sont surtout concentrées sur l'influence unidirectionnelle des formes et processus fluviaux sur les habitats aquatiques et l'écologie des eaux douces. Quelques études ont examiné l'impact de composantes biotiques sur la morphologie des rivières, telles que les effets du castor ou des embâcles de bois mort, mais les rétroactions entre la dynamique végétale et les processus hydrogéomorphologiques demeurent sous-étudiées (Buffin-Bélanger et al., 2024). Nous souhaitons donc dynamiser cet axe de recherche en proposant de nouvelles orientations centrées sur les rétroactions végétation-rivière. **Finalement, générer des pistes de réflexion dans un cadre de gestion et de restauration**. À partir des résultats de cette thèse, nous espérons apporter une compréhension des interactions entre les processus géomorphologiques, la dynamique végétale et les perturbations fluvioglacielles, afin de stimuler la réflexion et les discussions quant aux pratiques de gestion, de restauration et de conservation des milieux hydriques.

2. LES PRINCIPES DE LA BIOGÉOMORPHOLOGIE FLUVIALE

2.1 Les interactions fondamentales entre la végétation et l'hydrogéomorphologie

Les fondements de la biogéomorphologie fluviale reposent sur l'idée que les composantes fluviales (structure d'écoulement, transport de sédiments et formes fluviales) interagissent de manière bidirectionnelle avec la végétation (Figure 2). D'une part, la végétation riveraine est déterminée par les formes et processus hydrogéomorphologiques et en contrepartie, elle agit comme « ingénieur d'écosystème » (au sens de Jones et al., 1994) en influençant la capacité de l'écoulement à transporter les sédiments et en consolidant les sédiments déposés (Corenblit et al., 2007b; Kim & Lee, 2022). Le comportement et l'évolution d'un cours d'eau sont donc le reflet d'un équilibre dynamique entre le bilan sédimentaire, le régime de crue et la dynamique végétale (Bywater-Reyes et al., 2022a).

La distribution spatio-temporelle et la composition des communautés végétales riveraines sont fonction d'un ensemble de paramètres abiotiques et biotiques qui filtrent les

espèces et sélectionnent celles adaptées aux conditions locales d'un milieu (Götzenberger et al., 2012). Le régime de crue, les dynamiques sédimentaires et la topographie conditionnent la dispersion, le recrutement et l'établissement de la végétation (Naiman et al., 2005). Il a été observé à de nombreuses reprises que l'hydrochorie (c.-à-d., stratégie de dispersion des propagules par l'eau) participe significativement à structurer les communautés végétales le long des corridors fluviaux (Jansson et al., 2005; Kehr et al., 2014; Nilsson et al., 2010). Les crues facilitent le transport des propagules et maintiennent, avec l'élévation et la texture sédimentaire de l'habitat, un niveau d'humidité favorable à la germination et à la croissance des plantes. (Corenblit et al., 2020b; Edwards, 2024; Mahoney & Rood, 1998a; Sitzia et al., 2016). De plus, le régime de crue détermine la connectivité hydrologique entre le ou les chenaux et la plaine alluviale en créant des pulsations de transfert de matière et d'énergie sur un gradient transversal et longitudinal (« flood pulse »), procurant eau, matière organique et nutriments nécessaires au développement et au maintien de la végétation (Tockner et al., 2000). Inversement, la contrainte de cisaillement le transport des sédiments et le phénomène de submersion lors des crues peuvent nuire à la végétation soit par déracinement, enfouissement ou anoxie (Corenblit et al., 2007b; Politti et al., 2018).

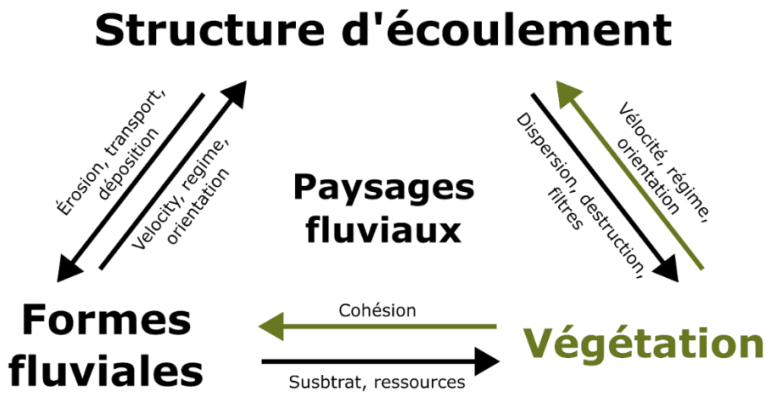


Figure 2 Schéma conceptuel des interactions entre la structure de l'écoulement, les formes fluviales et la végétation. Modifié de Corenblit et al. (2007)

Les effets du régime de crue sur la dynamique végétale sont toutefois modulés par les caractéristiques topographiques et sédimentaires d'un milieu qui influencent le degré d'exposition aux perturbations fluviales. Plus l'élévation d'un habitat est importante par rapport au chenal d'étiage, moins les inondations y sont fréquentes, conditionnant le niveau d'humidité et l'exposition aux stress mécanique et hydrique. La végétation se structure donc selon un ensemble de facteurs qui interagissent et génèrent une mosaïque changeante d'habitats et d'unités végétales (Corenblit et al., 2007b; Gurnell et al., 2016a). Conséquemment, chaque style fluvial (par ex., en anastomoses, à méandres mobiles, en îles en tresses, en tresses), caractérisé par des formes et processus distincts, conditionne la structure végétale en fonction des conditions spécifiques de leur milieu (Kui et al., 2017; Polvi & Sarneel, 2018). Par exemple, alors qu'un chenal linéaire en incision limite l'établissement végétal au sein du chenal actif et favorise la présence d'arbres matures sur les plaines, une rivière à méandres ou en îles en tresses offre une mosaïque plus diversifiée de stades de succession végétale (Gurnell et al., 2016a).

La végétation, quant à elle, influence la dynamique morphologique des rivières par l'entremise de son effet sur la structure de l'écoulement et la stabilisation des sédiments (Figure 3), agissant comme ingénieur d'écosystème qui transforme les conditions d'habitat (topographie, texture des sédiments, caractéristiques physicochimiques, quantité et qualité des ressources). Ces transformations facilitent généralement le recrutement de nouvelles espèces (Polvi & Sarneel, 2018). Premièrement, la végétation permet d'augmenter la cohésion des sédiments et la résistance au cisaillement. Le système racinaire stabilise les sédiments mécaniquement grâce à un réseau de fins filaments qui agit comme un filet de rétention, et hydrauliquement via les mécanismes d'évapotranspiration qui réduisent la pression d'eau interstitielle (Simon & Collison, 2002). De plus, les plantes flexibles peuvent avoir un effet « tapis » en protégeant les sédiments sans subir une force de trainée lorsqu'elles se couchent sous l'effet d'une crue (Zhu & Tsubaki, 2022). En stabilisant les morphologies fluviales et procurant une résistance au cisaillement, la végétation peut ainsi influencer de manière significative la structure et le fonctionnement des corridors fluviaux. Par exemple, des études ont montré que les variations spatiales de densité et d'abondance de la végétation

arbustive et arborescente le long des berges engendrent des taux d'érosion différenciés, modulant ainsi la largeur du chenal actif et la géométrie des méandres (González et al., 2019 a; Perucca et al., 2007). Ensuite, la structure aérienne de la végétation (tiges, feuillages et canopée) exerce une résistance mécanique à l'écoulement au sein de la zone végétalisée, ce qui réduit la vélocité et induit le dépôt de sédiments fins (Polvi & Sarneel, 2018). D'un point vue hydraulique, la résistance à l'écoulement offerte par les structures végétales aériennes a aussi comme effet de dévier le courant, pouvant intensifier localement l'érosion aux pourtours d'une plante individuelle ou d'un *patch* de végétation (petit groupe de plantes), et créer des zones de recirculation en aval où les sédiments peuvent y être déposés (Matte et al., 2022; Politti et al., 2018). En somme, la végétation redistribue l'énergie associée aux crues et influence les patrons d'érosion et d'accumulation autant à l'échelle du banc d'accumulation qu'à l'échelle du corridor fluvial.

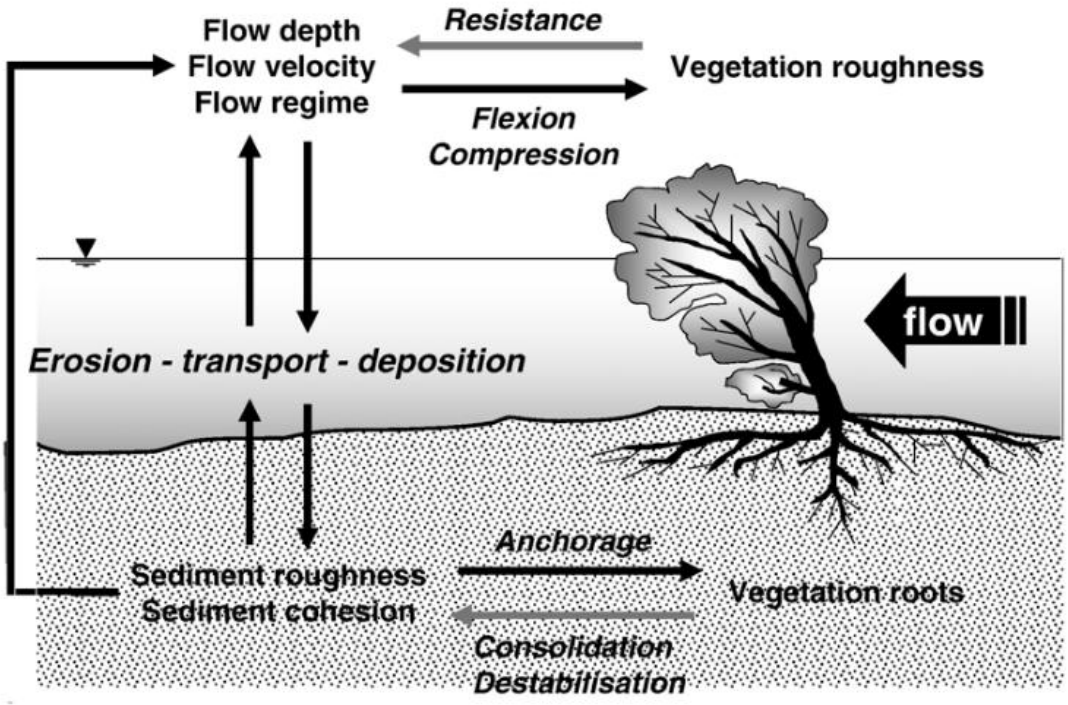


Figure 3 Modèle conceptuel des interactions entre la végétation, la structure d'écoulement et les dynamiques sédimentaires. Tiré de Corenblit et al. (2007).

2.2 L'importance des échelles spatio-temporelles

Il est maintenant reconnu que la végétation influence de manière significative la morphodynamique des cours d'eau, mais que la nature et l'importance de ces effets varient selon l'échelle d'analyse (Corenblit et al., 2024a). De l'individu et du *patch* jusqu'aux communautés et aux mosaïques végétales, la végétation peut induire une accumulation sédimentaire de quelques centimètres ou influencer profondément l'organisation morphologique d'un tronçon de rivière. Chaque échelle d'analyse demeure essentielle pour brosser un portrait complet des dynamiques biogéomorphologiques, puisqu'elles s'imbriquent au sein d'une dynamique d'effets en cascade. De petits changements à petite échelle peuvent, par effet cumulatif sur un temps donné, entraîner une chaîne de réactions à grande échelle, tandis qu'une perturbation à grande échelle peut provoquer des changements drastiques à petite échelle.

À l'échelle de l'individu et du patch, l'accumulation sédimentaire générée en aval par des courants de recirculation peut mener à la construction de formes de petite taille (par ex., trainées sédimentaires) (Bywater-Reyes et al., 2017). L'ampleur des effets associés à cette échelle est étroitement liée aux traits fonctionnels de l'espèce végétale, c'est-à-dire à des caractéristiques morphologiques, physiologiques, écologiques et phénologiques qui conditionnent la manière dont une espèce répond à son environnement et influence le fonctionnement de l'écosystème (Diehl et al., 2017). En effet, plusieurs traits fonctionnels caractérisant la végétation riveraine ont été associés à diverses fonctions géomorphologiques, telles que l'architecture racinaire, associée à la stabilisation des berges, ou la hauteur et la biomasse, associées aux patrons d'accumulation sédimentaire (Diehl et al., 2017). Par exemple, une plante développant des tiges plus longues et des feuilles plus grandes factorisera davantage l'accumulation de sédiments fins en augmentant la résistance à l'écoulement (Hortobágyi et al., 2017). Alors qu'un dépôt sédimentaire de quelques centimètres peut sembler insignifiant sur un tronçon de quelques centaines de mètres linéaires, il peut constituer une unité de base où s'instaure une boucle de rétroaction positive entre l'accumulation sédimentaire et la croissance végétale. En quelques années, cela peut

entraîner une reconfiguration majeure des chenaux et favoriser le développement d'une végétation arborée mature. (Bywater-Reyes et al., 2017; Corenblit et al., 2024a).

À l'échelle des communautés, l'émergence d'unités biogéomorphologiques telles que des îles végétalisées (Gurnell et al., 2001) ou des bancs de convexité boisés (Corenblit et al., 2016, 2018) peut considérablement modifier les patrons d'écoulement et le transport sédimentaire à l'échelle du corridor. Les unités biogéomorphologiques fluviales se définissent comme des formes (par ex., bancs d'accumulation, îles et plaines alluviales) façonnées par des interactions biogéomorphologiques (Corenblit et al., 2008). Lorsqu'une communauté végétale pionnière atteint un développement lui permettant d'induire une sédimentation significative, d'autres espèces peuvent coloniser ces habitats sous contrôle biotique. S'enclenche alors une boucle de rétroaction positive : la végétation favorise le dépôt de sédiments, de matière organique, de propagules viables et de nutriments, ces dépôts facilitant en retour la croissance et la succession végétale. La magnitude et le taux des rétroactions biogéomorphologiques sont toutefois fonction des caractéristiques de la communauté; ce n'est pas seulement la présence de la végétation, mais bien sa structure et sa composition qui déterminent son effet sur les dynamiques hydrosédimentaires (Kui et al., 2017). Par exemple, des études dans le sud-ouest des États-Unis ont exposé des taux d'accumulation significativement plus élevés lorsque les communautés étaient dominées par une espèce de tamaris que ceux où les communautés étaient dominées par le peuplier (Bywater-Reyes et al., 2022 a; Kui et al., 2017). Ainsi, la capacité des plantes à agir comme ingénieurs d'écosystème repose intrinsèquement sur les traits fonctionnels spécifiques des espèces qui composent la communauté.

L'établissement de nouvelles espèces au fil des constructions d'unités biogéomorphologiques entraîne une évolution de la composition fonctionnelle qui module la nature et l'intensité des rétroactions sur une échelle pluridécennale. Le modèle de succession biogéomorphologique fluviale (FBS; Corenblit et al., 2007) permet de représenter conceptuellement les différents stades de développement de ces unités biogéomorphologiques, en illustrant le basculement progressif d'une dynamique dominée

par les forçages physiques vers une dynamique contrôlée par les processus biologiques. Le cadre théorique de la FBS décrit un processus dynamique de co-construction entre les formes fluviales et les communautés végétales, caractérisé par une alternance de périodes de progression, de régression et de stabilité. Ce processus est modulé par plusieurs facteurs, notamment le régime de crue (Caponi et al., 2019; Corenblit et al., 2014; Garófano-Gómez et al., 2017), les dynamiques sédimentaires (Corenblit et al., 2009; Kim & Kupfer, 2016), l'accessibilité à l'eau souterraine (Bätz et al., 2016a) et les pressions anthropiques (Han et al., 2020). Elle se divise en quatre phases distinctes (Figure 4). La phase géomorphologique se caractérise par des formes fluviales dépourvues de végétation en raison d'un fort transport sédimentaire et de crues fréquentes. La phase pionnière commence lorsque des espèces végétales pionnières, qu'il s'agisse d'herbacées opportunistes ou de plantules d'espèces ligneuses, s'établissent. À ce stade, la végétation n'influence pas le transport sédimentaire hormis le captage de fines couches de sédiments fins, mais elle peut jouer un rôle déterminant en facilitant le recrutement d'espèces pionnières ligneuses comme le saule ou le peuplier (Corenblit et al., 2015). La phase biogéomorphologique débute lorsque des espèces ingénieures s'établissent et interagissent de manière significative avec l'écoulement, provoquant une accumulation sédimentaire. Enfin, la phase écologique est atteinte lorsque des communautés de fin de succession s'installent durablement et que les processus fluviaux n'affectent plus, ou très rarement, l'habitat. Généralement, la co-construction des formes et des communautés végétales progresse jusqu'à ce qu'une crue majeure réinitie l'habitat à un stade inférieur, ce qui entraîne une dynamique cyclique qui maintient une diversité d'habitats et de communautés.

Transposée à l'échelle du tronçon, l'émergence de formes pionnières (*sensu* Gurnell et al., 2014) telles que les îles fluviales et les processus de succession biogéomorphologique instaurent une dynamique d'auto-organisation spatiale des unités paysagères modulée par le régime de crues (Corenblit et al., 2008). La diversité, la distribution et la dimension des différentes unités biogéomorphologiques forment une mosaïque hétérogène qui influence le degré de contrôle de la végétation sur le morphodynamisme fluvial (Gurnell et al., 2016a). Ainsi, une dominance de la phase géomorphologique traduit une faible influence de la

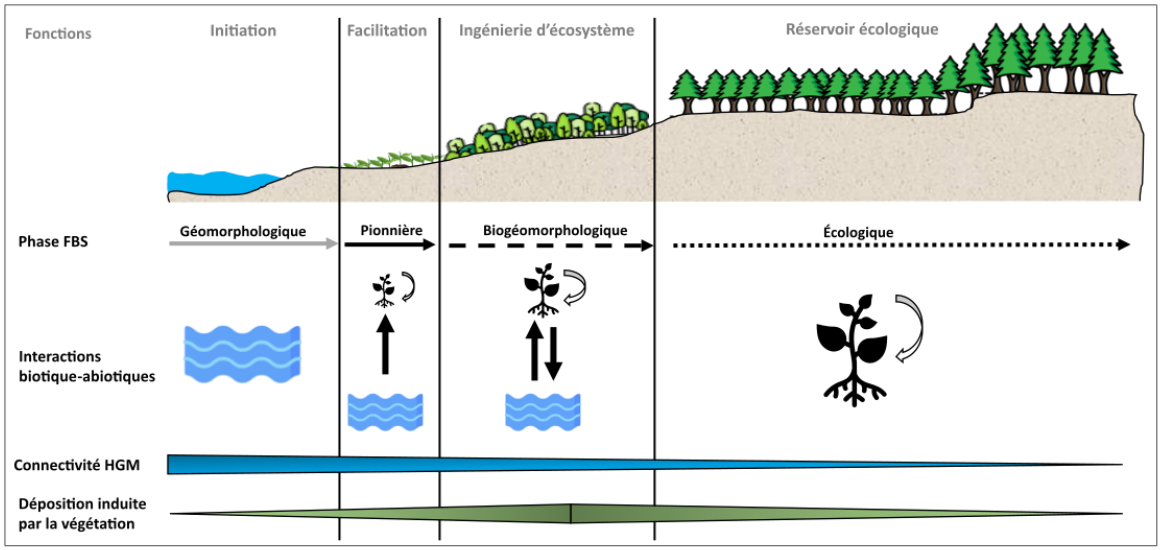


Figure 4 Représentation schématique des phases de la succession biogéomorphologique intégrant les fonctions écosystémiques, les interactions HGM-végétation dominantes, la connectivité hydrogéomorphologique et la force des rétroactions biogéomorphologiques. Figure adaptée de Corenblit et al. (2015) et Corenblit et al. (2009).

végétation, tandis qu'une dominance de la phase biogéomorphologique révèle un contrôle végétal significatif sur la dynamique fluviale. La distribution spatiale des communautés à différents stades de succession influence, quant à elle, les patrons d'écoulement et le transport sédimentaire, ce qui initie des mécanismes de co-ajustement entre les formes fluviales et les communautés végétales (Hortobágyi et al., 2017). Conséquemment, le comportement fluvial (c.-à-d., l'ensemble des formes et processus en réponse à son régime hydrologique) peut être intrinsèquement lié à la végétation qui influence les ajustements morphologiques pendant une crue (Gurnell et al., 2016b). L'intensité de ce couplage varie toutefois selon le contexte géomorphologique et hydrologique. En fonction du régime de perturbations, de la charge sédimentaire et de la mobilité latérale, le morphodynamisme d'un tronçon peut être dominé soit par des facteurs physiques (charge de fond et crues), soit par la végétation, soit par de fortes interactions réciproques (Corenblit et al., 2024a). Le régime de crues joue à cet égard un rôle déterminant en redistribuant matière et énergie sur toute la largeur du corridor, modulant ainsi les trajectoires d'ajustement et conditionnant l'influence relative de la végétation. La dynamique à l'échelle du tronçon résulte donc d'un équilibre variable entre le

forçage physique et l'influence végétale, soulignant la nature contextuelle et adaptative des trajectoires biogéomorphologiques fluviales.

Les interactions biogéomorphologiques propres à chaque échelle spatio-temporelle sont intrinsèquement reliées par une hiérarchie de processus susceptibles de créer des effets en cascade. Des changements à petite échelle peuvent entraîner une chaîne de réactions ascendante (*bottom-up*) et modifier la nature d'une rivière à l'échelle du corridor. Par exemple, l'introduction d'une espèce végétale envahissante a le potentiel de changer la nature des interactions biogéomorphologiques d'un écosystème en modifiant les traits fonctionnels et provoquer des changements géomorphologiques pouvant être conséquents et durables. Cela peut être illustré par l'envahissement du tamaris aux États-Unis, connu pour augmenter considérablement la résistance des berges grâce à ses racines profondes, provoquer une forte sédimentation et réduire la largeur active des chenaux (Fei et al., 2014). Dans un cas comme celui-ci, les changements dans la composition des communautés se répercutent sur le comportement biogéomorphologique du système en stabilisant les formes et en réduisant de manière drastique l'hétérogénéité des communautés dans le corridor. Inversement, des altérations à l'échelle du bassin-versant et/ou du corridor fluvial peuvent entraîner de profonds changements sur la structure des communautés et la morphodynamique fluviale. Un exemple clé est celui de la régulation hydrologique des cours d'eau : plusieurs études montrent que la réduction de la fréquence et de l'intensité des crues par un barrage transforme la dynamique biogéomorphologique des tronçons situés en aval, en favorisant le développement de la végétation vers des communautés post-pionnières et en réduisant les dynamiques de réorganisation spatiale par rajeunissement de la succession (Bejarano et al., 2018; Church et al., 2014; González del Tánago et al., 2015; Han et al., 2020). Somme toute, la compréhension des trajectoires d'ajustement biogéomorphologiques exige de considérer simultanément les structures et processus à diverses échelles, puisque c'est leur imbrication qui détermine la réponse d'un système à un forçage.

2.3 Une approche interdisciplinaire sur la taxonomie et les traits fonctionnels

En se fiant aux études des deux dernières décennies, il est possible d'identifier trois grands axes de recherche qui dominent les études dans la discipline de la biogéomorphologie, soit de déterminer (1) la manière dont les facteurs hydrogéomorphologiques structurent la végétation, (2) comment la végétation affecte les formes et processus hydrogéomorphologiques et (3) comment se manifestent les dynamiques d'ajustement réciproque entre morphodynamique fluviale et végétation. Les études portant sur la structuration de la végétation à l'échelle des communautés s'appuient davantage sur des méthodes issues de l'écologie, en identifiant des patrons entre les caractéristiques des assemblages d'espèces et celles des caractéristiques géomorphologiques, à l'aide d'un grand nombre de réplications d'échantillons. À l'inverse, les études portant sur les effets de la végétation relèvent plutôt des méthodes issues de la géomorphologie, où un nombre restreint de sites fait l'objet d'une quantification précise et détaillée de divers paramètres hydrosédimentaires afin d'en révéler les mécanismes sous-jacents (Haussmann, 2011). Pour étudier ces interactions à différentes échelles, plusieurs catégories de méthodes sont employées : l'obtention de données empiriques par des approches expérimentales et d'observation sur le terrain, des analyses spatiales via la télédétection et la géomatique, et la modélisation numérique (Corenblit et al., 2024 a; Haussmann, 2011; Viles, 2020). Alors que de plus en plus de modèles numériques sont développés pour tenter de modéliser les interactions réciproques entre la végétation et la morphodynamique fluviale (Bertoldi et al., 2014; Martínez-Fernández et al., 2018; Solari et al., 2016), il n'en demeure pas moins que les études sur le terrain demeurent essentielles pour quantifier et identifier les interactions entre la végétation et les processus fluviaux dans des contextes spécifiques.

Les analyses taxonomiques ont d'abord permis de générer d'importantes connaissances sur le rôle des contraintes hydrogéomorphologiques dans la structuration, la composition et la diversité de la végétation riveraine. Que ce soit à l'échelle d'une population, d'une communauté ou d'une mosaïque de communautés, la structure de la végétation et ses effets sur les cours d'eau ont été explorés dans divers environnements fluviaux pour identifier des

patrons associés au régime de crue, aux formes fluviales ou aux styles fluviaux (Dufour et al., 2007; Jolley et al., 2010; Picco et al., 2016). Les analyses taxonomiques peuvent suivre deux approches : l'une fondée sur la composition floristique en considérant l'abondance de chaque espèce (Egger et al., 2015; Nilsson et al., 1989; Suzuki et al., 2002), l'autre sur des indices écologiques tels que la richesse spécifique, la diversité et l'équitabilité (Brazeiro, 2001; Pielech, 2021). Combinées à des données géospatiales telles que des photographies aériennes historiques ou de l'imagerie LiDAR, les trajectoires d'ajustement hydrogéomorphologique et celles des communautés riveraines peuvent être quantifiées et décrites afin d'analyser les changements spatiaux et temporels (Garófano-Gómez et al., 2017; Surian et al., 2015; Vautier et al., 2016). Les approches taxonomiques ont aussi servi de base au développement de classifications à l'échelle de l'espèce et de la communauté qui reflètent des fonctions biogéomorphologiques quantifiables sur le terrain (Corenblit et al., 2009, 2024 b). Bien que ces approches aient contribué à l'approfondissement des connaissances sur les facteurs déterminant la dynamique de la végétation et leurs potentielles fonctions biogéomorphologiques, elles demeurent limitées dans une perspective de généralisation et de comparaison entre différents systèmes, puisque la composition floristique des communautés est sensible aux conditions locales et que les espèces peuvent varier d'une région à l'autre (Janssen, 2025).

L'approche par traits fonctionnels a rendu possible le transfert et la comparaison de résultats entre systèmes et s'est révélée efficace et plus puissante pour relier, en termes de réponses et d'effets, les caractéristiques des communautés riveraines aux processus hydrogéomorphologiques (Bejarano et al., 2018; Corenblit et al., 2024 b; Diehl et al., 2017). Cette approche, basée sur les traits fonctionnels des espèces végétales, permet d'abord de comprendre les mécanismes par lesquels la végétation persiste dans les conditions locales, mais aussi d'identifier les traits qui sont directement (traits morphologiques et biomécaniques) ou indirectement (traits d'histoire de vie) responsables des effets de rétroaction (Diehl et al., 2017). À l'échelle de la population d'individus, elle permet d'identifier les traits de réponses et d'effets responsables de leur maintien et de leurs fonctions dans les cours d'eau. Transposée à l'échelle de la communauté, cette approche

permet d'examiner comment la composition fonctionnelle module les interactions avec les processus fluviaux. Pour ce faire, plusieurs méthodes de généralisation existent, mais il y en a trois principales, soit de (1) calculer la moyenne des traits de chaque espèce pondérée par leur abondance, (2) définir des guildes fonctionnelles en regroupant des espèces partageant des traits fonctionnels similaires et (3) représenter la communauté dans un espace fonctionnel statistique (hypervolume) afin d'en mesurer l'étendue et la structure. Ces approches offrent toutes une vision différente et complémentaire : la moyenne pondérée renseigne sur les traits dominants, les guildes permettent d'identifier les stratégies d'adaptation générales, et l'hypervolume décrit la structure fonctionnelle (richesse, diversité, divergence). Ces méthodes peuvent être utilisées pour analyser la variation des traits selon différentes échelles spatiales ou temporelles, ou encore le long de gradients environnementaux (De Bello et al., 2021a; Funk et al., 2017; Janssen, 2025; Legras et al., 2020). La mesure des valeurs de traits fonctionnels sur le terrain ou en laboratoire peut toutefois nécessiter un temps considérable. Une alternative courante consiste à s'appuyer sur de grandes bases de données accessibles en ligne, telles que TRY (Kattge et al., 2020), où des chercheuses et des chercheurs à travers le monde contribuent à alimenter une compilation de valeurs par trait et par espèce. Bien que ces bases de données utilisent des valeurs moyennes qui ne reflètent pas la variabilité locale des traits au sein d'une même espèce (par ex., un taux de croissance et une morphologie qui varient en fonction de la position sur le gradient amont-aval du cours d'eau; voir Gurnell sur le Tagliamento), elles offrent un accès rapide à un large éventail de traits et d'espèce pouvant décrire les grandes stratégies écologiques employées par les plantes riveraines.

3. LA PARTICULARITÉ DES RIVIÈRES FROIDES

3.1 Processus fluvioglaciels

Les rivières de régions froides sont typiquement caractérisées par des environnements où les températures moyennes annuelles se retrouvent en dessous de 0 °C pendant au moins un mois consécutif dans l'année (Chassiot et al., 2020; Ettema & Kempema, 2012). De cette condition découle une gamme de processus fluvioglaciels qui interagissent avec les composantes fluviales tout au long de la saison hivernale (Figure 5) et qui peuvent laisser des traces morphologiques influençant les dynamiques fluviales aux autres saisons. Au cours d'une saison de glace, trois phases peuvent être distinguées : la période d'englacement, la période de croissance et la période de débâcle.

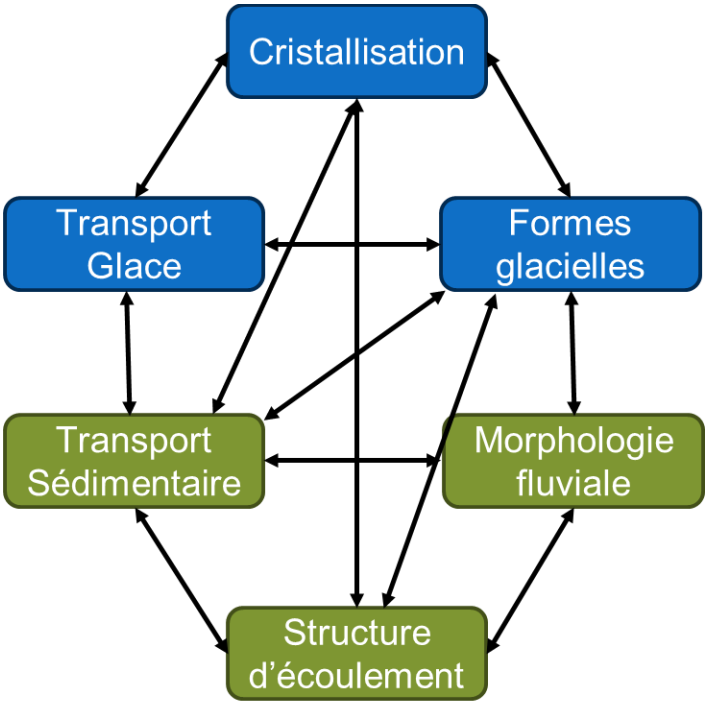


Figure 5 Modèle conceptuel des interactions entre les composantes hydrogéomorphologiques et fluvioglaciels. Modifiée de Allard (2010)

L'englacement débute lorsque les températures atteignent un seuil permettant la formation de cristaux de glace. Il est déclenché soit par la formation de glace de rives (c.-à-d., le gel thermique lorsque la température atteint 0 °C) qui s'étend dans l'entièreté du chenal, soit par un processus plus complexe lié à la production de frasil (Lindenschmidt, 2020). En conditions de surrefroidissement (c.-à-d. température < 0 °C) et en présence d'écoulements turbulents, la production de frasil peut mener à la formation de bouillies de glace (*slush*) et de glace en crêpes qui sont transportées vers l'aval, s'accumulent lorsqu'ils rencontrent un obstacle physique (p. ex. rétrécissement du chenal, couverture de glace stable, îles) et finissent par se consolider pour former une couverture de glace stable. Ces accumulations lors de la mise en place du couvert de glace, où embâcle de formation, peuvent provoquer de l'abrasion en berge et du débordement en plaine alluviale. Le frasil entraîné vers le lit du chenal, par exemple au niveau d'un seuil, peut adhérer au substrat et s'accumuler pour former de la glace de fond. Celle-ci peut croître jusqu'à la formation d'un seuil de glace, pouvant agir comme un barrage, réduisant la vitesse d'écoulement et augmentant le niveau d'eau en amont du seuil (Engström et al., 2011; Turcotte et al., 2011a). Dans certains cas, par exemple lorsque survient une accumulation importante de glace de fond dans un petit cours d'eau, l'air du chenal mouillé peut aller jusqu'à doubler et former un couvert de glace surplombant les berges de la rivière, connu sous le nom de glace riveraine (Engström et al., 2011; Lind & Nilsson, 2015). Le retrait d'une telle forme glacielle au printemps peut entraîner une érosion de surface des berges et, conséquemment, limiter le recrutement de plantes arbustives, ce qui structure les communautés végétales en favorisant le maintien d'espèces opportunistes. Dans d'autres cas, le frasil peut s'accumuler sous le couvert de glace et former des barrages suspendus qui affectent de manière importante les distributions de vitesse dans le chenal.

La période de croissance fluvioglacielle se définit par une stabilité du couvert de glace qui est entièrement formé et qui se développe verticalement au fil de l'hiver avec les accumulations de neige et les redoux qui créent des couches de glace en surface. Durant la période de croissance, la structure hydraulique de l'écoulement sous le couvert de glace est affectée; la face inférieure du couvert de glace applique une rugosité qui a comme conséquence de réduire la vélocité moyenne des écoulements (Beltaos & Prowse, 2009).

Toutefois, les effets directs de ce couvert stable sur le transport sédimentaire et la végétation riveraine sont négligeables.

Les processus fluvioglaciels ayant le plus grand impact sur les hydrosystèmes fluviaux se produisent lors de la phase de débâcle. Cette dernière se caractérise par la période de fonte et de dislocation du couvert de glace. Nous distinguons deux types de débâcles : la débâcle thermique et la débâcle mécanique (Beltaos, 2003). La débâcle thermique se produit lorsque le couvert de glace fond progressivement dû à la hausse des températures et l'ensoleillement. La débâcle mécanique, quant à elle, se produit lorsque le couvert de glace de la rivière se disloque et se met en mouvement à la suite d'un apport considérable en eau qui rehausse rapidement le niveau de la rivière, notamment lors de la fonte des neiges cumulée à de fortes pluies printanières (Boucher et al., 2009a). Vandermause et al. (2021) ont identifié trois processus distincts d'érosion liés à la glace qui se produisent lors des débâcles mécaniques : les amas de glace, les écoulements de blocs de glace (*ice floes*) et la congestion. L'érosion par amas de glace, caractérisée par des blocs de glace de 1 à 10 m de largeur, se manifeste par une érosion directe des sédiments et de la végétation selon deux mécanismes principaux : l'affouillement de la berge et l'érosion de surface. Ces processus entraînent un important déchaussement des berges et peuvent éroder la végétation en place (Chassiot et al., 2020). Les *floes* de glace, qui comprennent des blocs beaucoup plus grands, allant de 10 à 100 m de largeur, occupent l'ensemble du chenal et se déplacent vers l'aval à une vitesse relativement élevée; ils sont associés à d'importants épisodes d'érosion et de transport sédimentaire (Beltaos & Burrell, 2021; Vandermause et al., 2021). Associés à une force de cisaillement élevée, ces évènements peuvent entraîner le transport de grandes quantités de sédiments et affecter la végétation. Toutefois, l'ampleur de l'érosion dépend d'abord des caractéristiques du *ice floe* (p.ex., épaisseur et densité des blocs), qui déterminent la force de cisaillement, ainsi que des caractéristiques sédimentaires (densité, composition, texture) et du type de végétation en place qui influencent la résistance à l'érosion (Beltaos & Burrell, 2021). Bien que la végétation ait le potentiel d'atténuer l'érosion des berges, de nombreux impacts sur les communautés riveraines ont été documentés, tels que le bris de branches, le pliage ou le déracinement (Rood et al., 2007). Enfin, la congestion de glace survient lorsque des blocs de

glace s'immobilisent et s'accumulent contre des obstacles physiques, tels que des formes géomorphologiques surélevées ou des arbres riverains, ce qui entraîne l'éventuelle formation d'un embâcle de glace et l'obstruction du chenal.

3.2 Le cas des embâcles de glace

Les embâcles de glace sont connus comme des agents morphogènes importants dans les rivières des régions froides, provoquant d'importantes inondations et des épisodes d'érosion majeurs (Boucher et al., 2009 a; Chassiot et al., 2020; Rokaya et al., 2018). Leur formation est toutefois variable dans le temps et l'espace en fonction de nombreux facteurs climatiques, hydrauliques et géomorphologiques (Beltaos, 2002; De Munck et al., 2017). Les embâcles se forment préférentiellement dans des zones où le transport de glace est restreint, par exemple dans des méandres ou des segments où le chenal rétrécit abruptement, ou encore lorsque des ruptures de pente sont présentes dans le chenal principal (De Munck et al., 2017). Lors d'un embâcle, les niveaux d'eau en amont de l'obstruction peuvent s'élever de plusieurs mètres par rapport à une crue sans glace pour un même débit mesuré, générant d'importantes inondations (Rokaya et al., 2018). En raison de l'obstruction du chenal, les écoulements peuvent être déviés vers la base ou vers les côtés de l'embâcle, augmentant les contraintes de cisaillement sur le lit et les berges en raison de l'intensification des vitesses d'écoulement locales (Chassiot et al., 2020; Smith & Pearce, 2002). Lorsque les forces maintenant l'embâcle en place s'affaiblissent et qu'il cède, son démantèlement peut entraîner la formation d'une vague de propagation en aval qui transporte d'importantes quantités de glace. Ces vagues, appelées « *javes* » (contraction de *jam* et *waves*), peuvent rapidement rehausser les niveaux d'eau en aval et accroître considérablement la concentration en sédiments suspendus (Rood et al., 2007). Par exemple, sur la rivière Athabasca, une *jave* a été observée avec une hausse du niveau d'eau atteignant 4,4 mètres en seulement 15 minutes, accompagné d'une concentration de sédiments en suspension 4,2 à 6,5 fois plus élevée que lors des crues en eaux libres ayant des débits équivalents (Beltaos & Burrell, 2021).

Les processus d'inondation et d'érosion associés à la formation des embâcles de glace et aux *javes* peuvent avoir des effets considérables tant sur la morphologie des rivières que sur la végétation. Lors de la formation d'un embâcle, de fortes poussées glacielles peuvent entraîner d'importants transports sédimentaires et affecter les arbres des plaines inondables (Figure 6). Les forts volumes d'eau et de sédiments transportés jusqu'aux plaines alluviales lors de ces inondations peuvent favoriser l'aggradation des plaines alluviales et maintenir un niveau d'humidité assez élevé pour conditionner la composition de la végétation (Church et al., 2014; Hugenholtz et al., 2009; Tolkkinen et al., 2020; van Eck et al., 2006). De plus, la redirection et la concentration des écoulements causées par l'obstruction du chenal peuvent entraîner des avulsions et, par conséquent, reconfigurer la structure même d'un corridor fluvial (Smith & Pearce, 2002). Lors du démantèlement d'un embâcle, la propagation d'une *jave* constitue l'un des aléas les plus sévères des rivières froides et est considérée comme un agent majeur de leur façonnement (Chassiot et al., 2020; Rokaya et al., 2018). Si de tels évènements sont suffisamment fréquents, ils peuvent maintenir des formes typiquement fluvioglacielles, telles que des berges à deux niveaux (Boucher et al., 2009a). Dans certains cas, des forêts alluviales entières peuvent être détruites lorsque des blocs de glace surplombent les plaines alluviales (Vandermause et al., 2021). Somme toute, les effets des embâcles de glace sont variés et peuvent constituer des facteurs importants façonnant la structure biogéomorphologique des rivières.

3.3 Les embâcles : décrire un régime de perturbation

Les régimes d'embâcles de glace peuvent être caractérisés comme tout autre régime de perturbations, en identifiant leur fréquence, leur amplitude, leur durée et leur saisonnalité. Toutefois, la caractérisation de ces régimes demeure un défi, en raison du comportement stochastique des embâcles de glace et du manque de données disponibles. Dans les milieux anthropisés où les embâcles de glace présentent un risque important d'inondation, les données sont plus abondantes, car une surveillance est assurée par les municipalités et les gouvernements. Inversement, dans les milieux plus naturels où il n'y a pas de vulnérabilité des populations humaines, les évènements passés sont plus difficiles à identifier. Parmi les

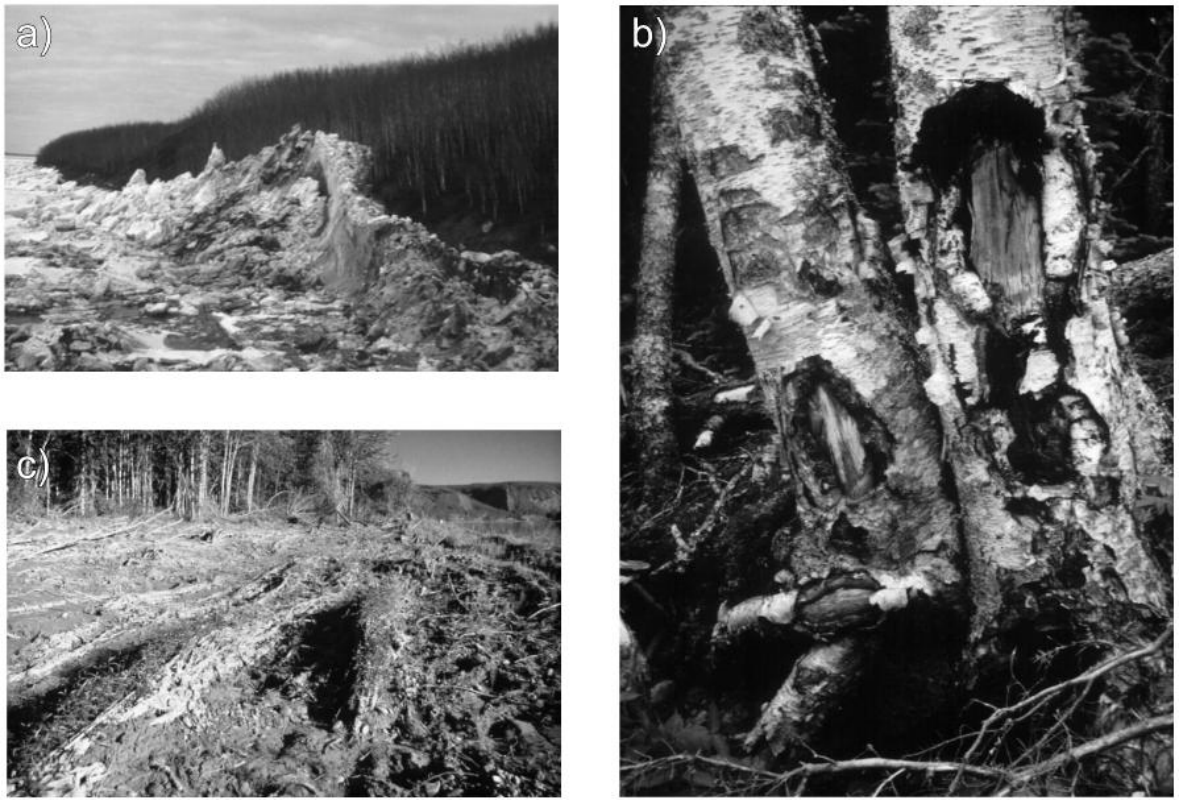


Figure 6. Exemple des potentiels impacts d'embâcles de glace, soit (a) des poussées glacielles en haut des berges, (b) des cicatrices glacielles laissées sur les arbres de rives et (c) écorchement glaciel laissé sur les berges après le passage d'un embâcle. Les photographies ont été tirées de Prowse et Culp (2003).

paramètres pouvant être caractérisés, l'amplitude d'un embâcle correspond au niveau d'eau atteint au moment de l'évènement. Dû au rehaussement du niveau d'eau causé par les glaces, il est impossible de se fier aux courbes de tarage qui mettent en relation le débit d'une rivière et la hauteur d'eau. De nombreuses études ont démontré que lors d'un embâcle (ou d'un *ice floe* important), le niveau d'eau pour un même débit peut être supérieur de plusieurs mètres à celui d'une crue sans glace (Beltaos & Burrell, 2010; Beltaos & Prowse, 2009; Krylenko et al., 2020). Une façon d'estimer le niveau d'eau atteint lors d'un embâcle consiste à mesurer la hauteur des cicatrices de glace laissées sur le tronc des arbres (Smith & Reynolds, 1983). Quelle que soit la marge d'erreur associée au risque que la cicatrice puisse surévaluer le

niveau d'eau lié au chevauchement des blocs de glace, cette hauteur demeure un proxy d'intérêt pour évaluer l'amplitude d'un évènement.

L'autre défi consiste à déterminer les années au cours desquelles des embâcles de glace ont eu lieu sur un site donné. Plusieurs méthodes ont été utilisées jusqu'à présent, dont des approches historiques, dendrochronologiques ou stratigraphiques (Kalinin, 2008; Lagadec et al., 2015; Livingston et al., 2009). Quoique moins abondantes dans les milieux naturels, plusieurs sources d'informations historiques permettent de documenter le lieu et la date d'évènements d'embâcles, soit à partir d'articles de journaux locaux, soit par des bases de données provenant des municipalités, des organismes de bassin-versant ou des gouvernements. Une approche couramment utilisée pour combler les lacunes historiques concernant les évènements d'embâcle est l'analyse dendrochronologique d'arbres impactés par des blocs de glace (Boucher et al., 2009b; Dahl et al., 2017; Lagadec et al., 2015; Lubiniecki et al., 2024). Les cicatrices sur les troncs d'arbres, causées par l'impact de blocs de glace, s'inscrivent dans la séquence des cernes de croissance et permettent de dater l'année à laquelle se sont produits les évènements (Figure 7). Une chronologie d'embâcle de glace peut alors être caractérisée en combinant les données provenant de plusieurs arbres et en aboutissant à une estimation de la fréquence de perturbations à une échelle spatiale donnée (p. ex., tronçon). Cette approche est toutefois limitée, d'abord parce qu'elle dépend de la présence d'arbres suffisamment âgés pour couvrir la période d'intérêt. Ensuite, la détection des arbres cicatrisés sur le terrain peut s'avérer complexe si les cicatrices ont été recouvertes par la croissance de nouveaux cernes, ce qui peut entraîner une sous-estimation d'un régime dû à un manque d'échantillons. Inversement, des risques de surestimations sont aussi présents si les cicatrices d'arbres échantillonnés proviennent de perturbations autres qu'un embâcle de glace, telles que par des chutes d'arbres ou du bois transportés durant une crue. Il est donc recommandé d'exploiter une variété de sources d'information (p. ex., sources historiques et dendrochronologiques) afin d'enrichir la caractérisation des chronologies et de limiter les erreurs d'estimation.



Figure 7. Exemple d'un échantillon ligneux (rondelle) provenant d'un thuya occidental ayant subi plusieurs perturbations par embâcles. Les cercles identifient les cicatrices visibles dans la chronologie des cernes. Comme illustré sur cette image, les cernes de croissance cessent de se former là où des cicatrices se sont formées, ce qui permet d'identifier l'année de la perturbation.

4. OBJECTIFS DE RECHERCHE

L'objectif principal de cette thèse est de **définir le rôle des perturbations fluvioglacielles, en particulier des embâcles de glace, sur la biogéomorphologie des rivières froides**. Alors que les influences des perturbations associées au régime de crues ont été largement explorées en biogéomorphologie fluviale, les rivières où sévissent des processus fluvioglaciels demeurent sous-représentées dans ce cadre théorique. Nous pensons toutefois que ces processus, par leurs effets mécaniques et physiologiques, peuvent influencer les trajectoires d'évolution et l'expression biogéomorphologique des rivières. En combinant deux échelles spatio-temporelles dans deux cours d'eau aux styles fluviaux contrastés, nous tentons d'identifier les patrons associés à la fréquence et à l'amplitude des embâcles de glace. Cette thèse tente ainsi d'apporter un éclairage sur les interactions biogéomorphologiques propres aux milieux froids et de stimuler la formulation d'hypothèses et de nouvelles questions de recherche.

Pour y parvenir, la thèse se décline en quatre objectifs spécifiques :

1. Quantifier la dynamique spatiale et temporelle des changements hydrogéomorphologiques et de la végétation riveraine des deux cours d'eau à l'étude, afin de caractériser les patrons d'ajustement observés en réponse aux évènements d'embâcle de glace sur la période 1963-2016.
2. Établir des relations entre la composition/diversité des communautés végétales riveraines et les paramètres du régime d'embâcle de glace (fréquence et magnitude) en tenant compte des variables hydrogéomorphologiques des corridors fluviaux, afin d'évaluer l'importance des embâcles de glace comme facteur structurant de la végétation.
3. Établir des relations entre les traits/guildes fonctionnels et les paramètres du régime d'embâcle de glace (fréquence et magnitude) en tenant compte des variables hydrogéomorphologiques des corridors fluviaux, afin d'identifier les stratégies de résilience et de résistance associées aux gradients de perturbations liées aux embâcles de glace.
4. Synthétiser les effets possibles des processus fluvioglaciels sur le comportement biogéomorphologique des rivières en régions froides afin d'émettre de nouvelles hypothèses de travail et d'identifier de futurs axes de recherche.

5. APPROCHE MÉTHODOLOGIQUE ET SITES D'ÉTUDE

Cette thèse repose sur une approche interdisciplinaire combinant des connaissances et méthodes issues de la géomorphologie et de l'écologie fonctionnelle. Elle s'ancre dans une analyse multiscalaire pour examiner la réponse des structures et dynamiques biogéomorphologiques à deux niveaux : à l'échelle du corridor fluvial sur une période pluridécennale (analyse diachronique), et à l'échelle locale des communautés riveraines face au régime de perturbations (analyse synchronique). Considérant l'importance des imbrications d'échelles, une telle approche permet de créer des liens et d'approfondir l'interprétation des systèmes à l'étude (Hortobágyi et al., 2017). Alors que les méthodes utilisées dans cette thèse s'appuient sur des techniques géomatiques et statistiques déjà éprouvées dans la littérature, son originalité tient à l'intégration de la fréquence et de l'amplitude des embâcles de glace. À l'aide de données historiques jumelées à des analyses

dendrochronologiques, des régimes de perturbations par embâcle ont été décrits afin d'analyser les patrons de réponse aux deux échelles d'analyse.

À l'échelle du corridor fluvial, des analyses diachroniques ont été réalisées à partir de photographies aériennes afin de quantifier et d'analyser les changements géomorphologiques et du couvert végétal au sein des corridors fluviaux. La description des trajectoires de changement, couplée aux régimes de crue et de glace, nous a ainsi permis d'identifier des patrons spatiaux et temporels associés aux perturbations par embâcle. À l'échelle locale des communautés, des méthodes d'ordinations multivariées contraintes ont été employées pour examiner la composition des communautés végétales de points de vue taxonomique et fonctionnel. L'analyse taxonomique repose sur une collecte de données *in situ*, au cours de laquelle 169 quadrats (variant de 2x2 à 10x10 mètre selon le type de végétation) ont été positionnés dans divers habitats afin de caractériser la végétation ainsi que des paramètres topographiques et sédimentaires. Par l'utilisation de l'analyse de redondance (RDA), nous avons d'abord comparé les communautés entre les deux rivières à l'étude et ensuite analysé leurs variations le long d'un gradient de régimes d'embâcle. L'analyse fonctionnelle repose quant à elle sur des données provenant de base de données en ligne (TRY et TOPIC). Combinées à l'abondance de chaque espèce, les valeurs de traits fonctionnels recueillies ont été moyennées à l'échelle des communautés et des guildes fonctionnelles ont été décrites, lesquelles ont été utilisées comme variables de réponses au travers des mêmes analyses de redondances utilisées pour l'approche taxonomique. Les analyses géomatiques ont été réalisées avec le système d'information géographique ArcGIS Pro (v3.6) et les analyses statistiques ont été effectuées avec le logiciel R (v.4.5.2).

Deux rivières gaspésiennes ont été sélectionnées dans le cadre de cette étude : la Matapédia et la Petite-Cascapédia (Figure 8). Initialement, quinze sites sur chaque rivière ont été sélectionnés pour la collecte *in situ* des données sur les habitats et la collecte d'échantillons ligneux. Dû à des imprévus et des contraintes rencontrées lors des campagnes de terrain, tels que l'inaccessibilité à certains sites ou le manque de temps, le nombre de sites où des données ont pu être récoltées, tant sur l'abondance des espèces que sur les évènements

d'embâcles, a été réduit à sept pour la Matapédia et à six pour la Petite-Cascapédia. Malgré cette réduction, les sites retenus ont permis de couvrir une diversité de tronçons reflétant les caractéristiques propres à chaque rivière.

La rivière Matapédia prend sa source au lac Matapédia et s'écoule en direction sud dans la rivière Restigouche, alors que la Petite-Cascapédia prend sa source dans les montagnes du parc de la Gaspésie et s'écoule, également en direction sud, dans la baie des Chaleurs. Ces deux cours d'eau présentent un caractère sédimentaire similaire avec une composition dominante du lit en galets grossiers sur toute leur longueur. De plus, le domaine bioclimatique (*Sapinière à bouleau jaune/Sapinière à bouleau papier*, MRNF, 2018) est identique dans les deux environnements. Les communautés végétales les plus abondantes sont des peuplements mixtes à dominance de peuplier baumier et des peuplements mixtes à dominance de sapin baumier (MRNF, 2018). Malgré ces similitudes, les dynamiques hydrogéomorphologiques sont contrastées. La rivière Matapédia est une rivière confinée présentant une très faible mobilité en raison d'affleurements rocheux et d'aménagements anthropiques (p. ex. enrochements, voies ferrées et routes). Son bassin-versant couvre 3 792 km², avec des débits journaliers variant de 5 à 940 $m^3 s^{-1}$, un débit annuel moyen de 56 $m^3 s^{-1}$ et un débit plein bord estimé à 414 $m^3 s^{-1}$ (MELCCFP, 2025). La rivière est régulièrement affectée par d'importants embâcles de glace qui ont historiquement causé des dommages majeurs aux infrastructures, ce qui a conduit à une documentation détaillée des évènements et des localisations d'embâcles (Beltaos & Burrell, 2010). Le tronçon d'étude s'étend sur environ 33 km entre la municipalité de Routhierville et la confluence de la rivière Restigouche, avec un indice de confinement moyen d'environ 0,59. À l'inverse, la Petite Cascapédia se caractérise par une forte mobilité latérale, avec des taux de migration latérale élevés et des évènements d'avulsion relativement fréquents au cours des 50 dernières années. Son bassin-versant couvre 1 449 km², avec des débits journaliers variant de 3 à 623 $m^3 s^{-1}$, un débit annuel moyen de 31 $m^3 s^{-1}$ et un débit plein bord estimé à 276 $m^3 s^{-1}$ (MELCCFP, 2025). Bien que la présence d'embâcles soit attestée par des cicatrices de glace sur les arbres riverains, les archives historiques formelles demeurent limitées. Le tronçon d'étude s'étend

sur 16 km dans la portion aval du système fluvial, où l'indice de confinement moyen est de 0,12, ce qui reflète un potentiel plus élevé de migration et d'ajustement latéral.

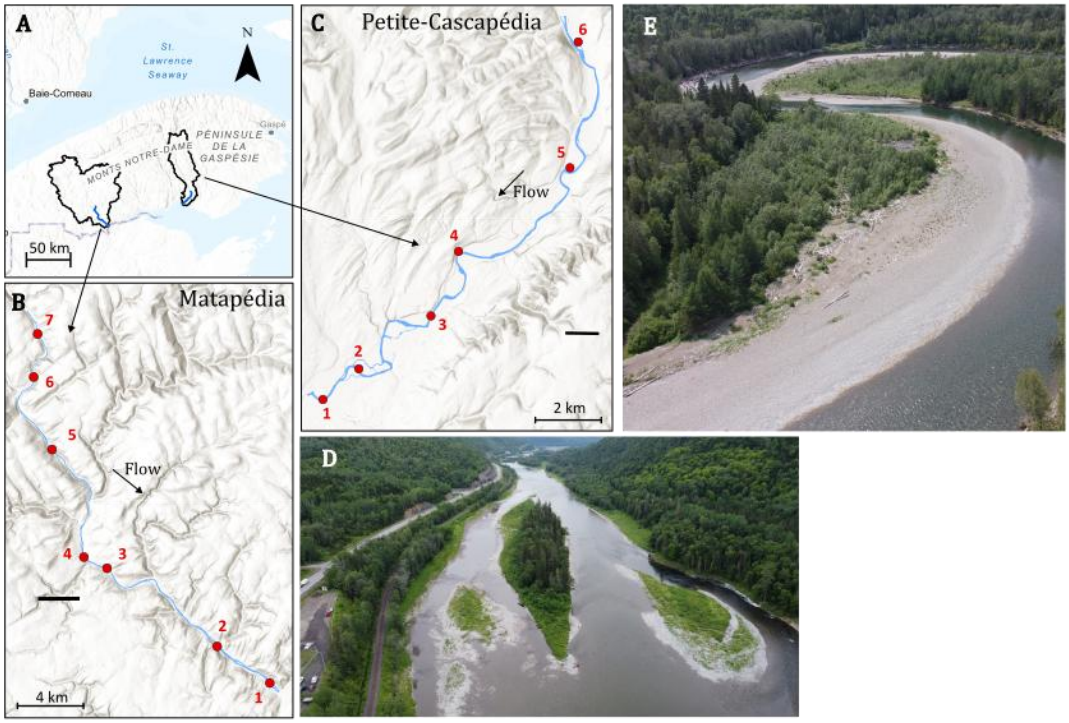


Figure 8 Localisation des segments de rivières sélectionnés dans le cadre de la thèse. Les boîtes représentent la délimitation des bassins-versants (A), les tronçons à l'étude de la rivière Matapédia (B) et de la rivière Petite-Cascapédia (C), ainsi que des photographies aériennes d'un tronçon de la Matapédia (D) et de la Petite-Cascapédia (E). Les points rouges représentent les sites d'échantillonnage où des données d'abondance et d'échantillons ligneux ont pu être recueillies.

Le choix de ces deux cours d'eau offre un cadre de comparaison, permettant d'apporter des nuances quant au rôle des perturbations fluvioglacielles dans les dynamiques biogéomorphologiques. D'une part, leurs similitudes en termes de végétation dominante et de composition sédimentaire permettent une comparaison directe entre les deux systèmes sans influence de gradients environnementaux majeurs (p. ex., précipitations et température). D'autre part, le contraste marqué de leur style fluvial permet d'explorer un gradient hydrogéomorphologique plus large et de comparer la manière dont chaque système réagit aux perturbations liées aux embâcles de glace dans un contexte régional similaire.

6. ORGANISATION DE LA THÈSE

Cette thèse s'articule autour de quatre articles correspondant aux quatre objectifs spécifiques de ce projet. Afin de brosser un portrait le plus complet des perturbations fluvioglacielles sur la biogéomorphologie des deux cours d'eau à l'étude, chaque chapitre se consacre à une échelle spatiale distincte (Figure 9). En plus de la complémentarité des échelles d'analyse, l'étude comparative de deux styles fluviaux permet de mettre en lumière les différences de réponses biogéomorphologiques et d'identifier les facteurs de contrôle propres à chaque style fluvial. Les trois premiers chapitres constituent des articles de recherche originaux axés sur la réponse hydrogéomorphologique et végétale face aux perturbations par embâcles de glace. Le dernier chapitre constitue, quant à lui, une synthèse permettant de formuler des réflexions générales sur le comportement biogéomorphologique des rivières de régions froides soumises à divers processus fluvioglaciels.

Le **Chapitre 1** présente une analyse géomatique de la trajectoire hydrogéomorphologique et végétale des deux cours d'eau à l'étude. Par photo-interprétation, la caractérisation des chenaux et des strates de la végétation a permis de quantifier les changements géomorphologiques et de succession chaque décennie entre 1963 et 2016. En parallèle de la caractérisation du régime d'embâcle de glace à l'échelle des tronçons homogènes, ces analyses mettent en évidence des patrons spatio-temporels récurrents dans les trajectoires directement attribuables aux régimes d'embâcle. Ce chapitre apporte ainsi des éclairages sur les ajustements biogéomorphologiques du corridor fluvial face aux perturbations par embâcle, tout en posant les bases nécessaires à la compréhension du dynamisme des deux systèmes pour les analyses subséquentes.

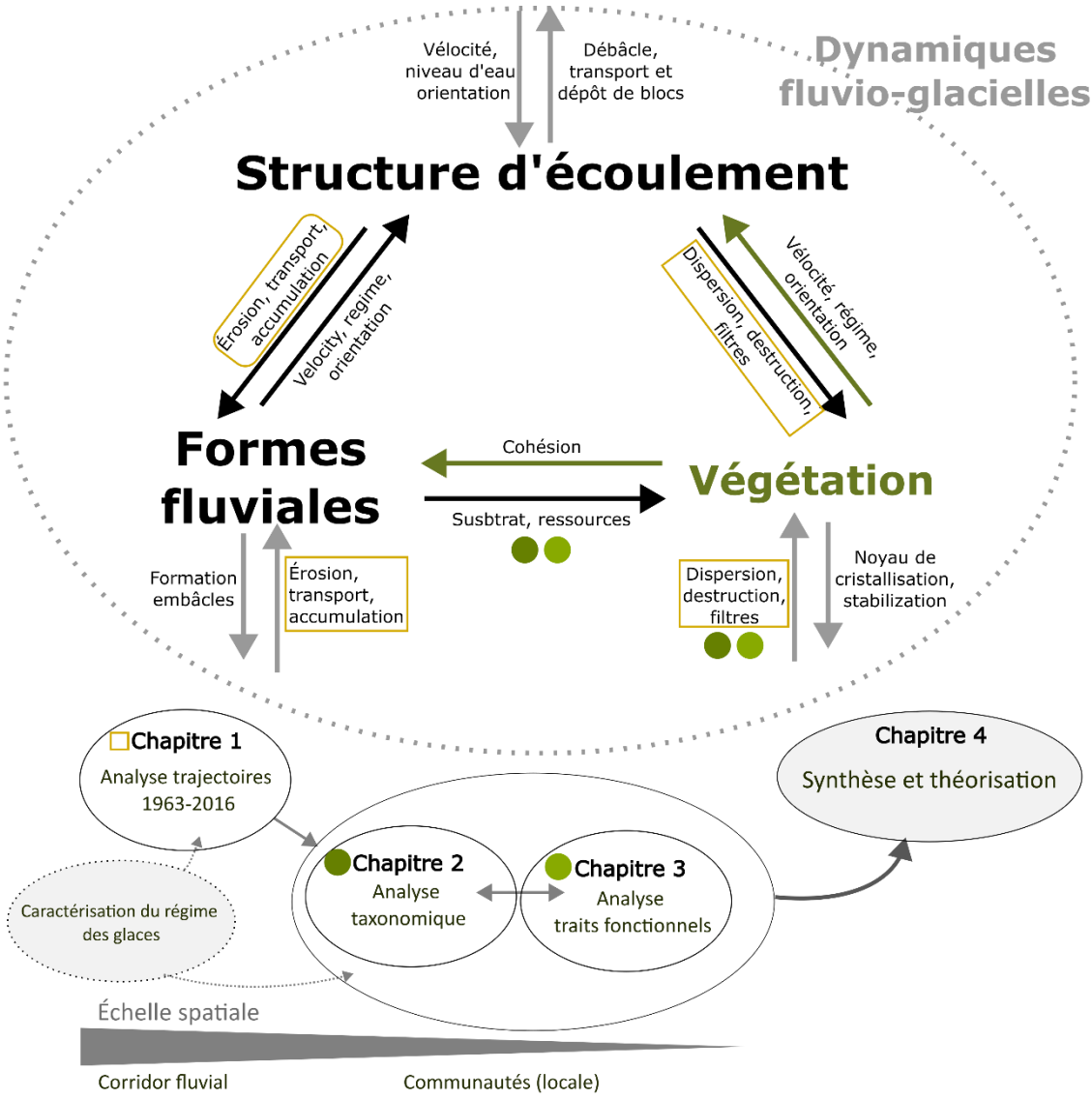


Figure 9 Schéma conceptuel intégrant les dynamiques fluvioglacielles (représentées par l'ellipse grise pointillée et les flèches grises) au cadre théorique de la biogéomorphologie fluviale proposé par Corenblit et al. (2007), accompagné d'un schéma situant l'organisation de la thèse. Les boîtes jaunes indiquent les interactions abordées au chapitre 1, tandis que les pastilles vertes correspondent aux interactions traitées dans les chapitres 2 et 3. Le gradient en bas de la figure illustre l'échelle spatiale propre à chacun de ces chapitres.

Le **Chapitre 2** et le **Chapitre 3** présentent des analyses statistiques pour identifier, à l'échelle de la communauté végétale, les différences de composition taxonomique et fonctionnelle le long d'un gradient de perturbations par embâcle de glace. En intégrant les variables de la végétation aux caractéristiques hydrogéomorphologiques et aux variables fluvioglacielles dans des méthodes d'ordination contraintes, ces analyses ont permis de distinguer les différences de structure des communautés riveraines entre les deux cours d'eau étudiés, le long d'un gradient de fréquence et d'amplitude d'embâcle. Le chapitre 2 présente les réponses taxonomiques fondées sur une collecte de données d'abondance *in situ*, tandis que le chapitre 3 présente les réponses fonctionnelles à partir de bases de données en ligne de traits fonctionnels. Pour l'analyse, les traits fonctionnels ont été moyennés pour chaque communauté, pondérés par l'abondance des espèces, et des guildes fonctionnelles ont été définies. Cette approche méthodologique a permis de déterminer le rôle des embâcles sur la structure fonctionnelle plus générale des communautés et d'identifier les traits fonctionnels clés qui confèrent un avantage adaptatif dans ces environnements. En complément de l'analyse des trajectoires à l'échelle du corridor fluvial (Chapitre 1), ces chapitres permettent ainsi d'approfondir la compréhension des mécanismes écologiques sous-jacents aux réponses observées à plus grande échelle et d'établir des liens entre le régime d'embâcle et la composition des communautés qui participent aux dynamiques biogéomorphologiques.

Finalement, le **Chapitre 4** présente un essai sur la conceptualisation des dynamiques biogéomorphologiques de rivières en régions froides. En intégrant les résultats des trois premiers chapitres à une revue de la littérature sur la biogéomorphologie et les dynamiques fluvioglacielles, ce chapitre explore les interactions biogéomorphologiques possibles à diverses échelles spatio-temporelles, allant du trait fonctionnel au paysage. Il vise à formaliser des hypothèses sur les rétroactions biogéomorphologiques impliquant la glace, la végétation et l'hydrogéomorphologie, afin de générer de nouvelles questions de recherche et d'orienter les futures études. Alors que les trois premiers chapitres se consacrent aux réponses géomorphologiques et écologiques, ce dernier les inscrit dans les cadres théoriques de la biogéomorphologie afin de proposer une généralisation des dynamiques propres aux environnements fluviaux des régions froides.

Ensemble, ces articles offrent une nouvelle perspective sur le rôle fondamental des processus fluvioglaciels dans le fonctionnement des hydrosystèmes, considérés non plus comme de simples facteurs d'érosion ou d'inondation sporadiques, mais comme des agents structurants inhérents à la dynamique biogéomorphologique des cours d'eau. Par une approche davantage inductive, centrée sur diverses échelles spatiales, les observations et analyses présentées dans cette thèse contribuent à affiner notre compréhension du comportement fluvial et des dynamiques végétales riveraines dans les régions froides et ouvrent la voie à de nouvelles hypothèses pour stimuler les recherches futures. Non seulement les résultats qui émanent de cette thèse soutiennent l'importance de développer le domaine de la biogéomorphologie au Québec, ils stimulent aussi la réflexion et la discussion quant à l'importance de considérer les interactions entre l'hydrogéomorphologie, l'écologie végétale et la glace dans un cadre de gestion et de restauration. Plus particulièrement, cette approche a été suggérée comme un outil utile pour le génie végétal (Prugne et al., 2024), et les résultats de cette thèse contribuent à enrichir la réflexion sur cette pratique, notamment en ce qui concerne la réponse des plantes face aux perturbations fluvioglacielles.

CHAPITRE 1
TRAJECTOIRES D'AJUSTEMENTS DES COMMUNAUTES RIVERAINES ET DES CHENAUX EN REGIONS FROIDES : LES EFFETS DES PERTURBATIONS FLUVIOGLACIELLES DANS DEUX COURS D'EAU GASPESIENS

1.1 RESUME EN FRANÇAIS DU DEUXIEME ARTICLE

La biogéomorphologie fluviale s'est révélée efficace pour comprendre l'évolution des rivières, en tenant compte des interactions entre les successions végétales et les ajustements hydrogéomorphologiques. Le rôle des crues en tant que principal facteur du régime de perturbation a été largement étudié, et nos connaissances sur leurs effets sur ces interactions ont considérablement progressé au cours des deux dernières décennies. Cependant, les rivières froides soumises à la dynamique des glaces (p. ex., embâcles et ruptures mécaniques) comme régime de perturbation n'ont pas encore été étudiées dans une perspective biogéomorphologique. Cette étude a examiné les effets à long terme de la dynamique des glaces sur les ajustements du chenal et les trajectoires de la végétation dans deux rivières aux comportements géomorphologiques distincts, l'une confinée (rivière Matapédia) et l'autre mobile (rivière Petite-Cascapédia), au Québec, Canada. En utilisant une analyse dendrochronologique, des données historiques et des photographies aériennes de 1963 à 2016, cette étude s'est consacrée à reconstruire la chronologie des embâcles de glace, à caractériser les régimes de crue et à analyser les changements hydrogéomorphologiques et de la végétation à l'aide d'une approche de photointerprétation. Les principaux résultats de cette étude indiquent que les impacts géomorphologiques des embâcles de glace ne sont pas significatifs à l'échelle décennale ni à l'échelle du tronçon, et qu'ils ne constituent probablement pas les principaux facteurs de contrôle géomorphologique à long terme. Cependant, les résultats montrent que la végétation est particulièrement sensible à ce type de

perturbations. Les tronçons soumis à des embâcles fréquents affichaient des taux élevés de régression et de renouvellement de la végétation, même lors d'années de très faibles crues, ce qui suggère que la dynamique des glaces accroît considérablement le stress de cisaillement sur les communautés végétales. Cette étude met également en évidence la résilience des deux rivières aux perturbations causées par les embâcles de glace, illustrant un rétablissement des formes fluviales et des communautés végétales affectées en moins d'une décennie. Compte tenu des incertitudes liées à l'échelle d'analyse de cette étude, nous proposons que les recherches futures instaurent des suivis à long terme à des échelles spatiales plus fines afin de mieux comprendre les mécanismes sous-jacents aux interactions complexes entre la dynamique des glaces, la végétation et les processus hydrogéomorphologiques.

Dans l'ensemble de cette thèse, ce premier chapitre s'inscrit dans l'analyse à l'échelle du corridor fluvial, où la réponse hydrogéomorphologique et végétale face aux embâcles de glace est examinée sur plusieurs décennies. Il offre un premier aperçu des deux environnements à l'étude, posant les bases sur lesquelles s'appuient les chapitres suivants. Rédigé sous la forme d'un article intitulé « *Vegetation and channel adjustment trajectories in cold regions: the effects of ice disturbances in two Gaspesian rivers* », il a été publié dans la revue internationale *Earth Surfaces and Landforms Processes* en avril 2025.

Contribution des auteurs : Cet article fut corédigé par moi-même, mon directeur, Thomas Buffin-Bélanger, et mes codirecteurs, Maxime Boivin et Dov Corenblit. En tant que premier auteur, j'ai développé l'idée originale, conceptualisé la collecte de données, organisé les campagnes de terrain, effectué l'acquisition et le traitement des images aériennes, procédé à leur analyse, produit les figures et rédigé la première version de l'article. Mon directeur et mes codirecteurs ont participé activement à chaque étape, notamment en apportant des conseils méthodologiques et analytiques, en interprétant les résultats et en révisant l'article. Finalement, la récolte des échantillons ligneux ainsi que leur préparation (sablage et scannage) ont été réalisées avec l'aide d'auxiliaires de recherche du Laboratoire de recherche en Géomorphologie et Dynamique Fluviale (LGDF) de l'UQAR (Zoé Martineu, Samuel Laroche et Alex Desliles)

1.2 VEGETATION AND CHANNEL ADJUSTMENT TRAJECTORIES IN COLD REGIONS: THE EFFECTS OF ICE DISTURBANCES IN TWO GASPESIAN RIVERS

Abstract: Fluvial biogeomorphology has proven to be efficient in understanding the evolution of rivers in terms of vegetation succession and channel adjustment. The role of floods as the primary disturbance regime factor has been widely studied, and our knowledge of their effects on vegetation and channel adjustment has grown significantly in the last two decades. However, cold rivers experiencing ice dynamics (e.g., ice jams and mechanical breakups) as an additional disturbance regime have not yet been studied within a biogeomorphological scope. This study investigated the long-term effects of ice dynamics on channel adjustments and vegetation trajectories in two rivers with different geomorphological behaviours, one laterally confined (Matapédia River) and one mobile (Petite-Cascapédia River), in Quebec, Canada. Using dendrochronological analysis, historical data, and aerial photographs from 1963 to 2016, this study reconstructed ice jam chronologies, characterized flood regimes, and analyzed vegetation and channel changes through a photointerpretation approach. The main findings of this study indicate that geomorphological impacts of mechanical ice breakups are not significant at the decadal and reach scales and that they might not be the primary factors of long-term geomorphological control. However, results have shown that vegetation was more sensitive to ice dynamics. Reaches presenting frequent ice jams depicted high regression rates and turnovers even during years with very low flood, suggesting that ice dynamics significantly increase shear stress on plant patches. This study also highlights the high resiliency of both rivers to ice jam disturbances, with vegetation communities and channel forms recovering within a decade. With the uncertainties following the reach/corridor and decadal scales, future research should focus on long-term monitoring and refined spatial scales to better understand the mechanisms behind the complex interactions among ice dynamics, vegetation, and hydrogeomorphological processes in cold rivers.

1.3 INTRODUCTION

The hydrological regime is a key aspect that has been extensively researched to understand its role on the biogeomorphological dynamics of rivers. Geomorphological-oriented studies have explored how it affects channel patterns and landform adjustments (Chen et al., 2019; Comiti et al., 2009; Dumitriu, 2020; Grams et al., 2020), while ecological-oriented studies have focused on vegetation richness and diversity (Jansson et al., 2005; Ochs et al., 2019; Steinberg et al., 2021), and succession trajectories (Garófano-Gómez et al., 2017; González et al., 2019b; Surian et al., 2015). Frequency, amplitude, timing and duration of floods are known to act as the principal pulse disturbance that maintains the riverscape configuration and modulates the rate and intensity at which feedbacks occur between plants and fluvial processes (Corenblit et al., 2024c).

Many authors have successfully established relationships between hydrological disturbance regimes and biogeomorphological feedbacks within river systems (Bollati et al., 2014; Corenblit et al., 2020b; Garófano-Gómez et al., 2022; Geerling et al., 2006; Lallias-Tacon et al., 2017; Scorpio & Comiti, 2024; Segura-Beltrán & Sanchis-Ibor, 2013; Serlet et al., 2018). Aerial photographs, satellite imagery and LiDAR mosaics have proven to be effective in qualitatively and quantitatively describing biogeomorphological feedbacks in the context of post-disturbance recovery (Mossa et al., 2020), ramp disturbances such as dam construction (Elderd, 2003; Han et al., 2020), biogeomorphological construction of floodplains and in-channel morphologies (Corenblit et al., 2014; Geerling et al., 2006; Gurnell & Bertoldi, 2020), and cyclic dynamics of turnovers and recovery (Surian et al., 2015). Many regions of the world have been studied through this scope, and our knowledge of the biogeomorphological dynamic equilibrium modulated by a range of flood regimes and bioclimatic contexts has significantly increased (Corenblit et al., 2024 a-c). However, rivers in cold-temperate and cold regions experiencing river ice dynamics as an additional disturbance regime have yet to be approached within a biogeomorphological scope.

River ice dynamics have been shown to act as major morphogenic and ecological agents in northern rivers through many processes and ice forms, such as low temperatures, short growing seasons, frequent freeze-thaw cycles, riparian ice, and anchor ice (Chassiot et al., 2020; Engström et al., 2011; Ettema & Kempema, 2012; Karle, 2003; Kimiaghalam et al., 2015; Lind & Nilsson, 2015; Turcotte et al., 2011a; Yumoto et al., 2006). The most impactful and studied processes are linked to mechanical ice breakup (i.e., physical disintegration of river ice due to thermal expansion, water flow, and mechanical forces), which causes an important quantity of ice blocks to be transported downstream. These ice blocks are of various sizes, and their associated shear forces are known to directly erode vegetation and sediment or indirectly reduce bank resistance to flood by exposing root systems (Beltaos & Burrell, 2021; Vandermause et al., 2021); however, the magnitude of these impacts is known to be modulated by the type of vegetation and breakup intensity at a given site (Karle, 2007; Poulin et al., 2019; Rood et al., 2007). Furthermore, ice blocks can accumulate when their movements are restrained by geomorphological or anthropic features, such as meanders or bridges, eventually causing ice jams (Boucher, 2017a; De Munck et al., 2017). Ice jams formation and release have been repeatedly shown to affect channel planforms and vegetation through scouring (Boucher et al., 2009b; Prowse & Culp, 2003; Uunila & Church, 2014), flooding (Kovachis et al., 2017; Livingston et al., 2009; Peters et al., 2016), and avulsions (Boivin et al., 2017; Jones & Schumm, 1999; Kramer & Wohl, 2014; Smith & Pearce, 2002; Smith et al., 1989). Many impacts of mechanical breakups and ice jams have been studied but there is a lack of knowledge on the medium-term to long-term effect on river decennial evolution and its role on the biogeomorphological equilibrium related to changes in channel and riparian vegetation patterns.

The main objective of this study was to analyze the adjustment trajectories of riparian vegetation and channel patterns in the context of mechanical ice breakups at the fluvial corridor and multidecadal scales. Two contrasting rivers were selected for the study, one laterally confined and one unconfined, to assess the differences in response to ice dynamics in contrasting geomorphological behaviours. The specific objectives of this study are to (1) reconstruct the ice jam chronologies from dendrochronological analysis along with historical

data and analyze the flood regime to characterize the disturbance regime in both rivers, (2) analyze both vegetation and channel trajectories from historical series of aerial photographs through photointerpretation to identify patterns related to the effects of disturbance regimes, and (3) assess the possibility of detecting significant impacts of ice dynamics on the biogeomorphological adjustment and recover processes in both study rivers.

1.4 STUDY RIVERS

The Matapédia and the Petite-Cascapédia Rivers located within the Gaspesian Peninsula in Quebec, Canada, were selected for this study (Figure 10A). They share similarities according to their sedimentary structure and vegetation, but they expose significant differences in their mobility. Both rivers are mountainous gravel-bed rivers, located in a cold-temperate/boreal bioclimatic domain in the presence of mixed stands of balsam poplar (*Populus balsamifera* L.), balsam fir (*Abies balsamea* [L.] Mill., 1768), and black spruce (*Picea mariana* [Mill.] BSP., 1888). Both are characterized by a nivo-pluvial flood regime with two periods of high discharges, one caused by snowmelt in the spring and one caused by intense rains in the autumn. The Matapedia River has virtually no mobility due to confinement by roc outcrops and rip raps to protect a road and railway line parallel to the river, while the Petite-Cascapédia River shows high lateral mobility and numerous avulsions. The combination of these similarities and differences offers an opportunity to analyze the impact of ice dynamics on two contrasting rivers.

The Matapédia River originates from Lake Matapédia and flows north-south into the Restigouche River. Its watershed has an area of approximately 3,792 km^2, with daily flow discharge ranging between 5 and 940 m^3s^{-1}, respectively. The mean annual flow is estimated to be approximately 56 m^3s^{-1} and the bankfull discharge is estimated at 414 m^3s^{-1}. The Matapédia River is frequently disturbed by important ice jams that cause major infrastructure damage, which has led to historical documentation about the year and location of different ice jams (Beltaos & Burrell, 2010). The study reach represents the downstream 33 km of the

river from Routhierville municipality to the Matapédia municipality at the confluence with the Restigouche River (Figure 10B), with a confinement index ($\frac{Channel\ width}{Valley\ width}$) around 0.65.

The Petite-Cascapédia River originates in the mountains of Gaspésie Park and flows north-south into Chaleur Bay. Its watershed's area is about 1449 km^2, less than half of Matapedia's watershed area, and its daily flow discharge range between 3 and 623 m^3s^{-1}, with a mean annual discharge of 31 m^3s^{-1}. The Petite-Cascapédia presents evidence of ice jams through ice-scarred trees, but very little historical data are available. It is a highly mobile river with a confinement index ($\frac{Channel\ width}{Valley\ width}$) around 0.12, with high rates of lateral migration and many avulsions that have occurred in recent decades. The study area consists of a section approximately 16 km upstream of the municipality of New Richmond (Figure 10C).

1.5 METHODOLOGY

1.5.1 GIS imagery

This study was based on a diachronic analysis of aerial photographs from 1963 to 2016. Sets of photographs covering both rivers were georeferenced based on a 2016 orthomosaic from the MELCCFP (*Ministère Environnement et Lutte aux Changements Climatiques et Forêts et Parcs*) with anthropic (e.g., roads and buildings) and natural (e.g., cut-off channel and deciduous trees patch) control points the closest to the channel as possible. Table 1 summarizes the scale of the photographs, mean RMSE from the georeferencing process, and mean and maximum discharges at the time the pictures were taken.

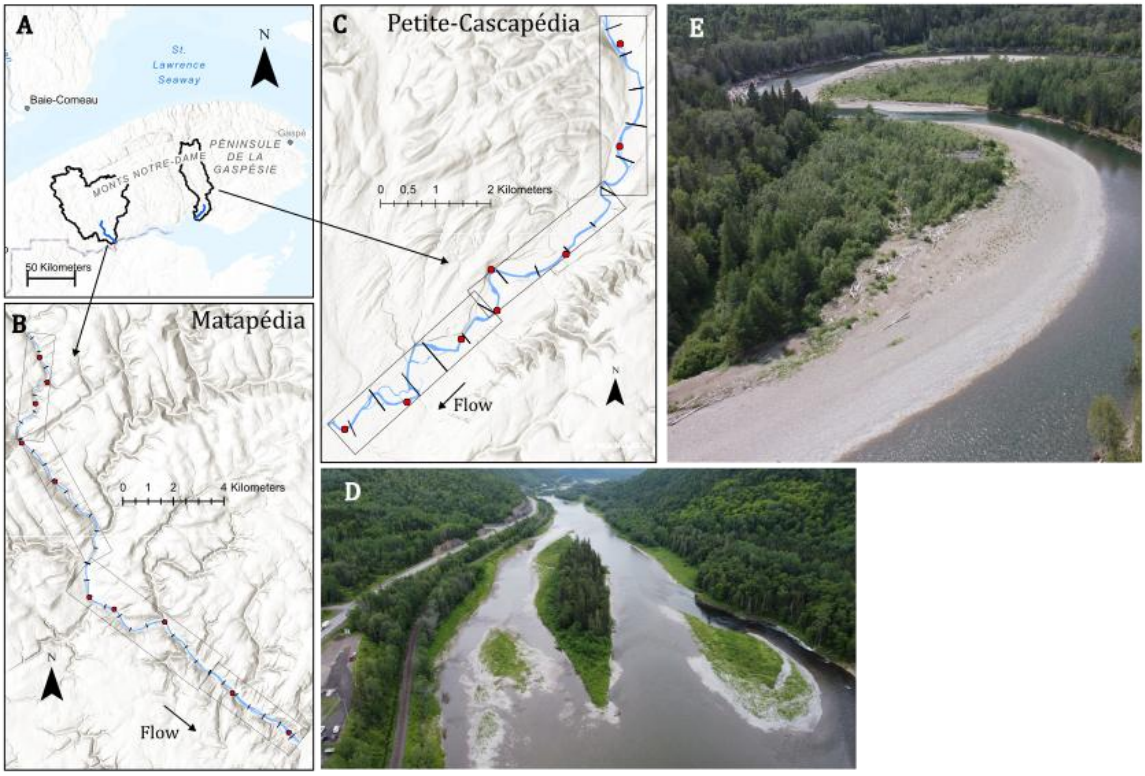


Figure 10 Figure of the study sites. *(A)* Location map of the two watersheds on the Gaspesian Peninsula, Canada. (B and C) Map of the studied river segments (B for Matapédia River and C for Petite-Cascapédia River); blue polygon represents the active channel, black squared outlines the study reaches, black lines along the channel represent the limits of the 1 km subreaches and red points identify the dendrochronological sampling sites. (D and E) Oblique photographs (camera angled between 30 and 60 degrees from vertical) of the Matapédia River (D) and the Petite-Cascapédia River (E).

1.5.2 Characterization of ice jam and flood chronologies

A chronology of ice jam disturbances was constructed using historical and dendrochronological sources. For each river, historical local newspapers from 1950 and later were searched through the BanQ (*Bibliothèque et archives nationales du Québec)* to find articles assessing the presence of impactful ice jams that occurred along the rivers, with which we identified the year of the event and its approximate location. Supplementary information was obtained from the local watershed organization OBVMR (*Organisme de bassin versant Matapédia-Restigouche*) and the MSP (*Ministère de la Sécurité du Québec)*,

who kept records of ice jams for the last couple of decades. Finally, a dendrochronological analysis of ice-scarred trees was performed to identify the location and years of ice jams (Lubiniecki et al., 2024; Taylor, 2009), as well as the height above the bankfull level of the scar. For both rivers, 200 tree cross-sections and wedges were collected from 18 different sites (Figure 10B-C). At each site, which was approximately 200 m long, samples were only taken from trees with visible scars. Samples were brought to the laboratory to be sanded and rings were counted, for which the latest ring was assumed to have grown in 2022. To avoid isolated events that could be misinterpreted as ice jams (e.g., impacts from large woody debris), we (1) took samples at a site only when multiple trees presented scars at the same height, assuring it came from mechanical breakups, and (2) considered ice jam years as confirmed only when a dated year was present in at least two different samples (Figure 11C).

Table 1. Aerial photographs and their characteristics used to analyze planform and vegetation trajectories

Year	Photo type	Scale/Resolution	Mean RMSE (m)	Mean Q (m^3s^{-1})	MaxQ (m^3s^{-1})
Matapédia					
1963	BW photographs	1:15,840	3.92	-	-
1975	BW photographs	1:15,000	2.79	21	67
1985	INF photographs	1:15,000	3.89	28	42
1993	INF photographs	1:15,000	3.48	41	52
2004	INF+BW photographs	1:15,000	2.69	61	406
2016	RGB Orthomosaic	0.3 m	-	25	-
Petite-Cascapédia					
1963	BW photographs	1:15,840	3.04	24	41
1975	BW photographs	1 : 15 000	-	16	22
1986	INF photographs	1:15,000	3.72	11	12
1992	INF photographs	1:15,000	3.72	22	31
2004	BW photographs	1:15,000	3.71	90	207
2016	RGB Orthomosaic	0.3 m	-	14	-

On the Matapédia river, water gauge stations 011507 (48° 5′ 19.00"N, -67° 6′ 2.02"W) and 011509 (48° 6′ 28.40"N, -67° 7′ 48.79"W) were used to analyze flow discharge time

series with available data from 1968 to 2023. On the Petite-Cascapédia River, the water gauge stations were the 010902 (48° 13′ 55.70"N, -65° 43′ 59.02"W), 010903 (48° 13′ 55.99"N, -65° 44′ 2.22"W) and 010901 (corrected data; 48° 11′ 26.89"N, -65° 48′ 38.6"W) with available data from 1963 to 2023. All the data came from the CEHQ (*Centre d'expertise Hydrique du Québec*) database. Flood recurrence intervals of 2, 5, 10, 20, and 50 years were calculated using the Weibull formula for each river and the number of floods was counted for each period. Each flood recurrence interval is annotated as Q_2, Q_5, Q_{10}, Q_{20} and Q_{50}. As the water gauge stations missed some recordings, the following years were discarded: 1993 for the Matapédia River and from 2006 to 2009 for the Petite-Cascapédia River. Important floods that occurred on the Petite-Cascapédia River damaged the water gauge stations and biaised the time series. To fill this gap, we used estimated discharges calculated by Buffin-Belanger et al. (2022) in a report submitted to the MAMH (*Ministère des Affaires Municipales et de l'Habitation,* governement of Quebec).

1.5.3 Analysis of geomorphological trajectories

To analyze the geomorphological adjustments and trajectories of both rivers, the active channel was photointerpreted and digitized for each decade on aerial photographs. The active channel was considered as the wetted part of the channel, including the unvegetated bars within the channel, estimating the area entirely covered by water for 2 years recurrence floods. The valley bottom was also traced to subdivide the study area into 1 km subreaches along the river (Figure 10). From these polygons, we calculated the channel width, lateral migration rate, and erosion-deposition rate at the subreach, reach, and river corridor scales. The channel width was measured as the ratio of the active channel area (A) to the thalweg length (L), by averaging the width of the active channel at a given scale. Lateral migration was measured using the Aggregated Migration rate index (AMI) from Jautzy et al. (2022), and the erosion and deposition areas were measured from the difference between active channel polygons of different years. Each planform change was further standardized to reflect the percentage of either the average channel width (i.e., width and lateral migration) or the average channel area (i.e., erosion and deposition). This standardization is useful because it

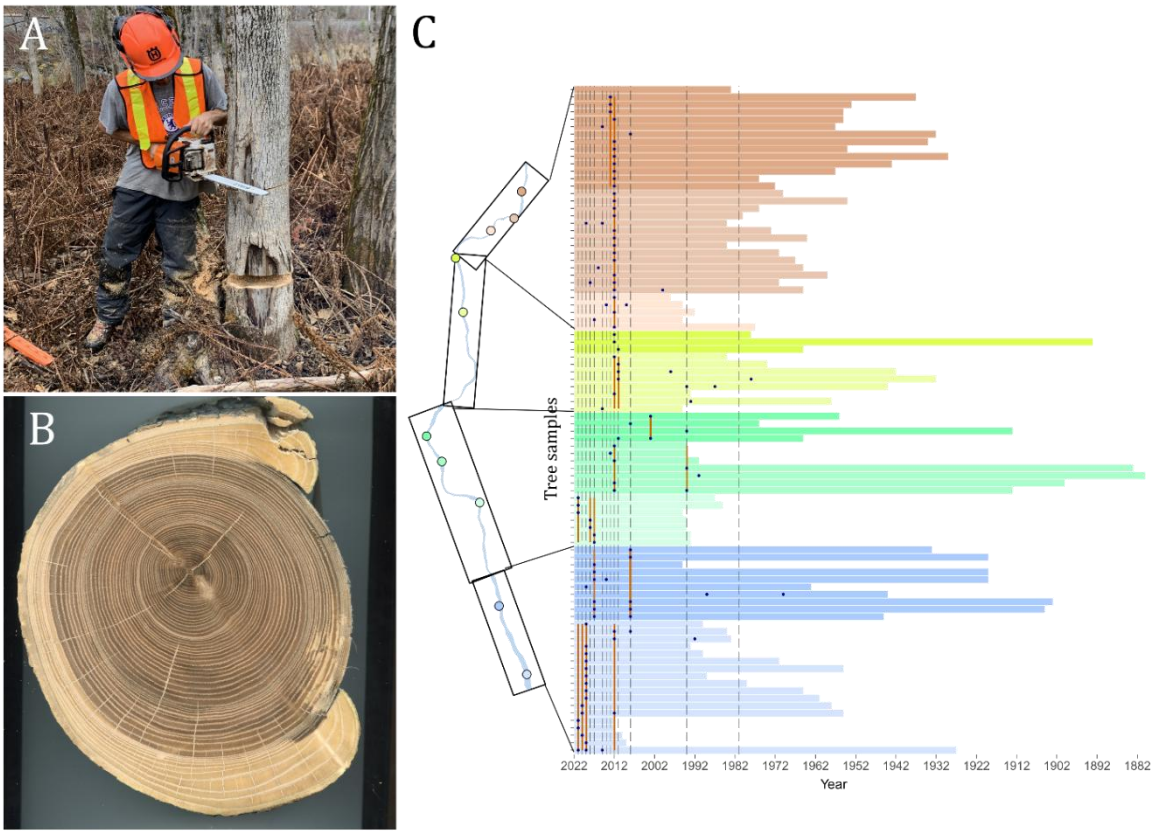


Figure 11 (A) Picture of the sampling method: cutting of wedges at two different identified scars. (B) Example of a scanned tree cross-section with visible ice scars forming a “cat’s paw”. (C) Graph showing results from dendrochronological analysis; tree samples are on the ordinate and dating year on the abscissa; colored bars (colors are according to river reach and tones to sampling sites) show the maximum rings counted for each sample, dark blue points indicate the dated ice jams events, and orange bars indicate the confirmed ice jams with respect to the rule of n>2.

enables the comparison of geomorphological changes across areas of varying sizes, ensuring that changes are proportionally represented relative to the channel dimensions. Finally, the sinuosity index was calculated for each year in each reach by dividing the channel thalweg length by the shortest straight line passing through each reach.

1.5.4 Analysis of vegetation succession processes

Adjustments of vegetation and succession trajectories were assessed based on the photointerpretation of six land cover classes (water bodies, bare surface, sparse vegetation, dense vegetation, forest, and anthropogenic) at the valley bottom to further identify the in-channel effect of ice and the potential ice-flood effect in the floodplain. These classes were chosen based on their generic characteristics. Differences in the angle and quality between the two photographs could make the differentiation between tall herbs and small shrubs quite difficult. By obtaining these large classes, we can reduce the photointerpretation error. Table 2 summarizes the principal descriptions and characteristics of each class and specifies the choices made.

Polygons of classes were compared from year to year at both the reach and sub-reach scales. For each subsequent pair of years (e.g., 1963–1974), the classified vectors were intersected to extract new polygons assessing the trajectory of change from one class to another (e.g., SV to DV). The categories of change were then aggregated into the following groups: progression, regression, and stability. For the analysis of natural changes, changes from and going to the anthropogenic class were excluded from the analysis.

Indices were used to characterize the trajectory of change based on the proportion of the total area that experienced changes. The indices followed the equation $I_{abc} = \frac{Progression - Regression}{Progression + Regression + Stable}$, where *progression* is the area for which the initial phase changed to a later state of development, *regression* is the area for which the initial phase change to a earlier state of development, and *stable* is the area for which the initial phase didn't change. It is important to note that these terms are used here as a simplified framework

Table 2. Description of each surface cover and their visual characteristics used for photointerpretation

Classes	Description	Visual characteristics
Water bodies (WA)	Area covered by water, both in the principal, cut off and abandoned channels.	Dark or blueish tint with homogeneous texture for each emulsion.
Bare surface (BS)	Composed principally of accumulation bars, the bare surface represents every area where no vegetation (0%) is present, representing high hydrological influences.	White or beige, these substrates were identified with light tint and homogeneous fine texture for each emulsion.
Sparse vegetation (SV)	Composed of areas where low vegetation starts to colonize. Principally present on accumulation bars, it represents areas where fluvial processes dominate the vegetation dynamic and where the habitats seem unstable.	Areas where vegetation can cover from 10 to 80% of bare substrate. Vegetation color varied between types of emulsions (red for infrared, dark grey for B&W and green for RGB) but they all showed similar grain effects produced by the contrast between bare substrate and vegetation.
Dense vegetation (DV)	Dense vegetation represents a large range of dense pioneer vegetation that seems stable. It comprises every community of tall and dense herbs, shrubs and young trees communities.	Areas where vegetation cover is of 100%. Depending on the type of communities, it could range from homogeneous and smooth texture to light textured caused by shrubs of low tree canopy.
Forest (FO)	Represents post-pioneer mature forest without distinction between coniferous or deciduous trees.	Highly textured produced from canopy cover. Large shadows near the canopy.
Anthropogenic (ANT)	This class encompasses all surfaces that are affected by human actions, including agricultural land, unnatural pasture and meadows, deforestation, riprap banks and inhabited spaces.	Agriculture, pasture, and meadow lands were identified from a highly homogeneous low vegetation with unnatural patch shape (e.g., perfect rectangle).

to describe the net trajectory of change between two specific years. We acknowledge that the actual dynamics of vegetation in riverine environments are often non-linear and may involve multiple intermediate states; thus, the progression–regression model should be viewed as an integrative summary rather than a detailed account of all temporal pathways. The sign of the

resulting index corresponds to the dominant process (positive for progression or negative for regression), and the value ranging from -1 to 1 represents the importance of the dominant process. The closer the number is to -1 or 1, the more important the proportion of change is, and an index of 0 means that there is no dominant process. This index was applied to the overall change dynamics (I_{all}) and for each cover type (Table 3).

Table 3. Change classes used to calculate the different indices. For example, the progression value for I_{BS} came from the sum of BS-SV (bare surface to sparse vegetation), BS-DV (bare surface to dense vegetation), and BS-FO (bare surface to forest).

Index	Progression	Regression	Stable
$\boldsymbol{I_{BS}}$	BS--> SV BS--> DV BS--> FO	BS--> WA	BS--> BS
$\boldsymbol{I_{SV}}$	SV-->DV SV-->FO	SV-->BS SV-->WA	SV-->SV
$\boldsymbol{I_{DV}}$	DV-->FO	DV-->SV DV-->BS DV-->WA	DV-->DV
$\boldsymbol{I_{FO}}$	-	FO--> DV FO--> SV FO--> BS FO--> WA	FO--> FO
$\boldsymbol{I_{all}}$	All of the above	All of the above	All of the above

1.6 RESULTS

1.6.1 Disturbance regime

Dendrochronological results depict a clear increase in ice-jam frequencies for both the Matapédia and Petite-Cascapédia rivers, where events were recorded almost annually as of 2008 (Figure 12). However, the confirmed ice jam showed high spatial variation. Jams rarely happen on the entire rivers' length. Instead, these events were localized, except for 2012 in the Matapédia River, where ice jams were confirmed at 7 out of 10 sites.

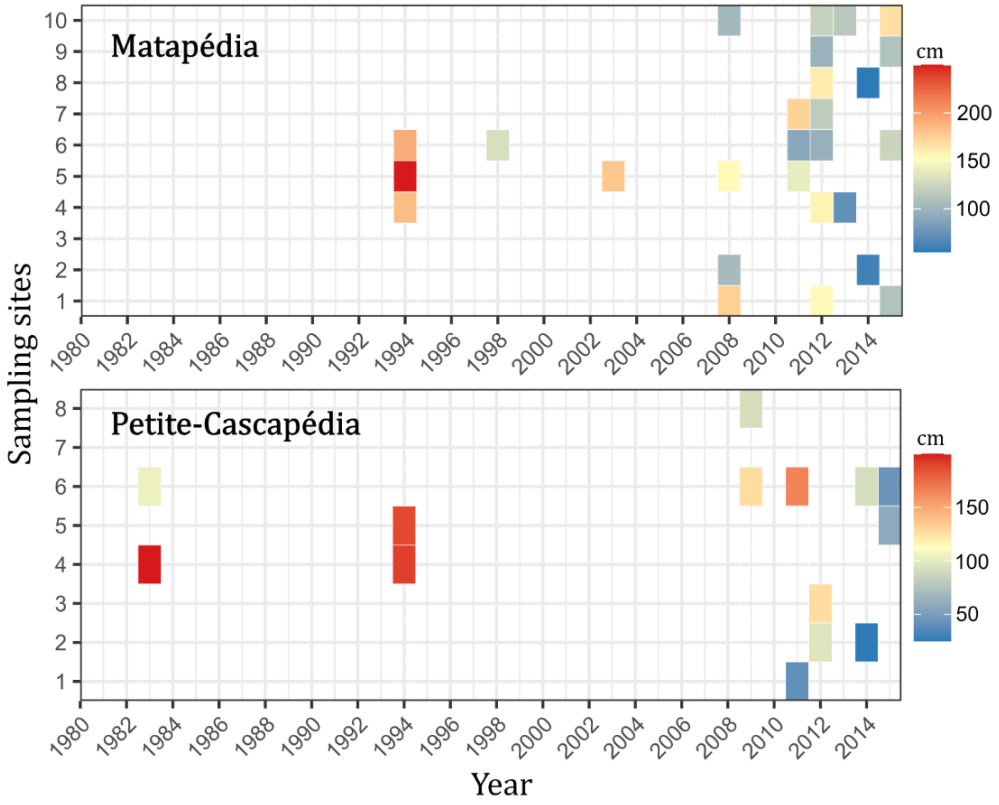


Figure 12. Site locations and dated years of confirmed ice jams. Y-axis represents the site number along the rivers in which the identified ice jam happened, and x-axis represents the dated years. The color gradients correspond to the average height (cm) of the scars above the bankfull level.

While ice jams were more frequent post-2008, the average height of the scars was lower than that of the oldest ice-jam years, suggesting a moderate ice-jam magnitude or potential channel incision, which lowered the riverbed. The highest magnitude jams occurred in 1994, with scars more than 2 m above the bankfull level. In fact, 1994 has been largely documented as it caused severe damages to anthropic structures along the Matapédia River. Additionally, the magnitude of jams seems to be highly variable from site to site when considering the average scar height within a site, ranging from 92 to 181 cm in the Matapédia River and from 40 to 199 cm in the Petite-Cascapédia River (Annexe I, Table 13). With trees being uprooted during high floods or severe mechanical ice breakups, we must consider the possibility of missing years in the dendrochronological analysis. However, historical data of ice jam records helped to confirm five additional years (1974, 1983, 1984, 1995, and 2009) in the Matapédia River and one more year (2015) in the Petite-Cascapédia River (Table 4).

The merged historical and dendrochronologically confirmed ice jam years were overlaid onto the discharge time series to display temporal trends in the magnitude and frequency of floods and jams (Figure 13). In the Matapédia River, the highest daily maximum discharge was 940 m^3s-1 in 1979, which corresponds to a flood recurrence interval of more than 50 years. The period of 1974–1985 was the most flood-impacted period, with Q_{50} (730 m^3s^{-1}) attained once, Q_{10} (550 m^3s^{-1}) attained twice, and Q_5 (496 m^3s^{-1}) attained four times (Annexe I, Table 14). On the other hand, the period of 1993–2004 was the lowest flood-disturbed period with only an Q_2 frequency of 0.4, meaning that more than half of this period was impacted by floods below the bankfull level. The highest recorded discharge on the Petite–Cascapédia River was 700 m^3s^{-1} in 2011, corresponding to a flood recurrence of 50 years. The period of 2004–2016 was the most affected period by flood, with one flood of Q_{50}, two floods of Q_{10} (600 m^3s^{-1}), and six floods of Q_2 (275 m^3s^{-1}). Period of 1986–1992 was the less disturbed in the study, with only three floods that attained the water level of Q_2.

Table 4. Years in which ice jams occurred based on dendrochronological analysis, historical newspapers, watershed organizations databases, and government databases and reaches in which they occurred.

Year	Dendro	Newspaper	OBVMR	MSP	Reach
Matapédia					
1974		x	x		1
1983		x			1
1984		x			1
1994	x	x	x	x	1, 2, 3
1995		x			1, 2
1998	x				3
2003	x				2
2008	x				1, 2, 4
2009		x		x	1
2011	x			x	1, 2, 3
2012	x				1, 2, 3, 4
2013	x				2, 4
2014	x	x	x	x	1, 4
2015	x			x	1, 3, 4
Petite-Cascapédia					
1983	x				2
1994	x			x	2
2009	x				2, 3
2011	x				1, 2
2012	x				1
2014	x				1, 2
2015				x	2

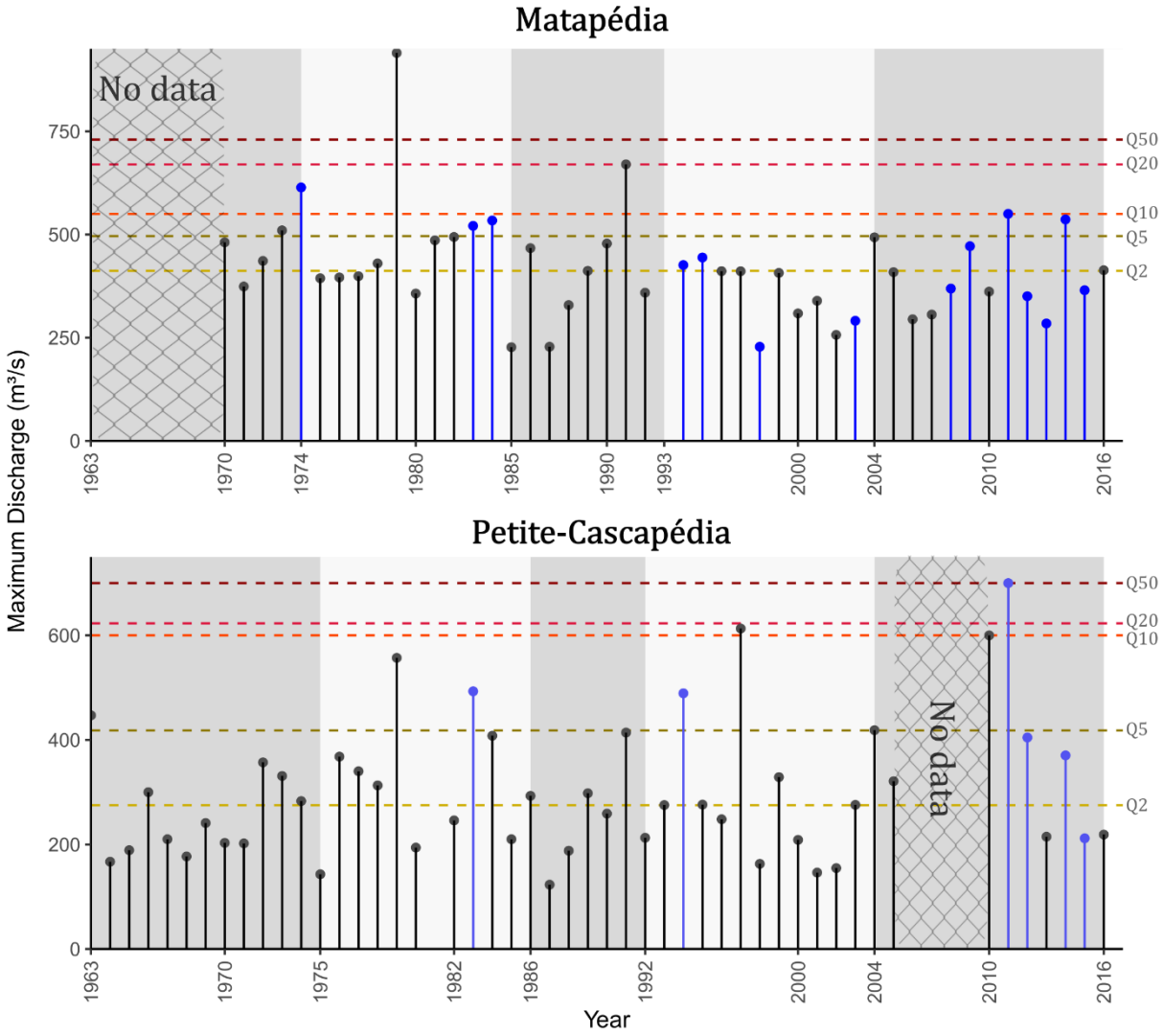


Figure 13. Time series of available maximum discharges for both rivers. The colored horizontal lines represent the discharges associated with flood recurrences Q2, Q5, Q10, Q20, and Q50. The blue points and vertical lines represent the years with known ice jam events. The alternating grey and white colors show the periods between the available series of aerial photographs. The hatched areas identify missing data of flood discharges.

Figure 14 summarizes the trends in the flood discharge and ice jam regimes over time (Figure 5A) and space (Figure 14B). For both rivers, the number of ice jams has increased over time. This trend is particularly evident for the Matapédia River, where the number of ice jams constantly increased from 1963 to 2016, except for the period of 1985–1993 where no ice jams were recorded. However, flood regime trends differed in both rivers. Matapédia depicts a marginal decrease in the mean peak discharge, from approximately 500 m^3s^{-1} to 400 m^3s^{-1}, with the lowest point in the period of 1993–2004. Conversely, the Petite-Cascapédia shows a significant increase with a mean peak discharge passing from 249 m^3s^{-1} to 392 m^3s^{-1}, with the lowest mean peak discharge in the period 1986-1986. While the discharge data can only be used at the river scale, we can spatialize the ice regime along the predefined reaches (Figure 14B). In the Matapédia River, the most downstream reach (1) was where the highest number of ice jams was recorded during the entire study period. In the Petite-Cascapédia River, the highest number of identified ice jams was in the middle reach (2).

1.6.2 Geomorphological planform adjustments

Geomorphological adjustments were assessed through the trajectory of change according to the river width, lateral migration, and erosion/deposition rate. The results were standardized to represent the changes as the proportion (%) of the average river width per subreach for the width change and lateral migration and as the proportion (%) of the average channel area per subreach for the erosion/deposition rate. Table 15 (Annexe I) summarizes the average width and area of the subreaches to scale the results presented in this subsection. Matapédia and Petite-Cascapédia are two contrasting rivers in terms of width and mobility (Figure 15). The downstream section of the Matapédia River (first 18 km) has an average channel width of 110m while the upstream section mean width is approximately 70m. The Petite–Cascapédia channel averages a smaller width of 74m but presented more variability over time (Figure 15B).

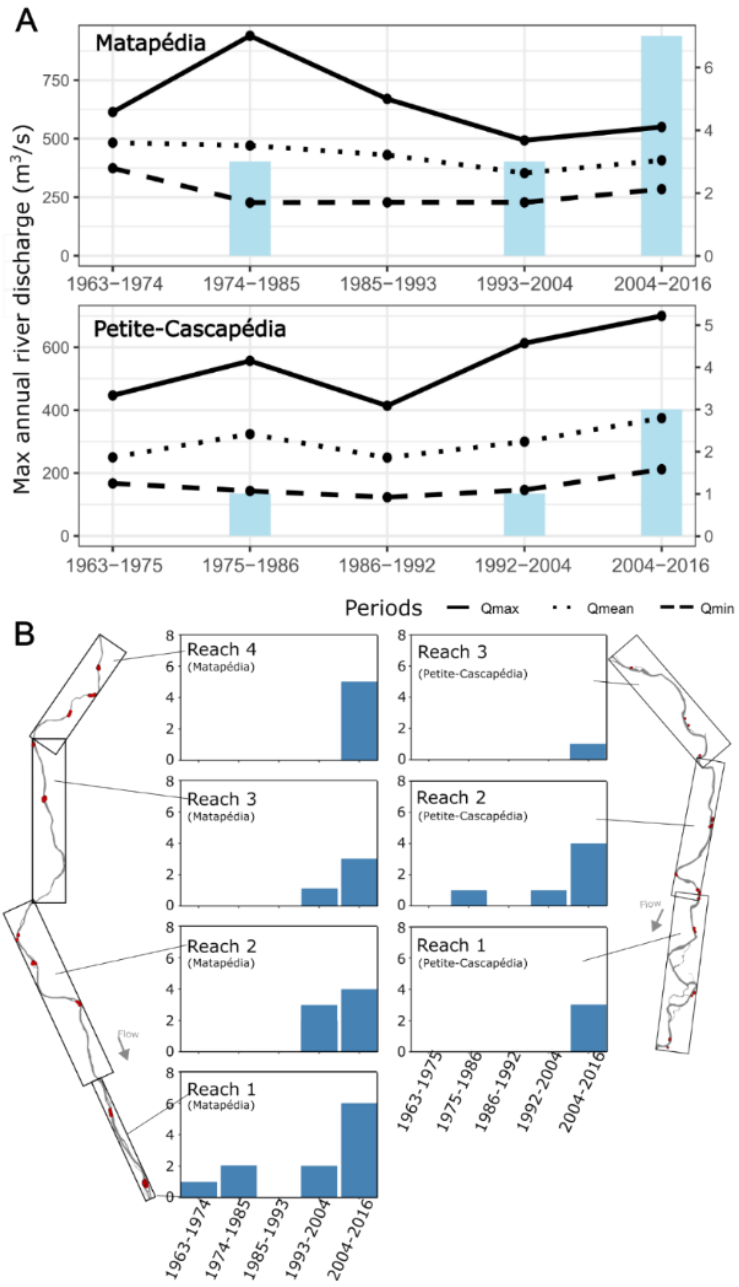


Figure 14. (A) Minimum, maximum, and mean discharges of the maximum discharges during periods covered with aerial photographs, where blue bars show the number of ice jams that occurred during the specified period. (B) Spatiotemporal description of the number of jams throughout the river reaches and periods

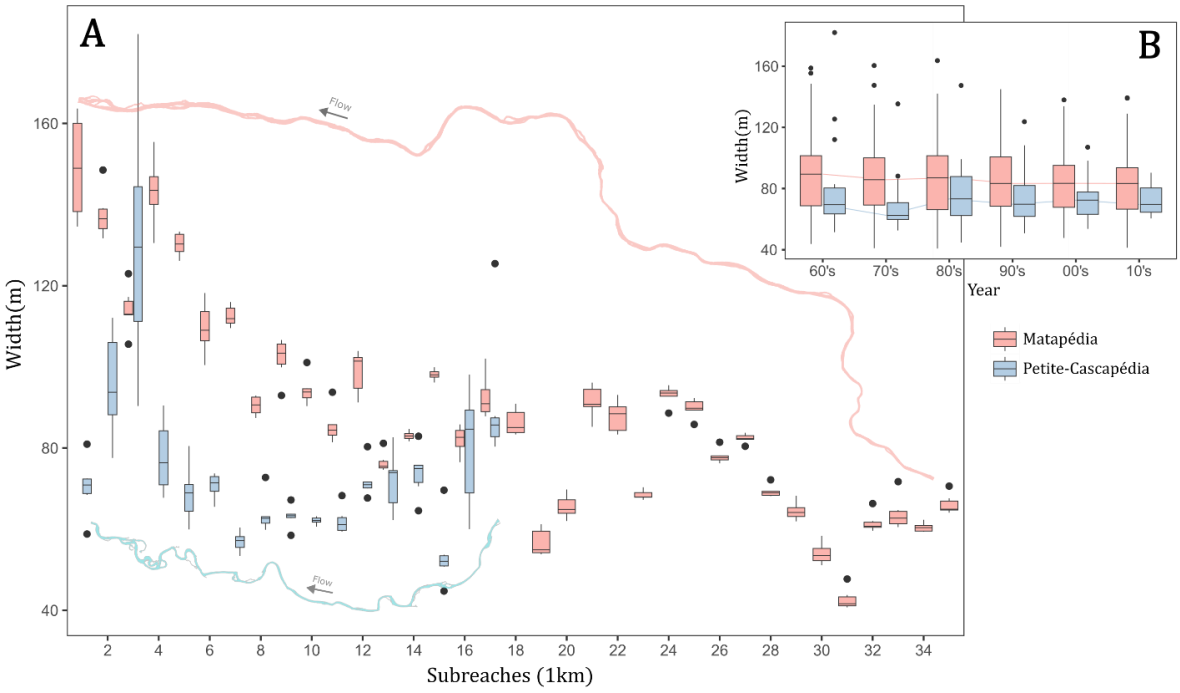


Figure 15. (A) Width variation across subreaches. (B) Width variation across years. Fill colors distinguish Matapédia (red) from Petite-Cascapédia (blue).

In Matapédia, the sinuosity index showed no significant changes over the years, bar surface areas significantly dropped in 2004 but were similar across the other dates, and width variation was marginal, except for reach 1, where the channel was narrowed by 14m in 2004 (Figure 16). Petite-Cascapédia showed higher sinuosity across all reaches and higher bar surface dynamics. The highest sinuosity variation occurred in reach 1, with a maximum of 1.42 attained in 2004 before dropping back to 1.37, while the bar surface areas presented high cyclical dynamics from year to year. While widths were smaller in the Petite-Cascapédia, their variations were more pronounced, especially in reach one, where it varied between 94 and 78 m.

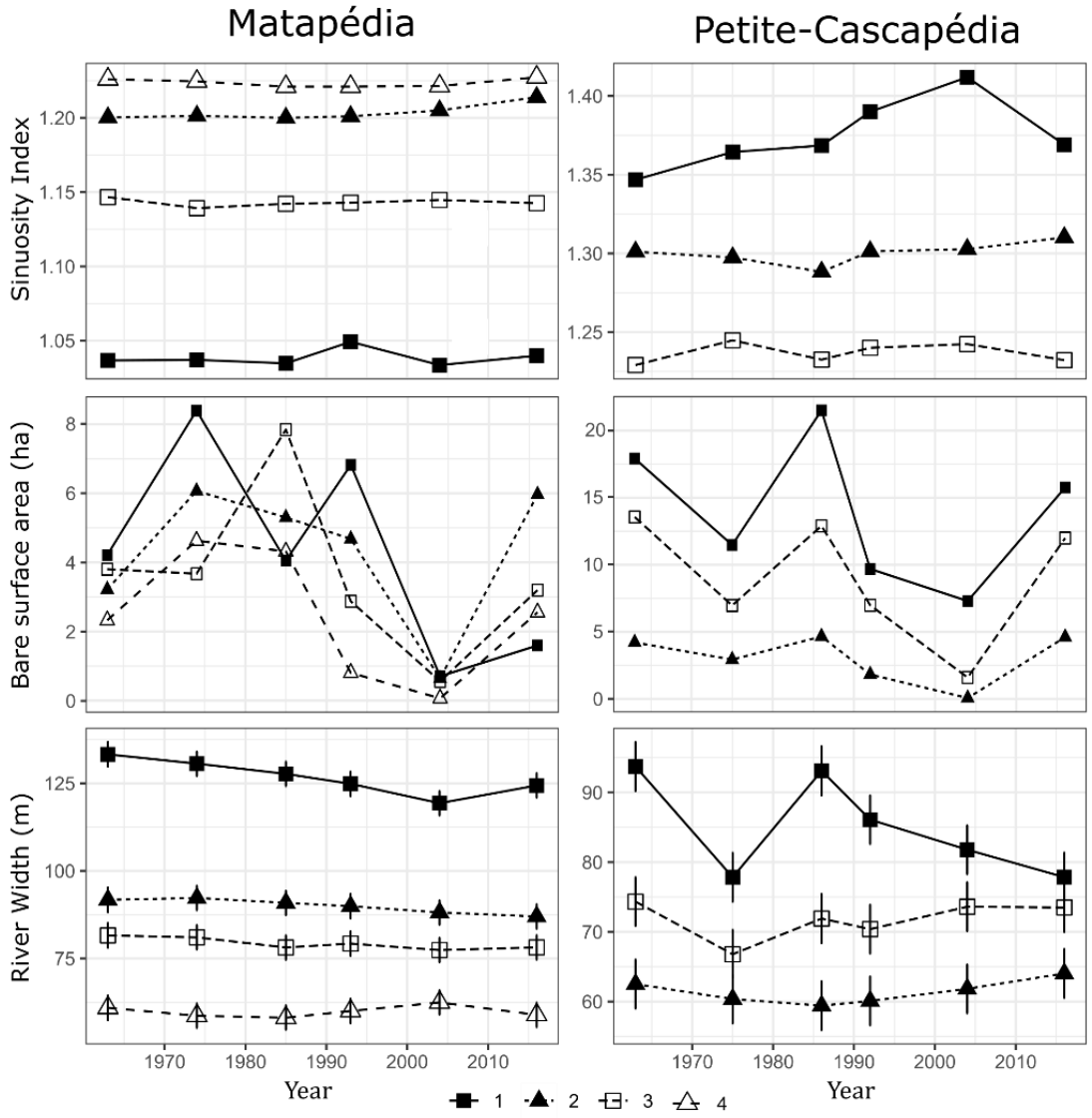


Figure 16. Variation in sinuosity index, bare surface area, and river width over time and selected reaches. Types of points and lines represent reaches from 1 to 4 for the Matapédia and 1 to 3 for the Petite-Cascapédia

The average width change rate in the Matapédia River ranged between 0.1%/yr and 0.2%/yr for the narrowing and enlargement processes (Figure 17A). Although most width changes in Matapédia were insignificant, some trends were evident. Narrowing dominated except for 1985–1993, where enlargement was prevalent. The rate of change varied across the sub-reaches. The highest narrowing rate was 2.4%/yr at subreach 1 (1985–1993), which

narrowed by almost 30 m. While reach 4 was measured as a high enlargement rate in 1993–2004 (1.5%/yr) and a high narrowing rate in 2004–2016 (1.5%/yr), these are the biases from the high flood of 400 m^3s^{-1} that occurred while the 2004 photograph was taken. The Petite-Cascapédia River showed higher rates of change with alternating narrowing and enlargement (Figure 17A). The highest narrowing rates were 0.9%/yr and 0.5%/yr during the period of 1963–1975 and 1986–1992, respectively. These were interspersed with increasing rates of 0.7 and 0.1%/yr during 1975–1986 and 1992–2004.

The inter-reach average mean width change rates showed temporal trends (Figure 17B). In Matapédia, each reach responded differently to the survey. Reach 3 and 4 had the highest enlargement rates (0.18 and 0.4%/yr) in 1985–1993. Reach 1 generally narrowed from 1963 to 2004, and then enlarged from 2004 to 2016. Reach 2 remained stable with minimal narrowing (0.15%/yr). The changes in the Matapédia River are marginal compared to those of the Petite-Cascapédia River, which show significant changes between -1.5 to 1.5%/yr. Reaches 1 and 3 alternated between narrowing and enlargement from 1963 to 1992, and then stabilized until 2016.

The Matapédia River shows very little lateral migration that is, furthermore, very constant throughout all the period, with an average aggregated migration rate index (AMI) varying between 0.2 and 0.4 (Figure 18A). However, some specific subreaches are relatively high compared with the rest of the river, attaining an AMI of 1, mostly in the middle reaches. In contrast, the Petite-Cascapédia River depicts a much higher average AMI index throughout the years, varying from 0.7 to 2.0, with its highest during the period 1986–1992. During this period, reach 7 attained an AMI of 6.8%/yr, which is equivalent to a migration rate of 3.8m/yr.

The analysis of the AMI at the reach scale helps define the general migration dynamics across homogeneous reaches (Figure 18B). Compared to the Petite-Cascapédia, reaches in the Matapédia are only marginally mobile, with an average AMI index varying between 0.1 and 0.6%/yr. Trajectories of change across reaches followed the same trends, where the peak migration was found in the period of 1985–1993, except for reach 2, where it was in 1963–

1974 with a constant decrease in the following years. As for the Petite-Cascapédia, the highest migration rate was identified in the first reach during the period of 1963–1975 with a constant decrease in the following periods. Reach 1 and 3 followed the same kind of trajectories but reach 2 was at its highest in the period of 1986–1992. Across every reach, the lowest migration rate occurred during 1963–1974.

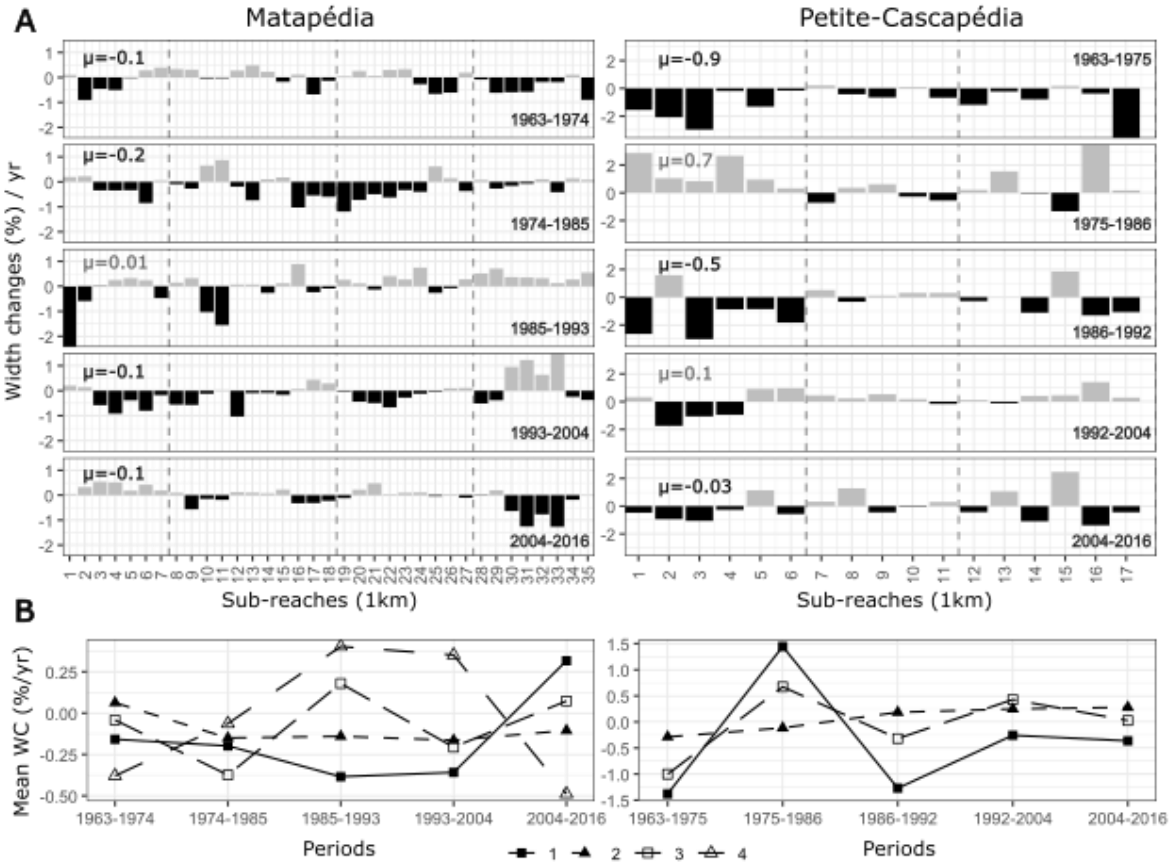


Figure 17 (A) Variation in width across periods and subreaches for both rivers. The colors of the bar distinguish narrowing (black) from widening (grey) processes. The increase/decrease in width was standardized by the mean width of each subreach and divided by the number of years in a given period. Vertical dotted lines mark the limits of each selected reach. (B) Mean changes in the standardized width change rate across the selected reaches. The line and point types distinguish the reaches.

In the Matapédia River, the average rate of eroded or newly formed areas (m^2/yr) was balanced, suggesting sediment equilibrium (Figure 19A). Slightly higher deposition occurred during 1963–1985 and 1993–2004. The period 1985–1993 saw more erosion than deposition but also the highest deposition rate (2.6%/yr), representing nearly 2 ha of sediment. In the Petite-Cascapédia River, the differences between erosion and deposition were more pronounced. Periods 1963–1975 and 1986–1992 were dominated by deposition, with the highest rate (2.1%/yr) in the latter. These periods were interspersed with a strong erosion period (1975–1986) averaging 1.7%/yr erosion compared to 1.1%/yr deposition, mainly due to downstream avulsion and upstream enlargement.

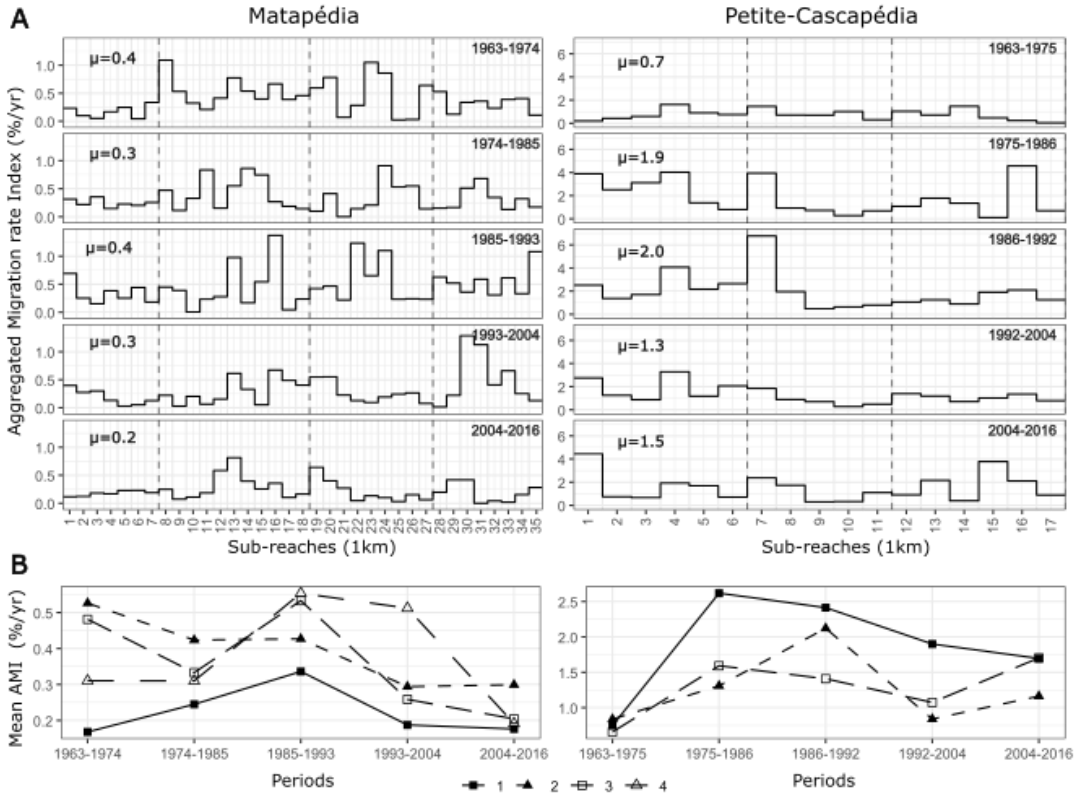


Figure 18 (A) Aggregated migration rate index (AMI) across periods and subreaches for both rivers. The AMI value was standardized using the mean width of each subreach. Vertical dotted lines mark the limits of each selected reach. (B) Mean changes in AMI across the selected reaches. The line and point types distinguish the reaches.

The differences in the reach-averaged deposition and erosion rates highlight significant events (Figure 19B). In the Matapédia River, the most significant erosion and deposition rates occurred in reach 1, where the deposition rate was dominant and increased until 2004, before abruptly changing to an erosion-dominated process between 2004 and 2016. In the Petite-Cascapédia, reach 1 shows strong variation with peaks in 1963–1975 and 1986–1992, and a low in 1975–1986. Reaches 2 and 3, although dynamic, show balanced trends with differences varying between -0.5 and 0.5%/yr.

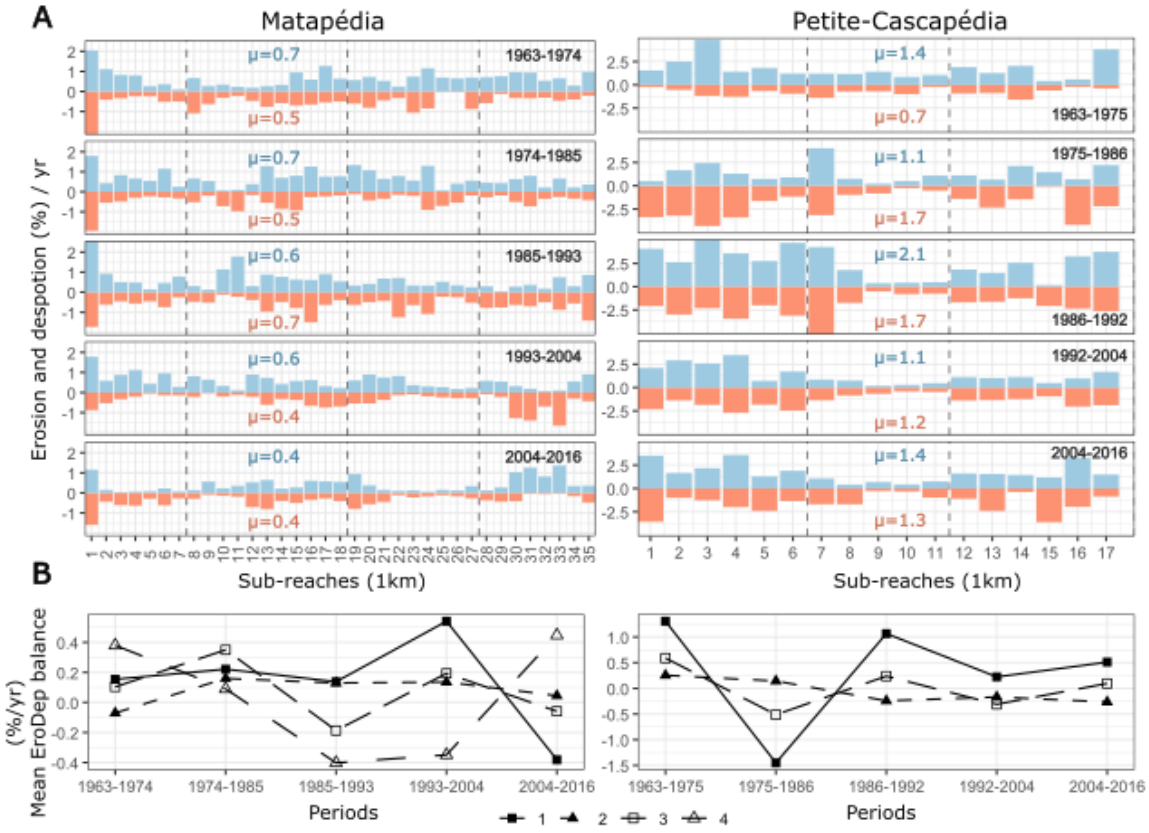


Figure 19 (A) Erosion and deposition rates across periods and subreaches for both rivers. The colors of the bar distinguish erosion (orange) from deposition (blue) processes. The erosion-deposition areas were standardized by the mean area of each subreach and divided by the number of years in each period. Vertical dotted lines mark the limits of each selected reach. (B) Mean balance of erosion-deposition rate (difference between deposition and erosion) across selected reaches. The line and point types distinguish the reaches.

1.6.3 Vegetation trajectory of change

The qualitative interpretation of land cover change shows that most of the changes occurred within the active channels (Figure 20). The main difference in terms of vegetation distribution across both rivers is the proportion of floodplains within the valley bottom, where the Petite-Cascapédia River has a much larger floodplain area, and thus an important forest proportion (Figure 21). Over the 60 years covered in this study, the overall trajectory of changes tended to increase vegetation cover and channel stabilization over both rivers.

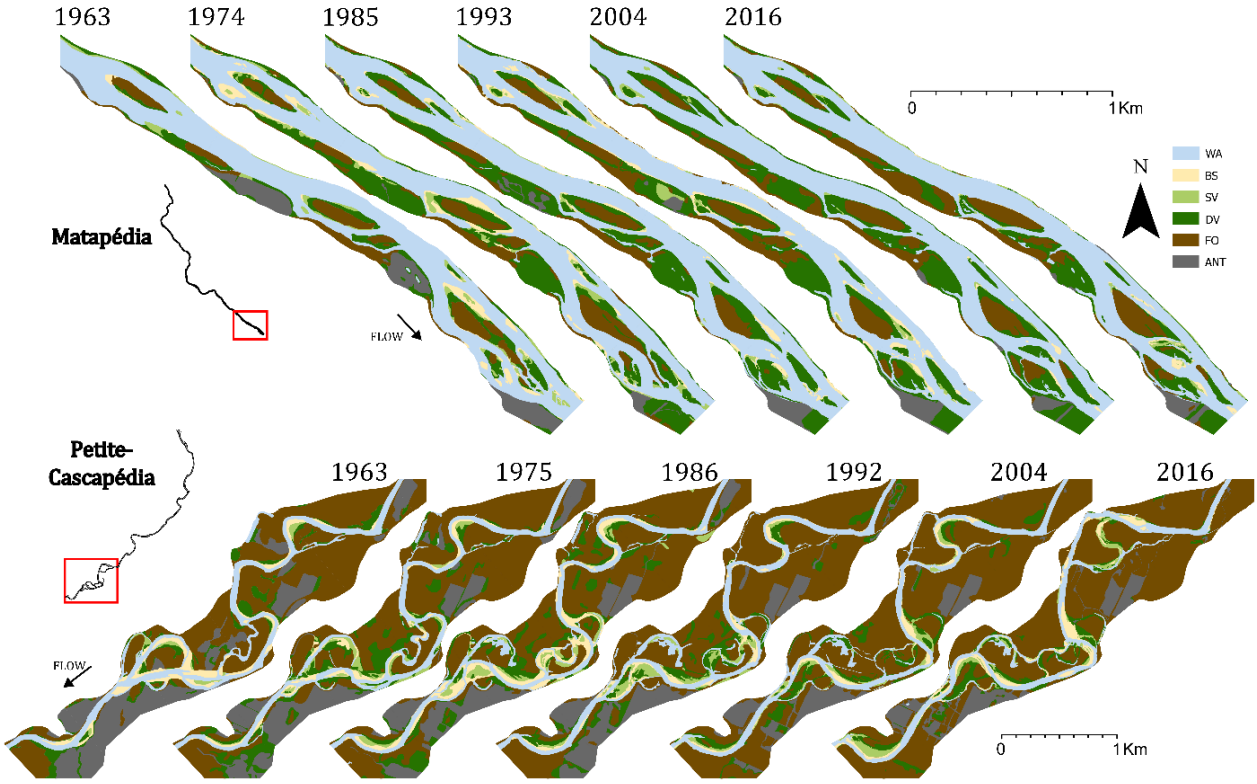


Figure 20 Classification map resulting from the photo-interpretation of the different land covers (WA: Water, BS: Bare surface, SV: Sparse vegetation, DV: Dense vegetation, FO: Forest, ANT: Anthropic). These are samples of the most downstream and dynamic reaches of both rivers

The proportion of the different land covers across the active floodplain clearly shows important differences between the Matapédia and the Petite-Cascapédia, where water cover is largely dominant in the former and forest is most abundant in the latter, mostly because of the vast floodplains of the Petite-Cascapédia River (Figure 21A). In both rivers, a general decrease in anthropic area was combined with a significant increase in forest cover, mainly due to the abandonment of agricultural lands. Matapedia's forest cover ranged from 87 to 117 hectares, while the forest cover of the Petite-Cascapédia River ranged from 371 to 443 hectares (Annexe I, Table 16). These were the most noticeable general changes observed. The bare surface, sparse vegetation, and dense vegetation classes varied throughout the years, depicting a dynamic of progression and regression.

The rate of gain and loss of cover varied significantly throughout the different periods for both rivers (Figure 21B). In the Matapédia River, important gains in forest and dense vegetation were observed during 1963–1974, which can be explained by the abandonment of agricultural lands that underwent colonization by natural plant communities. In the other periods, the gains and losses of all land-cover classes were strongly variable. However, one interesting fact is the important increase in dense vegetation combined with significant loss in bare surfaces and sparse vegetation in 1993–2004, suggesting the development of stable vegetated landforms through progression dynamics. Furthermore, this period was followed by a significant decrease in dense vegetation and an important increase in bare surfaces, depicting a period (2004–2016) of possible regression in many areas. In the Petite-Cascapédia River, important gains in forest cover were observed from 1963 to 2004. The period of 1986–1992 was the most active in terms of gain/loss, with large areas of bare and dense vegetated surface losses and significant gain in forest, suggesting a reconfiguration of the landscape mosaic. Other periods depicted sensitively similar changes according to the proportion of gain and loss of the different cover types. However, the period of 2004–2016 stands out with a significant gain in bare surface.

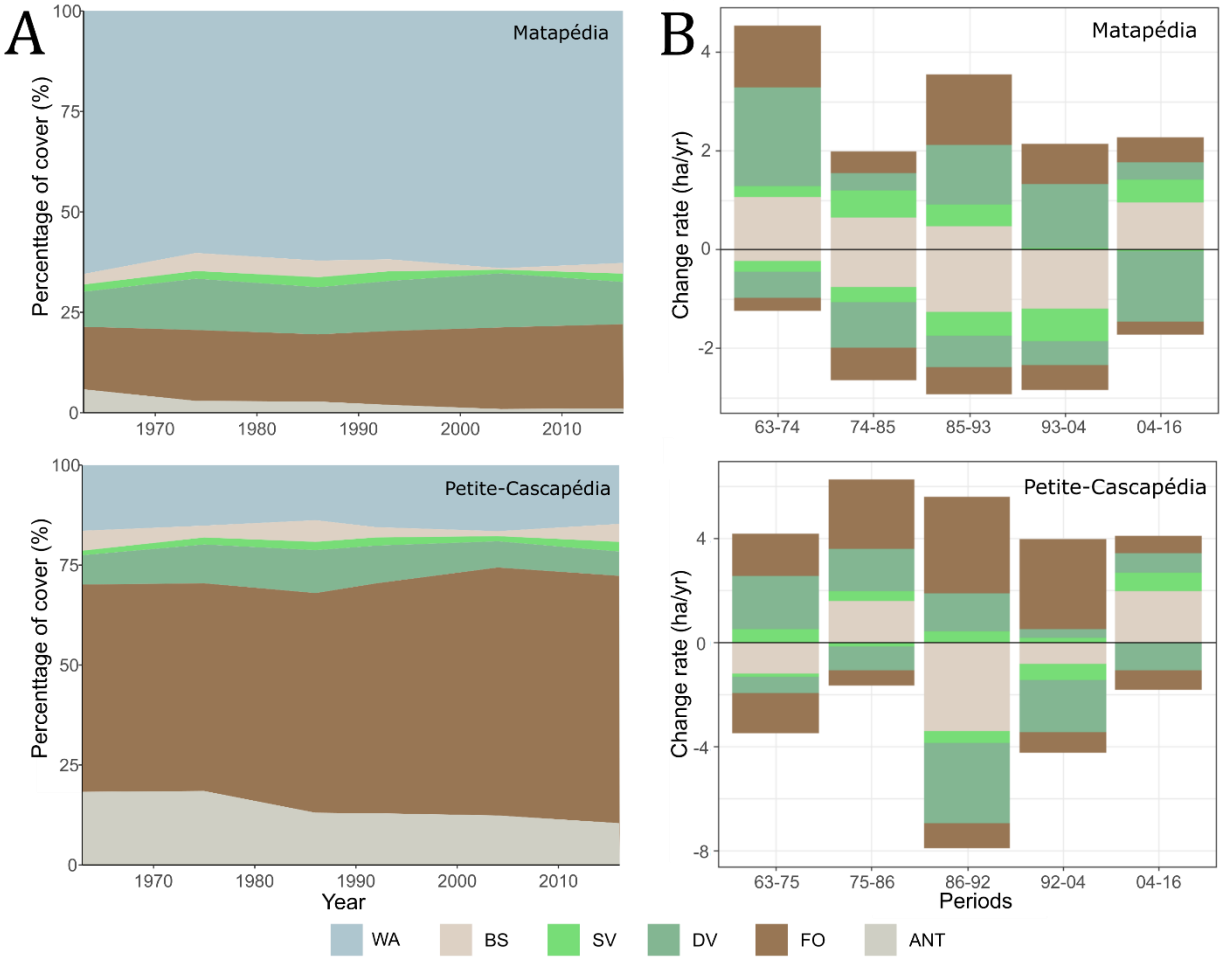


Figure 21 (A) Proportions of surface cover classes for each year. (B) Change rate of cover classes over time showing gain and loss between periods. Negative values represent loss surfaces and positive values represent gained surfaces between two years.

The pathway of succession progression and regression for each type of vegetation class highlights the important differences between the two corridors (Figure 22). Noticeable differences were observed within the bare surface and the dense vegetation trajectory of succession. Regression areas of the bare surface (BS to WA) were much higher in the Matapédia River than in the Petite-Cascapédia River, with the I_{BS} being negative or neutral. In the Petite-Cascapédia River, most of the bar surface areas progressed to a later successional state or stayed as is, where progression sometimes reached 40% of the total change, as in the period 1963–1975. Sparse vegetation progressed dominantly throughout all

periods, with an important peak between the 90's and the 00's. This result shows the important development of dense vegetation patches throughout pioneer landforms and floodplains of both rivers during the entire study period. The main difference between the two rivers relies on dense vegetation dynamics, where the Matapédia River is mainly characterized by stability and the Petite-Cascapédia River by progression.

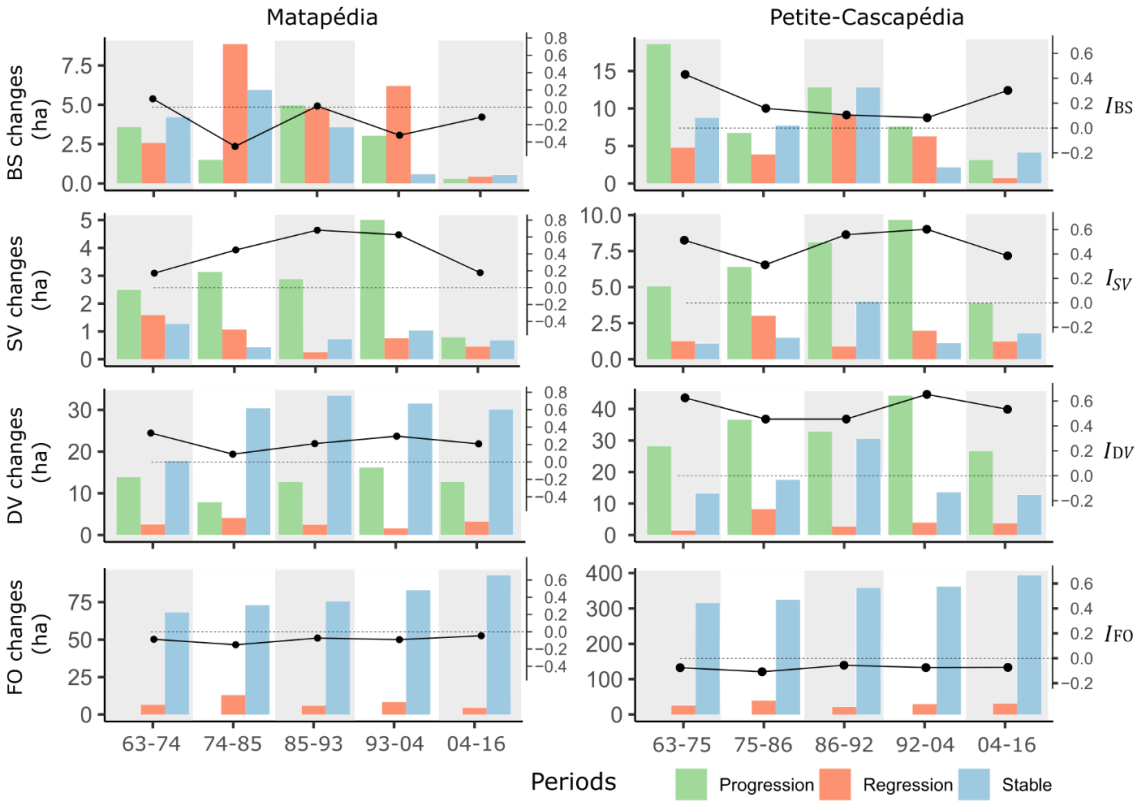


Figure 22 Trajectory of succession processes for each class of surface cover during different periods. The colored bars represent the area of progression (green), regression (red), and stability (blue). The progression area represents a change from the initial cover to a later successional state, regressing the area that passed from the initial cover to an earlier successional state and the stability of the area that depicted no change. The line graph on the secondary axis shows the trajectory of the indices measuring the dominant process and its importance compared to the total area of change.

At the reach scale, the general succession pathways (every class combined) show a clear progression-dominant process in most of the reaches and periods (Figure 23). While the

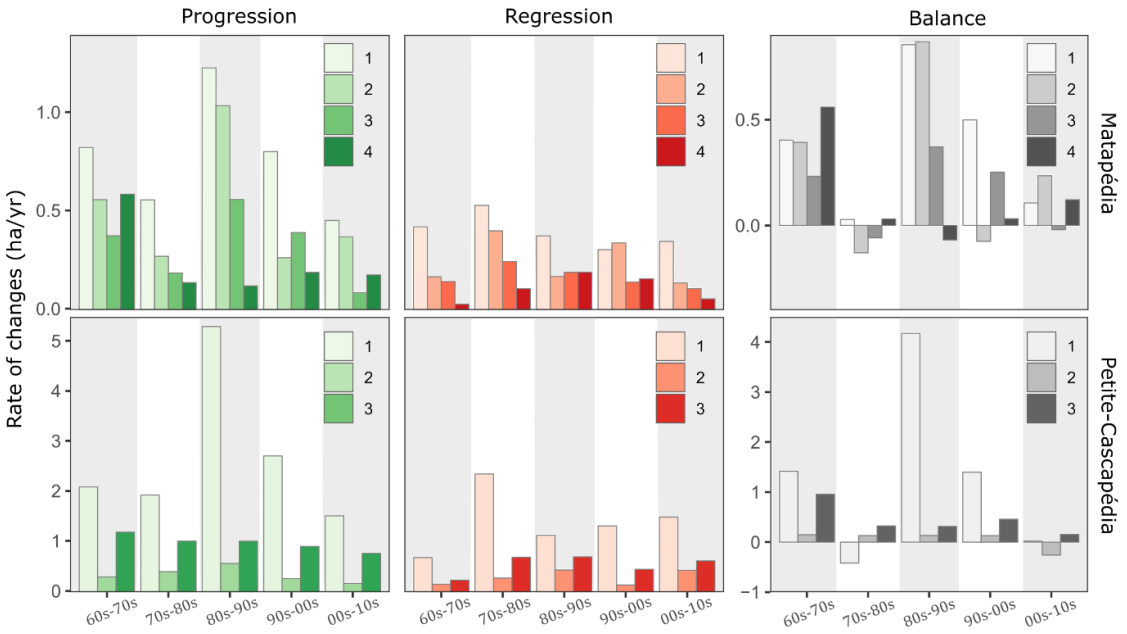


Figure 23 Rate of change in succession path through specific reaches and periods. Progression changes depict all progression pathways, similar to regression. Balance is the difference between the progression and regression rates. The colors of the bars represent the path of succession (green for progression; red for regression; grey for balance), and the color gradient represents the reach number (1 to 4: light to dark).

Petite-Cacapédia shows a balance of progression-dominant processes in all periods and all reaches (except for the period 1985–1993), the Matapédia show an alternating process of dominance between the periods. The periods of highest progression were 1963–1974 and 1985–1993 where a significant difference between progression and regression was shown, particularly for reaches 1 and 2. The periods 1974–1985 and 1993–2004 had more marginal areas of balanced succession, and some even tended to be a regression-dominant process. In the Petite-Cascapédia River, almost every reach during every period shows a progression-dominant dynamic, where Reach 1 (1986–1992) stands out according to the rate of changes. The only regression-dominated dynamics happened in Reach 1 during the period of 1975–1986 and in Reach 2 during the period of 2004–2016. Yet, the intensity of those regression dynamics remains very low when compared to the other rates of changes.

The overall index of succession (I_{all}) was calculated for every subreach to analyze the trajectories across spatial and temporal scales (Figure 24A). This representation helps to identify specific areas of progression- or regression-dominant processes, and the magnitude of these changes compared to the total area of change. When averaged across the entire rivers, indices balance out and depict a very small proportion of change, except for some exceptions such as the period 1963–1974 in the Matapédia River with an index of 0.2. However, the peaks of progression and succession can easily be identified through different subreaches and periods. Overall, the Matapédia River shows much higher variation along its rivercourse than the Petite-Cascapédia River. The period 1963–1974 significantly stands out compared to the other periods, with an average I_{all} stating that 20% of all changes were progression changes. On the other side, the period 1974–1985 shows the only negative I_{all}.

Upscaling to the reach scale helps to identify trends of I_{all} (Figure 24B). In the Matapédia River, reaches 1 and 2 are closely correlated according to their trajectories, with alternating periods of progression-dominance and regression-dominance. Reach 3 only varies between 0.08 and 0.11, showing very little dominant process. Regression peaks were found in reaches 2 and 4, at the period–1974–1985 and 1985–1993, respectively. In the Petite-Cascapédia River, reach 2 and 3 follow the same trajectory, but reach 1 stands out with two peaks of progression-dominance reaching an I_{all} of 0.15 accounting for 15% of total change equivalent to progression. The average reach index was positive along every reach of the PC, suggesting that progression is constantly the dominant area-related process.

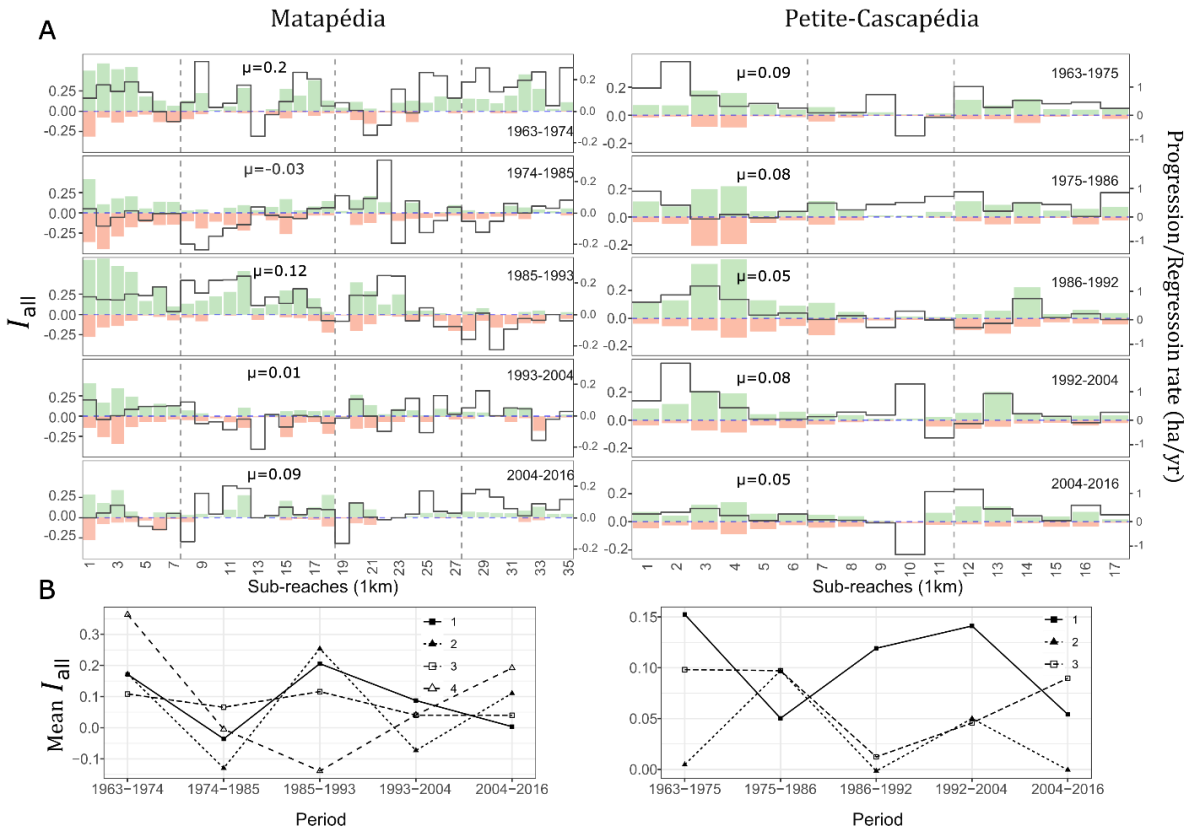


Figure 24 (A) The I_{all} index value across periods and subreaches for both rivers (left y-axis), along with the progression (green) and regression (red) rates of each subreach (right y-axis). I_{all} is calculated with every succession path (see Methods for details), where positive and negative values indicate a dominance process of progression and regression, respectively. The closer the value is to -1 or 1, the more important is the dominant process. (B) Mean I_{all} values across the selected reaches. Line and point types distinguish the reaches.

1.7 DISCUSSION

The results exposed important variations according to the vegetation and channel planform trajectories, both at the inter-river and inter-reach scales. A synthesis of the results is presented in Figure 25 to agglomerate the principal channel adjustments and vegetation progression/regression dynamics. The following section examines the role of ice jam dynamics on trajectories and discusses river-vegetation interactions from a biogeomorphological perspective.

1.7.1 Role of ice-jams and floods on channel planform and vegetation trajectories

Previous studies have explored the impact of ice jams on river channel dynamics such as channel enlargement, riverbed erosion patterns, riverbank morphology, and avulsion dynamics (Beltaos, 2016; Kolerski & Shen, 2015; Morin et al., 2015; Smith & Pearce, 2002). One specific study by Boucher et al. (2012) associated channel enlargement with recurrent ice jams, in which enlargement of up to 1.5 to 2 times the initial channel width was observed in reaches subjected to strong jamming, such as in the presence of meander or islands. These processes are caused by (1) the pressure exerted on the banks during the accumulation of ice blocks and (2) the release of jams that exert strong shear stress and remobilize the sediment (Boucher et al., 2009b; Boucher, 2017a). Although not true over each reach in our study, some observations corroborate this claim. For example, one of the largest enlargements in the Matapédia River occurred in reach 1 during the period of 2004–2016 when multiple ice jams occurred. However, enlargement also occurred in the fourth reach during the period of 1985–1993, which presented no sign of confirmed ice jam (Figure 16). These effects can be localized and affect a very restrained portion of a river because of channel morphological features (e.g., steep narrowing, meander, and slope change), fostering the formation of localized ice jams (De Munck et al., 2017). Figure 15 shows a high variability in channel width changes, with localized enlargements and narrowing throughout the subreach scale. Such results suggest that some of the localized important enlargement (e.g., subreaches 10 and 11 during the period 1974–1985) could be caused by local ice jam processes. However,

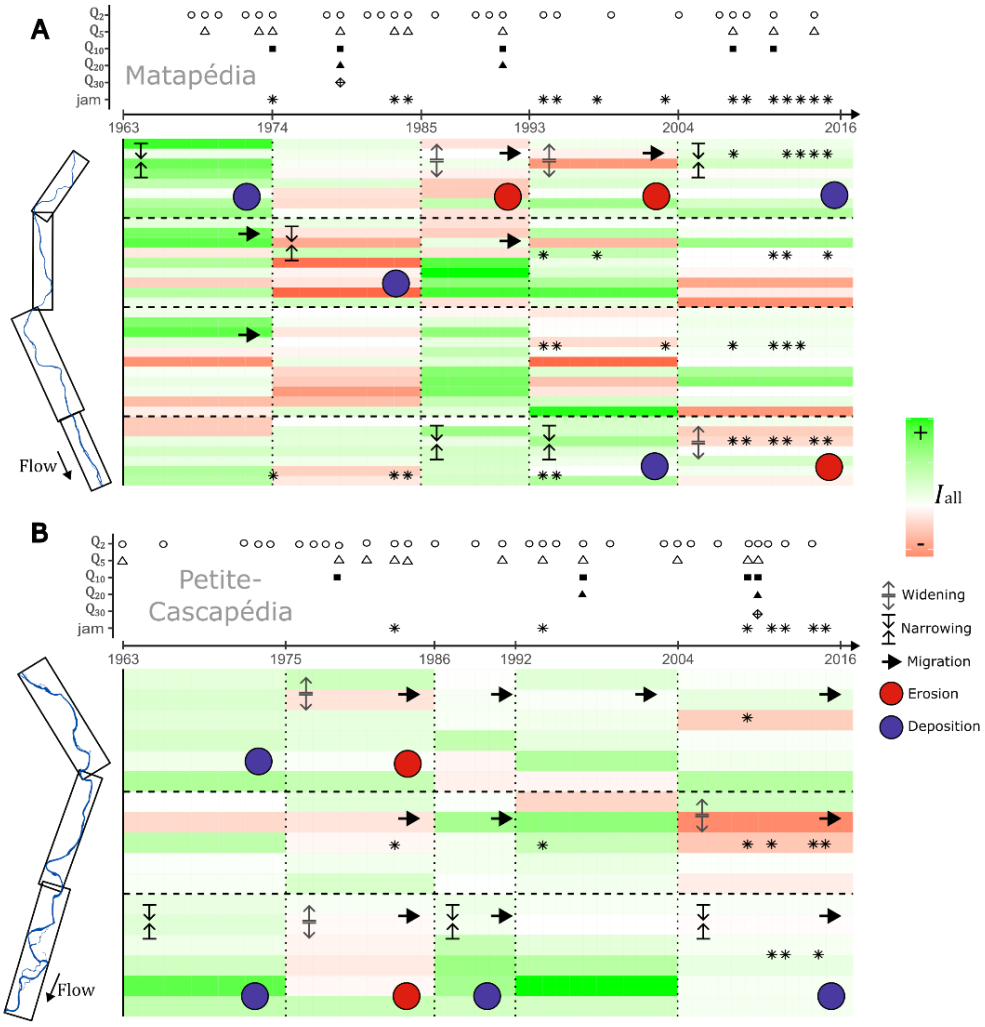


Figure 25. Synthesis figure agglomerating both dominant vegetation progression/regression dynamics at the sub-reach scale and significant/dominant channel adjustment at the reach scale, along with a summary of the disturbances. The timeline on the top of the graphs identifies years when a certain disturbance occurred (empty circle for Q_2, empty triangle for Q_5, solid square for Q_{10}, solid triangle for Q_{20}, lozenge for Q_{50}, and star for ice jams) at the corridor scale. Ice jam years (stars) were also reported spatially in the synthesis figure to spatialize known jams throughout the reaches. Circle and arrow symbols show the dominant hydrogeomorphological processes and are based on the average value. Migration (presence or absence of a lateral arrow) and widening/narrowing (diverging grey arrows for widening and converging black arrows for narrowing) are shown when the values are larger than the RMSE. Erosion (red circle) or deposition (blue circle) is shown when one of the processes is more important than the other in a given reach.

such variability also appears in periods without ice jams, indicating that ice jams are not the ultimate enlargement factors in such rivers that are also responsive to flood events.

In a modelling study, Kolerski and Shen (2015) found that during a moderate magnitude ice jam in 1984 on the St. Clair River (Michigan, USA), bed shear stress during the ice jam was not significantly higher than during free-flowing water floods, which was attributed to important water depth with thin ice jam. Aligned with the latest, both the Matapédia and Petite-Cascapédia rivers had the highest erosion rates during periods with low to no ice jam activity (Figure 25). This suggests that ice jams are not the principal factor contributing to channel erosion and sediment mobilization at the corridor scale. The highest erosion rates in the Matapédia River were observed between 1974 and 1993, when the highest floods were recorded (Q_{50} and Q_{20}). However, on the Petite-Cascapédia, the highest erosion rate was observed during the period (1986–1992) with floods as low as Q_5 and no ice jams events. This observation could be explained by the fact that the Petite-Cascapédia River is subjected to many avulsions and that this period could be dominated by strong bar push dynamics, increasing lateral migration. Furthermore, this supports the idea that ice dynamics might not be a critical factor in channel dynamics compared to sediment dynamics and flood regimes.

Ice jams can exert significant physical disturbances on vegetation stands by wounding, shearing, toppling and even uprooting ligneous species located on bars, riverbanks and floodplains, thus creating new colonizable open sites from vegetation to establish (Lind et al., 2014a; Rood et al., 2007; Vandermause et al., 2021). In a study on the Peace River (Canada), Uunila and Church (2014) have observed recurrent patterns linking the frequency and magnitude of ice jams with composition and age structure of riparian plant communities, suggesting that succession dynamics were significantly influenced by ice jams, especially in the lower riparian communities closest to the river. These turnover events were also observed by Rood et al. (2007) and Smith and Pearce (2000) on the Milk River (Alberta and Montana) and the Oldman River (Alberta), respectively. They both found areas where ice jams generated open sites with ideal conditions for the emergence and establishment of pioneer

ligneous species such as cottonwood and willow species. Matapédia's results effectively capture these dynamics where high regression happens during years of frequent ice jams. For every period where an ice jam happened 1 or 2 years prior to the latest photograph, the affected reach and subreaches within it depicted a dominant regression trajectory, suggesting a significative effect on the vegetation turnovers (Figure 25). These results align with previous studies stating that ice jams are the leading factor of vegetation rejuvenation within these systems. Furthermore, high regression rates were also observed in period with low magnitude floods but in the presence of ice jams. For example, reach 2 in the period of 1993–2004 shows high regression that can only be explained by the presence of multiple ice jams, as the only floods that occurred during this period were the equivalent of 2-year recurrence floods. This implies that ice dynamics can exacerbate the effect on vegetation rejuvenation during moderate flood that would probably cause no vegetation removal without ice. While similar patterns are observed on the Petite-Cascapédia, they are less pronounced, suggesting that confined rivers' vegetation communities are more prone to repetitive rejuvenation. Confined rivers are known to affect flow structure by increasing its water depth compared to a mobile river with the same discharge, thus increasing the shear stress and applying considerable drag forces onto riparian vegetation (Dufour et al., 2007). Ice impacts might behave alike and be more impactful in confined river compared to mobile rivers.

While uncertainties remain along the impact of floods against ice onto the channel trajectories and vegetation succession, our results suggest that ice dynamics control first and foremost vegetation rejuvenation. Other studies have quantified the important impact on sediment transport, erosion and deposition resulting from ice jams dynamics (Beltaos, 2016; Ettema & Kempema, 2012; Turcotte et al., 2011a; Vandermause et al., 2021), but the two-dimensional planimetric assessment of erosion and deposition presented in this study could not confirm a relationship between ice jams and erosion. This could be explained by two main reasons. First, it could be caused by the precision of the data where gaps of 10 years between photographs may not be sufficient to evaluate with precision the eroded area specifically provoked by mechanical ice erosion such as the year-scale assessment of erosion studied by Vandermause et al. (2021). This suggests that ice dynamics may play an important

role at the local and monthly/annual scale but that their effects are mitigated at the corridor and multidecadal scales. Second, it could be explained by the important water depth increase during breakups, which increase the distance between the riverbed and the ice blocks. As such, ice-related erosion forces might principally be applied on ligneous vegetation and not on the riverbed, causing vegetation scouring and uprooting without significant sediment erosion.

1.7.2 Biogeomorphological behavior interpretation

Fryirs (2017) defines river behaviour as the "adjustments to river morphology induced by a range of erosional and depositional mechanisms by which water moulds, reworks and reshapes fluvial landforms, producing characteristic assemblages of landforms at the reach scale". For the following discussion, we will focus on the biogeomorphological dynamics that participate in these sets of processes shaping river channels and planforms. More specifically, it concerns the dynamic and reciprocal interactions between plants and geomorphological processes, in order to assess the bidirectional effects between geomorphology and vegetation, the co-adjustment between landforms and vegetation type, and the emergence of biogeomorphological units fostered by these interactions (Bywater-Reyes et al., 2022a; Corenblit et al., 2007b, 2024a; Gurnell & Bertoldi, 2024). However, it is worth noting that disentangling cause-and-effect within biogeomorphological system is more complex at the reach and fluvial corridor scales, i.e., to discern whether vegetation primarily responds or drives geomorphological processes or if co-adjustment processes are dominant (Corenblit et al., 2024a). Our results cannot provide an absolute and clear interpretation of the ongoing dominant process within both rivers because of (1) the lack of annual aerial data and sparse historical information related to ice activities, and (2) the fact that we did not monitor sediment volume and plant traits through consecutive years to find relationships. However, our results remain a first step in the exploration of these dynamics in those understudied hydrosystems and suggest different behaviours and reactions to disturbances that can let us pose hypotheses onto the biogeomorphological dynamics driven by flood and ice disturbances.

Riparian vegetation is known to increase bank shear strength from root systems binding soil particles, decrease water shear stress by reducing flow velocities and promote sediment deposition by the reduced flow velocities (Andreoli et al., 2020; Bywater-Reyes et al., 2022a; Corenblit et al., 2007b). For instance, experimental studies from Tal and Paola (2010), Kyuka et al. (2021) and (Yang et al., 2018) all demonstrated that dense vegetation cover significantly reduced channel migration rates, fostered narrower and deeper channel, decreased erosion rate, and slowed down widening processes. These observations were also made in real-world study cases, for example in the Sacramento River and the Tarim River (Micheli et al., 2004; Yu et al., 2020). Our results on the trajectories of channel changes and vegetation succession indicate potential biogeomorphological feedbacks within both systems. While it was not part of the principal results due to its lack of statistical significance and qualitative nature, Figure 26 supports this idea by showing relationships between vegetation progression rates, width change rate and deposition rate. At the subreach scale, the higher the progression rate (i.e., development of dense vegetation cover), the higher the depositional rate and narrowing process. It remains hard to distinguish whether the channel changes have let vegetation to progress, vegetation forced the channel to adjust, or if complex interactions led to these results. We can, however, hypothesize that potential feedbacks have occurred based on the previous studies that confirmed these dynamics and the observations made in this study. The synthesis also strongly supports these hypotheses, depicting a pattern where periods following important turnovers and erosion are characterized by channel narrowing and vegetation progression.

In the Matapédia River, the period of 1974–1985 depicted the highest progression rate (Figure 21) and was instantly followed by channel narrowing processes ranging from 2 to 7 meters, combined with the lowest erosion rate and the lowest lateral migration rate over the entire study period (Figure 17, Figure 18 and Figure 19). Islands constantly aggraded since 1963 and some pioneer landforms such as lateral and central bars emerged since 1985. As island formation is known to be strongly impacted by vegetation and its effects on water flow (Bertoldi & Gurnell, 2020; Gurnell & Bertoldi, 2020), we can hypothesize that vegetation communities in the Matapédia River acts as stabilizing factor. Furthermore, some of the

emerging pioneer islands were maintained within the river for decades even after years of important ice jams activities, suggesting induced resistance from vegetation root systems stabilizing these pioneer landforms. Same patterns were also observed in the Petite-Cascapédia, where high progression rate from the period of 1986–1992 was followed by relatively low migration rate, little changes in river width and a positive ratio of deposition/erosion rate (Figure 17, Figure 18 and Figure 19). These observations suggest the extension of bar surfaces and emergence of new floodplain areas (in the case of channel migration), followed by vegetation encroachment and sediment stabilization leading to a narrowing process of the channel.

Resilience in the biophysical realm of rivers can be defined as the ability of a river system to return to its original state after a disturbance (Corenblit et al., 2024c). The rate at which landforms and vegetation recovered after a disturbance are great indicators of the potential resilience capacity of a system. Our study suggests high resilience potential in both rivers despite frequent mechanical ice breakups, which vary according to their unique behavioural regime. Based on the Green Balance Model (Bywater-Reyes et al., 2022a), the two studied rivers are great examples of rivers where vegetation acts as a geomorphological agent by narrowing the channel through sediment stabilization and accumulation. As depicted in Figure 24A, the rivers exhibited a dominant progression process in term of vegetation succession after each regression phases, indicating the potential of these systems to rapidly recover from disturbances. Despite localized vegetation turnovers and channel impacts (erosion/enlargement) that followed ice jams periods, relaxation time of less than 10 years were sufficient for vegetation encroachment and landforms stabilization. Figure 26 clearly shows this process. Despite years with some significative changes in channel structure and vegetation distribution, the rivers readjusted quickly to the same fluvial style it was beforehand. Ice disturbances thus might play a role in the turnover rates and as factors of channel changes but clearly don’t act as important inhibiting factors to the biogeomorphological dynamic equilibrium at play. These observations supports findings done in a Mediterranean river where general trends of vegetation progression was punctuated with irregular rejuvenation followed by high resiliency of the biogeomorphological structure

(Corenblit et al., 2010). The only difference between these observations is the source of disturbance, where rejuvenation rates were controlled by intense irregular floods in the Mediterranean context and by intense irregular ice jams events in our study.

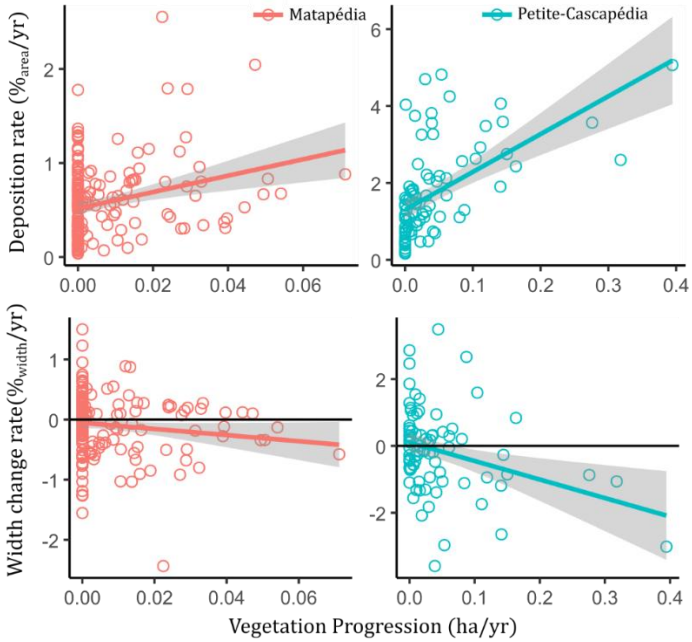


Figure 26 Relationship between sparse/dense vegetation progression rate and deposition/width change rate. Horizontal lines in the width change plots delimit narrowing (negative) and widening (positive). Each point (red for Matapédia; blue for Petite-Cascapédia) corresponds to a specific subreach in a specific period. The deposition rate was normalized based on the average channel area of each sub-reach. The width change rate was normalized based on the average channel width of each sub-reach. Regression line is based on the ordinary least squares.

Riparian species such as willows (*Salix sp.*) and poplars (*Populus sp.*) have evolved and adapted to regular and chaotic hydrogeomorphological regime by developing specific morphological and biomechanical traits allowing them to successfully establish, grow and disperse in these highly dynamic environments (Bornette et al., 2008; Edwards et al., 1999; Karrenberg et al., 2002; Lytle & Poff, 2004). Even though our results indicate high resilience of vegetation communities following ice disturbances, they also denote a lack of resistance by not withstanding period of ice jamming events. This observation suggests that the isolated

and sporadic regime of ice jams are not sufficiently regular for riparian species to develop long-term resistant adaptions to these specific disturbances. Thanks to their flood-related adaptions giving them the ability to resprout quickly, they can still maintain their presence in such environment through resiliency by avoiding high mechanical stresses.

1.8 CONCLUSION

This study examined the long-term effects of ice dynamics on channel planform adjustments and vegetation trajectories within two contrasting cold rivers: the confined Matapédia River and the mobile Petite-Cascapédia River in the Gaspé Peninsula of Quebec, Canada. The study used dendrochronological analysis, historical data, and a diachronic analysis of aerial photographs from 1963 to 2016 to evaluate the influence of ice dynamics on river evolution. Even though precise discernment between the impacts of flood versus ice was not noticeable, the results suggest many interesting points related to the long-term effects of ice jams on cold rivers biogeomorphological dynamics.

First, while previous studies have shown that ice jams could cause important channel erosion, no clear effects were observed at the multidecadal scale when compared with flood regime. This suggests that relaxation time between ice jam disturbances were sufficient to recover channel forms and plant communities. Second, ice jams first and foremost affect vegetation by causing turnovers. These rejuvenations could, however, have indirect effects on channel erosion due to the removal of vegetation-induced shear strength applied to banks. Third, presence of ice jams can exacerbate the potential of vegetation turnovers during periods of low discharge floods. Results have shown that high regression occurred during very low flood period with presence of ice jams, suggesting the role of ice in increasing shear strength. Fourth, construction of pioneer biogeomorphological units seems to be active despite the presence of ice dynamics, as shown by the relations between sediment deposition and rate of vegetation successional progression. Fifth, while being two contrasted behavioural systems with different responses to disturbances, both rivers exhibited biogeomorphological resilience. The Matapédia's resilience is showed by its quick

rejuvenation of vegetation communities that underwent turnovers. The Petite-Cascapédia, on its hand, was quickly adjusting to channel changes (e.g., migration and avulsion) and establishment of new communities.

These results are a first step towards the exploration of the interactions between ice disturbances, channel adjustment and vegetation succession. However, further research is needed to better quantify and assess the extent to which ice jam regime affect the turnover rate and the biogeomorphological construction of landforms. We propose that long-term monitoring of vegetation and geomorphological adjustments at the local and reach scales must be established to accurately understand the interactions between ice dynamics, vegetation and hydrogeomorphological dynamics.

Finally, this study focused on ice jams at the fluvial corridor scale with ice scars used for ice dynamic characterization. However, these proxies only reflect high magnitude events and do not consider mechanical breakups restrained below the floodplain level. Even if no ice jam or high magnitude breakup happens, we believe that the shear force associated with moderate ice breakups might play a role in vegetation development and succession. Exploring the response and effect functional traits of these communities would serve greatly to find relationships between plant communities' structure/composition and northern river ice dynamics. Future research must focus on these processes that might be much more frequent but less destructive than large ice jams breakup. These approaches are especially essential in a climate change context where mechanical ice breakups and ice jams might become more frequent due to more frequent winter thaws. Thus, tackling down the role of these disturbances on the moderate- to long-term evolution of rivers is essential for efficient management.

1.9 ACKNOWLEDGEMENTS

This research was financially supported by the Natural Sciences and Engineering Research Council of Canada (grand ID: RGPIN-2023-05431; grant owner: Thomas Buffin-Bélanger). Special thanks to all research professionals and assistants from the Laboratoire de recherche en dynamique et géomorphologie fluviale (LGDF) who helped gathering data during field work and helped with tree samples preparation. We also want to thank Dominic Arsenault from the UQAR for giving the access to his dendrochronological lab. Finally, we thank the reviewers who took the time to review this paper and provide constructive feedback to enhance the quality of writing and precision of content in the manuscript.

1.10 AUTHOR CONTRIBUTIONS

Matthieu Prugne: Conceptualisation, methodology, investigation, writing—initial draft, writing—reviewing and editing. **Dov Corenblit**: supervision, methodology, writing—reviewing and editing. **Maxime Boivin**: supervision, methodology, writing—reviewing. **Thomas Buffin-Bélanger**: funding acquisition, supervision, methodology writing—reviewing and editing.

CHAPITRE 2
L'EFFET DU REGIME D'EMBACLES DE GLACE SUR LA DIVERSITE ET LA COMPOSITION DES COMMUNAUTES VEGETALES RIVERAINES DIFFERE ENTRE DEUX RIVIERES GEOMORPHOLOGIQUEMENT CONTRASTEES

2.1 RESUME EN FRANÇAIS DU DEUXIEME ARTICLE

1. Les communautés végétales riveraines dans les régions tempérées froides et boréales sont fortement influencées à la fois par le régime d'inondation et par la morphologie du chenal, ainsi que par des événements de débâcles glacielles qui exercent des perturbations écologiques et géomorphologiques uniques.

2. Nous avons étudié comment les caractéristiques du régime d'embâcles (fréquence et magnitude) influencent la composition et la diversité des communautés végétales riveraines sur deux rivières contrastées d'un point de vue géomorphologique, au Québec, Canada : la rivière Matapédia (confinée) et la rivière Petite-Cascapédia (non confinée). Sur treize sites, nous avons reconstitué les régimes d'embâcles par dendrochronologie, en nous appuyant sur les cicatrices glacielles laissées sur les arbres lors de leur formation. De plus, nous avons inventorié des quadrats de végétation pour caractériser l'abondance des espèces, les conditions locales de l'habitat, et pour calculer des indices de richesse spécifique, de diversité et d'équitabilité.

3. Des analyses d'ordination contrainte ont montré que la composition des communautés végétales différait significativement selon les habitats et entre les rivières, et que les prédicteurs hydrogéomorphologiques expliquaient la majeure partie de la variation de la composition. Après avoir conditionné les analyses de redondance par les variables hydrogéomorphologiques, le régime d'embâcles expliquait une part significative des différences de composition, ces effets étant particulièrement prononcés dans la rivière non confinée. Les graminées et les arbustes répondaient le plus aux embâcles dans la rivière Matapédia, tandis qu'il s'agissait d'arbres matures des plaines alluviales dans la rivière Petite-Cascapédia. Malgré des réponses divergentes entre les deux rivières,

certaines tendances communes ont émergé, notamment la forte abondance de *Cornus sericea* sur les sites très perturbés. En revanche, la richesse spécifique, la diversité de Shannon et l'équitabilité étaient principalement structurées par le type de rivière et d'habitat, alors que les analyses de corrélation n'ont mis en évidence aucune relation significative avec les variables d'embâcles.

4. **Synthèse.** Notre étude montre que (i) l'hydrogéomorphologie contrôle majoritairement la composition de la végétation riveraine plutôt que les effets de la glace, (ii) les régimes d'embâcles imposent néanmoins des filtres écologiques supplémentaires, entraînant des changements de composition, et (iii) la force et la direction des effets d'embâcles dépendent des caractéristiques hydrogéomorphologiques. La pertinence de ces résultats réside d'abord dans l'approfondissement de nos connaissances sur l'écologie des plantes riveraines en régions froides, soulignant l'importance de considérer les interactions entre le contexte hydrogéomorphologique et les régimes de perturbation pour décrire les communautés.

Dans l'ensemble de cette thèse, ce deuxième chapitre s'inscrit dans une analyse à l'échelle des communautés riveraines, où la réponse taxonomique est examinée en fonction des contextes hydrogéomorphologiques et fluvioglaciels. Il permet d'identifier les grandes différences d'un point de vue taxonomique et propose un premier regard sur les effets structurants des régimes d'embâcle. Rédigé sous forme d'un article intitulé « *The effects of ice-jam regime on riparian plant diversity and community composition differ between geomorphologically contrasted rivers* », il sera soumis sous peu dans la revue *Journal of Ecology*.

Contribution des auteurs : Cet article fut corédigé par moi-même, mon directeur, Thomas Buffin-Bélanger, mes co-directeurs, Maxime Boivin et Dov Corenblit, ainsi que par deux collaborateurs internationaux, Eduardo González-Sargas et Aziz Syammach. En tant que premier auteur, j'ai développé l'idée de recherche, conceptualisé la collecte de données, organisé et supervisé les campagnes de terrain, procédé à leur analyse, produit les figures et rédigé la première version de l'article. Tout au long du processus, mon directeur (Thomas B-

B) et mes codirecteurs (Maxime B. et Dov C.) ont participé activement à chaque étape de ce projet, notamment en apportant des conseils pour améliorer les approches méthodologiques et analytiques, en contribuant à l'interprétation des résultats et en révisant l'article. Les deux collaborateurs s'étant joints à l'équipe dans le cadre de cet article ont apporté une aide considérable aux analyses statistiques, proposant de multiples idées et contribuant à l'interprétation. Ils ont de plus participé à plusieurs rondes de révision. Finalement, de nombreuses personnes ont été impliquées dans la collecte des données taxonomiques et topographiques, apportant une aide significative sur le terrain. Parmi celles-ci, nous notons l'aide d'une botaniste invitée (Kassandra Croteau) et la participation des auxiliaires de recherche du Laboratoire de recherche en Géomorphologie et Dynamique Fluviale (LGDF) de l'UQAR (Félix Lachapelle, Zoé Martineu, Samuel Laroche, Alex Desliles, Étienne Gariépy-Girouard et Étienne Gauthier-Dufour).

2.2 THE EFFECTS OF ICE-JAM REGIME ON RIPARIAN PLANT DIVERSITY AND COMMUNITY COMPOSITION DIFFER BETWEEN GEOMORPHOLOGICALLY CONTRASTED RIVERS

Abstract

1. Riparian plant communities in cold temperate and boreal regions are strongly influenced by both flood regime and channel morphology, with ice breakup events adding unique ecological and geomorphological disturbances.

2. We investigated how ice-jam regime characteristics (frequency and magnitude) influence riparian plant community composition and community-aggregated metrics across two geomorphologically contrasted rivers in Quebec, Canada: the confined Matapédia River and the unconfined Petite-Cascapédia River. At 13 sites, we reconstructed ice-jam regimes from tree scars using dendrochronology and surveyed vegetation plots to characterize species abundances and local habitat conditions, and to calculate richness, diversity, and evenness.

3. Constrained ordination analyses showed that plant community composition differed significantly among habitats and between rivers, with hydrogeomorphological predictors explaining most of the variation. After accounting for these factors, the ice-jam regime significantly contributed to composition differences, with stronger effects observed in the unconfined river. Grass and shrub species showed the strongest response in the confined river, while floodplain trees responded most significantly in the unconfined river. While species responses to ice disturbances varied between rivers, some general patterns emerged, such as high abundance of *Cornus sericea* in highly disturbed sites from the two rivers. By contrast, species richness, Shannon diversity, and evenness were mainly structured by river and habitat type and showed no significant relationships with ice-jam variables.

4. **Synthesis.** Our study shows that (i) hydrogeomorphology is the primary control on riparian vegetation when compared with ice effects, (ii) ice-jam regimes nevertheless

impose additional ecological filters leading to compositional changes, and (iii) the strength and direction of ice-jam effects depend on the hydrogeomorphological characteristics. These findings are relevant to our ecological understanding of riparian vegetation by highlighting how disturbance regimes interact with hydrogeomorphology to filter plant composition and emphasizing the need for case-specific assessments when predicting vegetation responses to changing ice and flood regimes.

2.3 INTRODUCTION

The composition and structure of riparian plant communities are driven by hydrological and geomorphological characteristics unique to each fluvial system. Dispersal, recruitment, establishment, growth, and survival of riparian plants are functions of the interactions between geomorphological conditions (Jolley et al., 2010; Kim & Kupfer, 2016; Pielech, 2021), and flood regime characteristics (González et al., 2019b; Kehr et al., 2014; Peters et al., 2016; Surian et al., 2015). Flood frequency, magnitude, and duration drive vegetation composition along transversal and vertical gradients by exerting varying levels of inundation and shear stress whose spatial distribution is mediated by the hydrogeomorphological context, resulting in mosaics of vegetation communities that differ across fluvial corridors (Corenblit et al., 2007b; Gurnell et al., 2016a; Hupp & Rinaldi, 2007). Vegetation response to a common disturbance regime may differ depending on the channel geometry and fluvial forms (and processes) characterizing an environment, as they influence sediment dynamics and hydraulic forces by concentrating or dissipating the energy (Church & Ferguson, 2015; Wohl & Merritt, 2001). For instance, vegetation structure, composition and diversity have been shown to significantly vary along a gradient of channel confinement, where the concentrated flows in confined reaches fostered incision and inhibited vegetation establishment (Dufour et al., 2007). The interactions between hydrogeomorphology and vegetation are now well documented and understood (Corenblit et al., 2024a; Gurnell et al., 2012), but most of the knowledge is based on flood-related disturbance regimes in temperate environments. In contrast, comparable ecological knowledge for cold-region rivers subjected to ice-related disturbances remains limited.

In cold-temperate and boreal regions, the presence of fluvial ice provides another source of disturbance, especially during mechanical ice breakup. These events typically occur in spring when rising temperatures and heavy rains destabilize the channel ice cover, causing it to break up and transport large ice blocks downstream (Beltaos, 2003, 2007; Burrell et al., 2023). These ice floes have been shown to exacerbate shear stress on both riverbeds and riverbanks, leading to significant sediment erosion and deposition, and

mechanical stress on vegetation stands (Prowse & Culp, 2003; Uunila & Church, 2014; Vandermause et al., 2021). If the movement of ice blocks is impeded by geomorphological features (e.g., meanders, islands) or human structures (e.g., bridges), ice can accumulate within the channel and form ice jams, which in turn generate substantial floodplain inundation (Beltaos, 2008; Lagadec et al., 2015; Rokaya et al., 2018). The release of ice jams can further result in flood surges composed of large ice blocks that can impact riverbank geometry (Boucher et al., 2009b; Morin et al., 2015), modulate sediment dynamics (Beltaos, 2016; Turcotte et al., 2011a), and damage riparian vegetation through scarring, bending, and uprooting (Chassiot et al., 2020; Engström et al., 2011; Lind et al., 2014a; Prowse, 2001). Ice breakups and ice jams result from specific climatic, geomorphological, and hydrologic conditions (De Munck et al., 2017; Lagadec et al., 2015). Thus, these events exhibit characteristic frequencies and severities, and their effects can be highly localized within a river network (Boucher et al., 2009a; Morin et al., 2015; Vandermause et al., 2021).

Research on the interactions between ice breakup and riparian vegetation remains sparse (Poulin et al., 2019; Prugne et al., 2024). Most authors addressing this subject focused on turnover dynamics and concluded that ice jam events play a crucial role in maintaining early-successional vegetation phases (Peters et al., 2016; Prowse & Culp, 2003; Uunila & Church, 2014). A recent study on the Susitna River in Alaska (Vandermause et al., 2021) quantified the erosional processes associated with ice breakups on vegetation and channel landforms and highlighted the importance of ice dynamics in shaping riparian vegetation distribution and river channel adjustments. It has also been proposed that ice-jam-related floods may influence vegetation composition on floodplains by controlling water and nutrient cycling (Peters et al., 2016; Rokaya et al., 2018). Up to now, research on the effects of ice jams on vegetation has either examined the impact of single events (Vandermause et al., 2021), compared species richness between sites with or without proxies of ice dynamics (Nilsson et al., 1989), or related ice jam frequencies with broader vegetation types (Boucher et al., 2009b; Uunila & Church, 2014). More recently, Prugne et al. (2025) linked vegetation succession and turnover spatial patterns with ice-jam frequencies in two rivers, revealing how the hydrogeomorphological context mediates ice-jam effects on vegetation landscape

dynamics. Yet vegetation response at the community scale, based on site-specific variation in the frequency and magnitude of ice jams, remains poorly examined.

In this study, we investigate the influence of ice jams on plot-scale vegetation composition and diversity across sites with varying disturbance regimes in two contrasting rivers, one confined and one unconfined. Specifically, we aim to identify the principal drivers of composition between the two rivers and to determine whether differences in the frequency and magnitude of ice jams contribute to shaping local riparian plant communities within those two contrasted fluvial corridors. As riparian vegetation responses to local disturbances vary across different fluvial contexts, we believe that the strength of influence associated with ice disturbances may also be mediated by hydrogeomorphological behaviours. This research thus aims to provide ecological knowledge that deepens our understanding of the interactions among vegetation composition, river hydrogeomorphology, and fluvial ice dynamics.

2.4 METHODOLOGY

2.4.1 Study area

This study examines the Matapédia River and the Petite-Cascapédia River in the Gaspesian Peninsula, Quebec, Canada (Figure 27). Both are mountainous gravel-bed rivers in a cold-temperate/boreal zone with mixed stands of balsam poplar (*Populus balsamifera* L.), balsam fir (*Abies balsamea* [L.] Mill., 1768), and black spruce (*Picea mariana* [Mill.] BSP., 1888). They are characterized by a nivo-pluvial flood regime with two flood peaks: one in spring after snowmelt and one in autumn during heavy rain. The Matapédia River is a confined river with very low mobility due to rock outcrops and anthropogenic features (e.g., ripraps, railways, and roads). Its watershed covers 3,792 km², with daily flows ranging from 5 to 940 $m^3\ s^{-1}$, a mean annual discharge of 56 $m^3\ s^{-1}$, and a bankfull discharge estimated at 414 $m^3\ s^{-1}$. The river is regularly impacted by large ice jams that have historically caused substantial damage to infrastructure, resulting in well-documented records of jam events and locations (Beltaos & Burrell, 2010). The study reach is about 33 km long between the town of Routhierville and the confluence with the Restigouche River (Figure 27B), with a mean confinement index of approximately 0.59 (Table 5). In contrast, the Petite-Cascapédia is characterized by high lateral mobility and channel avulsions (Prugne et al., 2025). Its watershed covers 1,449 km² with daily discharges ranging from 3 to 623 $m^3\ s^{-1}$ and a mean annual discharge of 31 $m^3\ s^{-1}$. Although evidence of ice jams is present through ice-scarred riparian trees, formal historical records are scarce. The study reach is 16 km long and spans over the downstream part of the fluvial system, where its mean confinement index is 0.12, reflecting its potential to migration and lateral adjustment.

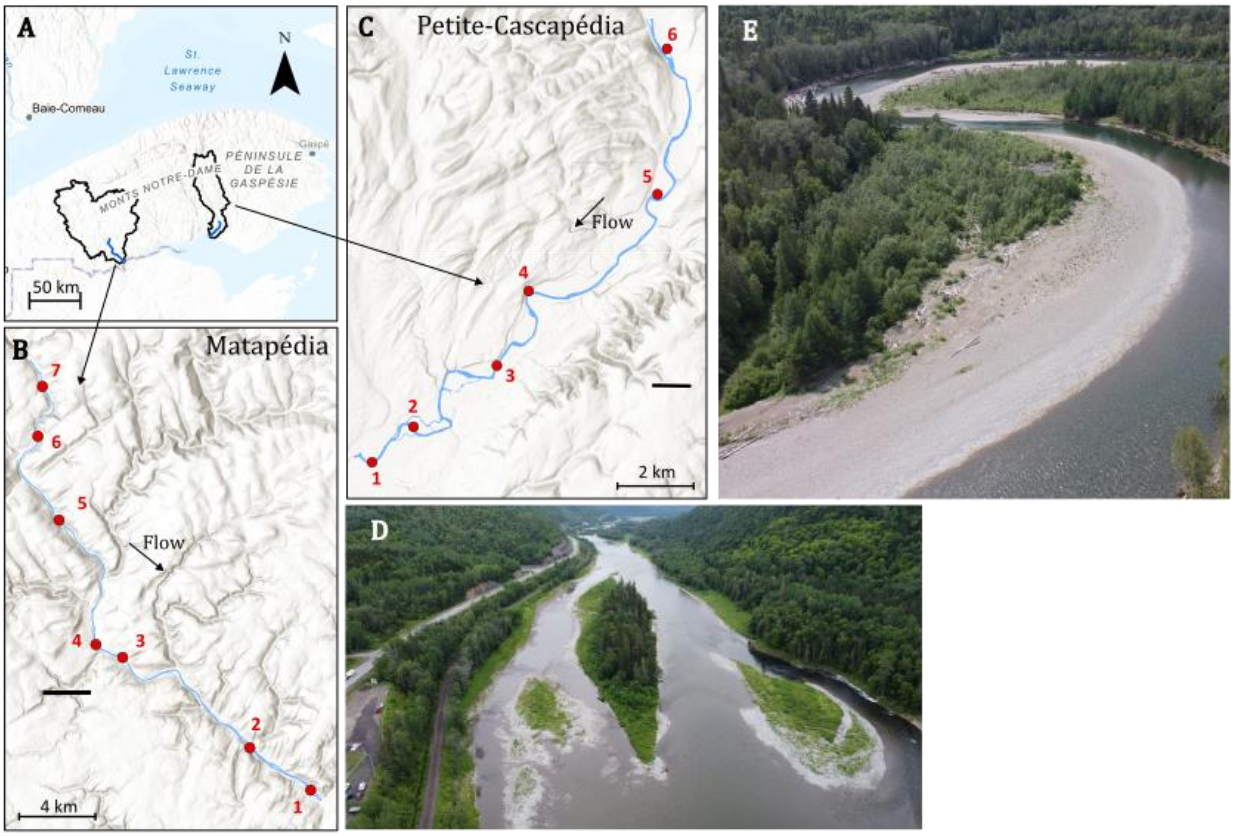


Figure 27 Location of the two study rivers and study sites. (A) Watersheds boundaries of the two rivers, in black, and segments studied, in blue lines. (B) and (C) River segments studied and the sites (red circles and red labels for site numbers) where dendrochronological and taxonomical samples were taken on the Matapédia and Petite-Cascapédia rivers, respectively. (D) and (E) Aerial views of characteristic reach in the Matapédia and Petite-Cascapédia rivers, respectively.

2.4.2 Sampling design and field campaigns

Fifteen sites on each river were initially selected, but constraints during field campaigns reduced this number to a total of thirteen sites (7 on the Matapédia River and 6 on the Petite-Cascapédia River). A field campaign was conducted in summer 2022 to collect sediment, topographic, and vegetation data. On each site approximating 200 meters long on the longitudinal river axis, three to four transects, oriented perpendicular to the main channel, were selected to capture most of the landscape diversity. On these transects, a total of 169

plots were established whenever vegetation community composition appeared visually distinct. The size of plots varied between 2 × 2, 4 × 4 and 10x10m whether communities were dominated by herbs, shrubs or trees, respectively. Another field campaign was conducted in winter 2022–2023 to collect tree samples for dendrochronological analysis, yielding a total of 200 tree cross-sections and wedges. During ice breakups and ice jams, the flow of ice blocks can mechanically scar trees. Through dendrochronology, these scars can be used to identify years of ice jams and construct a chronology of past events (Lubiniecki et al., 2024). Samples were sanded and scanned, and their growth rings counted using the software CDendro (v. 9.8.4), with the outermost ring assumed to correspond to 2022. To reduce the risk of misidentifying isolated disturbances such as damage from large woody debris, we (1) collected samples at a given site only when multiple trees displayed scars at the same height and (2) confirmed ice jam years only when the same dated scar appeared in at least two separate samples. We also supplemented the results with historical data on ice-jam years retrieved from local newspapers (*Bibliothèque et archives nationales du Québec*), local watershed organizations (*Organisme de bassin versant Matapédia-Restigouche*), and governmental databases (*Ministère de la Sécurité publique du Québec*).

2.4.3 Data

At the site-scale, we measured hydrogeomorphological characteristics from aerial photographs and digital elevation models (ANNEXE IV) and characterized the ice jam regime from historical data and dendrochronological analysis (Table 5). To estimate ice-jam frequency, site-scale frequencies were calculated by dividing the number of dated scars by the time elapsed since a reference point. As these estimates are sensitive to the choice of reference points and may alter site rankings along the disturbance gradient, we integrated frequencies derived from multiple methods into a single composite variable (PC1_freq) through Principal Component Analysis (ANNEXE V). Finally, we measured the elevation of ice scars relative to the bankfull height, which serves as a proxy for ice-jam magnitude (Smith & Reynolds, 1983).

Sediment, topography and vegetation community were characterized at the plot scale. The median grain size of coarse sediment (>0.1 cm) was derived from 50 pebbles B-axis measurements (Kondolf et al., 2003), and a soil probe was used to measure the depth of fine sediment deposition. We used both a Emlid differential GPS and a Leica robotic Total Station to measure the relative distance and elevation between the plots and the low flow water line. Each species was identified in the field using identification guides, and its cover was visually estimated by projection by a single person to avoid the observer bias. Community-aggregated metrics (taxonomic diversity) were calculated for each plot: species richness (S), Shannon's diversity (H), and Piélou's evenness (E).

Table 5. Mean and ± 1 SE of geomorphological and ice jam regime variables for each river.

River and sites	**Matapédia (confined)**	**Petite-Cascapédia (unconfined)**
Width (m**)**	94.5 ±12.4	70.6 ±5.0
Sinuosity (unitless**)**	1.02 ±0.01	1.21 ±0.06
Confinement (unitless**)**	0.59 ±0.04	0.12 ±0.01
Slope (unitless**)**	1.27 ±0.09	1.19 ±0.12
Unit Stream Power at bankfull discharge (W/m^2 x 10^3**)**	63 ± 12	45 ± 4
Ice-jam frequency gradient (PCA1 axis**)**	0.25 ±0.58	-0.29 ± 0.56
Ice scars relative height (cm**)**	135 ± 10	88 ± 15
Time since last ice jam (yr**)**	6.1 ±1.1	2.5 ±1.2

2.4.4 Statistical analysis

To test how ice dynamic effects might vary across different habitats, geomorphological variables (grain size, sediment depth, and relative elevation) and cover of different vegetation strata (<1m, 1–5 m, >5m) were used to conduct a hierarchical clustering of study plots

(ANNEXE VI). These analyses led to the definition of three distinct habitats, namely bar, ecotone and floodplain. Bars were characterized by coarse sediment and dominance of herbaceous communities. Ecotones were defined as zones of transition between bar habitat and forested floodplains, encompassing high benches, riverbanks, and young floodplain areas with noticeable fine sediment deposition and a dense cover of tall herbs, shrubs, or young trees (<5m high). Floodplains referred specifically to forested floodplains, defined as habitats with adult tree cover (>5 meters high) exceeding 80% (ANNEXE VI).

Community-aggregated metrics were averaged by habitat within each river. First, we used pairwise Wilcoxon tests with a Benjamini—Hochberg correction to assess whether the calculated metrics differed among habitats within each river and, for each habitat type, between rivers. This nonparametric test was chosen because the data did not meet the assumptions of normality and homogeneity of variance for analysis of variance. Second, to determine whether community-aggregated metrics varied along the ice-jam gradients within the same habitat and river, we conducted multiple Kendall's Tau correlations between the three community-aggregated metrics (richness, diversity and evenness) against plot-scale hydrogeomorphological variables (D50, fine sediment depth, relative distance and relative elevation) and ice disturbance variables (ice jam frequency gradient, ice scars height). After a Benjamini—Hochberg correction, the adjusted p-values were all non-significant. However, given the exploratory nature of this analysis, uncorrected p-values are also reported.

Two different ordination techniques were used to explore the relationships between communities' composition and hydrogeomorphological variables. We ran a Redundancy Analysis (RDA) on Hellinger-transformed plant species abundance data to emphasize dominant species and account for double-zeros (Legendre & Gallagher, 2001), and a Correspondence Analysis (CCA) on a presence-absence matrix to emphasize subsidiary species (Legendre & Legendre, 2012). Species occurring in fewer than four plots (2.5% of total plot count) were excluded from the CCA to minimize the disproportionate influence of rare species on the ordination. Before constructing the models, Variation Inflation Factor (VIF) was used to identify predictors that were highly correlated, and we removed variables

until the highest VIF was <5. From this new set of variables, we then conducted a forward selection for each ordination to identify the most relevant predictors. Permutation tests were used to assess the overall significance of the RDA and CCA models. Additionally, we ran permutational analysis (permutations = 999) of variance (PERMANOVA) on the abundance matrix (Hellinger-transformed) and presence-absence matrix to test for significant differences between rivers and habitats.

To disentangle the effects of ice disturbance variables from other environmental factors, we used variation partitioning with three defined families of variables (Table 6; reach-scale hydrogeomorphology, plot-scale hydrogeomorphology, and ice-jam regime), and tested the significance of each group using permutation tests (permutations = 999). A partial RDA on the Hellinger-transformed abundance matrix and partial CCA on the presence—absence matrix was conducted separately for each river. This approach allowed us to isolate the unique contribution of ice-jam regime to riparian plant composition within each system, after accounting for hydrogeomorphological controls. For each ordination conditioned on hydrogeomorphological variables, a VIF analysis was conducted to remove collinear variables. The dispersion of site scores in the partial RDA and CCA ordination spaces was then analyzed through descriptive statistics to assess the extent of turnover along the ice-jam regime gradient across habitat types within each river. A greater dispersion of sites within a group indicates greater variability in species composition in response to a common ice-jam regime gradient.

We conducted all data analysis in RStudio v.2024-12.1.563 (Posit team, 2025). Community-aggregated metrics were calculated with the package *BiodiversityR* (Kindt & Coe, 2005). Wilcoxon and Kendall's tau tests were computed with R base *stats* package and visualization of paired comparison was done using the *multcompView* package (Graves et al., 2024). Abundance matrix transformation and multivariate analyses were performed in the vegan package (Oksanen et al., 2025), including the following functions: *decostand()* for Hellinger and presence-absence transformation, *rda()* for redundancy analysis, *cca()* for canonical correspondence analysis, *varpart()* for variation partitioning, *adonis2 ()* for

Table 6 List of variables used in the multivariate statistical analyses, with abbreviations, descriptions and relevance as environmental variables. The family represents the defined groups of variables used in Variation Partitioning, and each variable is associated with the model(s) to which it was retained after forward selection.

Family	Variable and abbreviation	Description and relevance
Reach-scale hydrogeomorphology	Confinement	Ratio of active channel width to valley floor width; indicates lateral constraints on channel mobility and floodplain extent.
	Sinuosity	Ratio of channel length to valley length; reflects channel curvature, related to sediment deposition patterns and habitat heterogeneity.
	Unit stream power (bankfull discharge) (USP)	Quantifies the energy available to move water and sediment per unit channel area; relevant as a proxy for erosive power.
Plot-scale hydrogeomorphology	Coarse sediment median size (D50)	Median diameter of coarse sediment; relevant as a proxy to sediment transport and hydraulics.
	Fine sediment depth (Sdepth_moy)	Depth of fine-textured sediment overlaying coarser material; indicates sediment depositional processes or low-energy.
	Relative distance (dist_lf)	Distance of plot to the limit of the wetted channel; indicates connectivity to water table and flooding.
	Relative elevation (height_lf)	Elevation of plot to the limit of the wetted channel; indicates connectivity to water table and flood.
Ice-jam regime	Ice jam frequency (PC1_freq)	Composite variable (first axis of PCA) representing the frequency of ice jam; indicates the frequency of disturbances provided by ice jam
	Ice scars elevation (Havg)	Relative elevation of ice scars to the bankfull level; relevant as a proxy for ice jam magnitude

PERMANOVA, and *betadisper()* with *permutest()* for multivariate dispersion. Finally, the variance partitioning visualization was produced with the package *eulerr* (Larsson & Gustafsson, 2018) and all other graphs were constructed with the *ggplot2* package (Wickham, 2016) and some enhanced with Inkscape v1.4 (2024).

2.5 RESULTS

2.5.1 Vegetation patterns between rivers and main hydrogeomorphological driving factors

We identified a total of 115 species (27 at genus level), of which 66% were shared between both rivers (Annexe II, Table 17). The mean cover by habitat and river of a selection of 30 species highlights important differences in dominant species abundance (Figure 28). The mean cover of balsam poplars (*Populus balsamifera)* on the floodplains was more than three times higher in the unconfined river than in the confined river, with a mean cover of 73% and 22%, respectively. In the ecotones, the confined river was characterized by a high abundance of pioneer shrubs, including willows (*Salix sp*.) and red-osier dogwood (*Cornus sericea*). In contrast, the unconfined river's ecotones showed dominance of balsam poplars across different age stands. Bars in the confined river were dominated by *Eupatorium maculatum* and showed high species diversity. In contrast, the only abundant species present on the unconfined river bars were *Melilotus albus* and *Tussilago farfara*. High cover of the fern species *Matteuccia struthiopteris* was found in both rivers' floodplains, mostly in combination with *Fraxinus nigra* stands. Grass plots, mainly found on bars and ecotones, showed a high abundance of *Poa* and *Agrostis sp.* in the confined river and *Poa sp.* and *Phalaris arundinacea* in the unconfined river.

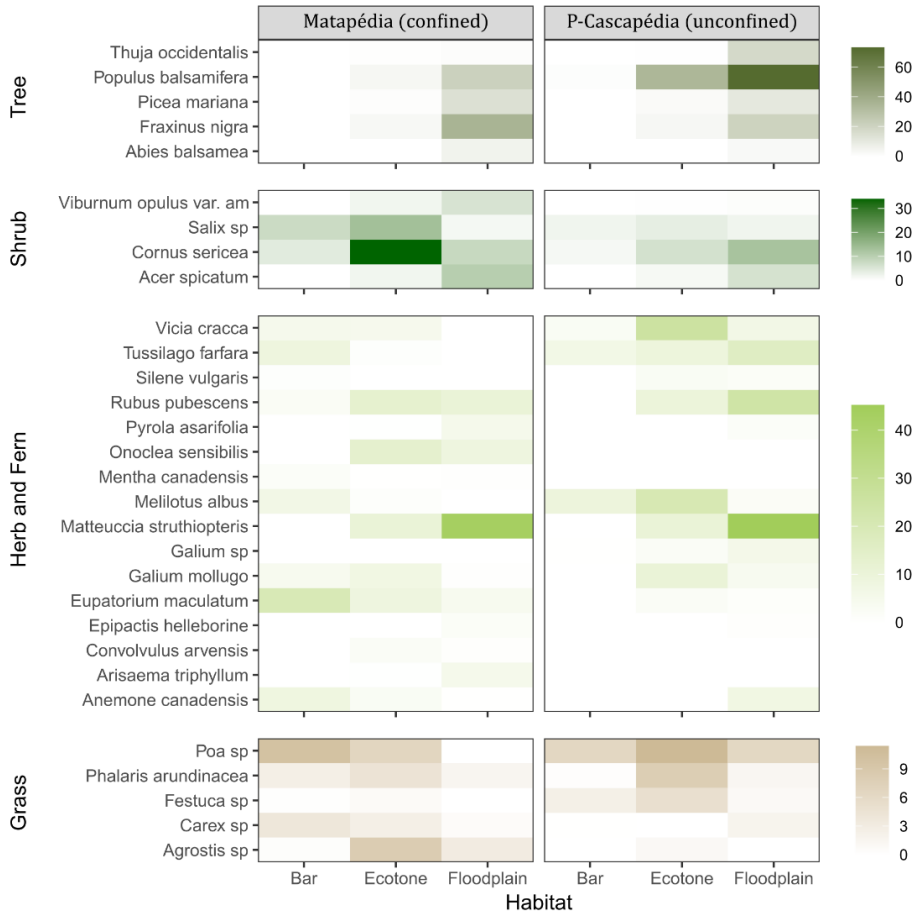


Figure 28 Mean cover of 30 species across habitats and rivers that were identified by their high loadings in a preliminary Principal Component Analysis (PCA). The colors of the heatmap discriminate the life form of the species, and the color gradient shows the mean cover in %.

Significant differences in plot composition (Hellinger-transformed abundance) were found between each group of river and habitat (Annexe II, Table 18, PERMANOVA, F = 10.76, R^2 = 0.25, p = 0.001). The Redundancy Analysis (RDA; Figure 29) showed a significant effect of environmental variables on community composition (F = 6,0, p = 0,001, adj-R^2 = 0,17). The first constrained axis RDA1 (8.8% explained variance) separated plots across the habitats, from the bars (negative end) to the forested floodplains (positive end). On this gradient, high median grain size and high unit stream power were driving high abundance of *Eupatorium maculatum*, *Salix sp.* and *Poa sp*. In contrast, high fine sediment

depth, along with long distance and high elevation relative to the wetted channel, were driving the abundances of *Fraxinus nigra*, *Matteuccia struthiopteris,* and *Populus balsamifera*. The second constrained RDA axis (RDA2, 6.9% of explained variance) distinguished plots between the two rivers. Plots in the confined Matapédia River (positive RDA2) were associated with *Onoclea sensibilis*, *Cornus sericea*, and *Fraxinus nigra*. In contrast, plots in the unconfined Petite-Cascapédia River (negative RDA2) were linked to *Vicia cracca*, *Melilotus albus*, and *Populus balsamifera*.

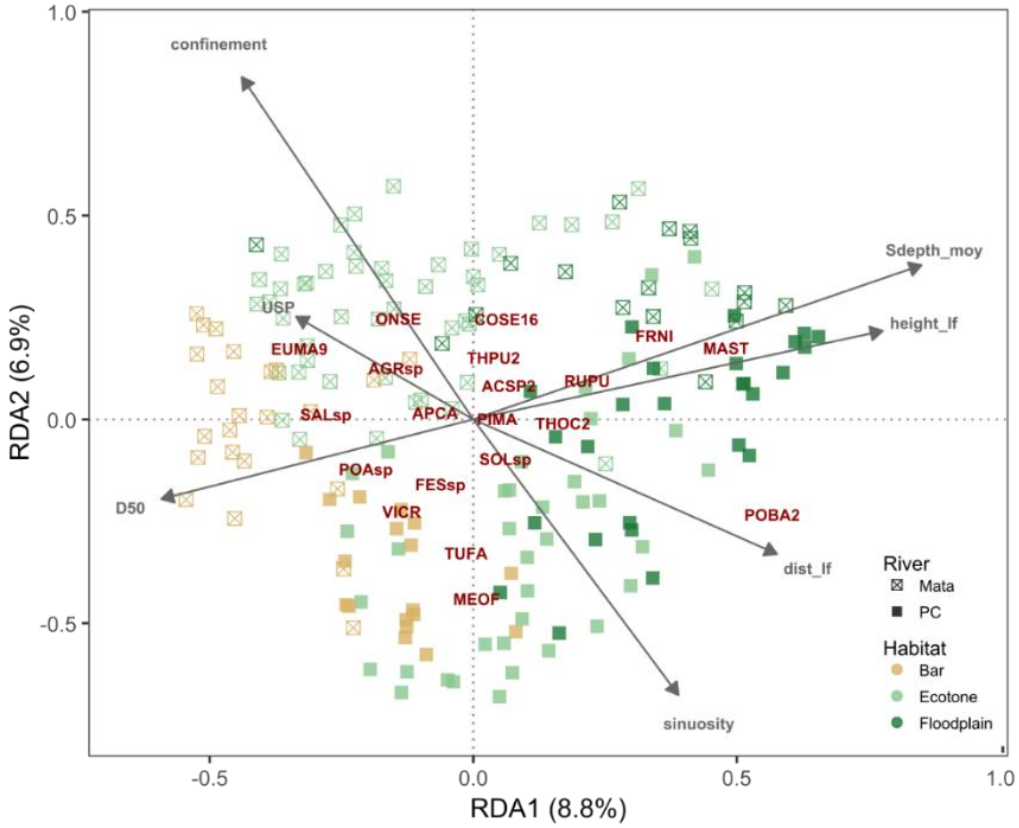


Figure 29 Redundancy Analysis (RDA) diagram of the 169 vegetation plots composition (Hellinger-transformed), constrained by selected environmental variables. The positions of the 20 species with the highest loading scores are indicated with red code labels (see Annexe II Table 17 for full species name). Predictors illustrated by arrows in grey and associated labels were first filtered through a Variance Inflation Factor (VIF) and then a forward selection was applied (see Methods for the name of the acronyms).

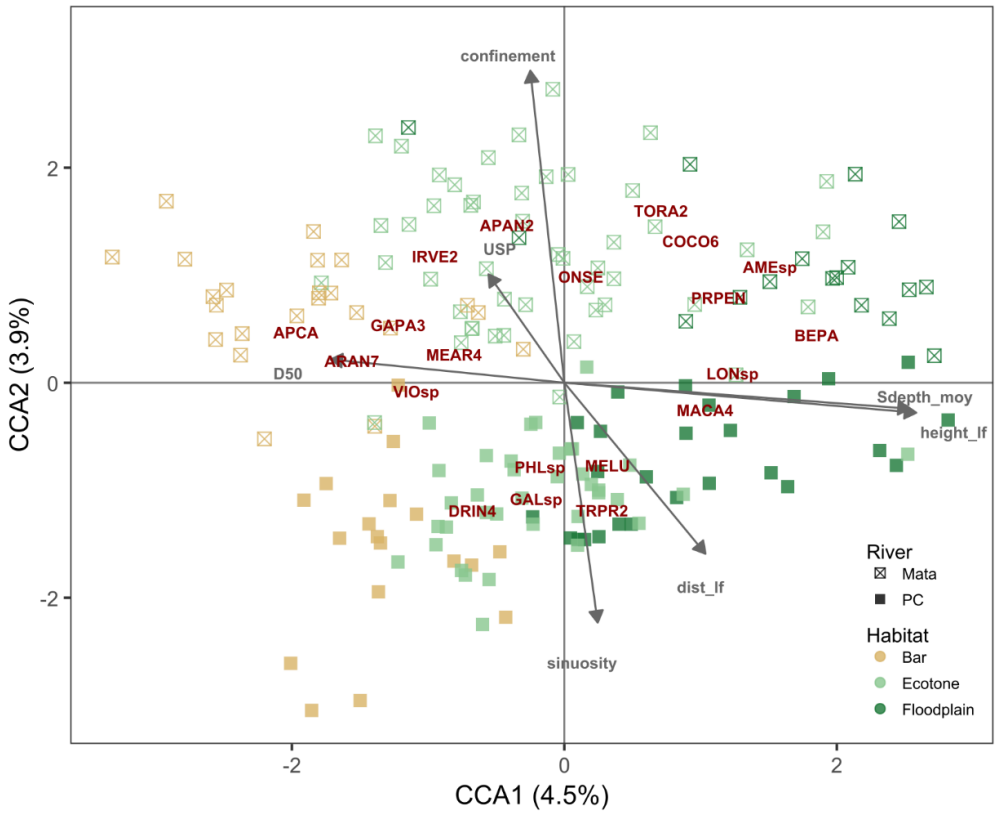


Figure 30 Canonical correspondence analysis (CCA) diagram of the 169 vegetation plots composition (presence-absence), constrained by selected environmental variables. The positions of the 20 species with the highest loading scores are indicated with red code labels (see Annexe II Table 17 for full species name). Predictors illustrated by arrows in grey and associated labels were first filtered through a Variance Inflation Factor (VIF) and then a forward selection was applied (see Methods for the name of the acronyms).

Significant differences in plot composition were also found between each group of river and habitat for presence-absence matrices (Annexe II, Table 19, PERMANOVA, F = 12.76, $R^2 = 0.28$, p = 0.001). The Canonical Correspondence Analysis (CCA; Figure 30) also showed a significant effect of environmental variables on community composition (F = 3,4, p = 0,001, adj-R^2 = 0,09). The first constrained axis CCA1 (4.5% explained variance) represents the same habitat gradient as in the RDA, dividing plots between habitats from bars to forested floodplains. Bar habitats, driven mainly by high median size grain, were associated with the presence of *Apocynum cannabinum* and *Potentilla anserina*. In contrast,

floodplain habitats, driven mainly by fine sediment depth and elevation above the wetted channel, were associated with the presence of *Betula papyfera*, *Amelanchier spp.* and *Lonicera spp.* The second constrained axis CCA2 (3.9% explained variance) also distinguished differences between river, where the confined river (positive values) was driven by high confinement and unit stream power, and the unconfined river by high sinuosity and distance from the wetted channel. The former showed high presence of *Apocynum androsaemifolium* and *Toxicodendron radicans*, while the latter was more associated with *Trifolium pratense*, *Dryas integrifolia* and species from the *Galium* genus.

Community-aggregated metrics differed between habitats and rivers (Wilcoxon test; Figure 31; Annexe II, Table 20). Mean species richness of the bar habitat was consistently the lowest among the habitats, but was significantly higher in the confined river (mean = 8) than in the unconfined river (mean = 5.7). Conversely, species richness in the floodplain habitat was 1.6 times higher in the unconfined river (mean = 15.6) compared to the confined river (mean = 9.9). Furthermore, in the unconfined river, floodplains' species richness was significantly higher than that of ecotones, but Shannon diversity was identical. The average evenness of communities across habitats and rivers showed the least variation among all community-aggregated metrics. The only difference was found in the unconfined river, where the floodplains and ecotones had significantly lower average evenness than all the other habitats throughout the study.

2.5.2 Ice-jam regime effects on community composition and diversity

The ice-jam regime significantly affected community composition in both rivers, as indicated by Hellinger-transformed data that emphasize dominant species, after accounting for all other hydrogeomorphological variables; however, the patterns and strength of these effects varied between the two systems. For both rivers, variation partitioning revealed a significant contribution from each family of explanatory variables, but the ice-jam regime was revealed to have little to no overlaps with reach-scale and plot-scale hydrogeomorphological variables (Figure 32, Annexe II, Table 21).

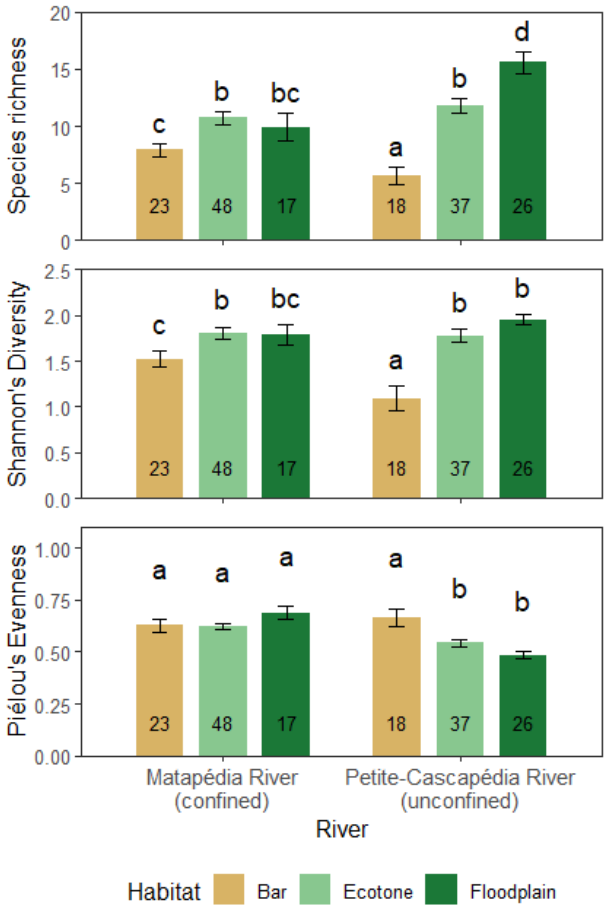


Figure 31 Mean values ± 1 SE (error bar) of (a) species richness, (b) Shannon's H diversity and (c) Piélou's evenness. Each community-aggregated metric was calculated for each habitat in each river. A pairwise Wilcox test was used to assess significant differences between river-habitat groups. The multcompLetters function (R Package MultcompView, version 0.1-1) was used to apply letters for the groupings. Different letters depict a significant difference between the means of two groups. The numbers in the graph bars represent the sample sizes for each group.

In the confined river, the main effects of ice-jam frequency and magnitude explained 2.4% (adjusted R^2) of the total variation in dominant species composition (Figure 32A, Annexe II, Table 22). The first pRDA axis was mainly driven by the ice-jam magnitude and associated and grey alder (*Alnus incana*) in high magnitude (negative values) and spotted joe-pye weed (*Eupatorium maculatum*) in low magnitude (positive values). The second pRDA axis was primarily influenced by ice jam frequency, with white sweetclover (*Melilotus*

albus) and red-osier (*Cornus sericea*) associated with high-frequency sites. In contrast, black spruce (*Picea mariana*) and species of the genus *Salix* were associated with low-frequency sites. Grass species from the *Agrostis* and the *Poa* genus were associated with both high frequency and magnitude. Floodplain habitat showed the lowest species variation across sites within the pRDA space constrained by the ice-jam regime, as indicated by the lowest point dispersion. In contrast, bars showed the highest species variation.

The main effects of ice-jam frequency and magnitude explained 4.7% (adjusted R^2) in the unconfined river, almost twice as much as in the confined river, of the dominant species composition total variation (Figure 32B, Annexe II, Table 22). The first pRDA axis explained most of the variation and was the only significant axis. Both the ice frequency and magnitude drove it, but the latter had a higher effect size. High magnitudes and frequencies (positive values of pRDA1) were associated with *Fraxinus nigra*, *Rubus pubescens*, *Matteuccia sthrutiopteris* and *Picea mariana*. In contrast, low magnitudes and frequencies were associated with *Melilotus albus* and species of the *Salix* and *Solidago* genus. While the second axis was not significant ($p = 0.103$), the high position of *Cornus sericea* along this axis indicates a possible effect of ice-jam frequency on its abundance. Compared to the confined river, all habitats showed a similar magnitude of species turnover along the gradient, as indicated by comparable mean point dispersion.

A similar pattern was observed in the analyses based on presence—absence data (CCAs), which emphasized subsidiary species. The ice-jam regime significantly affected community composition in both rivers, after accounting for all other hydrogeomorphological variables, and showed different patterns and strengths of effect between the two rivers. For both rivers, variation partitioning revealed contribution from each family of explanatory variables, but the ice-jam regime was shown to have little to no overlaps with reach-scale and plot-scale hydrogeomorphological variables (Figure 33, Annexe II, Table 23).

In the confined river, the main effects of ice-jam frequency and magnitude explained 1.4% (adjusted R^2) of the subsidiary species composition total variation (Figure 33A, Annexe II, Table 24). The first pCCA axis was the only significant axis and was driven by

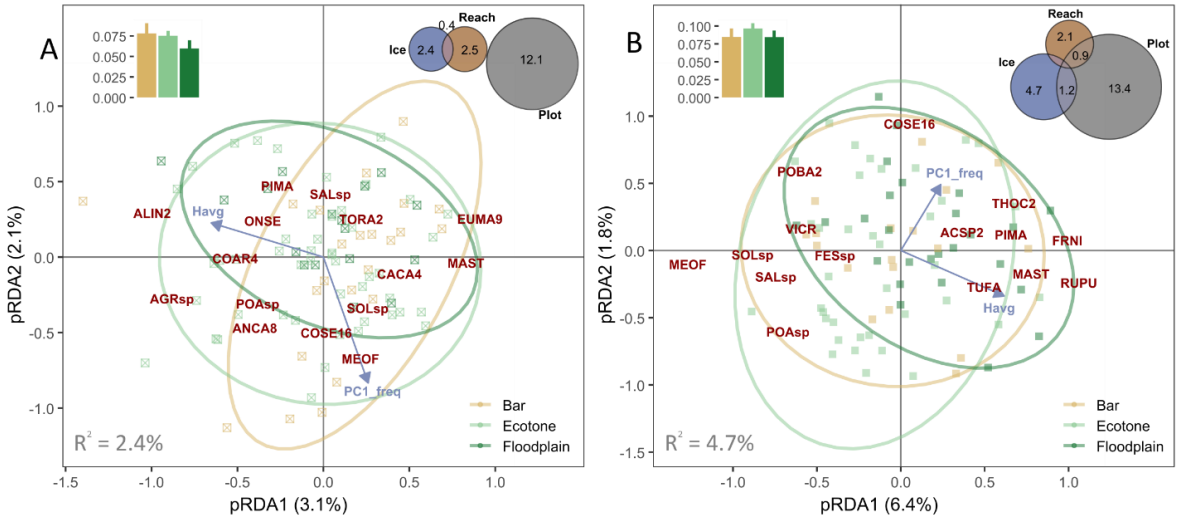


Figure 32 Partial Redundancy Analysis (pRDA; Ice Regime | Reach + Plot hydrogeomorphology) of vegetation abundance (Hellinger-transformed) constrained by ice disturbance variables (Havg: ice scars height, PC1_freq: ice jam frequency gradient) and conditioned by all the other hydrogeomorphological variables in the (A) Matapédia and (B) Petite-Cascapédia rivers. The 15 species with the highest loadings are shown with red code labels, and their scores were multiplied by 5 for better visuality. Scaling: 2 scores are shown by open squares (Matapédia River — Panel A) and filled squares (Petite-Cascapédia River— Panel B). Colors of squares and ellipses represent the three habitats. Ellipses were set at a level of 0.95 to capture most of the dispersion. Ice-jam regime variables are represented as blue vectors and labels. Bar graph at the top left shows the mean dispersion of points for each habitat measured on scaling 1 scores for better emphasis on Euclidean distance, with SE + 1 represented by the tick. On the top right is a Venn diagram from the variation partitioning of plot communities (Hellinger-transformed) against the three groups of variables described in the methodology. The numbers in the circles represent the % of explained variability in plot composition. The Venn diagram is the result of plotting an "Euler" function object (Package *eulerr*; Larssen, 2021).

both the frequency and the magnitude. However, the effects of both variables were in opposite directions and drove the presence of different species. High frequency (positive CCA1 values) was associated with *Lotus corniculatus*, *Lycopus americanus* and species from the *Sonchus* genus, while high magnitude (negative CCA1 values) was associated with species from the *Lonicera* and the *Pyrola* genus, *Silene vulgaris* and *Cornus corniculatus*. In contrast with the dominant species, the highest dispersion of points within the constrained canonical space of subsidiary species occurred in the floodplain habitat, with the highest turnover among habitats.

In the unconfined river, the main effects of ice-jam frequency and magnitude explained 3.0% (adjusted R^2), almost twice as much as in the confined river, of the subsidiary species composition total variation (Figure 33B, Annexe II, Table 24). The first pCCA axis explained most of the variation and was the only significant axis. This axis was mainly driven by ice-jam magnitude, but ice-jam frequency still had a marginal effect. High magnitudes and frequencies (negative values of pCCA1) were associated with *Cornus canadensis*, *Galium asprellum*, and *Lysimachia ciliata*, while low magnitudes and frequencies were associated with *Helianthus tuberosus*, *Lotus corniculatus* and *Echium vulgare*.

Regarding community-aggregated metrics, richness, diversity, and evenness across rivers and habitats all revealed no significant correlations related to variation in ice-jam regime variables after Benjamini-Hochberg correction (Annexe II, Table 21). However, Kendall's tau tests revealed potential trends before correction for multiple comparisons. For instance, species richness and diversity in the confined river's floodplains were negatively correlated with ice-jam frequency ($t = -0.38$ and -0.48, uncorrected $p < 0.05$), and richness was positively correlated with time since the last ice jam ($t = 0.44$, uncorrected $p < 0.05$).

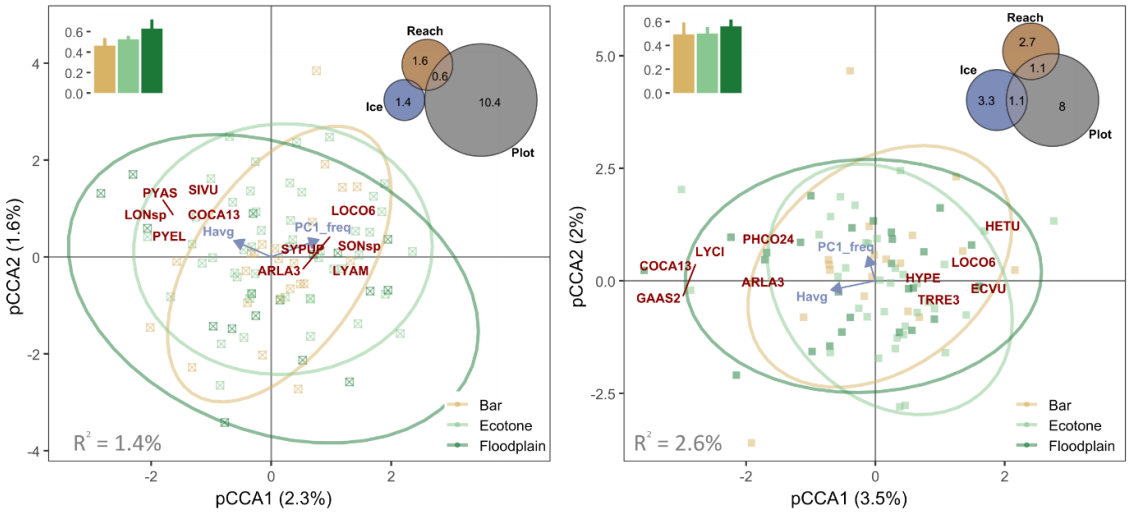


Figure 33 Partial Canonical Correspondence Analysis (pCCA; Ice Regime | Reach + Plot hydrogeomorphology) of vegetation composition (presence-absence) constrained by ice disturbance variables (Havg: ice scars height, PC1_freq: ice jam frequency gradient) conditioned by all the other hydrogeomorphological variables in the (A) Matapédia and (B) Petite-Cascapédia rivers. The 5 species with the highest loadings in the pCCA1 positive values and the 5 with the highest loadings in the pCCA1 negative values are shown as red code labels, and the scaling 2 scores of plots are shown by open squares (Matapédia River) and filled squares (Petite-Cascapédia River). Colors of squares identify the three studied habitats, and ellipses were set at a level of 0.95 to capture most of the dispersion for the three habitats (two rivers combined). Ice-jam regime variables are represented as blue vectors and labels. The bar graph at the top left shows the mean dispersion of points for each habitat, with SE + 1 represented by the tick. On the top right is a Venn diagram from the variation partitioning of plot communities (presence-absence) against the three groups of variables described in the methodology. The numbers in the circles represent the % of explained variability in plot composition. The Venn diagram is the result of plotting an "Euler" function object (Package *eulerr*; Larssen, 2021).

2.6 DISCUSSION

The results of this study revealed that hydrogeomorphological contrasts between the two rivers drove significant differences in riparian plant composition, and that ice-jam regimes exerted an additional, significant influence on riparian community composition. Using variation partitioning and constrained ordinations, we found that ice-jam frequency and magnitude together explained a portion of community composition in both the confined Matapédia River and the unconfined Petite-Cascapédia River, independently of hydrogeomorphological factors. Aligned with previous research and review papers that showed the role of ice processes in shaping vegetation structure and dynamics (Boucher et al., 2009b; Lind et al., 2014; Prowse, 2001; Uunila, 1999), this study further highlights that not only do ice-jam regimes influence riparian vegetation, but that their ecological effects vary depending on the hydrogeomorphological behaviour of the river system. Both the ice-jam regime effect size and the community species response differed between the two rivers, suggesting that the effects are context-dependent. Furthermore, the observed effects of hydrogeomorphological context and ice regimes affected not only dominant but also subsidiary species. However, richness, diversity, and evenness did not appear to be affected by the ice-jam regimes covered in this study, suggesting that ice-jam dynamics principally drive species composition and turnover rather than altering diversity patterns.

2.6.1 Differences in vegetation composition between hydrogeomorphological settings

Hydrogeomorphological variables explained the highest percentage of community composition, with 17% for dominant species and 9% for subsidiary species. Communities were significantly different across all combinations of river and habitat, indicating the critical role of local- and reach-scale hydrogeomorphological variables in shaping riparian vegetation. The highest driving factors were related to hydrological connectivity (relative distance and elevation of plots to the main channel) and sediment transport (median grain size and fine sediment depth), where high cover of pioneer herbs, grasses and well-adapted

shrubs (such as *Salix sp*.) thrived in sites closely linked to high fluvial disturbances, characteristic of early-successional communities in cold-region rivers (Egger et al., 2015; Helm & Collins, 1997; Nilsson et al., 2013). With an increase in elevation and fine sediment depth, the cover of black ash (*Fraxinus nigra*), ostrich fern (*Matteuccia sthruptiopteris*) and balsam poplar (*Populus balsamifera*) considerably increased, reflecting sites of established floodplain forests relying on periodic flooding, nutrient-rich sediment input and relatively stable substrate to allow growth and persistence (Shaw et al., 2001; Tardif & Bergeron, 1999). Even though over 65% of all species were common to both rivers, reach-scale hydrogeomorphological characteristics significantly differentiated the community's composition, highlighting the importance of fluvial behaviour, i.e., the typical patterns of channel dynamics resulting from erosion and deposition processes under prevailing hydrological and sedimentary conditions (Fryirs, 2017). High river confinement concentrates flood energy, typically leading to increased shear stress and channel incision that limit vegetation succession (Choné & Biron, 2016). In contrast, meandering dynamic rivers dissipate flood energy across floodplains, attenuating shear stress and allowing for greater landform heterogeneity and interaction between fluvial disturbances and cycles of vegetation succession-rejuvenation (Corenblit et al., 2007b; Gurnell et al., 2016a; Prugne et al., 2025). Consistent with these patterns, the confined river's ecotones were dominated by disturbance-adapted shrubs such as *Cornus sericea* and *Salix sp*. At the same time, pioneer trees were largely absent, likely due to limited lateral migration and high shear stress caused by confined flows onto these habitats. Conversely, poplar-dominated communities characterized the unconfined river's ecotones, where greater lateral mobility and flood energy dissipation may facilitate tree establishment by allowing weaker shear stress on these habitats.

Beyond ecotones, these hydrogeomorphological differences also shaped forested floodplain communities. In the unconfined river, richness and diversity were significantly higher, with balsam poplar as the dominant species. In contrast, the confined river exhibited lower diversity but greater occurrence of late-successional conifers. Poplars are known as key early successional tree species in North American rivers (Egger et al., 2015; González et al., 2018), usually associated with high and diverse understorey cover of shrubs and herbs

(González et al., 2016), and closely associated with frequent flood disturbances (Corenblit et al., 2014; Egger et al., 2015). High richness and diversity in the unconfined river's floodplains can thus be explained by the dynamic behaviour of that river, characterized by a high rate of lateral mobility and channel planform changes (Prugne et al., 2025), leading to disturbed environments that enable the establishment of various ruderal and stress-tolerant species. In contrast, floodplains in the confined river are exposed to less lateral migration (Prugne et al., 2025), which can provide more stability and increase the establishment of competitive species. Indeed, many floodplain plots were composed of late-successional conifer-dominated communities or early-successional forests dominated by the co-occurrence of black ash and ostrich fern, two species that strongly compete for light and limit the establishment of other understory plants (Brockett, 2023; Fraver et al., 2022; Pierce, 2002). Thus, the limited understory development in these habitats likely contributed to the overall low species richness and diversity observed in these confined river floodplains.

2.6.2 Ice-jam regime effects on riparian vegetation composition and diversity

After accounting for hydrogeomorphological effects, the ice-jam regime significantly influenced community composition, though responses differed between rivers. This indicates that the impact of ice-jam disturbances, while some might be partly generalized across systems, is modulated by local hydrogeomorphological conditions and species pools. In the unconfined river, *Fraxinus nigra* was most abundant in sites with frequent and high-magnitude ice-jam floods, suggesting their potential role in maintaining the moist soil conditions that favour black ash growth and persistence (Looney et al., 2018; Tardif & Bergeron, 1999). Ice-jam floods can cause overbank inundation even during moderate spring flows, which may deliver water and nutrients to floodplains at a higher rate than in less-affected sites (Beltaos & Burrell, 2021). However, in reaches experiencing frequent and intense ice runs, in-channel vegetation can be entirely removed, resulting in an abrupt transition between unvegetated riverbanks and mature floodplain forests, with little or no intermediate vertical vegetation gradient (Prowse & Culp, 2003; Uunila & Church, 2014). This pattern is reflected in the RDA results (Figure 32), where *Picea mariana* abundance

increased with ice-jam frequency in the Petite-Cascapédia River, likely indicating that intense ice disturbance prevents poplar establishment in ecotones, leaving mature conifer stands as the dominant community near the channel. In contrast, the most abundant species in highly disturbed sites of the confined river were mostly early-successional shrubs, such as *Alnus incana* and *Lonicera* spp., and grasses from the *Poa* and *Agrostis* genus. These responses align with previous research stating that frequent ice runs maintain early stages of succession in fluvial corridors through mechanical scour rejuvenation and selecting for species tolerant to erosion (Boucher, 2017b; Uunila & Church, 2014).

Despite these differences, one possible common response across each river was the high abundance of red-osier dogwood (*Cornus sericea*) over willows (*Salix sp.*) in sites highly disturbed. This pattern was clear at sites of high ice-jam magnitude in the Matapédia River, but caution is warranted for the Petite-Cascapédia River. Even though *Cornus sericea*'s position in the RDA space (Figure 32B) suggested an association with ice-jam frequency, the concerning axis was found not significant (p.value = 0.1). While this finding cannot be considered statistically robust for the Petite-Cascapédia River alone, the convergent pattern across both rivers strengthens the inference that *Cornus sericea* may be favoured under ice-jam disturbances. This pattern was, however, unexpected given prior research highlighting the adaptability to ice disturbance of willows for their flexible stems, strong rooting systems and high regenerative capacity after erosion (Lind et al., 2014; Uunila, 1999). Both willows and dogwoods are considered disturbance-tolerant shrub species that can thrive in fluvial environments due to their strong vegetative reproduction and propagation ability (Edwards, 2024; Gucker, 2012). However, compared to willow species whose been extensively studied according to their tolerance and resilience traits (Amlin & Rood, 2001; Keita et al., 2021a; Pasquale et al., 2014), dogwoods lack comparable quantitative assessments. Although their regenerative ability, fast growth, and broad environmental tolerance are acknowledged (Charles-Dominique et al., 2010; Davis et al., 2014; Gucker, 2012), existing knowledge in the literature remains largely limited to occurrence-level observations, and further research is needed to support a clear quantitative comparison with

willows. Nevertheless, these results suggest that ice-jam regimes may introduce an additional filtering mechanism that shapes species composition even among disturbance-adapted taxa.

Interestingly, the effect size of ice-jam regime on community composition differed between rivers, with frequency and magnitude explaining roughly twice as much variation in the unconfined river as in the confined river, both for dominant (4.7% vs. 2.4%) and for subsidiary (3.3% vs. 1.4%) species. This disparity may reflect fundamental differences in how each river can physically and ecologically respond to ice-jam disturbances. Ice runs are known to cause a diverse set of depositional and erosional features such as fine sediment aggregates, ice-pushed ridges and scour holes (Beltaos & Burrell, 2021; Prowse & Culp, 2003; Uunila & Church, 2014). In unconfined rivers, greater lateral adjustment capacity may allow these ice-induced features to persist and foster microhabitat heterogeneity. Because such heterogeneity facilitates the coexistence of species occupying different ecological niches (Masaki et al., 2007; Suzuki et al., 2002), ice-jam disturbances may exert a more substantial influence on community composition in these systems. Furthermore, the highly diverse communities and well-developed understorey layers in the unconfined river's floodplains likely encompass a greater diversity of species-specific adaptations and tolerance to fluvial disturbances (Catford & Jansson, 2014; Naiman et al., 2005). This greater functional diversity means that ice-jam disturbances may trigger a broader range of species-specific responses, amplifying compositional turnover in the unconfined system. In contrast, communities along the confined river's fluvial corridor may be less structured by ice runs, as concentrated flows already impose high shear stress during ice-free floods, homogenizing habitats and diluting the relative influence of ice-jam disturbances.

Unexpectedly, the magnitude and frequency of ice jams did not affect the community-aggregated metrics, despite previous studies linking ice-jam disturbances to increased species richness (Nilsson et al., 1989, 2013). Instead, richness and diversity patterns were primarily driven by river and habitat type, with floodplains in the unconfined river being significantly richer and more diverse than those in the confined river. While disturbance frequency and intensity can affect local-scale species richness (Brown et al., 2016), only disturbances of

sufficient severity and recurrence tend to alter community-aggregated metrics (Brown et al., 2001). In our case, the absence of correlation between ice-jam regimes and diversity suggests that the variations in frequency and magnitude among sites were probably too slight to produce detectable changes, and that such metrics may not be the best indicators for assessing the effects of ice-jams compared to composition. Moreover, richness and diversity in the forested floodplains of the confined river tended to decline with increasing ice-jam frequency, as revealed by Kendall's Tau test (before BH corrections). While Nilsson et al. (1989, 2013) attributed higher richness to open patches created by ice scour after a specific event and colonized by opportunistic species, our results suggest that frequent ice-jam floods may reduce species richness and diversity in established floodplain forests, possibly through extended inundation or burial that filters for a few tolerant and/or competitive species. In the unconfined river, however, the generally high baseline richness and habitat heterogeneity may buffer against such effects, diluting the influence of ice-jam disturbance on the overall community-aggregated metrics even though composition turnover seemed higher than in the confined river.

2.6.3 Challenges in studying ice dynamics in rivers and future research

Studying ice-jam and mechanical ice-breakups presents considerable challenges due to their complex, dynamic and stochastic nature. As a result, their ecological effects have been poorly studied (Engström et al., 2011; Rood et al., 2007) and as of today, little is still known about their impact on riparian vegetation. In this study, we identified years of past ice-jam events from tree scars to explore how the composition of riparian stands varied along an ice-jam regime gradient. However, tree scar analysis can lead to underestimation of frequency, if scarred trees were removed by subsequent floods or if scars healed and became undetectable (Zhong et al., 2023). Conversely, overestimation might happen if certain scars resulted from causes other than ice jams, such as impacts from various floating materials. However, from Smith and Reynolds's perspective (1983), ice is still considered the most probable cause of large scars. Nevertheless, the consistency of patterns across our results

strengthens confidence in our findings and highlights the need to study these effects at a finer scale to better understand the mechanisms underlying these responses.

Tree scars, while useful, capture only moderate to high-magnitude ice-jam events, providing no evidence of low-magnitude ice runs and jams that do not reach bankfull height (Prugne et al., 2025; Smith & Reynolds, 1983). Yet, weaker mechanical ice breakups may still accelerate bank erosion and increase shear stress on riparian banks and bars (Morin et al., 2015). While focusing on high-energy ice jams provide valuable insights into one of the most impactful disturbance types, a more complete understanding of ice-vegetation interactions will require examining the ecological effects of other forms (e.g., frazil ice, surface ice, ice dams) and processes (e.g., freeze-up, slush jam, ice push) (Engström et al., 2011; Lind et al., 2014a; Nilsson et al., 2013; Prowse & Culp, 2003; Rood et al., 2007).

To address these limitations, long-term monitoring is recommended to improve the characterization of ice processes and their effects on vegetation. For instance, establishing permanent plots in reaches prone to mechanical ice breakups, alongside the continuous characterization of ice forms (such as block deposition location, ice sheet extent, and inundation duration) and processes (including freeze—thaw cycles, mechanical abrasion, and flooding), would provide the detailed observations needed to link specific ice-related disturbances to vegetation structure and changes. Furthermore, to adequately capture the inherent spatial variability of ice dynamics and their diverse, often localized impacts on geomorphology and vegetation (Boucher et al., 2009b; Engström et al., 2011; Morin et al., 2015; Rood et al., 2007), a robust systematic sampling strategy is crucial (e.g., establishing equally spaced plots at high spatial density). This would allow researchers to better capture how various ice forms and processes alter riparian composition and structure from small-scale scour and deposition to broader patterns of mechanical and physiological stresses.

2.7 CONCLUSION

Our study provides field-based evidence that the frequency and magnitude of ice-jam regimes act as an ecological filter, modulating riparian plant composition in cold-region

rivers. We detected consistent species-turnover patterns along an ice-jam gradient using a descriptive, ordination-based analysis across two geomorphologically contrasting systems. Our results enabled us to highlight species associated with high and low ice-jam intensity and to propose mechanisms driving species composition from bars to forested floodplains across the two studied rivers. Although these effects explained only a small proportion of the variance and our analyses were mostly descriptive, they nonetheless revealed broad patterns suggesting that variation in ice-jam frequency and magnitude can influence vegetation composition, though the hydrogeomorphological context mediates this effect. Future work should explicitly model vegetation responses to ice disturbances to better predict future changes in cold river riparian plant composition. With climate change, river-ice regimes are expected to change, but their trajectories remain uncertain. Spring and midwinter ice-jam frequency could increase due to more frequent winter thaws or decrease due to fewer cold spells (Burrell et al., 2023). Ultimately, more robust statistical modelling is essential to precisely assess how the ice regime structures riparian communities. Such models will enable better prediction of vegetation turnovers under a changing climate and ice regime, providing the fundamental insights needed for riparian management and conservation in cold-region environments.

2.8 ACKNOWLEDGEMENTS

This research was financially supported by the Natural Sciences and Engineering Research Council of Canada (grand ID: RGPIN-2023-05431; grant owner: Thomas Buffin-Bélanger). Special thanks to all research professionals and assistants from the Laboratoire de recherche en dynamique et géomorphologie fluviale (LGDF) who helped gathering data during field work and helped with tree samples preparation. We also want to thank Dominic Arsenault from the UQAR for giving the access to his dendrochronological lab.

2.9 AUTHOR CONTRIBUTIONS

Matthieu Prugne: Conceptualisation, methodology, investigation, statistical analysis, writing—initial draft, writing—reviewing and editing. **Dov Corenblit**: supervision, methodology, writing—reviewing and editing. **Maxime Boivin**: supervision, methodology, writing—reviewing. **Eduardo González-Sargas**: statistical analysis, writing—reviewing. **Aziz Syammach**: statistical analysis, writing—reviewing. **Thomas Buffin-Bélanger**: funding acquisition, supervision, methodology writing—reviewing and editing.

CHAPITRE 3
LE CONTEXTE HYDROGEOMORPHOLOGIQUE MODULE LA REPONSE FONCTIONNELLE DE LA VEGETATION RIVERAINE AUX PERTURBATIONS LIEES AUX EMBACLES DE GLACE

3.1 RESUME EN FRANÇAIS DU DEUXIEME ARTICLE

1. Les communautés végétales riveraines des rivières dans les régions froides sont soumises à divers processus liés à la dynamique de la glace fluviale. La formation et la rupture des embâcles exercent d'importantes contraintes mécaniques et physiologiques. Pourtant, les réponses de la végétation à ce type de perturbations demeurent peu étudiées, en particulier sous l'angle des traits fonctionnels.

2. Nous examinons ici comment la fréquence et l'amplitude des embâcles peuvent façonner la structure fonctionnelle de la végétation riveraine dans deux rivières contrastées d'un point de vue géomorphologique (confinée vs non confinée) de la péninsule gaspésienne, dans l'est du Canada. Nous utilisons des analyses dendrochronologiques sur treize sites pour reconstruire les régimes d'embâcles, des données floristiques pour estimer l'abondance des espèces, et des bases de données de traits fonctionnels pour regrouper les espèces en guildes fonctionnelles et calculer les moyennes pondérées par l'abondance de chaque espèce pour chaque trait. Nous explorons ensuite, à l'aide d'analyses d'ordination et de corrélations, les différences clés de composition fonctionnelle entre (1) les deux rivières et (2) les sites soumis à différents régimes d'embâcles.

3. La rivière confinée présentait une forte abondance d'arbustes à croissance rapide et tolérants aux perturbations, tandis que la dynamique de la rivière non confinée favorisait l'établissement de peuplements dominants d'arbres pionniers. Sous des

régimes d'embâcle intenses, les sites de la rivière Matapédia répondaient par une augmentation de traits associés à des stratégies d'évitement, représentée par des guildes de graminées clonales (flexibilité) et de bisannuelles (cycle de vie court). Dans la rivière Petite-Cascapédia, les sites soumis à des régimes d'embâcle intenses présentaient une proportion plus élevée d'espèces de milieux humides établies sur les plaines alluviales. Dans les deux rivières, les espèces arbustives à croissance rapide, les herbacées clonales et les traits associés à une propagation végétative aérienne augmentaient le long du gradient de régime d'embâcles, dénotant la propagation végétative comme un trait d'intérêt associé aux perturbations par embâcles de glace.

4. **Synthèse** : Cette étude révèle que (1) le contexte hydrogéomorphologique est un facteur déterminant dans la structuration fonctionnelle de la végétation riveraine et (2) le régime d'embâcles sélectionne des traits spécifiques tels qu'une forte capacité de propagation végétative, mais que l'ampleur et les effets de cette sélection dépendent du contexte hydrogéomorphologique et du *pool* local d'espèces. Ces résultats soulignent l'importance de prendre en compte la dynamique des embâcles dans l'étude de la végétation riveraine des rivières en régions froides et appellent à de futures mesures *in situ* et quantitatives sur les traits fonctionnels, afin de mieux saisir les mécanismes locaux et de prédire les réponses sous des régimes de glace en changement.

Dans l'ensemble de cette thèse, ce troisième chapitre s'inscrit dans une analyse à l'échelle locale des communautés riveraines et constitue un complément au deuxième chapitre, où la réponse fonctionnelle est examinée en fonction ds contextes hydrogéomorphologiques et fluvioglaciels. Il permet d'identifier les principales différences d'un point de vue fonctionnel et offre un premier aperçu des effets structurants des régimes d'embâcle. Rédigé sous la forme d'un article intitulé « *Hydrogeomorphological context mediates the functional response of riparian vegetation to ice-jam disturbances* », il sera soumis sous peu à la revue *Journal of Ecology*.

Contribution des auteurs : Cet article fut corédigé par moi-même, mon directeur, Thomas Buffin-Bélanger, mes co-directeurs, Maxime Boivin et Dov Corenblit, ainsi que par deux collaborateurs internationaux, Eduardo González-Sargas et Aziz Syammach. En tant que premier auteur, j'ai développé l'idée originale de la recherche, conceptualisé la collecte des données, organisé et supervisé les campagnes de terrain, récolté et traité les données issues des bases de données de traits fonctionnels, procédé à leur analyse, produit les figures et rédigé la première version de l'article. Tout au long du processus, mon directeur (Thomas B-B) et mes codirecteurs (Maxime B. et Dov C.) ont participé activement à chaque étape de ce projet, notamment en apportant des conseils pour améliorer les approches méthodologiques et analytiques, en contribuant à l'interprétation des résultats et en révisant l'article. Les deux collaborateurs s'étant joints à l'équipe dans le cadre de cet article ont apporté une aide considérable aux analyses statistiques, en proposant de multiples idées et en contribuant à l'interprétation. Ils ont de plus participé à plusieurs rondes de révision. Finalement, de nombreuses personnes ont été impliquées dans la collecte des données taxonomiques et topographiques, apportant une aide significative sur le terrain. Parmi celles-ci, nous notons l'aide d'une botaniste invitée (Kassandra Croteau) et la participation des auxiliaires de recherche du Laboratoire de recherche en Géomorphologie et Dynamique Fluviale (LGDF) de l'UQAR (Félix Lachapelle, Zoé Martineu, Samuel Laroche, Alex Desliles, Étienne Gariépy-Girouard et Étienne Gauthier-Dufour).

3.2 HYDROGEOMORPHOLOGICAL CONTEXT MEDIATES THE FUNCTIONAL RESPONSE OF RIPARIAN VEGETATION TO ICE-JAM DISTURBANCES

Abstract

1. Riparian vegetation communities in cold-region rivers are subjected to various forms and processes related to fluvial ice dynamics. The formation and release of ice jams exert significant mechanical and physiological stresses on riparian vegetation. Yet, vegetation responses to such disturbance remain understudied, particularly from a functional perspective.

2. Here, we explore how ice-jam frequency and magnitude may shape the functional structure of riparian vegetation in two geomorphologically contrasting rivers (confined vs. unconfined) in the Gaspesian Peninsula, eastern Canada. We used dendrochronological analyses at 13 sites to reconstruct ice-jam regimes, floristic data to estimate species abundance, and online functional trait databases to cluster species into functional guilds and calculate community-weighted means for each trait. We then explored, through a series of ordinations and correlations, the key differences in functional composition between (1) the two rivers and (2) sites of different ice-jam regimes.

3. The confined river exhibited a high abundance of fast-growing disturbance-tolerant shrubs, while the unconfined river dynamics enabled the establishment of dominant pioneer tree stands. Under intense ice regimes, confined sites shifted toward avoidance strategies such as clonal grasses (i.e., flexibility) and biennials. In the unconfined river, sites of intense ice regimes exhibited a higher proportion of wetland species established on the floodplains, along with the absence of in-channel pioneer trees. Across both rivers, fast-growing resprouters, clonal herbs and the above-ground vegetative propagation trait increased along the ice-jam regime gradient, highlighting vegetative propagation as a key response trait to ice-jam dynamics.

4. **Synthesis:** This study revealed that (1) the hydrogeomorphological context is a key factor in shaping the functional structure of riparian vegetation and (2) the ice-jams regime selects for specific traits such as strong vegetative propagation, but its effect size and outcomes depend on the hydrogeomorphological context and local species pool. These findings emphasize the importance of accounting for ice-jam dynamics when studying riparian vegetation in cold-region rivers, and call for future *in situ*, quantitative trait measurements to better capture local-scale mechanisms and predict ecosystem responses under changing ice regimes.

3.3 INTRODUCTION

Riparian ecosystems are structured by a hierarchy of processes, from climate and geology to flow structure and sediment dynamics (Naiman et al., 2005). Within the same region, differences in plant communities can arise from distinct hydrogeomorphological characteristics. For instance, composition, distribution, and turnover dynamics can differ substantially between confined and unconfined river systems. Key differences between confined and unconfined rivers relate to channel migration potential, flow regime, shear stress, sediment size, and moisture level (Dufour et al., 2007). Channel mobility in confined rivers is restricted by natural (e.g., rocky outcrops) or anthropogenic factors (e.g., embankments), and the concentrated flows exacerbate bed shear stress. Consequently, confined reaches are subjected to incision processes, inhibition of in-channel landforms deposition (e.g., bars) and limited vegetation succession (Choné & Biron, 2016). Inversely, unconfined rivers have a higher capacity of lateral adjustment to floods due to their ability to migrate and their larger freedom of space on the valley floor (Buffin-Bélanger et al., 2015; Fryirs, 2017; Reid & Brierley, 2015). The extended floodplains and point bars in such systems enable flood energy to dissipate and modulate shear and inundation stresses, thereby supporting a more complex mosaic of vegetation communities (Camporeale et al., 2013; Corenblit et al., 2007b).

In cold regions, rivers are subjected to additional disturbances associated with ice-related processes that interact with flow and sediment regimes (Allard, 2010), such as abrasion, erosion and inundation (Chassiot et al., 2020; Engström et al., 2011; Prugne et al., 2024; Rood et al., 2007). During mechanical breakups, i.e., the process by which the ice cover breaks apart due to specific hydroclimatic conditions that leads to the transport of large ice blocks downstream the river (Beltaos, 2003), geomorphological and anthropogenic features may restrain ice floes and induce ice jams (Beltaos, 2002; De Munck et al., 2017; Turcotte et al., 2020). Ice jams formation and release have been observed to promote channel and riverbank erosion (Boucher et al., 2009b; Chassiot et al., 2020), modulate sediment dynamics (Beltaos & Burrell, 2021) and generate substantial floodplain inundations

(Boucher et al., 2009b; Peters et al., 2016; Rokaya et al., 2018), leading to mechanical and physiological disturbances on vegetation. Direct ice scours can inhibit in-channel vegetation establishment (Boucher et al., 2009b; Uunila & Church, 2014) or foster heterogeneous mosaics of successional stage (Nilsson & Jansson, 1995), while ice-jam induced floods may influence floodplain species composition and distribution (Boucher et al., 2009b; Peters et al., 2016; Rokaya et al., 2018). The degree of control exerted by ice-related disturbances in riparian ecosystems, however, remains a function of the hydrogeomorphological characteristics that modulate habitat exposure to such disturbances (Smith & Pearce, 2000b; Uunila & Church, 2014; Vandermause et al., 2021). For instance, Smith and Peace (2000b) observed that poplar establishment was more hindered by ice floes in braided reaches than in meandering reaches.

Studies of ice-related disturbances on riparian vegetation remain sparse and mainly focused on taxonomical or diversity approaches. However, these cannot reveal underlying mechanisms that link species responses to their environment and limit the generalization of results (Corenblit et al., 2024b; Janssen, 2025; Janssen et al., 2024). The functional traits approach, on its hand, has allowed transferability of results across systems and has proved efficient in linking riparian vegetation traits to hydrological and drought regimes, physical disturbances, geomorphological characteristics (e.g., river types) and anthropogenic pressures (Bejarano et al., 2018; Corenblit et al., 2024b; Diehl et al., 2017). The association between morphological, ecological, phenological and life history traits with diverse hydrogeomorphological components have contributed to a better understanding of the mechanisms underlying colonization, establishment, growth and succession of riparian vegetation (Violle et al., 2007). However, patterns of functional traits related to ice-jam disturbances are still lacking, despite some studies that highlighted some key resilience and resistance traits to such disturbances (Catford & Jansson, 2014; Engström et al., 2011). Thus, it is necessary to assess whether traits related to flood disturbances and variations can also explain community responses to ice-jam disturbances.

Here, we explore the role of ice-jam regimes in shaping the functional structure of riparian vegetation communities in two Gaspesian rivers, Canada. This study builds on our previous taxonomic analyses (Prugne et al., *In prep*), which revealed that ice-jam regimes significantly affected plant community composition and that community responses differed between the two rivers. To understand the underlying mechanisms behind these taxonomical responses, we aim to (1) determine how hydrogeomorphological characteristics shape community functional composition, and (2) evaluate how ice-jam regimes influence the direction and magnitude of functional responses in two contrasting rivers. Using global plant traits databases, we analyze functional composition through guild abundances to identify broad response strategies, and community-weighted means to identify key traits related to ice jams. This approach allows us to assess whether traits and guilds commonly associated with flooding responses can also explain vegetation responses to ice-jam disturbances, and, if so, which are most relevant.

3.4 MATERIALS AND METHODS

3.4.1 Study area and sampling design

Two mountainous gravel-bed rivers located in the Gaspesian Peninsula (Quebec, Canada) were selected for this study (Figure 34), the Matapédia River and the Petite-Cascapédia River. The former is characterized by natural and anthropogenic confinement, low lateral migration, and a steep longitudinal slope. Most of the reaches are linear with the absence of point bars but the presence of central bars and fluvial islands. The latter is characterized by high lateral mobility and avulsions, in the presence of numerous point bars and broad floodplain areas (Prugne et al., 2025). The Petite-Cascapédia River exhibit a higher rate of vegetation turnover due to its high mobility. While they are contrasted geomorphologically, they share many similarities. First, they are both located in a cold-temperate and boreal bioclimate with their floodplains dominated by mixed stands of balsam poplar (*Populus balsamifera L.*), balsam fir (*Abies balsamea* [L.] Mill., 1768), and black spruce (*Picea mariana* [Mill.] BSP., 1888). While the species pools differ across the two

rivers, they share over 60% of their species (Prugne et al., *In prep.*). Second, they share the same type of flood regime, characterized by a nivo-pluvial regime with two flood peaks: one caused by spring snowmelt and the other by autumnal heavy rains. Third, both rivers are subjected to mechanical ice breakups, which affect channel and vegetation dynamics (Prugne et al., 2025).

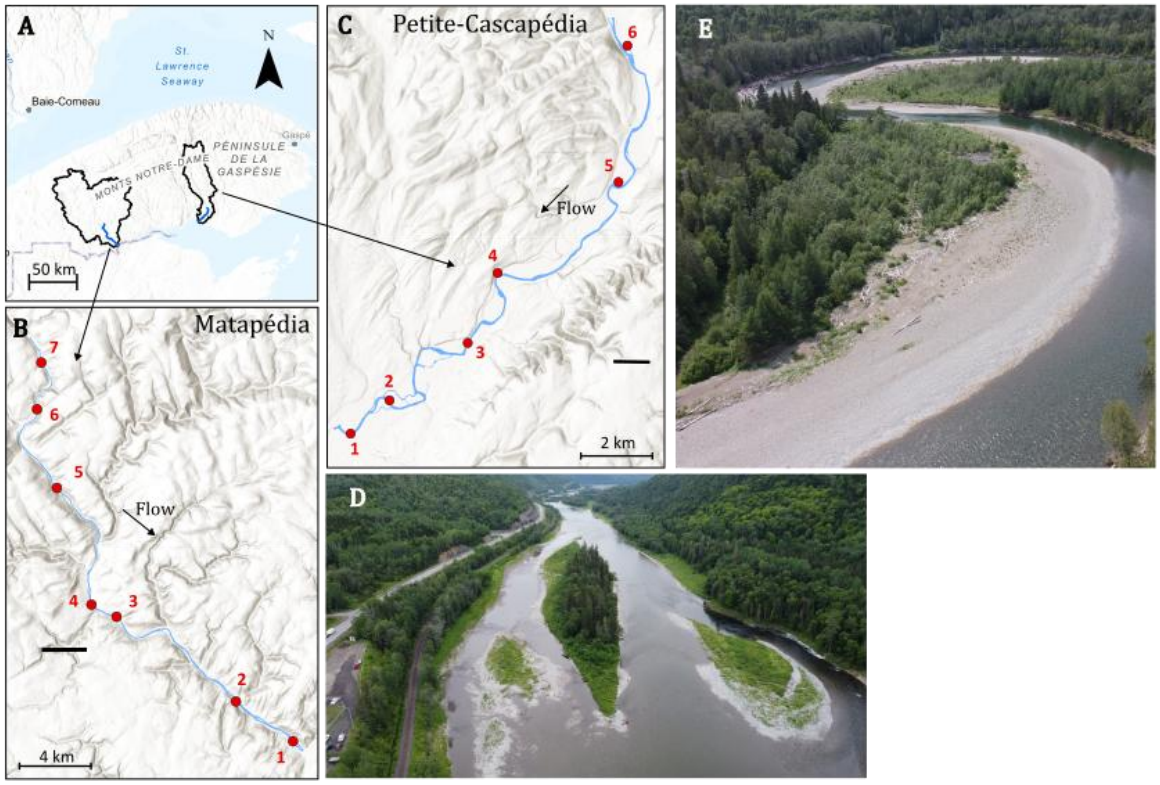


Figure 34 Location of the two study rivers and study sites. (A) Watershed boundaries of the two rivers, in black, and segments studied, in blue lines. (B) and (C) River segments studied and the sites (red circles and red label for site numbers) where dendrochronological and taxonomical samples were taken on the Matapédia and Petite-Cascapédia rivers, respectively. (D) and (E) Aerial views of characteristic reach in the Matapédia and Petite-Cascapédia Rivers, respectively.

A total of thirteen sites were selected along the two rivers, seven on the Matapédia River and six on the Petite-Cascapédia River. Two field campaigns were organized to gather floristic data during the growing season, in Summer 2022, and dendrochronological data during dormancy season in the Winter of 2022–2023. On each site, extending approximately

200 meters along the river's longitudinal axis, three to four transects were laid out perpendicular to the main channel to capture the greatest possible landscape diversity. Along these transects, a total of 169 plots were established wherever the vegetation community composition appeared visually distinct. Plot sizes varied between 2 × 2 m, 4×4 m, and 10 × 10 m, depending on whether the communities were dominated by herbs, shrubs, or trees, respectively.

3.4.2 Data

3.4.2.1 Environmental data

We characterized both hydrogeomorphological and ice-jam regimes at the reach-scale (Table 7). Aerial photographs and digital elevation models were used to measure the active channel width, longitudinal slope, sinuosity and confinement index, and the unit stream power was calculated based on the 2-year discharge interval (ANNEXE IV). For the ice-jam regime, we performed dendrochronological analysis on 98 tree cross-sections sampled across the study sites, using scars left on trees by ice impacts (Dahl et al., 2017; Lubiniecki et al., 2024). Samples were collected and sanded, and tree rings were counted using the Cdendro v.9.8.1 software. Frequencies of ice jams at the site scale were then calculated by dividing the number of years since a reference point by the number of dated scars. Because frequency estimates vary with the chosen reference point and can misrepresent site rankings along the disturbance gradient, we combined the frequencies from different methods into a composite variable (PC1_freq) using a Principal Component Analysis (ANNEXE V). Ice scars elevation above the bankfull level were also measured in the field and averaged at the site scale to be used as a proxy for ice-jam magnitude (Smith & Reynolds, 1983).

We also measured hydrogeomorphological-related variables at the plot scale to assess environmental characteristics of each community. We measured the B-axis length of 50 pebbles per plot when present and calculated the median grain size (Kondolf et al., 2003). When fine sediment deposition was present, we used a soil probe to reach the underlying

riverbed and measure the sediment depth. Finally, we used both an Emlid differential GPS and a Leica robotic Total Station to measure the perpendicular distance and elevation between the plots and the low-flow water line.

Table 7 Mean and ± 1 SE of geomorphological and ice jam regime variables for each river.

River and sites	**Matapédia (confined)**	**Petite-Cascapédia (unconfined)**
Width (m**)**	94.5 ±12.4	70.6 ±5.0
Sinuosity (unitless**)**	1.02 ±0.01	1.21 ±0.06
Confinement (unitless**)**	0.59 ±0.04	0.12 ±0.01
Slope (unitless**)**	1.27 ±0.09	1.19 ±0.12
Unit Stream Power (W/m^2 x 10^3**)**	63 ± 12	45 ± 4
Ice-jam frequency gradient (PCA1 axis**)**	0.25 ±0.58	-0.29 ± 0.56
Ice scars relative height (cm**)**	135 ± 10	88 ± 15
Time since last ice jam (yr**)**	6.1 ±1.1	2.5 ±1.2

3.4.2.2 Floristic data

At each of the 169 plots in the study, we identified all species present using identification guides directly in the field. Identification was made at the species level; otherwise, we identified only the genus. For each species in a plot, the absolute cover (in %) was estimated visually by a single person to avoid observer bias. Cover was recorded for all species across all vegetation strata; when multiple strata were present, each was estimated independently, so total plot cover could exceed 100%.

3.4.2.3 Functional traits data

We collected values for fourteen functional traits through multiple online databases (Table 8). Most of the traits were retrieved from the TOPIC (Aubin et al., 2020), TRY (Kattge et al., 2020) and USDA Plants (NRCS, 2019) plant databases, and a literature review was conducted to fill missing values until each trait covered at least 50% of each plot of the study (ANNEXE III). For species identified at the genus level, we selected three to four riparian species per genus, calculated the mean for quantitative traits, and determined the mode for categorical traits. For all traits, most plots had trait cover of 95% or higher. The lowest coverage was for specific leaf area, where about 15% of the total number of plots had a cover of between 50 and 80% (Annexe III, Figure 50). Traits were grouped in three broader categories: morphological, life history, and ecological (Table 8). For morphological traits, the morphotype and maximum rooting depth may be related to resistance against flood or ice scouring and uprooting, either through bending flexible stems (e.g., shrubs and grasses) or deep anchorage providing shear resistance (Bywater-Reyes et al., 2022a; Diehl et al., 2017). Specific leaf area (SLA) indicates the strategy used for resource acquisition, whether it is conservative or not, for which a high value has been linked to fast growth (Gibert et al., 2016; Liu et al., 2017; Pittaro et al., 2024). Seed weight indicates mechanisms by which dispersal can be promoted, such as lighter seeds being more easily carried by the wind or a persistence strategy where heavier seeds tend to withstand more stress (Westoby, 1998). The maximum height is a proxy for competitive ability for light and avoidance strategy by escaping total submergence (Westoby, 1998).

The selected life history traits describe how species survive and reproduce in disturbed environments. Raunkiaer life-form categories capture the position of overwintering buds relative to the soil or water surface and have been linked to fluvial disturbances and ice formation (Abgrall et al., 2017; Engström et al., 2011). Life cycle (annual, biennial or perennial), reproduction mode (seed, vegetative or mixed) and vegetative propagation vectors are all connected to disturbance and resilience, providing potentially fast regeneration and recolonization of disturbed patches (Catford & Jansson, 2014; Fischer et al., 2021).

Table 8 Functional traits selected for the analyses, grouped by trait category. For each trait, the variable type, unit of measurement (or modalities), and the abbreviation used in subsequent analyses are provided. See Table 33 (ANNEXE VII) for trait values and references used to retrieve them.

	Traits	Type of variable	Description and abbreviation
Morphological	Morphotype	Categorical	Morphotype_h = herbs Morphotype_s = shrubs Morphotype_t = trees Morphotype_f = ferns Morphotype_g = grasses Morphotype_h = herbs Morphotype_p = horsetail
	Maximum height	Continuous	Maximum height a species can reach (m)
	Specific Leaf Area (SLA)	Continuous	Ratio of leaf area by dry leaf weight (cm^2/g)
	Maximum rooting depth	Continuous	Maximum root depth (cm)
	Seed weight	Continuous	Weight of 1000 seeds (g)
Life history	Raunkiaer life form	Categorial	Raunkiaer_t = therophyte Raunkiaer_g = geophyte Raunkiaer_h = hemicryptophyte Raunkiaer_ch = chamaephyte Raunkiaer_mc = microphanerophyte Raunkiaer_mg = macrophanerophyte
	Vegetative propagation	Categorical	a = absent ab = aboveground organs (e.g., stolon, stem sprouts, root collar, layering) be = belowground organs (e.g., corm, rhizome, tuber)
	Life cycle	Categorical	1 = annual 2 = biennial 3 = perennial
	Reproduction mode	Categorical	s = seed only vp = principally vegetative svp = mixed
	Dispersal vector	Categorical	wi = by wind wa = by water an = by animal
Ecological	Seed persistence	Ordinal	1 = absent 2 = semi-persistent 3 = persistent
	Resprouting ability	Binary	Resprout_y = yes Resprout_n = no
	Water preference	Ordinal	1 = Dry 2 = Facultative dry 3 = Facultative generally 4 = Facultative humid 5 = Humid
	Shade tolerance	Ordinal	1 = intolerant 2 = moderately tolerant 3 = shade tolerant

Dispersal vectors represent adaptations to fluvial environments, for which hydrochorous species have an advantage in dispersing over long distances (Catford & Jansson, 2014; Merritt & Wohl, 2002).

Ecological traits included both traits related to environmental requirements and traits associated with survival strategies. Seed persistence and resprouting ability are both associated with recovery capacity after scouring events, either by regeneration from a viable seedbank or from underground and aboveground parts of a plant (e.g., rhizomes, root collars, bulbs) that can regrow after breakage of burial (Catford & Jansson, 2014; Klimešová et al., 2018). Water preference and shade tolerances relate to the ecological requirements of each species, measuring their affinity to wetlands and their light requirement which are usually linked to the successional trajectory (Lienard et al., 2015).

3.4.3 Data processing

3.4.3.1 Definition of habitat

To evaluate how the influence of ice-jam regimes differed among habitats, geomorphological attributes (grain size, sediment depth, and relative elevation) together with estimates of vegetation strata cover (<1 m, 1–5 m, >5 m) were used to group study plots into homogeneous habitat types (ANNEXE VI), leading to three main habitat types: bar, ecotone, and floodplain. Bars are areas characterized by coarse sediment and a low vegetation cover (mostly herbaceous). The term “ecotone” specifically describes transitional areas between bars and forested floodplains, including high benches, riverbanks, and young floodplain zones marked by fine sediment accumulation and dense cover of tall herbs, shrubs, or young trees (<5 m tall). The floodplain habitat refers specifically to forested floodplains, defined as zones where canopy cover by adult trees (>5 m in height) exceeds 80% (ANNEXE VI).

3.4.3.2 Functional guilds

To explore broader patterns of functional composition across habitats and rivers and along gradients of ice-jam regime, we clustered species into functional guilds. As suggested by Janssen (2025), we limited the number of traits representing different plant parts to optimize clustering and ensure results transferable to other studies. To avoid growth-form masking of variation in other functional traits, we conducted separate clustering analyses for woody and non-woody species. Woody and herbaceous species exhibit fundamentally different functional strategies in response to disturbances (Funk et al., 2017; Stromberg & Merritt, 2016), and separating them enabled the detection of finer-scale functional differentiation within each life-form group. For the woody subset, a total of five traits were selected from the database: maximum height, specific leaf area, maximum rooting depth, reproduction mode and resprout capacity. We believe this selection allows us to capture the main differences into growth strategies and competitiveness (e.g., maximum height and SLA), resistance to uprooting (maximum rooting depth) and resilience (resprouting ability). For non-woody species, resprouting ability was removed due to low trait differentiation among species (providing minimal clustering separation) and replaced by morphotype traits to distinguish herbaceous life forms. For each subset, we calculated a species-by-species trait dissimilarity matrix using generalized Gower distances to account for both quantitative and qualitative traits. This method accounts for multiple trait types and can apply group-wise weighting, balancing contributions across traits while minimizing redundancy via the optimized weighting algorithm of the *gawdis()* function from *Gawdis* R package (De Bello et al., 2021b). Hierarchical clustering using the Ward's method was then applied to the dissimilarity matrices, and a silhouette analysis over 2 to 15 clusters was performed to select the optimal number of clusters. The Analyses of Similarities test (ANOSIM) was performed with 999 permutations using the trait dissimilarity matrices to test whether species within the same guilds are functionally more similar than species in other guilds. Finally, we performed a principal coordinate analysis (PCoA) on the Gower dissimilarity matrices, followed by a permutation test (999 permutations) of vector fitting to test the strength and significance of

traits distinguishing the guilds. Continuous traits were fitted as vectors, while categorical variables were transformed to dummy-coded levels and treated as binary predictors. Each species was then assigned to its guild, and we quantified plot-level guild abundance as the sum of the percent cover of all member species.

3.4.3.3 Community weighted mean

For each of the fourteen traits, we computed community-weighted means (CWMs) to summarize the functional composition of each plot. CWMs were obtained by averaging species' trait values, weighted by their relative abundances. For continuous traits (e.g., maximum height, SLA, and maximum rooting depth), we therefore calculated the weighted mean of all species' trait values using their proportional abundances in the community. Binary and categorical variables were first converted into sets of dummy (0/1) variables with fuzzy coding applied, where taxa could express more than one category. The CWM for each dummy variable was then computed as the abundance-weighted mean of these binary values. Seed persistence, water preference, and shade tolerance were treated as ordinal traits. Each modality was assigned an integer value (0 to the highest category), and the ordinal scales were then analyzed as continuous variables.

3.4.4 Statistical analysis

We followed the same workflow for both the functional guild abundances and CWMs. To compare patterns across rivers and habitats without assuming normality, we applied pairwise Wilcoxon rank—sum tests (two-sided Mann—Whitney U) to assess whether guild abundances and CWMs differed significantly between rivers within the same habitat, for which we recorded the Wilcoxon W statistic and controlled false discovery rates using Benjamini—Hochberg correction. Differences in composition were further assessed using a multivariate permutational analysis of variance (PERMANOVA; 999 permutations) with river-habitat interactions as a fixed factor. To explore the role of hydrogeomorphology, we ran Redundancy Analyses (RDA) constrained by plot-scale and

Table 9 List of the variables used in the multivariate statistical analyses, their description and relevance as environmental variables. The family represents the defined groups of variables used in Variation Partitioning, and each variable is associated with the model(s) for which it was retained after forward selection. This table was reproduced from Prugne et al. (*In Prep.*)

Family	Variable and abbreviation	Description and relevance
Reach-scale hydrogeomorphology	Confinement	Ratio of active channel width to valley floor width; indicates lateral constraints on channel mobility and floodplain extent.
	Sinuosity	Ratio of channel length to valley length; reflects channel curvature, linked to sediment deposition patterns and habitat heterogeneity.
	Unit stream power (USP)	Quantifies the energy available to move water and sediment per unit channel area; relevant as a proxy for erosive power.
Plot-scale hydrogeomorphology	Coarse sediment median size (D50)	Median diameter of coarse sediment; relevant as a proxy to sediment transport and hydraulics.
	Fine sediment depth (Sdepth_moy)	Depth of fine-textured sediment overlaying coarser material; indicates sediment depositional processes or low-energy.
	Relative distance (dist_lf)	Distance of plot to the limit of the wetted channel; indicates connectivity to water table and flood.
	Relative elevation (height_lf)	Elevation of plot to the limit of the wetted channel; indicates connectivity to water table and flood.
Ice-jam regime	Ice-jam frequency (PC1_freq)	Composite variable (first axis of PCA) representing the frequency of ice jams; indicate the frequency of disturbances provided by ice jams
	Ice scars elevation (Havg)	Relative elevation of ice scars to the bankfull level; relevant as a proxy for ice jam magnitude

reach-scale hydrogeomorphological variables (

Table 9) on Hellinger-transformed guilds composition and on scaled (Z-scores) CWMs composition. Before constructing these models, a Variance Inflation Factor (VIF) analysis was conducted to identify highly correlated predictors, and variables with VIF> 5 were excluded. We included all remaining variables and assessed the effect sizes and significance of both the overall models and each predictor's marginal effects using permutation tests (n = 999). To disentangle the impact of ice disturbances, we ran a series of partial redundancy analyses for each river. The models were conditioned on plot-scale and reach-scale hydrogeomorphological variables and constrained by ice-jam frequency and magnitude. For the functional guilds, this approach allowed us to compare the effect size of ice-jam characteristics between the two rivers and identify both similarities and differences in responses. For CWMs, we further partitioned the analysis by trait group (morphological, life-history, and ecological; Table 8) and ran partial RDAs for each subset, conditioned with the plot-scale and reach-scale hydrogeomorphological variables and constrained with ice-jam regime variables. This enabled us to assess which trait categories were most responsive to ice-jam disturbances and, therefore, most representative of community responses to ice regimes.

All data processing and statistical analyses were conducted in RStudio v.2024.12.1+563 (Posit team, 2025). To characterize trait dissimilarities among species, we used the function *gawdis* from the *gawdis* R package (De Bello et al., 2021b) and performed hierarchical clustering with *hclust* function from the base stat package and silhouette analysis with *silhouette* function from the *Cluster* package (Maechler et al., 2025). Community-weighted means were calculated using the *functcomp* function from the *FD* package (Laliberté et al., 2014). Principal coordinate analyses were conducted using the *pcoa* function from the *ape* package (Paradis & Schliep, 2019). The *vegan* package (Oksanen et al., 2025) was used to test differences in trait composition across guilds with the function *anosim*, fit environmental vectors onto PCoA with the function *envit*, Hellinger-transform guild's abundances with the *decostand* function, run constrained ordinations with the *rda*

function and permutations tests with the function *anova.cca*, and conduct variation partitioning with the function *varpart*. Graphs were computed with the package *ggplot2* (Wickham, 2016) and enhanced with Inkscape v1.4 (2024) when necessary.

3.5 RESULTS

3.5.1 Functional guilds

3.5.1.1 Guild classification

The classification of the 115 identified species resulted in a total of 14 functional guilds (Table 10) that differed in morphological, life history and ecological traits. Woody species were segregated into six guilds (Figure 35, $R_{ANOSIM} = 0.877$, $P < 0.001$). Trait—ordination fitting (envfit, 999 perms) indicated that maximum height and rooting depth were the dominant gradients ($R^2 = 0.83$ and 0.66, both $P = 0.001$), with SLA also significant ($R^2 = 0.43$, $P = 0.006$). Reproductive strategy strongly structured the ordination, contrasting vegetative-only and mixed reproduction modes ($R^2 = 0.78$, $P = 0.001$). Resprouting ability had a weaker relationship to the guilds but was still significant ($R^2 = 0.47$, $P = 0.004$). Non-woody species were segregated into eight functional guilds (Annexe III, Figure 51, $R_{ANOSIM} = 0.865$, $P < 0.001$). Maximum height ($R^2 = 0.61$, $P = 0.001$) and morphotype composition ($R^2_{Morphotype\_h} = 0.80$ and $R^2_{Morphotype\_g} = 0.60$, both $P = 0.001$) showed the strongest correlations, while specific leaf area and rooting depth were weaker but still significant ($R^2_{SLA} = 0.28$; $R^2_{rooting\_depth} = 0.18$; $P \leq 0.005$). Similar to the woody guilds, reproductive mode significantly contributed ($R^2_{reprod\_vp} = 0.53$, $P = 0.001$; $R^2_{reprod\_s} = 0.36$, $P = 0.001$; $R^2_{reprod\_svp} = 0.16$, $P = 0.022$) to guild segregation.

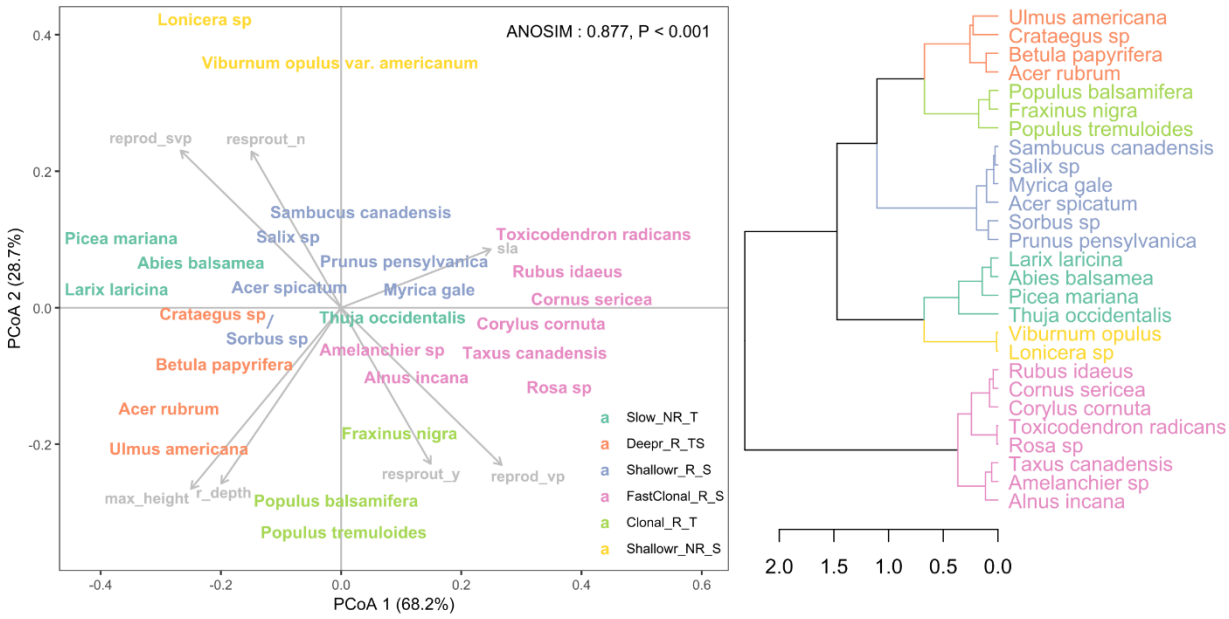


Figure 35 A) Principal coordinate analysis (PCoA) diagram of the 27 woody species based on a set of five functional traits (maximum height, specific leaf area, rooting depth, reproduction mode and resprout capacity), clustered into six distinct functional guilds. Labels' colors correspond to distinct guilds, and the plotted vectors with grey labels represent the significant traits after envfit () analysis. B) Dendrogram from the hierarchical clustering illustrating the functional similarity among the 27 woody species. Distances were computed using the Gower dissimilarity optimized with the gawdis algorithm, and species were grouped using Ward's minimum variance method.

Table 10 Functional guilds identified from clustering of species. Each guild is described by its main representative characteristic trait combination, along with the number of species included and representative examples. The first six rows correspond to woody guilds, and the remaining rows to non-woody guilds.

Guilds	Description	Nb. of species
Slow_NR_T	Tall, slow-growing trees with low specific leaf area that have no resprouting ability.	4 (e.g., *Abies balsamea, picea mariana, Thuja occidentalis*)
Deepr_R_TS	Trees and shrubs with deep roots and resprouting ability.	4 (e.g., *Acer rurbum, Crataegus sp., Ulmus americana*)
Shallowr_R_S	Shrubs with shallow roots and resprouting ability that reproduce vegetatively and sexually.	6 (e.g., *Acer spicatum, Salix sp., prunus pensylvanica*)
FastClonal_R_S	Small fast-growing shrubs with high specific leaf area and resprouting ability that mainly reproduce through vegetative reproduction.	8 (e.g., *Alnus incana, Cornus sericea, Rubus idaeus*)
Clonal_R_T	Trees with high maximum height that mainly reproduce vegetatively and have resprouting ability.	3 (i.e., *Fraxinus nigra, Populus balsamifera, Populus tremuloides*)
Shallowr_NR_S	Small shrubs with shallow roots without resprouting ability.	2 (i.e., *Lonicera sp.* and *Viburnum opulus var. americanum*)
FastSmall_H	Small fast-growing herbs with high specific leaf area.	20 (e.g., *Actaea rubra, Silene vulgaris, Vicia cracca*)
DeeprClonal_tall_H	Tall herbs with deep roots that mainly reproduce vegetatively.	11 (e.g., *Agrimonia striata, Eupatorium maculatum, Solidago sp..*)
Clonal_G	Graminoids that mainly reproduce vegetatively.	11 (e.g., *Agrostis sp., Carex sp., Poa sp.*)
SmallClonal_H	Small herbs that mainly reproduce vegetatively.	30 (e.g., *Apocynum cannabinum, Aster sp., Oxalis stricta*)
TallSlow_bi_H	Tall biennial herbs with heavy seeds reproducing only sexually.	3 (i.e., *Arctium lappa, Lathyrus latifolius, Melilotus albus*)
Fast_bi_H	Biennial fast-growing herbs with high specific leaf area that reproduce only by seeds.	7 (e.g., *Cirsium vulgare, Echium vulgare, Medicago lupulina*)
DeeprSmall_P	Small horsetails with deep root that reproduce mainly vegetatively.	2 (i.e., *Equisetum arvense* and *Equisetum sylvaticum*)
FastClonal_F	Fast-growing ferns with high specific leaf area that reproduce mainly vegetatively.	4 (e.g., *Matteuccia struthiopteris, Onoclea sensibilis, Osmunda claytoniana*)

3.5.1.2 Guild composition across rivers and hydrogeomorphological characteristics

Composition of functional guilds significantly differed between each group of river and habitat (Annexe III, Table 26 PERMANOVA, $R^2 = 30.9\%$, $F = 14.56$, $P < 0.001$). All the guilds were present throughout both the confined Matapédia and the unconfined Petite-Cascapédia rivers, but their abundance varied across both systems (Figure 36). In bars, the Matapédia River exhibited significantly higher coverage of *shallow-rooted resprouting shrubs*, *small clonal herbs,* and *deep-rooted clonal tall herbs*. In ecotones, *fast-growing resprouting shrubs, clonal ferns,* and *deep-rooted clonal tall herbs* were significantly more abundant in the confined river, but the unconfined river exhibited higher coverage of *clonal-resprouting trees* and *fast-growing small herbs*. Floodplains in both systems showed marginally greater similarity, but the unconfined river showed significantly higher coverage of *small clonal herbs* and *grasses*.

The abundances of the fourteen identified functional guilds were significantly structured by the hydrogeomorphological factors (Figure 37, RDA, adj-$R^2 = 22{,}6\ \%$, $F = 8{,}0$, $P < 0.001$). Marginal permutation tests showed that fine sediment depth (Sdepth_moy) had the strongest unique effect ($F = 12.57$, $P = 0.001$), followed by confinement index ($F = 5.65$, $P = 0.001$), relative elevation ($F = 3.44$, $P = 0.001$), median grain size ($F = 2.74$, $P = 0.007$) and unit stream power ($F = 2.72$, $P = 0.012$). The first canonical axis of the redundancy analysis (RDA1) explained 13% of the total variance and represented a gradient of plot-scale hydrogeomorphological variables distinguishing the three habitats. Negative values of RDA1 were associated with high sediment grain size and non-woody functional guilds, including *clonal grasses* and *biennial herbaceous* plants. The positive values, mostly driven by fine sediment deposition, were associated with high abundances of *ferns* and *clonal resprouting trees*. The second canonical axis (RDA2) explained 8.9% of the total variance and represented a gradient of reach-scale hydrogeomorphological variables distinguishing the two rivers. Negative values of RDA2 were driven mainly by high sinuosity and associated with *tall biennial herbs* and *clonal resprouting trees*. In contrast, the positive values were

driven by high confinement index and associated with deep-rooted *clonal herbs* and *fast-growing resprouting shrubs*.

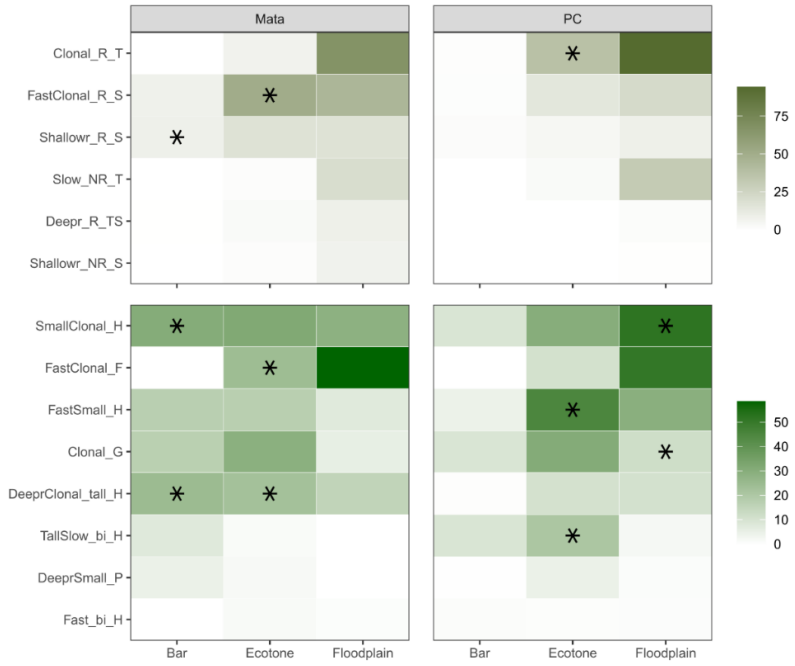


Figure 36 Mean cover of the 14 functional guilds across habitats and rivers, where colors distinguish woody (olive greens) from non-woody (dark greens) guilds and where color intensity shows the mean cover in %. Asterisks denote significant differences between rivers within the same habitat, based on Wilcoxon tests, where the marked habitat in one river shows significantly greater cover of the corresponding guild compared to the same habitat in the other river. Statistics from the Wilcoxon tests are presented in Table 27 (Annexe III).

3.5.1.3 Effects of ice-jam regime on guild composition

The ice-jam regime significantly affected Hellinger-transformed guild composition in both rivers, even after accounting for all other hydrogeomorphological variables. Still, the patterns and strengths of these effects varied between the two systems. For both rivers, variation partitioning revealed a significant contribution of each independent group of variables, and ice-jam regime shared variation with reach-scale hydrogeomorphological variables in the Matapédia River (1.1% shared variation), but not in the Petite-Cascapédia River (Figure 38).

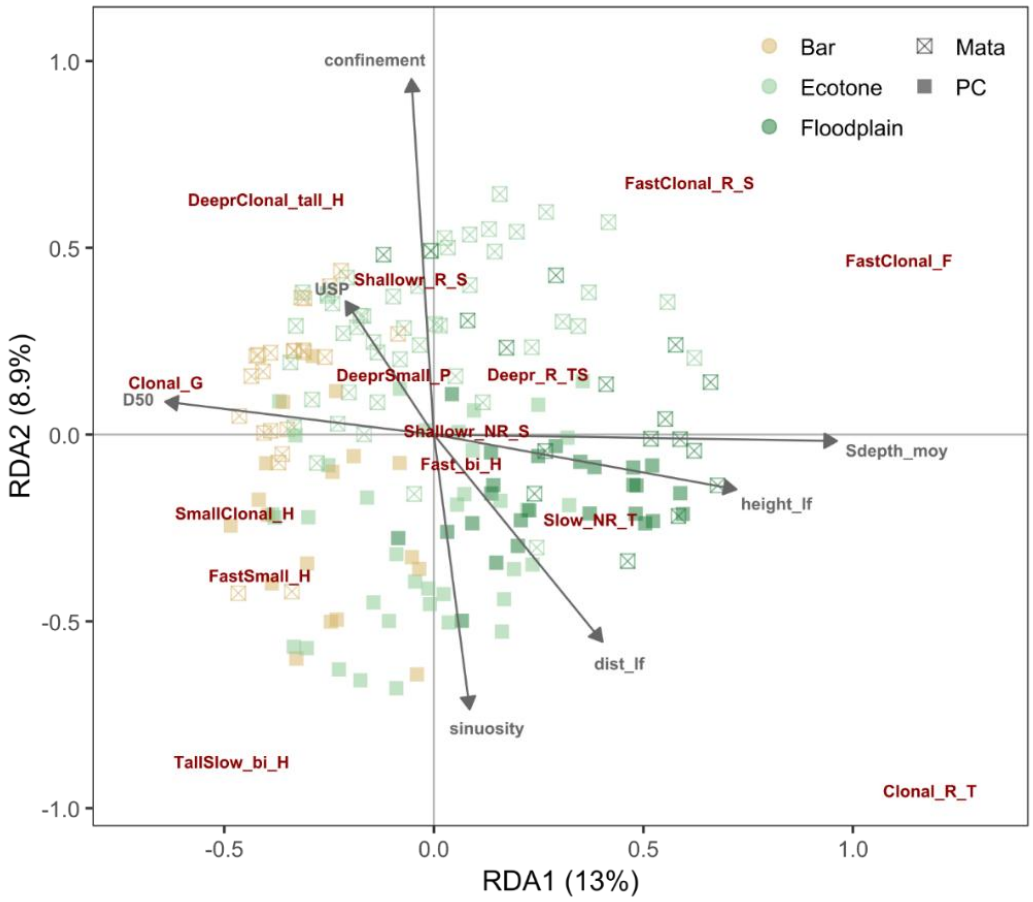


Figure 37 Redundancy Analysis (RDA) ordination of 169 vegetation plots based on the Hellinger-transformed functional guilds abundances, constrained by selected environmental predictors. Species scores (scaling 2) of the 14 guilds (multiplied by 2 for better visualization) are displayed in red code labels, and grey arrows and labels represent environmental variables. The selected environmental predictors were retained following a Variance Inflation Factor (VIF) to remove collinear variables.

In the confined river, the main effects of ice-jam frequency and magnitude explained 2.7% (adjusted R^2) of the guild composition total variation (Figure 38A). The first pRDA axis was mainly driven by the ice-jam frequency, where *clonal grasses* were driven by high frequency (negative values), and both *deep-rooted clonal tall herbs* and *shallow-rooted resprouting shrubs* by low frequency (positive values). The second pRDA axis was primarily influenced by ice jam magnitude, with *fast-growing resprouting shrubs* and *small clonal herbs* associated with high-magnitude sites (negative values). In contrast, *clonal ferns* and

deep-rooted small horsetails were linked to low-magnitude sites. In the unconfined river, the main effects of ice-jam frequency and magnitude explained 7.0% (adjusted R^2), more than twice as in the confined river, of guild composition total variation (Figure 38B). The first pRDA axis explained most of the variation and was the only significant axis. Both the ice frequency and magnitude drove it, but the latter had a higher effect size. High magnitudes and frequencies (positive values of pRDA1) were associated with *small clonal herbs*, *clonal ferns* and *slow-growing non-resprouting trees*, while low magnitudes and frequencies were associated with *fast-growing small herbs* and *slow-growing biennial tall herbs*.

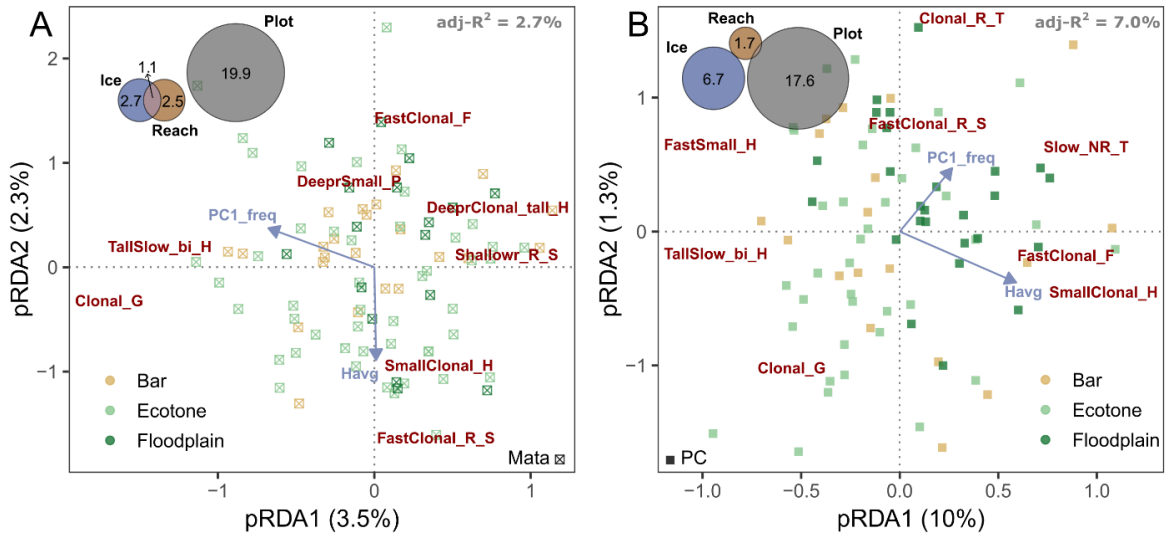


Figure 38 Partial Redundancy Analysis (pRDA; Ice Regime | Reach + Plot hydrogeomorphology) of Hellinger-transformed functional guild abundances constrained by ice disturbance variables (Havg: ice-scar height; PC1_freq: ice-jam frequency gradient) and conditioned by hydrogeomorphological variables, in (A) the Matapédia and (B) the Petite-Cascapédia rivers. Guilds are displayed in red labels, and ice-jam vectors are displayed in blue labels and vectors. Plot scores are shown in Scaling 2 as open squares (Matapédia, Panel A) and filled squares (Petite-Cascapédia, Panel B), with colors indicating the three habitat types. The inset Venn diagram (top left) summarizes variation partitioning of functional composition (Hellinger-transformed) among three groups of predictors (see Methods). Values inside circles indicate the percentage of explained variation, and the diagram was produced using the "euler" function from the eulerr package (Larssen, 2021).

3.5.2 Community-weighted mean

3.5.2.1 Differences in CWM across rivers and habitats

The community-weighted means of functional traits were significantly different across habitats and rivers (PERMANOVA, F = 8.5, R^2 = 20.7, P <0.001). Pairwise permutational analysis of variance revealed that all combinations of river x habitats were different in terms of functional traits abundance, except for bars and ecotones within the unconfined river (Annexe III, Table 28). While many traits were comparably abundant in both rivers, some key differences were found (Figure 39, Annexe III, Table 29). In the bar habitat, the strongest differences were related to ecological and regeneration traits, for which the confined river had communities with higher water preference and higher proportions of biennial species. The ecotones had the highest number of traits that significantly differed between rivers. In the confined Matapédia River, communities were characterized by higher SLA, higher proportion of species dominantly propagating vegetatively through aboveground organs, higher water preference and higher proportion of resprouting species, while the unconfined Petite-Cascapédia River showed higher proportions of species with wind-dispersal strategy, deeper roots and higher maximum height (Annexe III, Table 29). Finally, floodplain traits mainly differed in ecological and life-history traits. The confined river showed greater shrub coverage, higher SLA, and heavier seeds, while the unconfined rivers had higher proportions of water dispersion strategies and slightly more propagation by fragments.

The CWMs composition was significantly structured by hydrogeomorphological factors (Figure 40, RDA, adj-R^2 = 6,5 %, F = 2,67, P < 0.001), but the effect size was much lower than for functional guilds composition. Furthermore, only two environmental predictors (fine sediment depth and distance to low-flow) were significant after accounting for other variables in a marginal permutational test, indicating strong shared variance across the predictors. The first canonical axis of the redundancy analysis (RDA1) explained 12.8% of the total variance and represented a gradient of plot-scale hydrogeomorphological variables distinguishing the three habitats. Negative values of RDA1 were driven by high

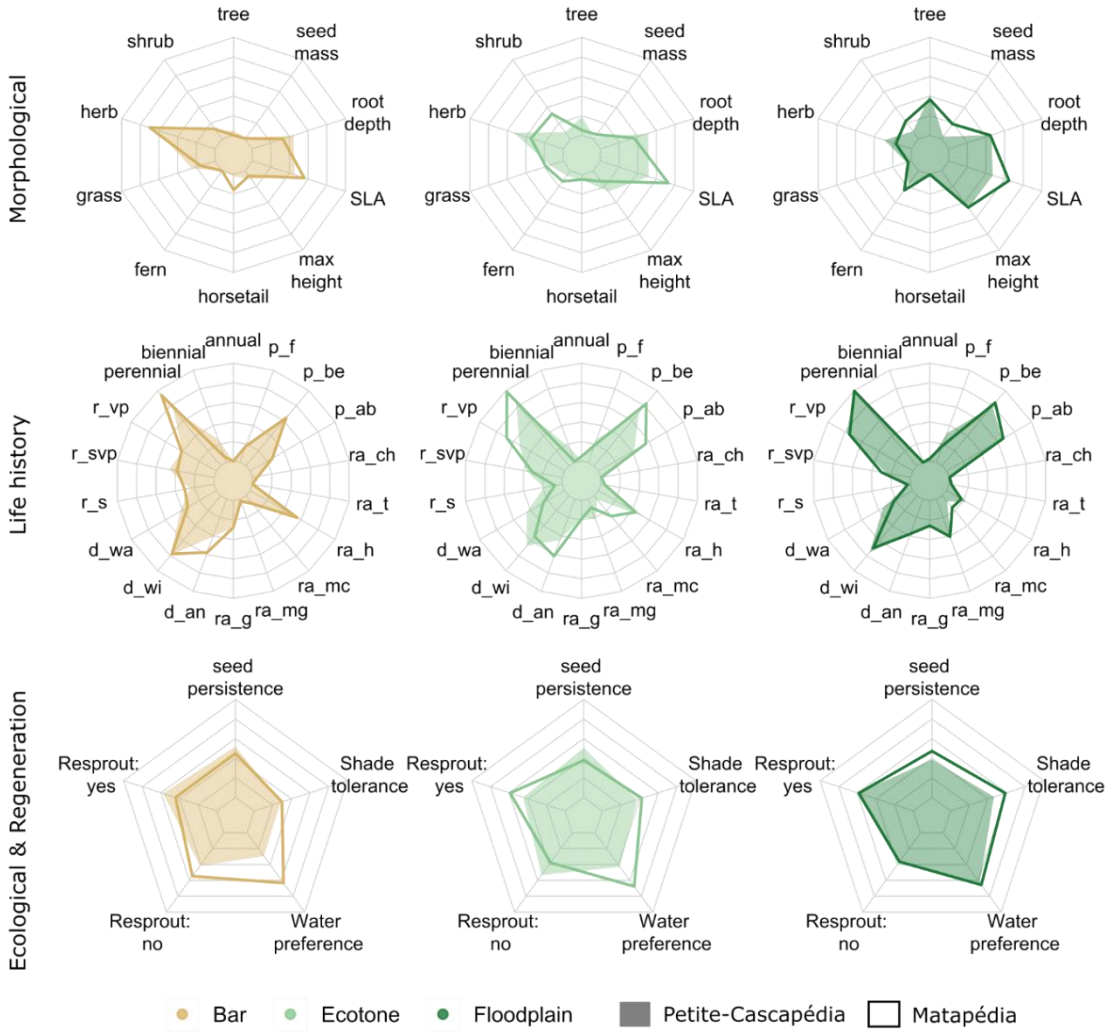


Figure 39 Radarcharts of the community-weighted means averaged to the scale of the habitat and river. Each row represents a group of traits (Morphological, Life history, Ecological), columns are divided by habitat, and filled/solid polygons identify the river. For better visual representation, all traits were scaled to 0–1 before averaging. Full names of the trait's abbreviations can be found in *Table 8*. Radarcharts were constructed with the *fmsb* R package (Nakazawa, 2024).

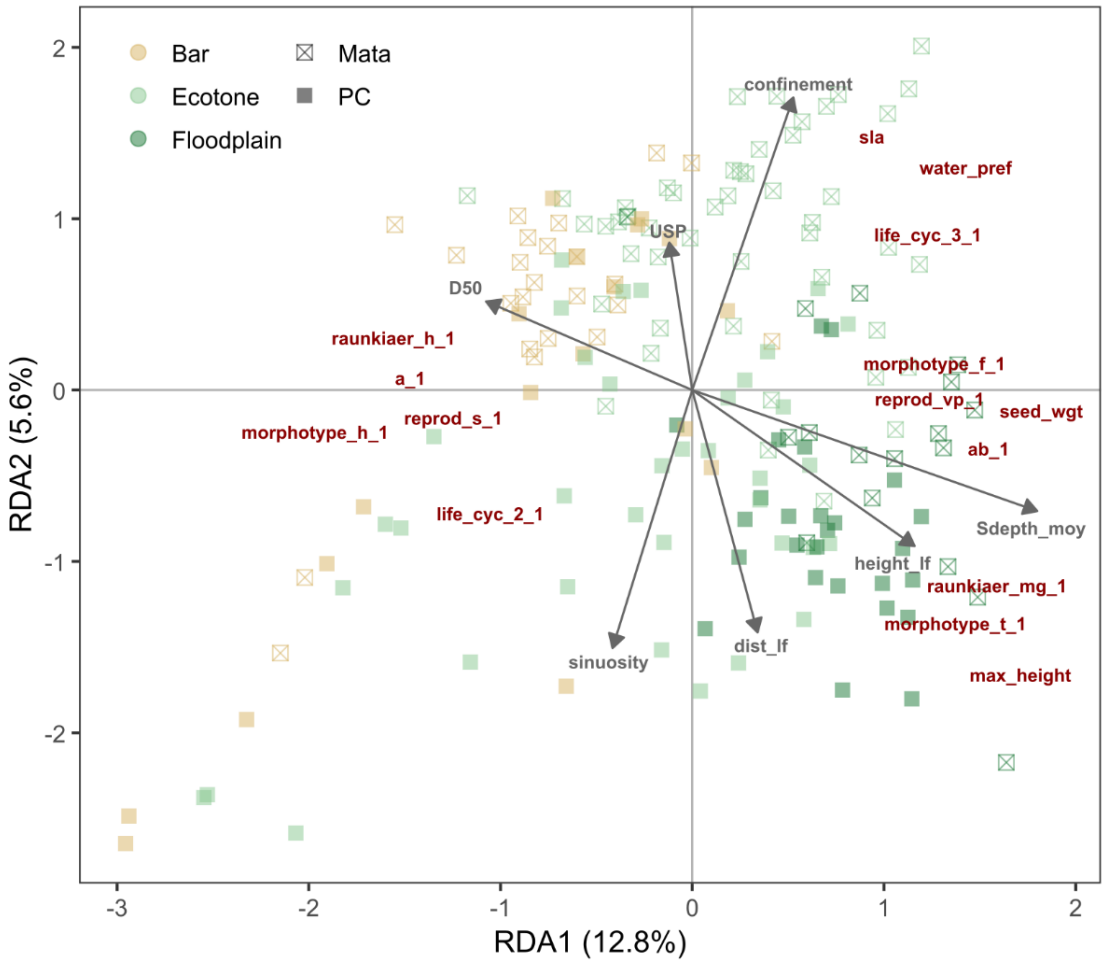


Figure 40 Redundancy Analysis (RDA) ordination of 169 vegetation plots based on community-weighted traits composition, constrained by selected environmental predictors. Species scores (scaling 2) of the 15 traits with the highest loadings (multiplied by 2 for better visualization) are represented in red code labels and grey arrows, and labels represent environmental variables. The selected environmental predictors were retained following a Variance Inflation Factor (VIF) to remove collinear variables

sediment grain size and were associated to herbaceous morphotype, hemicryptophyte Raunkiaer lifeform and absence of vegetative propagation strategy. The positive values, driven mainly by fine sediment deposition, were associated with higher seed weight, perennial species, an aboveground propagation strategy, and a vegetative-dominant reproduction mode. The second canonical axis of the redundancy analysis (RDA2) explained 5.6% of the total variance and represented a gradient of reach-scale hydrogeomorphological variables distinguishing the two rivers. Negative values of RDA2 were mainly driven by high sinuosity and were associated with tree morphotype and maximum height. In contrast, the positive values were driven by high confinement index and unit stream power and were primarily associated with high specific leaf area and water preference.

3.5.2.2 Ice-jam regime effects on CWM

Ice-jam regime significantly influenced the community-weighted means of all trait groups (morphological, life-history, and ecological) in both rivers (Table 11). However, the explained variation was consistently greater in the unconfined Petite-Cascapédia River (R^2 = 4.30–5.50%) than in the confined Matapédia River (R^2 = 1.70–2.90%). Among trait groups, life history traits showed the strongest response in the Petite-Cascapédia River, followed by ecological and morphological traits. Both ice-jam regime predictors significantly influenced all trait groups, except ecological traits, for which only frequency was significant. In contrast, ecological traits showed the strongest response in the Matapédia River, followed by life history and morphological traits. Morphological traits were mainly influenced by magnitude, life history traits by frequency, and ecological traits by both factors.

Morphological traits were the least responsive to ice-jam characteristics compared to the other trait groups, with adjusted R^2 of 1.70% for the Matapédia River and 4.30% for the Petite-Cascapédia River (Table 11). In the confined river, neither of the constrained axes reached significance (Annexe III, Table 30) but the overall model still revealed significant effects ($F = 1.91$, $p = 0.025$). Caution is therefore warranted in interpreting trait—environment associations. Nonetheless, species positions in trait space suggest that shrub morphotypes

Table 11 Results of partial redundancy analysis models testing the effects of ice-jam regime on community-weighted means of plant traits in each river (Matapédia and Petite-Cascapédia). For each trait group (morphological, life-history, and ecological), the overall model effect is reported by its F-statistics and p-value from the anova.cca () function, along with the adjusted R^2 calculated with the RsquareAdj() function in the vegan R package (Oksanen et al., 2025). Marginal effects for ice-jam frequency (PC1_freq) and magnitude (Havg) are also reported, along with F statistics and associated p-values. P <0.050 in bold.

	Matapédia			**Petite-Cascapédia**		
Morphological	Adj-R2	F	P	Adj-R2	F	P
Main model	1.70%	1.91	**0.025**	4.30%	3.13	**0.001**
frequency		1.83	0.072		3.61	**0.003**
magnitude		2.16	**0.034**		2.72	**0.011**
Life history						
Main model	2.50%	2.19	**0.004**	5.30%	3.45	**0.001**
frequency		2.84	**0.006**		3.75	**0.003**
magnitude		1.07	0.365		3.24	**0.003**
Ecological						
Main model	2.90%	2.27	**0.030**	4.70%	3.19	**0.018**
frequency		2.47	**0.047**		4.38	**0.018**
magnitude		2.97	**0.026**		2.08	0.119

may be linked to high-magnitude sites, while grasses may be more common in high-frequency sites (Figure 41A). In the unconfined river, the first and only significant RDA axis explained 6.5% of the variation ($F = 5.12$, $p < 0.001$), and was driven by both the ice-jam frequency and magnitude. Sites of high disturbance level (positive RDA1) were associated with heavier seeds, higher maximum height and a high proportion of ferns and trees, while low-intensity sites (negative RDA1) were associated with deeper roots and a higher proportion of herbaceous species (Figure 41D).

In the confined river, life-history trait composition was mainly structured by ice-jam frequency, with the first RDA axis explaining 4.0% of the total variation (Figure 41B). Sites with high-frequency of ice jams were characterized by a greater proportion of species with wind-dispersal strategies, biennials, and geophytes, whereas perennial species were more abundant in low-frequency sites. In the unconfined river (Figure 41E), the first RDA axis

was also the only significant axis and explained 7.1% of the variation. There, frequency and magnitude acted in the same direction along RDA1: high-intensity sites (positive scores) were associated with vegetative reproduction and aboveground propagation, while low-intensity sites (negative scores) were associated with water-dispersal, greater abundance of hemicryptophytes, and exclusive seed reproduction.

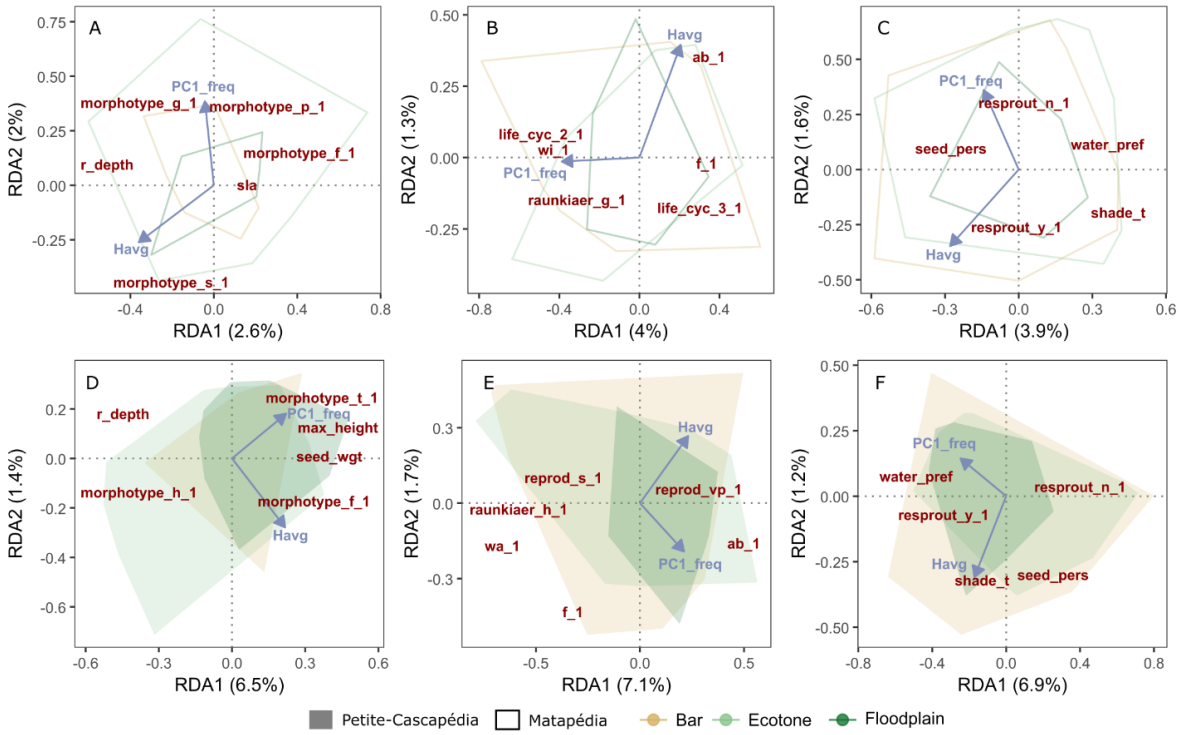


Figure 41 Partial Redundancy Analysis (pRDA; Ice Regime | Reach + Plot hydrogeomorphology) of Z-score scaled CWM traits constrained by ice disturbance variables (Havg: ice-scar height; PC1_freq: ice-jam frequency gradient) and conditioned by hydrogeomorphological variables. Each model was computed for each river (A-C Matapédia, D-F Petite-Cascapédia) and trait-group (A&D morphological, B&E life history, C&F ecological). Species scores (scaling = 2) of traits are displayed in red labels, and environmental scores of ice-jam vectors are displayed in blue vectors and blue labels. In each model, environmental vector scores were divided by 2 for better visualization. Convex hulls encompass the site by habitat.

In the confined river, despite the RDA model being overall significant ($p = 0.03$) for the ecological traits group, the axes were borderline to nonsignificant (RDA1; $p = 0.07$, RDA2; $p = 0.26$). Positions of the traits nevertheless indicated possible effects of ice, with low values of magnitude and frequency associated with higher water preference and shade tolerance, while high values of magnitude and frequency were associated with longer seed persistence (Figure 41C). For the unconfined river, the effects of ice-jam regime were more apparent, for which the first axis of the RDA was significant ($p = 0.02$) and both frequency and magnitude were in the same direction. High-intensity sites (negative RDA1) were associated with higher water preference and resprout capacity, while low-intensity sites (positive RDA1) were associated with a lower proportion of resprouting-capable species.

3.6 DISCUSSION

Our results revealed that while fluvial dynamics remained the most determinant factor structuring riparian vegetation functional composition, the ice-jam regime also contributed to explaining a portion of that variability. The notable differences both in functional guilds abundance and community-weighted means (CWM) found between the two rivers highlight the influence of hydrogeomorphological behaviour in shaping ecological strategies of riparian vegetation communities, consistent with previous studies that have shown how riparian vegetation response traits differ across different hydrogeomorphological contexts (Bejarano et al., 2018; Bywater-Reyes et al., 2022a; Corenblit et al., 2024b; Nilsson et al., 2010). Concerning ice-jam disturbances, the results revealed contrasting responses to frequency and magnitude across the two rivers, indicating that ice jams' influence on vegetation depends on the hydrogeomorphological context. However, general patterns were also identified along the ice-jam gradient in both rivers, suggesting that ice-jam dynamics may influence functional characteristics shared across systems. While the functional guild analysis revealed broad vegetation patterns linked to varying ice-jam intensities, the examination of individual CWM trait groups revealed that key traits responding to ice jams differ between rivers. Together, these results provide insights into how ice dynamics

influence riparian functional structure across contrasting rivers and point toward future research directions to better link functional traits with ice dynamics.

3.6.1 The hydrogeomorphological context explains most of plant community functional structure

Contrasts in functional guild abundances and community-weighted means between the two rivers reflect the dominant ecological strategies of riparian communities under different hydrogeomorphological constraints. In confined rivers, channels are usually more incised and flows are more concentrated, resulting in higher shear stress on in-channel landforms and less frequent flooding of the floodplains (Dufour et al., 2007). A positive correlation was observed between the confinement index and specific leaf area (SLA), suggesting the dominance of a resource-acquisitive strategy within the confined river. SLA has been linked to rapid growth, allowing plants to capitalize on a suitable environment during the period between disturbances (Catford & Jansson, 2014; Gibert et al., 2016). This is further supported by the greater abundance of *fast-growing shrub* guilds (characterized by high SLA) found in the confined river ecotones compared to unconfined river ecotones. The strong response of the *deep clonal tall herb* guild to river confinement further suggests that spatially homogeneous distribution of high shear stress across the entire channel may prevent tree establishment, selecting instead for species with uprooting-resistant traits such as flexible stems or deep roots (Bywater-Reyes et al., 2022a; Catford & Jansson, 2014; Karrenberg et al., 2003). Conversely, the high abundance of *clonal trees* guild in the unconfined ecotones reflects a strategy of persistence relying on clonal regeneration (Kozlowski & Pallardy, 2002) and long-distance colonization (Andersson et al., 2000). Because flow energy dissipates more easily, the shear stress on pioneer trees is lower, allowing them to establish. Furthermore, the community-weighted deeper roots, lighter seeds, and higher proportion of hydrochorous species indicate that they rely on flood disturbances to establish and propagate (Catford & Jansson, 2014; Corenblit et al., 2024b). This contrasts with the communities of the confined river, which display a resistance strategy to high-energy flows. The higher community-weighted seed weight of the confined river (forested) floodplains, which relates to seedling

survival under less disturbed and drier conditions (Stromberg & Merritt, 2016), suggests that these habitats are not flooded as frequently as in the unconfined river, due to the more incised channel. Conversely, the higher proportion of vegetative propagation from fragments and water vector dispersal in the unconfined floodplains suggests that recurrent fluvial disturbances shape them. Indeed, hydrochory dispersion is a dominant trait for riparian species that promote rapid colonization of disturbed sites (Andersson et al., 2000; Nilsson et al., 2010), while propagation by fragments may further promote resilience and resistance to mechanical disturbances (Catford & Jansson, 2014).

3.6.2 Ice-jam disturbances affect plant community functional structure

Along the ice-jam disturbance gradient, a high abundance of fast-growing resprouting shrubs and small clonal herbs was associated with sites of frequent and high-magnitude ice jams. The main ice-jam characteristic driving these patterns, however, differed across rivers, where these guilds were principally driven by magnitude in the confined river and by frequency in the unconfined river. Such pioneer and stress-tolerant species are generally characterized by having a high specific-leaf-area, allowing plants to withstand submergence by enhancing underwater gas (Diehl et al., 2017) and promoting high resource acquisition (Janssen et al., 2022). Despite the increased flooding and shear stress ice jams are known to cause, SLA was not associated with ice disturbances in the community-weighted means ordinations, suggesting that ice-jam dynamics do not favour high-SLA species beyond the selective effects already exerted by fluvial disturbances (Surmacz et al., 2024). However, the aboveground propagation trait (including layering, stem sprouts and root sprouts) was positively associated with ice-jam frequency and magnitude. This life history trait enables species to thrive in severely disturbed environments, providing them with the ability to resprout and propagate efficiently (Bartušková et al., 2021; Kenefick et al., 2024). Interestingly, this trait was characteristic of both the *fast-growing resprouting shrubs* and *shallow-rooting resprouting shrub* guilds, but only the former was positively affected by ice disturbances in the confined river, highlighting the potential role of rooting depth in providing sufficient shear resistance to withstand frequent mechanical stress.

3.6.3 Functional responses to ice disturbances are mediated by fluvial behaviour

While increased cover of clonal herbs and shrubs appeared to be a common response to ice disturbances in both systems, our results also revealed distinct filtering effects from the ice-jam regime in each river, underscoring the importance of considering hydrogeomorphological characteristics when studying disturbance regimes' effects on riparian plant communities.

In the confined river, clonal grasses and tall biennial herbs cover increased along the ice-jam gradient, suggesting that frequent and high-magnitude ice jams select for species with avoidance strategies that enable species to minimize the detrimental effects of disturbances (Puijalon et al., 2011). For instance, avoidance of fluvial mechanical stresses may be achieved by morphological traits such as increased flexibility to reduce drag force (Corenblit et al., 2024b). While flexibility units (e.g., flexural rigidity per unit area) were not measured in this study, the clonal grasses guild is a good indicator of this trait. Moreover, these sites were associated with deeper rooting depth, a trait that enhances anchorage against uprooting while also improving access to soil water during drought (Catford & Jansson, 2014; Diehl et al., 2017). Thus, the prevalence of clonal grasses and deep roots suggests that frequent ice disturbances filter riparian communities towards species that minimize mechanical damage through growth form, persist via clonal propagation, and secure stability and resources through deeper rooting. Avoidance can also be achieved through a short life cycle and a persistent seedbank that allows regeneration between floods (Diehl et al., 2017). The positive responses of *biennial herbs* guild abundance and seed persistence trait to high ice-jam frequency thus reflect this strategy, supporting previous studies stating that ice jams favored annual and biennial species (Lind et al., 2014a; Rood et al., 2007; Uunila & Church, 2014). Taken together, these results suggest that ice-jam regimes filter riparian communities in confined rivers towards species with morphological traits that reduce mechanical impact and life-history strategies that limit exposure to disturbances.

In the unconfined river, patterns of avoidance strategies were not as evident. Instead, we detected two different structuring effects on riparian communities. First, the higher proportion of species with a wetland affinity (i.e., water-preference trait) in sites with high ice-jam intensity may reflect the role of ice-jam floods in delivering a high rate of water and nutrient input to the floodplains (Beltaos & Burrell, 2021). Ice jams have the potential to cause overbank flooding even during low discharge flows, thereby increasing the rate of inundation and potentially maintaining wetland habitats (Peters et al., 2016; Rokaya et al., 2018). This result supports our previous taxonomical study that linked black ash (*Fraxinus nigra*), a species favored by high moisture levels (Looney et al., 2018; Tardif et al., 2021), to sites of frequent ice jams. Second, the dominance of the *non-resprouting trees* guild, composed of typical boreal late-successional species such as black spruce or balsam fir (Egger et al., 2015; Helm & Collins, 1997), points to a sharp boundary between in-channel landforms disturbance and floodplain forest dynamics. Previous studies have shown that severe and frequent ice jams can erode vegetation across the entire active channel, leaving a clear trimline that separates eroded banks from late-successional, mature forests (Morin et al., 2015; Uunila & Church, 2014). The prevalence of these well-established floodplain species in sites with high-magnitude ice jams therefore suggests a decrease in the abundance of pioneer trees. As mentioned previously, early successional communities in the unconfined river (mainly in ecotones) were dominated by the *clonal trees* guild, with *Populus balsamifera* being particularly abundant. Poplars have been observed to be especially sensitive to ice disturbance compared to low-lying shrubs, as they are more easily broken or toppled when established in areas where ice blocks move freely across bars, benches, and banks (Smith & Pearce, 2000b; Vandermause et al., 2021). Thus, it suggests that the mobile hydrogeomorphological character of the unconfined river, which allows pioneer trees to establish on its bars and benches due to lower shear stress applied on these habitats, also supports an initial species pool that makes early successional communities especially vulnerable to mechanical damage from ice-jam dynamics.

The CWM analyses further support these differences, revealing that the trait families most sensitive to ice-jam disturbance varied between rivers, where ecological traits

responded more strongly in the confined river. In contrast, life-history traits were more responsive in the unconfined river. The high frequency and magnitude of ice jams in the confined river shifted the functional composition toward increased seed persistence and decreased shade tolerance, reflecting increased cover of clonal grasses and biennial herbs, species generally known to form seedbanks (Souza et al., 2019; Williams et al., 2008). As persistent seedbanks reflect a resilience strategy under variable disturbance regimes (Casanova, 2015), this pattern indicates that ice-jam disturbances (irregular and high-energy) preferentially select species that regenerate from seed banks rather than those that rely primarily on resprouting. In contrast, vegetative reproduction and propagation were the two most responsive traits to ice-jam disturbances in the unconfined river. These can provide both resistance and resilience to flood disturbances by easily resprouting and propagating through the production of suckers, tillers, or buried shoots (Catford & Jansson, 2014). For instance, species from the Salicaceae family, including *Populus spp.* and *Salix spp.*, are very well adapted to fluvial dynamics, notably because of their capacity to propagate via fragments and rhizomes (Edwards, 2024). Instead, our results showed that the main propagation vectors associated with ice-jam disturbances were aboveground organs produced by layering, stem sprouts, or root collar sprouts. Root sprouting promotes survival and spatial expansion in frequently and severely disturbed environments by enhancing resprouting capacity (Bartušková et al., 2021), while stem sprouting promotes lateral propagation and potential resistance to hydraulic forces by stimulating multi-stemmed growth after physical damage (Fischer et al., 2021). Aligned with the proposition from Rood et al. (2007), mentioning that willows and poplars may benefit from ice damage fostering clonal propagation, our results suggest that vegetative propagation may be a key trait selected by ice-jam disturbances.

3.7 IMPLICATIONS AND CONCLUDING REMARKS

While the ordination analyses enabled us to describe functional composition patterns along an ice-jam disturbance gradient and across two contrasted rivers, the limited number of sites prevented the use of more robust regression models (e.g., generalized linear mixed model), which would have allowed a more precise quantification of trait—environment relationships. Furthermore, the use of trait values from global databases cannot capture intraspecific variability in trait expression (Albert et al., 2010; Violle et al., 2012), which is essential for understanding trait-environment interactions at the local scale (Li et al., 2022; Westerband et al., 2021). Additionally, traits of interest for environments disturbed by ice dynamics, such as stem flexibility or mechanical root strength (Catford & Jansson, 2014; Engström et al., 2011), are still sparsely documented in global databases such as TRY or TOPIC. Thus, to better capture the ecological effects that are specific to ice-jam regimes, it is recommended to use a few selected traits that would be measured *in situ* following a standardized framework (Pérez-Harguindeguy et al., 2013).

Nevertheless, the consistency of our results linking ice-jam regimes to functional responses underscores the need to account for those disturbances when studying riparian vegetation in cold rivers. This study revealed that the ice-jam regime induces slight differences in riparian vegetation response traits and suggests that trait selection is mediated by the functional diversity initially fostered by fluvial behaviour. To support this, our results showed that (1) in confined rivers, shrub-dominated assemblages shaped by high open-water shear stress buffer ice scour through resistance and avoidance traits, resulting primarily in turnovers within disturbance-tolerant guilds; whereas (2) in unconfined rivers, pioneer tree communities promoted by greater channel mobility are inherently more susceptible to ice mechanical stress despite their adaptation to fluvial morphodynamics (Corenblit et al., 2014), while ice-jam floods sustain floodplain species with high water preference. As response traits can also be associated with effect traits that influence both ecological dynamics and hydrosedimentary processes (Corenblit et al., 2024b), there is a need to quantify the local-scale effects of such disturbances better. It is even more important given that ice regimes are

anticipated to shift in the future, either intensifying due to more frequent freeze-thaw or weakening through lower frequency of cold spells (Burrell et al., 2023). To better predict the future trajectories of these riparian ecosystems, further research should focus on disentangling the effects of ice dynamics on local variation in selected functional traits. Ultimately, integrating ice dynamics into our understanding of riparian vegetation would strengthen management frameworks for cold-region rivers, supporting conservation and restoration efforts in a context of climate change.

3.8 ACKNOWLEDGEMENTS

This research was financially supported by the Natural Sciences and Engineering Research Council of Canada (grand ID: RGPIN-2023-05431; grant owner: Thomas Buffin-Bélanger). Special thanks to all research professionals and assistants from the Laboratoire de recherche en dynamique et géomorphologie fluviale (LGDF) who helped gathering data during field work and helped with tree samples preparation. We also want to thank Dominic Arsenault from the UQAR for giving the access to his dendrochronological lab.

3.9 AUTHOR CONTRIBUTIONS

Matthieu Prugne: Conceptualisation, methodology, investigation, statistical analysis, writing—initial draft, writing—reviewing and editing. **Dov Corenblit**: supervision, methodology, writing—reviewing and editing. **Maxime Boivin**: supervision, methodology, writing—reviewing. **Eduardo González-Sargas**: statistical analysis, writing—reviewing. **Aziz Syammach**: statistical analysis, writing—reviewing. **Thomas Buffin-Bélanger**: funding acquisition, supervision, methodology writing—reviewing and editing.

CHAPITRE 4
LA BIOGEOMORPHOLOGIE DES RIVIERES FROIDES : L'INTEGRATION DES DYNAMIQUES FLUVIOGLACIELLES

4.1 RESUME EN FRANÇAIS DU DEUXIEME ARTICLE

Des progrès significatifs ont été réalisés dans le domaine de la biogéomorphologie fluviale au cours des deux dernières décennies afin de comprendre les mécanismes de co-ajustement entre la végétation et les formes fluviales qui façonnent les rivières. Cependant, la compréhension des comportements biogéomorphologiques qui en a émergé repose largement sur des études menées dans des régions tempérées, avec un accent principalement orienté vers le régime de crue. Alors que plus de 20 % de la surface continentale mondiale se situe en climat froid, les rivières de ces régions demeurent largement sous-représentées en biogéomorphologie. À l'instar des rivières en milieu tempéré, les rivières de régions froides sont soumises à un éventail de formes et processus fluvioglaciels reconnus pour affecter la structure de l'écoulement, la dynamique sédimentaire, les formes fluviales et la végétation par le biais de perturbations liées aux inondations et à l'abrasion glacielle.

Cet article de synthèse est présenté sous la forme d'un essai visant à intégrer la dynamique des glaces fluviales aux concepts biogéomorphologiques afin de générer de nouvelles hypothèses sur le comportement des rivières en climat froid. Il passe d'abord en revue la littérature sur la dynamique fluvioglacielle, identifiant et décrivant les formes et processus de glace, ainsi que leurs effets sur le paysage fluvial, susceptibles d'avoir des implications significatives pour les mécanismes de co-ajustement rivière-végétation. Cet article discute ensuite de la manière dont la dynamique des glaces peut moduler l'expression et la structure des interactions biogéomorphologiques. À partir de différents cas d'étude, nous proposons l'idée que les dynamiques fluvioglacielles jouent un rôle potentiellement

important dans l'évolution et les trajectoires d'ajustement des rivières. Nous utilisons des cadres fondamentaux de la biogéomorphologie, tels que la succession biogéomorphologique fluviale, pour retracer ces modulations à travers diverses échelles spatiotemporelles, allant des traits fonctionnels à l'organisation spatiale du paysage.

Les réflexions et hypothèses présentées tout au long de cette discussion révèlent le large éventail de contrôle que la dynamique des glaces peut exercer sur différents contextes fluviaux et mettent en évidence les lacunes et les avenues de recherche essentielles pour accroître notre compréhension. Nous proposons de consacrer des efforts au suivi à long terme, aux études comparatives et à la modélisation numérique afin de tester différentes hypothèses et de cerner la place de la dynamique des glaces dans les processus biogéomorphologiques. Non seulement ces suggestions présentent un intérêt particulier pour les avancées théoriques dans la compréhension du comportement des rivières de régions froides, mais elles pourraient également fournir des perspectives utiles pour une meilleure prévision et gestion des cours d'eau dans un contexte de changements climatiques.

Dans l'ensemble de cette thèse, ce quatrième chapitre s'inscrit dans une démarche synthétique et propose une interprétation biogéomorphologique des résultats exposés précédemment. Alors que les trois premiers chapitres se sont concentrés sur les réponses géomorphologiques et écologiques à diverses échelles spatiales et temporelles, le présent chapitre vise à transposer ces conclusions dans une discussion apportant un éclairage sur les mécanismes par lesquels les perturbations fluvioglacielles peuvent influencer le fonctionnement biogéomorphologique des cours d'eau à plusieurs échelles. Rédigé sous la forme d'un article intitulé « *The biogeomorphology of cold rivers: Integration of fluvial ice dynamics* », il sera soumis au cours de l'année 2026 à la revue *River Research and Applications*.

Contribution des auteurs : Cet article fut corédigé par moi-même, mon directeur, Thomas Buffin-Bélanger, ainsi que mes co-directeurs, Maxime Boivin et Dov Corenblit. En tant que premier auteur, j'ai développé l'idée de recherche, conçu les figures et rédigé la première version de l'article. Après leur conception, les figures ont été retravaillées par un collègue du Laboratoire de recherche en Géomorphologie et Dynamique Fluviale (LGDF), Félix Lachapelle, afin d'améliorer le design graphique. Tout au long du processus, mon directeur (Thomas B-B) et mes codirecteurs (Maxime B. et Dov C.) ont participé activement à chaque étape de ce projet, notamment au travers d'innombrables discussions, qui ont suscité de riches réflexions, ainsi qu'en révisant l'article.

4.2 THE BIOGEOMORPHOLOGY OF COLD RIVERS: INTEGRATION OF FLUVIAL ICE DYNAMICS

Abstract

Significant progress has been made in the field of fluvial biogeomorphology in the last two decades regarding how vegetation and fluvial landforms co-adjust to shape rivers within different rivers and disturbance regimes. However, the understanding of biogeomorphological behaviours that emerged is largely built on studies made in temperate regions with a focus on the flood regime. While over 20% of the continental surface worldwide lies in cold climates, rivers in these regions have been largely underrepresented in biogeomorphology and warrant exploration given the presence of fluvial ice dynamics. These rivers are subjected to an array of ice forms and processes that are known to affect flow structure, sediment dynamics, fluvial landforms and vegetation through ice-related flood and scour disturbances.

This review paper presents an essay that aims to integrate fluvial ice dynamics into existing biogeomorphological concepts to generate new hypotheses about river behaviour in cold climates. It first reviews the literature on fluvial ice dynamics, identifying and describing ice forms and processes, and their effects on the riverscape (e.g., river morphology, sediment dynamics, and vegetation structure), which may have significant implications for river-vegetation co-adjustment mechanisms. The work then discusses how fluvial ice dynamics may modulate the expression and structure of biogeomorphological interactions. Based on different case studies, we emphasize that ice dynamics play a significant role in the trajectories and evolution of cold rivers. We use core frameworks from the field of biogeomorphology, such as the fluvial biogeomorphological succession, to trace these modulations across scales, from individual plant traits to landscape spatial organization.

Reflections and hypotheses presented throughout this discussion reveal the wide range of control ice dynamics can exert across different fluvial contexts and highlight key research gaps and avenues to increase our understanding. It is proposed that efforts should be made to

support long-term monitoring, comparative studies, and numerical modelling to test different hypotheses and frame the role of ice dynamics in biogeomorphological processes. Not only are these suggestions of particular interest for advancing theoretical understanding of cold rivers' behaviour, but they would also provide invaluable insights for better prediction and management in the context of climate change.

4.3 INTRODUCTION

The field of biogeomorphology has been extensively studied over the last two decades, resulting in a multitude of concepts and models designed to understand how organisms contribute to the development of landforms, and how geomorphological processes shape the distribution, composition and diversity of these organisms (Coombes, 2016; Viles, 2020). As a subfield of geomorphology, fluvial biogeomorphology has been predominantly focusing on the interactions between hydrosedimentary processes (e.g., flood, erosion, transportation and deposition), fluvial landforms and vegetation dynamics (e.g., dispersal, recruitment, establishment and succession), and has made considerable advancements to our understanding of rivers' behaviour and dynamics (i.e., understanding how landforms and vegetation co-adjust in various fluvial contexts). A paradigm shift has been crossed in the field of fluvial geomorphology, where we now fully appreciate the role of plants, not as a passive factor of rugosity interacting with flow, but rather as an active, adaptive and plastic agent modulating geomorphological processes at multiple spatiotemporal scales through a variety of mechanisms (Larsen et al., 2020).

Vegetation's main effects on fluvial landforms and hydraulic structure can be summarized into two distinct mechanisms. First, the root system increases shear stress resistance by mechanically stabilizing sediments through the formation of rootmats (Perucca et al., 2007) and by reducing the interstitial water pressure through evapotranspiration (Simon et al., 2004). Second, aerial parts (e.g., stems, branches, and leaves) add resistance to water flow, thereby reducing flow velocity and promoting sediment deposition within and downstream of vegetated patches (Gurnell et al., 2012; Polvi & Sarneel, 2018). Each species has its unique set of characteristics that modulate the extent to which it interacts with hydrogeomorphological processes, manifested as functional traits that respond to and affect fluvial processes (Corenblit et al., 2024b). Community structure of morphological and biomechanical traits (e.g., maximum height, stem density and width, flexibility), physiological (e.g., aerenchymas providing resistance to hypoxic condition during floods), phenological (e.g., timing of seed release and growth season duration) and ecological (e.g.,

type of reproduction, competitiveness, tolerance) traits are known to convey resistance and resilience to flood disturbances and modulate the magnitude and extent of vegetation communities' feedbacks on fluvial processes (Diehl et al., 2017; Janssen et al., 2020; Viles & Coombes, 2022). For instance, Corenblit et al. (2009) have observed significant differences in sediment accretion fostered by vegetation throughout different types of communities, where net accretion was about four times higher in pioneer shrubs and young trees compared to herbaceous or post-pioneer tree communities, which can be attributed to high stem density and hydrological connectivity (Politti et al., 2018).

Riparian plant community physiognomy and composition are the product of complex interactions between abiotic and biotic components (Catford & Jansson, 2014). The interaction between sediment dynamics, fluvial landform morphology, and the flood regime actively impacts the dispersal, recruitment, establishment, and survival of riparian vegetation. The flood regime (i.e., amplitude, duration, and frequency of floods) dictates vegetation distribution through various mechanisms. For instance, it promotes propagule dispersion by water flow during the rise and fall of floods (Jansson et al., 2005); it contributes to nutrient cycling by the process of deposition and erosion (Pinay et al., 2002); and it acts as an ecological filter to select species adapted to fluvial-related disturbances such as submergence, shear stress or sediment burial. Landform geomorphology, on its hand, controls communities' composition by its sedimentary texture (e.g., silt, sand or gravel) and topographic dimensions (e.g., area and elevation) that mediate the degree of exposure to flood-related stresses (Corenblit et al., 2007) and the connectivity of riparian species to groundwater (Bätz et al., 2016b).

Biogeomorphology focuses extensively on the principles of co-adjustment, the process by which vegetation communities undergo development and succession, or destruction, concomitantly with the construction or erosion of fluvial landforms. It considers not only the direct effects that landforms have on biota and vice versa, but also how those two components interact bi-directionally to shape landscapes both through time and space. Biogeomorphological studies that focus on biotic-abiotic interactions in fluvial hydrosystems

have been done in many environments. Mobile, regulated and confined rivers (Corenblit et al., 2020b; Garófano-Gómez et al., 2017; Han et al., 2020; Serlet et al., 2018) have been studied in temperate, semi-arid and arid environments (Corenblit et al., 2010; Egger et al., 2015; González del Tánago et al., 2015; Stromberg & Merritt, 2016). River's biogeomorphological dynamics are now well understood. However, rivers in cold regions that experience fluvial ice dynamics, such as ice jams and dynamic breakups, have never been addressed within the scope of biogeomorphology.

Cold-climate rivers are typically characterized by regions in which the average daily temperature remains below 0 °C for a minimum of one month each year (Chassiot et al., 2020; Ettema & Kempema, 2012). However, this definition encompasses a broad array of bioclimatic regions and biomes, including cold-temperate forests, boreal forests, and tundra (Rohli et al., 2015). For the purposes of this review, the focus is redirected to rivers that are located within cold climate regions as defined by the Köppen-Geiger system (i.e., -3 °C and below for at least a month). We have further refined that range to specifically focus on cold-temperate and boreal forests situated in continental and subarctic regions (Figure 42), excluding polar regions. Cold climate, through a long period of low temperature and the presence of snow, affects the species pool by selecting species with a short growing season lasting from 3 to 6 months (Hoppenreijs et al., 2022). Typical successional pathways of riparian forest in such environments have been described in three main successional phases: (1) pioneer deciduous species such as balsam poplars and willows, (2) early successional species such as white birch mixed with the recruitment of young spruces, and (3) late successional coniferous forest composed of cedars and balsam firs (Bonan, 1989; Egger et al., 2015; Helm & Collins, 1997). These biomes represent a significant portion of the globe's bioclimatic regions, constituting over 20% of the worldwide continental surface, and exceeding 50% within North America (Peel et al., 2007). In the northern hemisphere, more than one river out of two experiences ice dynamics (Rokaya et al., 2018), emphasizing the need for a better understanding of these processes on riverscapes.

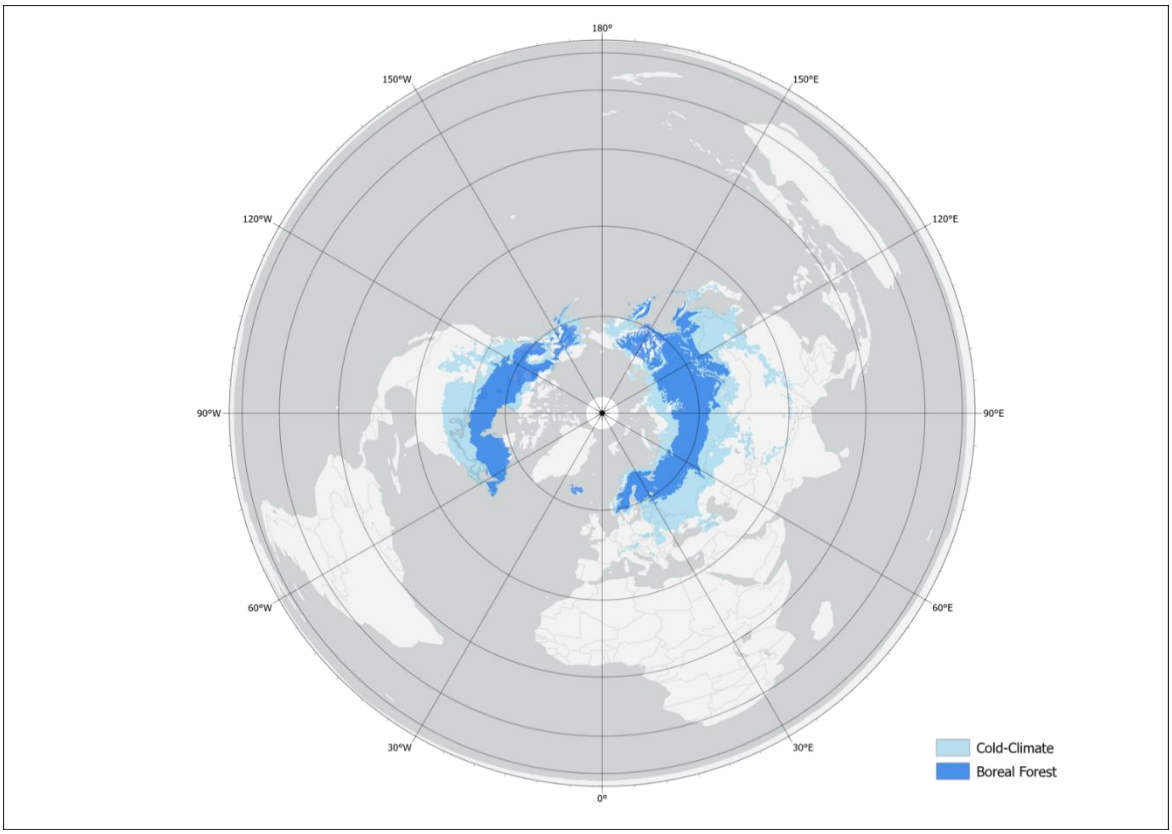


Figure 42 Location of the regions with potential presence of ice-related dynamics, where temperatures reach values below -3 ˚C for over a month in a year. The map is based on the Köppen-Geiger climate classification, for which data were taken from Beck et al. (2023).

The purpose of this synthesis paper is to examine how fluvial ice processes affect the biotic and abiotic components of rivers and to discuss their potential effects on biogeomorphological dynamics (i.e., co-adjustment dynamics, successional processes, and spatiotemporal distributions and structures) in cold-region rivers. We first describe key ice-related processes and their known effects on riverscapes. We then position ice dynamics as an environmental driver within the biogeomorphological frameworks by proposing hypothetical processes and scenarios. Presented as an essay, this paper aims to deepen reflections on the biogeomorphological character of cold-region rivers, generate hypotheses to guide future research, and stimulate work in these understudied regions.

4.4 ICE DYNAMICS AS A DISTURBANCE REGIME

A variety of ice-related forms and processes have been covered in the last decades to highlight their effects on hydraulics, geomorphology and vegetation (Table 12), revealing how their frequency and magnitude highly vary both spatially and temporally because

Table 12 Main ice-related processes and their known effects on hydraulics, geomorphology and vegetation.

Processes	Hydraulic effects	Geomorphological effects	Impacts on vegetation	Reference
Freeze-thaw		Preparatory subaerial processes Needle-ice formation and lost cohesiveness of riverbanks		Turcotte et al., 2011; Yumoto et al., 2006
Ice dam (anchor ice)	Reduced backwater velocity Increased backwater depth Riverbank flooding Redirected flow	Fine-sediment local deposition Localized erosion from redirected flow	Physiological stress—Anoxia from inundation and burrowing	Lind and Nilsson, 2015
Bankfast and riparian ice		Erosion and transport of sediment	Mechanical stress—Bank failure entraining vegetation — Physiological stress	Engström et al., 2011; Turcotte et al., 2011
Ice abrasion	Increased shear stress Increased water depth Inundations	Important erosion and transport of sediment—Ice-scoured banks Inundation and floodplain aggradation	Mechanical stress—Scarring, bending, fracturing, shearing, toppling, uprooting	Beltaos, 2003; Vandermause et al., 2021; Lind et al., 2014; Boucher et al., 2012
Ice Jam formation	Decreased backwater velocity Increased backwater depth Important floodplain inundations Redirected flow	Erosion—Bank erosion from lateral ice pushing; creation of gullies and scour holes Deposition—Floodplain aggradation from inundation and pushed sediment forming levees	Inputs of nutrients in the floodplain Mechanical stress—Erosional processes	Smith and Pearce, 2002; Beltaos, 2003; Vandermause et al., 2021; Boucher al., 2012
Ice Jam release	Increased shear stress Increased water depth Inundations	Important erosion and transport of sediment—Ice-scoured banks Inundation and floodplain aggradation	Mechanical stress—Scarring, bending, fracturing, shearing, toppling, uprooting	Smith&Pearce, 2002; Beltaos, 2003; Vandermause et al., 2021; Boucher al., 2012

of the complex interactions between ice dynamics (i.e., crystallization, ice transport and ice forms) and fluvial dynamics (i.e., water flows, sediment erosion, transportation and deposition, bedform adjustments) (Allard, 2010; Bergeron et al., 2011). They represent important disturbance regimes that drive the geomorphological and ecological structures and functions of cold rivers (Rokaya et al., 2018). The disturbance regime can be defined as the recurrent nature of events that affect ecosystems physically and biologically over space and time, characterized by the types of disturbances (e.g., flooding, fire, anthropogenic pressures) and their frequency, intensity, and duration. It is a central concept in the study of river systems, as it provides a framework for understanding how they respond to and adjust to different disturbance regimes. To understand how ice operates as a disturbance regime, it is necessary to describe the two phases during which its geomorphological and ecological impacts are most pronounced: freeze-up and breakup.

The freeze-up phase is defined as the transitional period when the river begins to freeze and gradually shifts from open waters to total channel icing (Beltaos, 2013; Lindenschmidt, 2020). It is triggered either by border ice formation (i.e., thermal freezing when temperature attains 0 °C) or through a more complex process initiated by frazil production (Lindenschmidt, 2020). In supercooling conditions (i.e., temperature <0°C) and turbulent flows, the production of frazil ice leads to the formation of ice slush and ice pans that are transported downstream, accumulate when facing a physical barrier (e.g., channel narrowing, stable ice cover, islands), and ultimately consolidate to form a stable ice cover. Frazil ice that is pushed toward the channel bed, such as in a riffle section, may also adhere to the substrate and build up to form an anchor ice. Acting like a dam, it can reduce upstream flow velocity, promote sediment deposition and increase backwater level (Turcotte et al., 2011b). In some cases, e.g., a highly developed ice dam within a small river, the wetted area of the fluvial corridor can double (Engström et al., 2011; Lind & Nilsson, 2015). Flooded riparian habitats may then be disturbed by riparian ice, which can cause frost burn or uproot plants trapped in an ice sheet when it is displaced.

The breakup phase is defined as the period when the river ice is being removed and is divided into two types (Beltaos, 2003): mechanical (also known as active) and thermal (or passive). Thermal breakups manifest as a slow thawing of ice through the increase of temperature and insolation, a process that progressively diminishes the river ice cover and moderately increases the water level (Beltaos, 2003). Conversely, mechanical ice breakups occur when the ice cover fractures, resulting in the transport of ice blocks downstream in the river. These typically occur when a substantial input of water (e.g., spring heavy rains) meets a solid, intact ice cover, but depend on an array of hydroclimatic conditions (e.g., temperature and precipitation) and ice cover characteristics (e.g., thickness, strength, density). Vandermause et al. (2021) have identified three distinct ice-related erosion processes that occur during mechanical breakups: ice rubbles, ice floes, and ice congestion. Erosion caused by ice rubble, consisting of ice blocks 1 to 10 meters wide, happens mainly through two mechanisms: grinding the bank surface and scouring the near-surface of the bank. These processes lead to significant undercutting of riverbanks. (Chassiot et al., 2020). In contrast, ice floes, which entail much larger ice blocks spanning from 10 to 100 meters in width, occupy the entirety of the channel and move downstream with relatively high speed, and have been associated with important events of erosion and sediment transport (Beltaos & Burrell, 2021; Boucher et al., 2009b; Vandermause et al., 2021). However, the extent of erosion is influenced by the magnitude of the erosive forces, as well as the structural characteristics and size distribution of the sediments, and the protective capacity conferred by vegetation (Beltaos & Burrell, 2021). Lastly, ice congestion occurs when stabilized ice blocks build up and become stuck against physical barriers such as elevated geomorphological features or riparian trees, leading to block immobilization, channel obstruction, and an eventual ice jam.

Ice-jams display substantial spatial and temporal variability due to a range of climatic, hydraulic, and geomorphological factors (Beltaos, 2002; De Munck et al., 2017). De Munck et al. (2017) identified five major factors that initiate ice congestion and potential ice jams: (1) high sinuosity where ice blocks stabilize in the outer bends of meanders, (2) sudden width decreases downstream in linear channels, reducing the transit capacity of ice blocks, (3)

confluences where breakup events are not triggered simultaneously, (4) the presence of fluvial islands leading to ice block stabilization at the head of the island or congestion on either side due to virtual width reduction, and (5) anthropogenic structures such as bridges that impede the passage of ice blocks. During ice jams, water levels upstream of the obstruction can rise by many meters for the same recorded discharge, resulting in significant flooding (Rokaya et al., 2018). Because of the obstructed channel, flows may be redirected toward the bottom or sides of the jams, increasing bed and bank shear stress through the intensified local flow velocities they generate (Chassiot et al., 2020; Smith & Pearce, 2002). The release of an ice jam can lead to a surge of fast-flowing water carrying a large number of ice blocks of various sizes downstream. These surges, known as "javes" (for *ja*m and wa*ves*), can rapidly elevate water levels downstream and considerably increase the flow sediment concentration (Rood et al., 2007). For example, in the Athabasca River, a jave was observed to increase downstream water levels by up to 4.4 meters in just 15 minutes, with suspended sediment concentrations 4.2 to 6.5 times higher than during open-water floods with equivalent discharges (Beltaos & Burrell, 2021).

4.5 KNOWN EFFECTS OF ICE DYNAMICS ON RIVERSCAPES

Direct and indirect disturbances generated by ice processes have only been sparsely investigated in recent decades. Still, growing research efforts are now improving our understanding of how they affect water flows, geomorphology, and vegetation. Going from frazil and anchor ice formation to dynamic breakups and ice jams, many reviews have attempted to synthesize the effects of ice on geomorphology and vegetation (Chassiot et al., 2020; Lind et al., 2014a; Rokaya et al., 2018; Rood et al., 2007), leading to the identification of distinctive geomorphological and vegetation pattern signatures linked to ice-related disturbances that are absent from ice-free temperate systems (Figure 43). In this section, we describe the key features reported in the literature that are most relevant to a biogeomorphological framework by integrating vegetation and fluvial landforms into the descriptions and discussing how the hydrogeomorphological context and the ice-jam regime mediate channel dynamics and vegetation responses. To provide a clearer overview of how

ice disturbances act across different parts of the fluvial system, we grouped them into three broad categories of fluvial forms and landscapes: active channel, riverbanks, and floodplains.

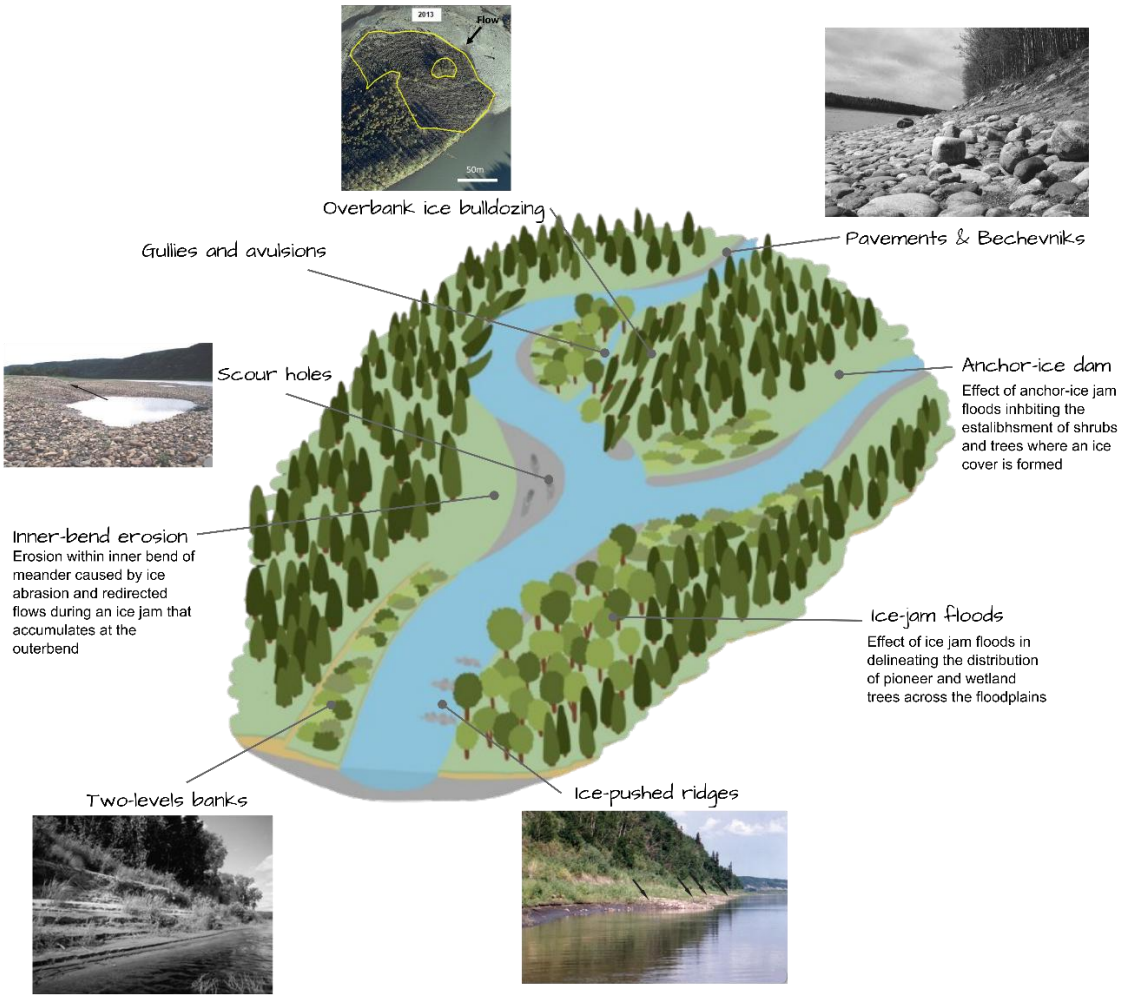


Figure 43 Schematic representation of all the ice forms and processes impacts left as visible markers within the fluvial corridor that are discussed in the following section. The illustration synthesizes the main features generated by ice dynamics across the active channel (scour holes, pavements, inner-bend erosion), riverbanks (two-level banks, Bechevniks, ice-pushed ridges), and floodplains (gullies, avulsions, overbank ice bulldozing, ice-jam flood extent). Annotations highlight the various forms and processes, while photographs provide field examples from cold-region rivers. Pictures were taken from Uunila and Church (2014), Prowse and Culp (2003), and Vandermause et al. (2021).

4.5.1 Active channels

Geomorphological units comprised within the active channel are subjected to frequent sediment reworking by bankfull floods and encompass a wide range of in-stream landforms (e.g., alluvial bars, benches and pools) for which their assemblage and diversity are functions of the river style and hydrological regime (Fryirs & Brierley, 2022). By extension, the active channel and in-stream geomorphological units are highly susceptible to ice disturbances, either through direct mechanical ice-push mechanisms or through indirect hydraulic forces resulting from ice-induced alterations in flow direction. Some authors even suggest that the geomorphological structure of cold rivers may be dominantly shaped by long-term adjustment to local ice conditions (Boucher, 2017). For instance, previous research showed that in reaches subjected to frequent ice jams, the active channel width could be enlarged by 1.5 to 3 times compared to ice-free similar environments (Boucher et al., 2012; Smith, 1979; Uunila & Church, 2014).

High pressure applied by ice movement on bed sediment can create extended pavements, generally composed of boulders and cobbles, or generate ice-pushed ridges and scour holes on river bars (Uunila and Church, 2014). Prowse and Culp (2003) observed on the Mackenzy and Yukon rivers pavements going from 7 to 30 meters wide over a longitudinal distance of hundreds of kilometers, highlighting the considerable effects of ice runs in structuring the active channel sedimentary template and constraining the establishment of in-stream riparian vegetation. Indeed, the inhibition of pioneer species establishment, such as poplar species, in favour of more opportunistic forb species has been repeatedly reported (Nilsson & Jansson, 1995; Smith & Pearce, 2000b; Uunila & Church, 2014), suggesting that ice dynamics may limit vegetation succession. In many studies, sites frequently affected by ice floes were characterized by a clear trimline separating mature floodplain communities from in-channel ephemeral species, with no in-between successional species (Peters et al., 2016; Prowse & Culp, 2003). Uunila and Church (2014) and Prowse and Culp (2003) further suggest that trees' ages on benches and low-lying islands could indicate last ice-jam events. However, caution must be taken with this interpretation, as the

magnitude of these effects depends on both the severity of the ice regime (e.g., dominant processes, frequency, magnitude) and the hydrogeomorphological context.

Homogeneous reaches and their fluvial styles exhibit specific characteristics of flood and sediment regime, assemblage of geomorphological units and mosaics of vegetation patches (Fryirs & Brierley, 2022; Gurnell et al., 2016a). Thus, the inherent characteristic of a system may mediate ice effects within the active channel by influencing both species selection and geomorphological-driven exposure. For instance, a study in two contrasting rivers in Eastern Canada suggested that vegetation removal by ice jams was greater in a meandering river than in a confined one, as the latter's high-energy flows initially favored flexible, disturbance-tolerant shrubs, whereas the former supported poplar-dominated early successional communities known to be more sensitive to ice damage (Prugne et al., *In Prep.*). In dynamic meandering rivers, ice jams that accumulate on the outer bend of a meander can, furthermore, reverse the usual erosional pattern by redirecting flows within the inside bend and cause substantial erosion on point bars, an effect not observed in ice-free systems (Smith & Pearce, 2002). Moreover, geomorphological units themselves modulate exposure to ice abrasion. Vandermause et al. (2021) observed, on the Susitna River, Alaska, that low-lying benches were more prone to ice scouring erosion during ice jams. Finally, while severe ice-jam regimes inhibit succession and constrain vegetation establishment, more moderate breakup conditions may instead foster heterogeneity, generating a dynamic mosaic of geomorphological units and vegetation patches at different successional stages (Nilsson & Jansson, 1995). It is thus the complex interplay between river style, geomorphological setting, vegetation, and ice regime that ultimately governs whether ice disturbances dominantly control the ecogeomorphological structure of active channels or participate in a dynamic equilibrium.

4.5.2 Riverbanks

Riverbanks are particularly prone to ice disturbances as the movement of ice blocks applies direct shear stress on river margins during the breakup phase, remobilizing sediment

and mechanically disturbing vegetation communities (Chassiot et al., 2020; Uunila & Church, 2014). In many rivers across the northern hemisphere, authors have identified typical ice-related riverbanks with geomorphological characteristics not observed in temperate rivers (Egger et al., 2015; Uunila & Church, 2014; Vandermause et al., 2021). For instance, pavements can be generated on the riverbanks during ice runs due to heavy ice push and may lead to the formation of *Bechevniks*, a typical ice-induced riverbank resulting from eroded riverbed coarse sediments being deposited onto the upper part of a bank usually much higher than the bankfull level (Boucher, 2017b; Hamelin, 1979). Such types of riverbanks typically exhibit a relatively steep slope and the absence of vegetation, for which their establishment is limited by frequent high shear stress and the lack of fine substrate washed away during subsequent open-water floods. The effects of ice runs on riverbanks, however, vary with the position along a river. Uunila and Church (2014) observed considerable differences in riverbank responses to ice dynamics across reaches along the Peace River in Canada, highlighting the importance of fluvial context. In erosional environments (e.g., upstream reaches with steep slopes), ice-disturbed reaches were mainly associated with clean-scoured riverbanks, followed by undercutting processes. In contrast, downstream sites with wider floodplains showed a higher cover of early successional shrubs, which seemed to be frequently rejuvenated by ice.

One of the most well-known riverbank ice-scoured features is the two-level bank formed by ice-jam releases. Two-level banks result from ice runs eroding the tops of riverbanks and subsequent fluvial floods reworking sediment into a flat surface. They are typically characterized by a lower ice-scoured flat surface and an upper terrace or floodplain (Boucher et al., 2009; Chassiot et al., 2020; Uunila & Church, 2014). However, their presence might be maintained only at a specific ice-jam frequency (Boucher et al., 2009); otherwise, fluvial floods would rework sediments and reshape the banks. The lower ice-scoured level is usually colonized by early successional shrubs such as willows and poplars, which are supposedly rejuvenated at each ice jam. However, some species may tolerate ice runs and persist. It has been shown that ice-jam frequency can select for species adapted to such scouring events (Prugne et al., *In Prep.*), suggesting that rejuvenation may not occur

systematically. For instance, Prugne et al. (*In Prep.*) found that sites with high disturbance frequency were associated with increased *Cornus sericea* cover and decreased *Salix* species cover in two rivers in eastern Canada. Moreover, other fast-growing, flexible species, such as *Alnus rugosa*, are thought to thrive in highly ice-disturbed environments (Boucher, 2017). While extreme events can cause significant erosion and rejuvenate communities, some species established on riverbanks are well adapted to avoid mechanical stress and persist. Thus, it seems that the ice-jam regime plays a significant role in determining riverbank vegetation composition.

While ice jams are known to foster considerable changes both geomorphologically and ecologically, other forms of less severe ice disturbance also seem to play a role in the vegetation composition and physiognomy. Studies have shown that river reaches experiencing important anchor-ice dynamics had significantly higher species richness and diversity than free anchor-ice reaches due to the inhibition of woody species establishment and facilitation of herbs and forbs (Engström et al., 2011; Lind et al., 2014b; Nilsson et al., 1989). The riparian ice fostered by ice-dam exert sufficient physiological stress through frost burns to inhibit the establishment of first successional woody species, resulting in frequent turnovers caused by the creation of open habitats, which are then colonized by fast-growing and opportunistic herbaceous species

4.5.3 Floodplains

During ice-jam events, water levels can significantly exceed those of equivalent open-water discharges, leading to significant sediment deposition and contributing to floodplain aggradation (Uunila and Church, 2014). Such ice-related depositional processes result in a high volume of light alluvial materials at higher elevations than an ice-free flood could (Prowse and Culp, 2003). Those sediments are thus beyond the reach of subsequent fluvial erosion during open-water floods. Livingston et al. (2009) identified ice-related flood beds in the Yukon River with thicknesses ranging from 1.7 meters to 2.65 meters within three stratigraphic profiles. Similarly, Hugenholtz et al. (2009) documented stratigraphic increases

of 1 to 3 meters in the Athabasca and Peace Rivers. These evidences collectively underscore the significant influence of ice-jam flooding on the elevation and structure of floodplains. Ice-related flood dynamics may also play a crucial role in sustaining high levels of moisture and nutrient cycling in floodplain areas that would not be inundated during ice-free floods (Rokaya et al., 2018). Prowse and Culp (2003) emphasize that ice-jam induced high-elevation floods are essential in maintaining riparian wetlands at the upper limits of floodplains. This observation is also supported by Prugne et al. (*In Prep.*), who found that black ash (*Fraxinus nigra*) was most abundant in reaches with high-frequency, high-magnitude ice jams. Furthermore, Peters et al. (2016) also suggest that the extent and persistence of poplars is favored by such ice-jam floods, as major floods naturally generate pulses of dispersion and recruitment throughout floodplains. Altogether, these examples reveal how ice-jam floods contribute to the structure, composition, and dynamics of floodplain forests by exacerbating the spatial extent and frequency of flooding (Prowse and Culp, 2003). Thus, one can argue that ice dynamics may contribute to regional biodiversity by maintaining local winter-flood tolerant floodplain species (Tolkkinen et al., 2020).

4.6 FROM TRAITS TO LANDSCAPES: HOW ICE DYNAMICS MAY MODULATE THE EXPRESSION OF BIOGEOMORPHOLOGICAL DYNAMICS AND ADJUSTMENTS

It is understood that rivers are the product of a complex balance between water discharge, sediment supply and vegetation that co-adjust in time and space (Bywater-Reyes et al., 2022b). The bidirectional interactions between flow structure, fluvial landforms development and vegetation dynamics have been extensively explored and modelled through different conceptual, statistical and modelling approaches (Corenblit et al., 2007b; Gurnell et al., 2016a; Larsen et al., 2020). We now fully acknowledge the effects of vegetation on river morphodynamics, and studies from the last decades revealed that the strength of interactions (i.e., degree of control on river) varies both across bioclimatic regions and river types (Corenblit et al., 2024a). A given system might be controlled either by physical forcings (water flows and sediment transport), vegetation morphodynamic effects, or feedbacks; ultimately, the dominant condition depends on the system's environmental characteristics

(e.g., climate, geology, flood regime) that determine the presence or absence of key plants acting as ecosystem engineers. More particularly, disturbance regimes play an essential role in determining vegetation assemblages by selecting well-adapted species through mechanical and physiological stresses (Naiman et al., 2005; Bornette et al., 2008). In doing so, they select for specific functional traits that allow avoidance, tolerance, and dispersion strategies (Catford & Jansson, 2014). These response traits often coincide with effect (and feedback) traits that influence how vegetation interacts with and affects flow structure and sediment dynamics (Corenblit et al., 2024b; Diehl et al., 2017). Consequently, vegetation's influence on river morphodynamics is closely tied to the disturbance regime. However, very little is known about the role of ice-related disturbances in such a framework.

We believe that the direct and indirect effects of ice dynamics on the riverscape components (Figure 44) may result in distinctive biogeomorphological adjustments of rivers compared to more temperate systems, thus emphasizing the need to theorize possible outcomes. Here, we link insights from the biogeomorphology discipline to what is known about ice dynamics and their effects on riverscapes, highlight some key research questions and propose scenarios of possible feedback loops and adjustments at various spatial and temporal scales.

4.6.1 Plants: establishment, growth and dispersion

Foundation engineer species in fluvial systems, such as species from the Salicaceae family (e.g., poplars and willows), are closely connected to fluvial dynamics at every stage of their life cycle (i.e., dispersal, recruitment, establishment, sexual maturity) through adaptive traits (Corenblit et al., 2014). For seeds to germinate and seedlings to grow, hydrogeomorphological conditions must be met, including sediment texture and humidity, relative elevation to low flow, flow variability and shear stress, and sediment dynamics (Corenblit et al., 2020a). Two distinct models have been developed to assess and predict the successful recruitment of riparian species on fluvial landforms. First, the recruitment box model (Mahoney & Rood, 1998b) links the timing of seed release and germination to river

stage recession and landform elevation by defining the spatial and temporal limits within which optimal conditions for seed germination are met. Second, the Windows of Opportunity model (Balke et al., 2011) defines the time needed for a plant to develop sufficient resistance to a subsequent disturbance and persist. Both models have been used across different riparian species and fluvial styles (Balke & Nilsson, 2019; Dixon et al., 2002; Fivash et al., 2021; Lytle & Merritt, 2004), but we know little about the influence of ice dynamics.

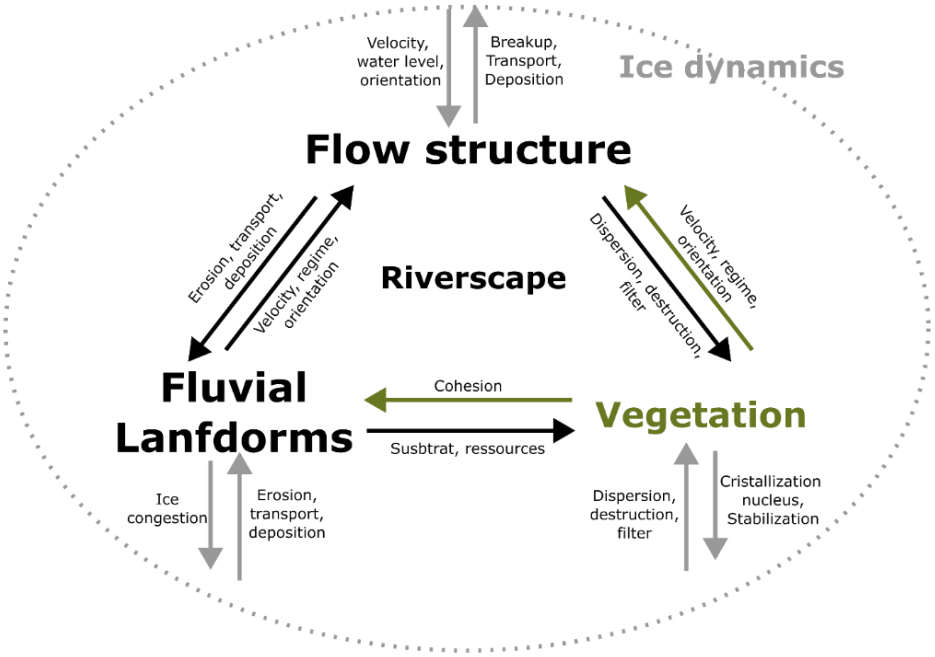


Figure 44 Conceptual models illustrating the interactions between flow structure, fluvial landforms, vegetation and ice dynamics that shape riverscapes.

Those models should be applied and tested on rivers experiencing various forms and intensities of ice disturbances to better capture how ice processes may modulate vegetation recruitment. Substrate and landform elevation have been recognized as key factors for seedling recruitment and survival because they influence inundation frequency, moisture retention, and substrate stability (Corenblit et al., 2020b; Gilvear et al., 2007). Thus, sediment texture and relative elevation of geomorphological features generated by ice-related erosion

and deposition (e.g., pavements and ridges) may influence the availability and spatial distribution of sites within the germination/regeneration niche. Because recruitment boxes are species-specific (Dixon & Turner, 2006), these controls may indirectly filter which species can establish. Beyond these indirect effects on habitats, the survival rate of newly established seedlings may be further reduced by mechanical stress from ice scouring. To our knowledge, no model has quantitatively linked ice breakups to vegetation recruitment. However, Dixon and Turner (2006) designed a simulation model of recruitment and survival of different species on the Wisconsin River (USA). Although they lacked sufficient data to parameterize ice dynamics, they achieved good agreement between simulated and observed variation in first-year seedling density by applying a simple ice penalty: when ice was present, survival was reduced by a factor of 5 for a given flood depth and shear stress. This implies that ice exerts significant control over recruitment and underscores the need to properly quantify its degree of control.

According to the Windows of Opportunity (WoO), a riparian plant growing sufficient root strength to resist a subsequent disturbance may be able to persist and establish. Two principal factors in cold regions might modify these timeframes. First, the cold climate may increase the time required for the roots to develop sufficient strength due to lower temperatures. Previous studies have consistently shown that low temperatures reduce root growth in deciduous and evergreen temperate species (Alvarez-Uria & Körner, 2007; Schenker et al., 2014; Wan et al., 1999). One could argue that in cold regions, the probability that seedlings do not achieve sufficient root growth to resist a subsequent disturbance is higher than in more temperate regions. Second, the mechanical stress from ice runs and ice floes may necessitate a stronger anchorage compared to ice-free rivers, as moving ice blocks exert higher shear stress than open waters (Lind et al., 2014b; Prowse & Culp, 2003; Smith & Pearce, 2000b). However, high-flexibility woody species (e.g., young poplars and willows) also have the capacity of bending instead of breaking or being uprooted (Karle, 2007; Rood et al., 2007). Conversely, more rigid stems are known to be more vulnerable to breakage during ice floes due to the lack of bending capacity. This suggests a time window during which pioneer species such as poplars can establish and withstand ice disturbance, up

to the point where growth reduces their flexibility and increases their vulnerability to ice runs (Figure 45). Altogether, these mechanisms imply that the WoO in cold rivers may be both delayed and narrowed, with seedlings requiring longer disturbance-free intervals to reach anchorage thresholds while facing higher mechanical stress during ice breakup, and that these pioneer species may become more vulnerable once the flexibility threshold is crossed.

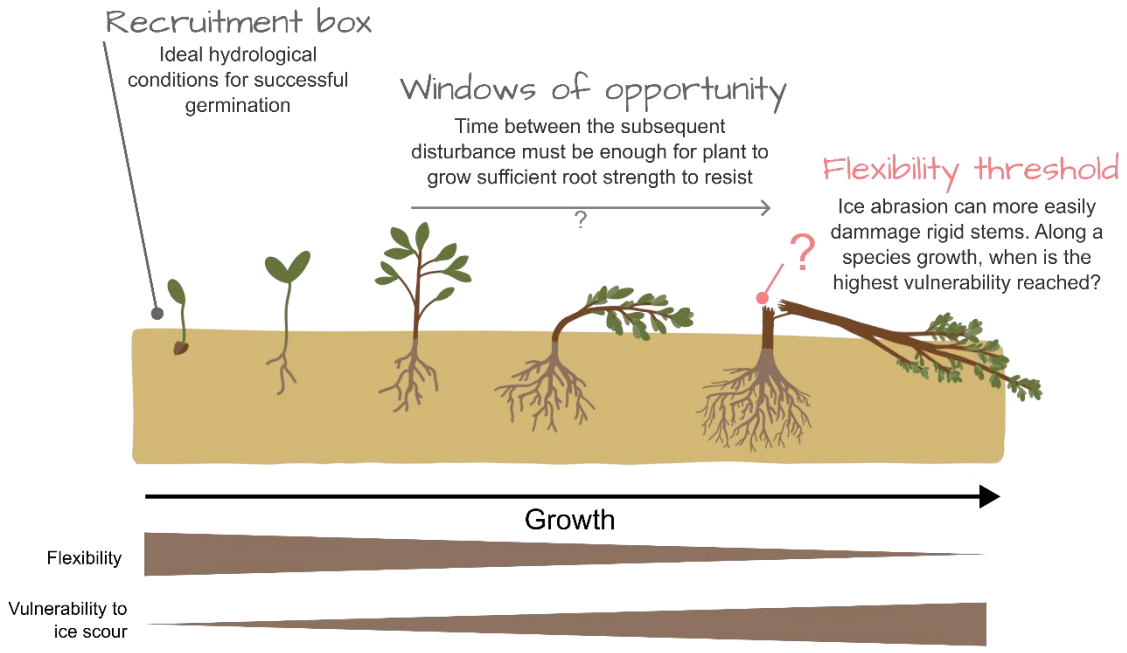


Figure 45 Schematic representation of a pioneer tree recruitment and growth under ice abrasion constraints, illustrating (1) the inverse relation between plant growth and flexibility, (2) the requirements for successful establishment from the recruitment box to the WoO model, and (3) highlighting the need to identify thresholds associated with ice abrasion vulnerability. To note that dimensions and relative proportions are exaggerated for clarity.

Hydrochory (i.e., transport by water) and anemochory (i.e., transport by wind) are dominant dispersal strategies in rivers, enhancing species richness and diversity in flooded areas (Andersson et al., 2000; Jansson et al., 2005; Nilsson et al., 2010). Notably, species from the *Salicaceae* family that produce a high quantity of very small seeds have the capacity to disperse over long distances and are known as river specialists (Edwards, 2024). To our knowledge, no research has been conducted on the dispersal mechanism via fluvial ice as a

vector, but field evidence indicates that flowing ice could be a significant agent exploring. Archival photographs and videos repeatedly shown that ice floes can transport large volumes of wood and other propagules. We hypothesize that ice dynamics could further benefit species that do not rely on wind and water for dispersal by transporting and depositing viable propagules along rivers' longitudinal and lateral gradients. For instance, red-osier dogwood (*Cornus sericea*) is widespread in eastern Canada floodplains and is particularly abundant compared to willows in sites frequently affected by ice jams (Prugne et al., *In Prep.*). Interestingly and in contrast to the *Salicaceae* species, *Cornus sericea* has heavy seeds that disperse mainly by animals, but also has a strong capacity for vegetative propagation (Gucker, 2012). Despite its dominance in many rivers, it remains understudied mainly in the scientific literature, making it a compelling case. Its high occurrence and abundance in North American rivers may simply reflect animal dispersal and slow lateral spread, but a previous study by Prugne et al. (*In Prep.*) suggests that future research should consider the role of ice dynamics in this species' life cycle. Another illustrative case comes from a study on the Etchemin River in Eastern Canada (Matte, 2020), where it was observed that Japanese knotweed (*Reynoutria japonica*), an exotic invasive species, can spread hundreds of meters within floodplains through ice blocks that transport and deposit propagules. Such observations imply that ice dynamics may disperse species in areas where they would not if mechanical ice breakups were absent, underscoring their potentially important role in vegetation dispersal mechanisms.

4.6.2 Communities: linking functional traits to feedbacks

Community composition and structure result from a hierarchy of filters (e.g., dispersal, environmental, biotic) that select species adapted to local conditions (Götzenberger et al., 2012). Communities along river corridors are shaped by the selection of species that respond primarily to flood-related disturbances and stresses, expressing a set of traits that allow them to withstand mechanical forces and physiological stresses (Catford & Jansson, 2014). Notably, riparian species exhibit key ecological response traits associated with hydrogeomorphological disturbances, including fast acquisition of resources, water-use

efficiency, competitive ability, mechanical stability, and reproductive characteristics that enable them to thrive in highly dynamic environments (Diehl et al., 2017). Recent studies have extended this functional approach to the ecogeomorphological processes, showing that many response traits overlap with effect (and feedback) traits that interact with hydrosedimentary dynamics (Corenblit et al., 2024b; Diehl et al., 2017; Lytle et al., 2017; Merritt et al., 2010). For instance, vegetative propagation by pioneer shrubs in response to frequent disturbances can expand the vegetated area and increase community density, thereby amplifying effects on sediment deposition. The type, rate and strength of interactions (e.g., volume of sediment deposited by vegetation influence on flow velocity and turbulence) furthermore depends on the functional structure of communities, which can be assessed by the mean trait value weighted by the species abundances or by indices measuring the community functional richness, redundancy and diversity (De Bello et al., 2021a; Janssen, 2025; Lepš & de Bello, 2023). For instance, communities with high flexibility may decrease sediment trapping and erosion (Zhu & Tsubaki, 2022), whereas more rigid and dense communities may increase sediment deposition (Montakhab et al., 2012).

Recent studies have explored the role of ice in structuring the functions of riparian ecosystems and highlighted multiple morphological, ecological, and phenological traits associated with resistance and resilience to ice dynamics. Catford and Jansson (2014) suggest that low shoot: root ratio, high flexibility, fast-growing roots, lateral spread, high growth rate, and early reproduction are all functional traits that promote the persistence of species in ice-disturbed environments. Prugne et al. (*In Prep*.) observed that sites with frequent ice jams had high abundances of fast-growing, resprouting shrubs and a dominance of vegetative propagation traits (stem and root sprouting), suggesting that the ice-jam regime acts as an environmental filter selecting traits that enable species to resist or avoid ice-jam disturbances. Consistent with this, previous studies indicated that some species may even benefit from ice scour, either by increasing vegetative propagation via stem and branch breakage or by achieving greater persistence through quick resprouting in a context of frequent ice-scour removal (Keita et al., 2021b; Prowse, 2001; Randall, 2015; Rood et al., 2007). In certain fluvial contexts (e.g., confined reaches), intense ice dynamics appear to favour highly flexible

species such as graminoids (Prugne et al., *In Prep*.), indicating further community structuring by the ice-jam regime. All these insights support the evidence that ice dynamics act as an environmental filter, shaping the functional composition of riparian plant communities and, in turn, their biogeomorphological functions.

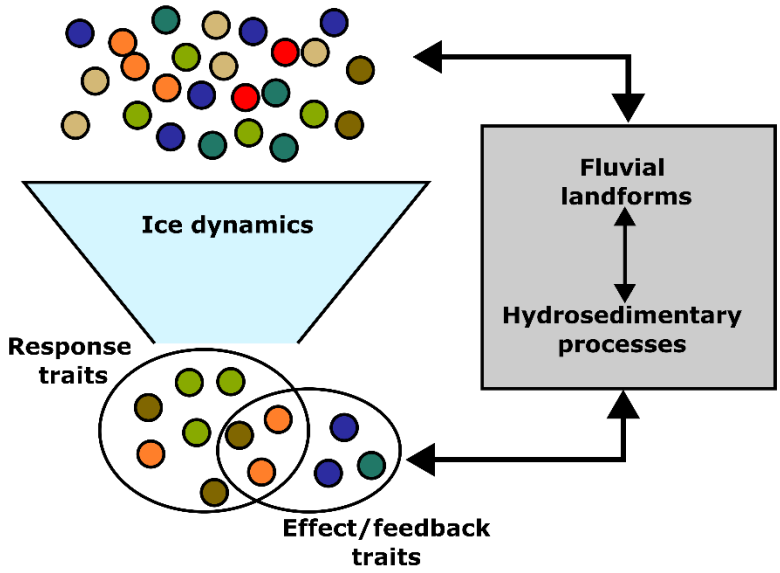


Figure 46 Schematic representation of ice dynamics as an environmental filter shaping community functional composition and biogeomorphological feedbacks. Points represent individual traits (e.g., height, reproduction, flexibility) while colors distinguish different families of traits (e.g., ecological, morphological, biomechanical). From a pool of traits initially shaped by fluvial processes, ice dynamics select for specific response traits that confer resistance or resilience to ice-related disturbances. These selected response traits often overlap with effect traits (indicated by the ellipses' intersection) that subsequently influence hydrosedimentary processes and fluvial landform development, thereby modulating the nature and strength of biogeomorphological feedbacks.

We hypothesize that filters imposed by different ice forms and processes select for response traits that diverge from those favored under ice-free regimes, thereby modulating community feedback mechanisms on hydrosedimentary processes and shaping the medium—to long-term biogeomorphological adjustments of rivers. For example, the selection of vegetative propagation by stem breakage from ice jams (response trait) may indirectly increase the patch area and density of a community (effect traits), thereby

strengthening positive feedbacks on sediment deposition and stabilization. Conversely, selecting for high stem flexibility (both response and effect traits) may reduce sediment deposition feedbacks but increase riverbank resistance to erosion, thereby stabilizing landforms. Available case studies remain sparse and rely on qualitative characterizations of ice forms and processes rather than quantitative links to vegetation dynamics. Building robust, predictive understanding will require quantitative measurements and statistical models that distinguish among ice processes (e.g., frazil/anchor ice, stable ice cover, mechanical breakup and jam floods) and estimate their effects on riparian recruitment, survival, and community structure. Such insights will furthermore be essential for a better assessment of the strength of subsequent biogeomorphological feedback from these communities.

4.6.3 Biogeomorphological landforms: biotic-abiotic co-construction and succession dynamics

Fluvial landforms shaped by the interplay between hydrosedimentary processes and vegetation are known as biogeomorphological units, comprising alluvial bars, islands and floodplains (Corenblit et al., 2016). Resulting from the positive feedbacks of vegetation development and sediment trapping, these units exhibit various processes and functions throughout their development stages. A model used to reflect the evolution of such landforms is the Fluvial Biogeomorphological Succession (FBS; Corenblit et al., 2007), which highlights four distinct phases linking the vegetation succession state with their biogeomorphological functions: geomorphological, pioneer, biogeomorphological, and ecological. The geomorphological phase features vegetation-free landforms due to intense sediment transport and flooding. The pioneer phase starts when pioneer species establish, but are unidirectionally controlled by hydrosedimentary dynamics (Corenblit et al., 2020b). While vegetation does not significantly influence sediment dynamics at this stage, it can trap and stabilize fine layers of sediment and, especially, facilitate the recruitment and establishment of early successional species (e.g., willows and poplars). The biogeomorphological phase occurs when vegetation grows sufficiently to significantly

interact with flow structure and sediment transport, leading to deposition and landform construction. Within this stage, the timeframe in which feedbacks occurs has been defined as the Biogeomorphological Feedback Window (BFW) that describes the boundary conditions at which feedbacks can initiate and stop (Eichel et al., 2016). Finally, the ecological phase is reached when late-successional communities are allowed to establish once the habitat is disconnected from flooding (Corenblit et al., 2007). It is important to note that the FBS is a nonlinear process that varies in time and space, for which its progression, retrogression and cyclicity are influenced by many factors, including hydraulics and flood regime (Caponi et al., 2019; Corenblit et al., 2014; Garófano-Gómez et al., 2017), sediment dynamics and topography (Corenblit et al., 2009; Kim & Kupfer, 2016), regulation (Han et al., 2020) and groundwater variability (Bätz et al., 2016a).

Considering that ice dynamics influence both geomorphology and vegetation functional composition, we believe they may influence the trajectories of biogeomorphological landform construction. The spatial and temporal variability of ice dynamics, however, makes it challenging to capture the full range of its possible effects. Yet, the documented ice-disturbance impacts allow us to outline plausible scenarios on the trajectories of biogeomorphological landforms under ice-driven regimes. Because many ice processes remain poorly quantified, and their geomorphological and ecological impacts are unevenly studied, we focus specifically on mechanical ice breakups and ice jams. We propose hypotheses on how variation in their magnitude and frequency could modulate the progression, regression, and cyclic dynamics of the development of biogeomorphological units.

Controls on the emergence of pioneer landforms. For biogeomorphological succession to initiate, two criteria are essential. First, the emergence of new pioneer landforms (e.g., bars or islands) with ideal physical and environmental conditions to support early successional species to establish. Already at this stage, the influence of ice runs on channel geometry and bedload sediment may alter the availability of potential colonization sites, either through the formation of flattened pavements or ice-pushed ridges that modulate flood connectivity and

shape sediment texture. Second, the WoO must be achieved for pioneer engineers to persist and start interacting with hydrosedimentary dynamics. As described before, the frequency and amplitude of mechanical ice breakups could influence the successful establishment of early shrubs and trees, so it is unlikely that pioneer landforms (*sensu* Gurnell et al., 2016a) emerge in reaches subject to frequent, high-energy breakups. Yet, this only represents the upper bound of the ice disturbance gradient. Generally, mechanical ice breakups do not occur on an annual basis and have spatially heterogeneous effects on channels; moreover, the formation of vegetated river bars has been observed in many cold rivers (Morin et al., 2015; Prugne et al., 2025; Vandermause et al., 2021), indicating that models of biogeomorphological unit construction may apply to cold rivers. No comparison of the emergence of pioneer landforms between morphologically similar rivers with and without ice has yet been conducted to our knowledge. Still, such research directions could provide insights into the degree of control ice breakups may exert.

Deposition of large wood (LW) within channels has also been identified as a key process in the initiation of pioneer islands, supporting further biogeomorphological construction (Gurnell et al., 2012). The obstruction caused by LW accumulations interrupts flow patterns and allows for sediment and propagule retention downstream of large wood jams, which can eventually be colonized by engineering species and extend landforms through biogeomorphological feedbacks (Gurnell et al., 2019). Dynamics of LW thus have significant implications as they can shape the distribution of biogeomorphological landforms (Gurnell & Bertoldi, 2024). Because ice breakups have been shown to interact with LW dynamics, they may indirectly influence the emergence of pioneer landforms through the spatial organization of wood jams. A study on the Saint-Jean River (Gaspé, Canada) revealed that the transport rate of LW increased during years with ice breakup, even at low discharge (Boivin et al., 2015, 2017). The increased water level and roughness from the presence of ice blocks allow for the mobilization of a large volume of dead wood, but do not necessarily increase LW recruitment. Boivin et al., (2015) thus suggest that mechanical ice breakups may restructure the distribution of large wood jams along a river by remobilizing unstable large wood jams in reaches where ice jams occur and supplying wood to downstream sections.

Thus, critical zones for biogeomorphological unit construction (*sensu* Gurnell et al., 2016) fostered by LW dynamics could significantly be modulated by ice-jam regimes, but future research is needed to assess their contribution.

Increased resets and turnovers. No studies have yet mechanistically analyzed co-construction within cold rivers to properly model or statistically test the rate and strength of biogeomorphological feedbacks, as it has been done in more temperate regions (Bertoldi et al., 2014; Corenblit et al., 2009; Serlet et al., 2018; Sitzia et al., 2016). However, a recent study that coupled ice jam regimes with vegetation and hydrogeomorphological trajectories over a period of 60 years in two gravel-bed rivers revealed a potential relationship between landform extension and vegetation succession progression (Prugne et al., 2025). Aligned with other studies suggesting that the reset of pioneer shrub communities often occurs during ice jams (Prowse & Culp, 2003; Uunila & Church, 2014), vegetation turnovers happened almost systematically after years of ice jams, but rapid recovery of vegetation followed and was met with geomorphological adjustment in subsequent years. This indicates that ice jams do not inhibit biogeomorphological co-construction on a decennial scale but rather impact their trajectories in time by forcing more frequent turnovers.

Yet, ice jams may not erode landforms on which vegetation rejuvenation recurrently happens. For instance, Vandermause et al. (2021) observed dense rootmats that were not representative of *in situ* vegetation structure, suggesting that multiple ice scours led to vegetation removal, followed by resprouting and root system densification. These observations have two key implications for biogeomorphological co-construction theories in cold rivers. First, repeated vegetation removal followed by resprouting may strengthen root systems over time, enhancing sediment cohesion and increasing resistance to fluvial erosion. This suggests that, rather than eroding the underlying landform, ice jams may periodically "reset" only the aboveground vegetation while allowing subsurface structures to accumulate strength. Second, it points to a theory of pulse-driven mode of biogeomorphological development (Figure 47). When vegetation cover reaches the Biogeomorphological Feedback Windows, feedbacks promoting sediment deposition and landform stabilization

can operate and contribute to construction if open water floods occur in subsequent years. When (and if) ice scours remove the vegetation, feedbacks are temporarily interrupted, but the remaining landforms maintained by rootmats allow for efficient resprouting that restores biogeomorphological functions. This implies that co-construction may not be prevented but rather slowed and fragmented into recurrent cycles of interruption and recovery timed with mechanical ice breakups.

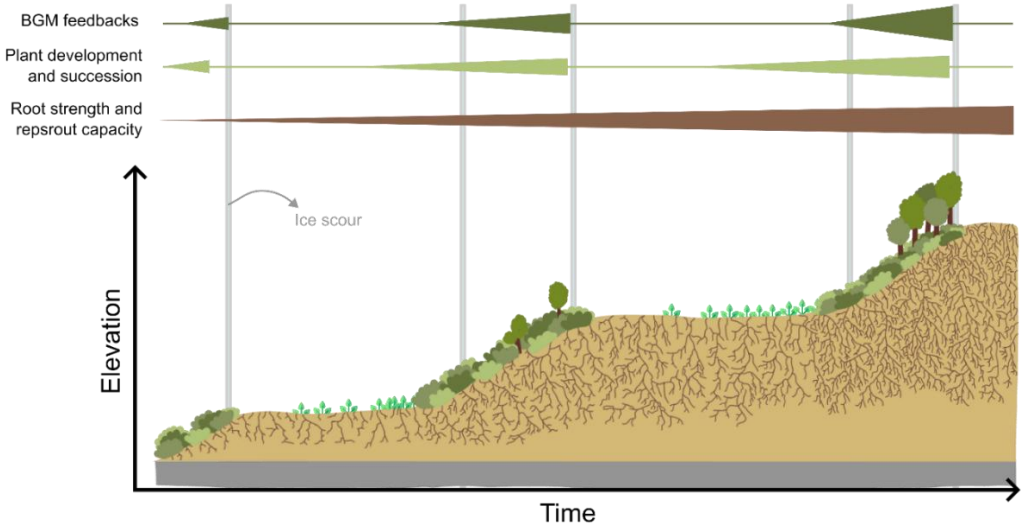


Figure 47 Schematic representation of pulse-driven biogeomorphological development in ice-affected systems. The figure illustrates that ice-scouring events vary in their impact: some are insufficient to remove established vegetation, while others cause aboveground reset without eroding landforms. Following severe ice scour, rootmats densify and enhance both sediment cohesiveness and resprout capacity, while biogeomorphological feedbacks resume during subsequent ice-free periods after reaching sufficient plant development and succession (i.e., reaching the Biogeomorhpological Feedback Window).

Influences on aggradation and sediment retention. The strength of biogeomorphological feedbacks and retention of fine sediment within river active channels and planforms are strongly influenced by sediment supply and vegetation composition (Bywater-Reyes et al., 2022a; Gurnell & Bertoldi, 2022); the concentration of suspended sediment controls the potential for deposition, while vegetation functional traits influence the rate of deposition. The high suspended sediment concentration (SSC) and elevated water level caused by mechanical ice breakups could thus amplify these feedbacks in locations that

cannot be mechanically disturbed by ice scouring. For instance, Beltaos and Burrell (2021) observed an SSC increase from 70 mg/L during pre-breakup to 1067 mg/L during ice floes on the Liard River. These short-lived but intense pulses of sediment could thus considerably increase the potential for sediment deposition compared to an ice-free environment, provided the established vegetation can trap them. However, no studies have yet quantified the depositional rate of such ice-related floods in vegetation patches of different composition. Normally limited by the bankfull flood elevation (Gurnell & Bertoldi, 2022), the storage capacity of fine sediment in rivers subjected to ice-jam floods may be exacerbated. This is supported by the hypothesis that in rivers subject to ice-jam flooding, floodplain surfaces build up to elevations higher than the typical open-water bankfull level (Uunila & Church, 2014), allowing for the retention of higher volumes of sediment (Figure 48). By aggrading these planforms above the "normal" bankfull stage, they may indirectly control floodplain-channel connectivity and modulate floodplain communities' functions, leading to two distinct trajectories. If the ice-jam flood frequency and amplitude are maintained or increased, the frequent disturbances may sustain connectivity and the persistence of early-to-mid successional communities that interact with flows at higher elevation. Conversely, a decline or cessation of the regime may result in reduced connectivity, triggering the habitat's development toward the ecological phase (*sensu* FBS).

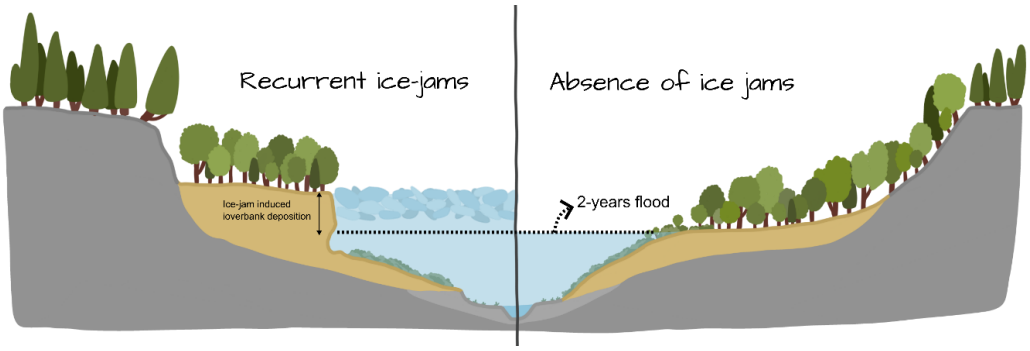


Figure 48 A conceptual model of differences in floodplain aggradation between rivers affected by frequent ice-jam floods versus the absence of ice dynamics based on a theoretical common discharge.

4.6.4 Reach scale: Spatial organization and adjustment

River reaches, defined as sections possessing a set of homogeneous processes leading to similar geomorphological and ecological characteristics (Gurnell et al., 2016b), allow for the identification and classification of different homogeneous sections along a watercourse, depicting specific sets of fluvial styles (e.g., straight, braiding, sinuous, meandering, wandering, anastomosing). They manifest distinct behavioural regimes, reflecting past and ongoing hydrogeomorphological (and biogeomorphological) processes and adjustments, expressed through specific process-form interactions that shape fluvial landforms and riparian vegetation distribution within the reach (Fryirs, 2017). The influence of vegetation on reach-scale morphodynamics, however, does not emerge from its mere presence but rather from its spatial organization within the reach that modulates its spatial and temporal effects on hydraulics and sediment transport, thereby controlling where and when biogeomorphological feedbacks can occur (Box, 2018; Vargas-Luna et al., 2015). The strength of biotic control at the reach scale thus depends on the spatial organization (e.g., size, shape, spacing, and composition) of vegetated patches, which creates spatially heterogeneous flow pathways and deposition patterns. While a specific configuration reflects a particular state of biogeomorphological dynamics, these patterns exist potentially within a shifting steady-state mosaic controlled by the fluvial regime, where episodic floods either promote succession or force resets and turnovers (Corenblit et al., 2010; Gurnell et al., 2016a). Consequently, reach-scale biogeomorphological organization represents a dynamic equilibrium between vegetation-driven landform construction and disturbance-driven resets, with spatial mosaic patterns reflecting the frequency, magnitude, and spatial distribution of disturbances relative to vegetation colonization, establishment and succession rates.

Ice effects on sediment transport, water flow, and vegetation can thus significantly influence the structure and distribution of fluvial landforms and vegetation patches, indirectly affecting the biogeomorphological behavior of river reaches. Depending on their type, magnitude and frequency, ice forms and processes may yield a wide range of outcomes for rivers' adjustment dynamics. There is a need to assess the degree of control they have over

these dynamics, whether they are just sporadic events to which river reaches adjust punctually, or whether they maintain a shifting mosaic of successional phases specific to ice-related disturbance regimes. This is especially important as ice regimes are anticipated to shift with climate change, either through an increase in mechanical ice breakups caused by more frequent freeze-thaw cycles or a decrease caused by a lower frequency of cold spells (Burrell et al., 2023). While many processes could have implications for the spatial organization of vegetation and landforms, we propose here a gradient of effects specifically focused on mechanical breakups and ice runs, which appear to be the most direct disturbances that can initiate change. Depending on the frequency and amplitude of such events, we believe their control on river reach spatial organization can manifest in an array of forms, ranging from the total control of morphodynamics by restraining the presence of vegetation, to strong interactions with floods and fluvial morphology that increase mosaic heterogeneity and thus the biogeomorphological expression within a reach. Figure 49 shows an attempt to position the different effects that mechanical breakup frequency and amplitude can have on reach-scale vegetation and landform spatial organization.

Effects on morphodynamics and spatial reorganization. In cases where severe ice runs occur very frequently (e.g., <5-year recurrence), the high shear stress and sediment reworking could inhibit the establishment of pioneer plants acting as ecosystem engineers, thereby maintaining the active channel entirely in the geomorphological phase (*sensu* FBS). In such cases, morphodynamics would thus be mainly driven by the ice-jam regime and subsequent floods. Because ice dynamics are largely influenced by channel geometry and usually happens repeatedly at precise locations with ideal conditions (e.g., ice jam formation and release) (Ettema, 2002; Lagadec et al., 2015; Morin et al., 2015), the resulting control may be the consequence not only from the ice effect alone but rather from the interactions between channel morphology and ice dynamics. While ice runs may not act as a long-term dominant morphodynamic agent if high-magnitude events occur only rarely, they may, however, cause periodic spatial reorganization within reaches. For example, the formation of gullies from ice-jam-redirected flows, a process known to generate secondary channels within alluvial bars or precipitate avulsions (Chassiot et al., 2020; Smith & Pearce, 2002), could, in

consequence, modify fluxes of matter and energy throughout the fluvial corridor. Consequently, these isolated events may abruptly reorganize the spatial configuration of feedbacks, after which the system would readjust primarily through flood-driven processes until the next major ice disturbance. This frequency gradient of high-magnitude events highlights the capacity of ice runs to shape reach-scale spatial organization, either through sustained or punctuated modes of influence, with implications for how cold-river reaches may respond to shifting ice regimes under climate change.

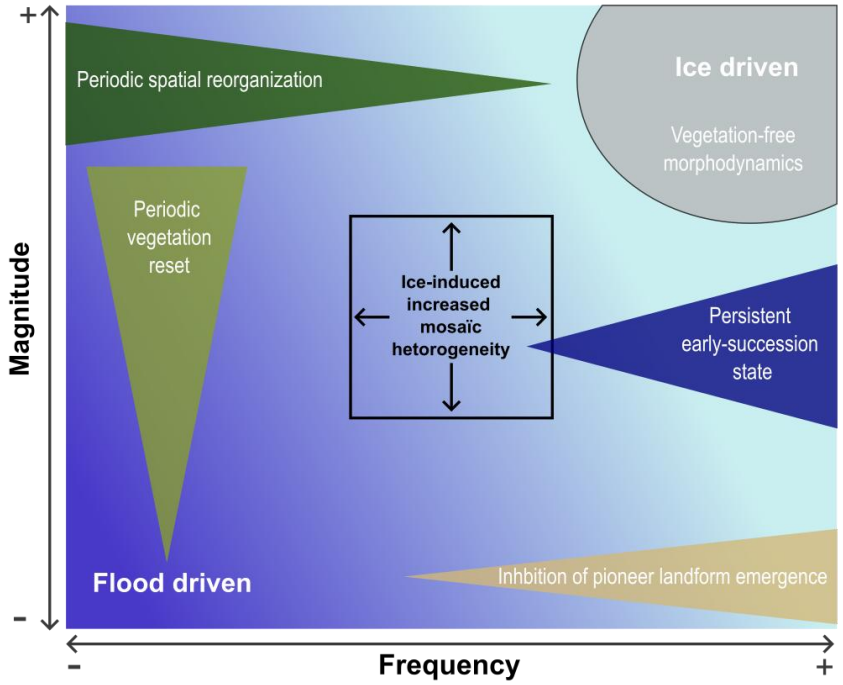


Figure 49. Conceptual model illustrating the range of effects that mechanical ice breakup frequency and magnitude may have on reach-scale vegetation and landform spatial organization. The color gradient spans from flood-driven systems (lower left), where ice exerts minimal influence, to ice-driven systems (upper right), where frequent high-magnitude events maintain vegetation-free conditions. Intermediate conditions (centre) may foster ice-induced increases in mosaic heterogeneity. Along the frequency axis, high-frequency low-magnitude events may inhibit pioneer landform emergence, while along the magnitude axis, infrequent high-magnitude events may cause periodic spatial reorganization or vegetation reset. The succession inhibition zone (right) represents conditions in which early communities are maintained by frequent disturbance.

Effects on succession and distribution. In-channel pioneer landforms mosaic usually alternate between progression toward mature and stable stages, and abrupt rejuvenation caused by exceptional floods (Corenblit et al., 2010; Gurnell et al., 2001). The frequency of ice jams may be a main factor controlling this cyclic biogeomorphological behavior by maintaining persistent early-succession states and limiting the progression to mature stages. The example from the Matapédia River (Prugne et al., 2025) revealed systematic rejuvenation of vegetation stands after ice-jam events, even during periods of low flood levels, followed by rapid recovery of dense vegetation and narrowing of the active channel. Following this study, a relationship between ice-jam frequency and community composition was also revealed, with pioneer shrubs more abundant in sites disturbed more frequently (Prugne et al. *In Prep.*). These observations exemplify the long-term effects that moderate to high frequency ice runs could have on successional stages, and by extension, on the biogeomorphological behavior of reaches subjected to such regimes. However, if magnitude is sufficient to rejuvenate vegetation but insufficient to reshape landforms, and frequency remains very low, ice runs may act merely as sporadic agents of vegetation rejuvenation within systems whose long-term biogeomorphological dynamics remain principally flood-driven. Conversely, if the magnitude is too low to affect established in-channel patches but the frequency is very high, the mechanical actions restrained to low elevations may nonetheless be sufficient to repeatedly disturb seedlings and saplings before they achieve the Windows of Opportunity, thereby preventing the emergence of pioneer landforms and the extension of existing biogeomorphological units. Collectively, these scenarios illustrate how the interplay between ice-run frequency and magnitude can generate markedly different successional outcomes, ultimately shaping the spatial distribution of vegetation communities and the biogeomorphological expression within river reaches

Increasing mosaic heterogeneity. At intermediate levels of ice run frequency and magnitude, ice dynamics may neither fully control morphodynamics nor act as mere sporadic disturbances, but instead contribute to the spatial complexity of reach-scale biogeomorphological organization. Erosional and depositional patterns generated from ice runs can promote substrate heterogeneity and vegetation patchiness across the fluvial

corridor (Nilsson et al., 1989; Prowse & Culp, 2003). For instance, the formation of ice-pushed ridges, scour holes, and localized pavements may create topographic variability that modulates flood connectivity and sediment texture in potential habitats, thereby influencing the distribution and dynamics (e.g., establishment and growth) of vegetation at different successional stages. Moreover, localized erosion and deposition may generate microtopographic variability that fosters a higher diversity of ecological niches, facilitating species coexistence (Masaki et al., 2007; Suzuki et al., 2002) and influencing functional composition of communities. Because ice runs are spatially heterogeneous in their erosional impact and because landform elevation modulates exposure to these disturbances (Prowse & Culp, 2003; Vandermause et al., 2021), moderate ice regimes may selectively rejuvenate certain patches while allowing others to progress toward more advanced successional stages, generating a spatially heterogeneous assemblage of communities at different phases. By reworking patch geometry and distribution, influencing species sorting through trait selection, and interacting with fluvial landforms, ice dynamics at intermediate intensity may thus participate in maintaining a dynamic shifting mosaic of communities and landforms, ultimately modulating where and when biogeomorphological feedbacks operate within the reaches.

4.7 CHALLENGES AND PERSPECTIVES

4.7.1 Developing techniques and tools to characterize ice dynamics

The various forms and stochastic behavior of ice dynamics make it a difficult component to analyze in river systems. Despite decades of research, there is a need for a clear framework to characterize and quantify ice forms and processes. Even though predictive models for ice-jam formation have been developed and are currently under development for flood management purposes (Krylenko et al., 2020; Madaeni et al., 2020; Rokaya et al., 2022), identifying past events to characterize an ice-jam regime remains challenging. Previous studies have used historical records, dendrochronology, floodplain stratigraphy, and geomorphological signatures to estimate the regime, but each approach has its limitations.

While ice jams have received growing attention, most studies have focused on risk management, and their role as environmental filters has been studied much less. The effects of anchor ice on vegetation have been explored (Engström et al., 2011; Lind et al., 2014b), but research on mechanical breakups across all levels of intensity is needed. We believe that even moderate mechanical ice breakups may play an important role in shaping the biogeomorphological template of cold rivers, adding another layer of disturbance to pioneer landforms and vegetation communities, and interacting with both hydrology and sediment dynamics. Tools and methods to assess these processes should be developed to more accurately quantify different characteristics of those disturbances, such as areas of high abrasion and flooding or associated shear stress. Frameworks and methods must be designed with clear, systematic ways to characterize, at both small and large scales, the various forms and processes of ice. For instance, remote sensing technologies could be used to describe their spatial distribution and movements during breakups, which could further be linked to the spatial organization of biogeomorphological units.

4.7.2 Quantitative assessments and threshold identification

There is a lack of studies linking ice dynamics with vegetation functional structure and landforms evolution. Prugne et al. (*In Prep.*) have identified potential relationships between 14 community-weighted functional traits and ice-jam regimes, but the results remain exploratory due to low replication and reliance on online trait databases. They proposed that ice dynamics may have local effects on functional response and that future research should focus on establishing links between *in situ* functional traits and ice dynamics to better assess the mechanistic effects that ice dynamics have on vegetation functional response. Based on a clear characterization of ice dynamics, whether it is related to a regime or to specific characteristics from a single event, applying the functional approach to determine the response of individual plants and communities would offer great insights into how it may modulate subsequent interactions with hydrosedimentary processes. Furthermore, as described in section 4.1, resistance of plants to ice runs may be associated with thresholds in both the magnitude of the ice disturbance and changes in the plant's morphological traits

(i.e., loss of flexibility that increases vulnerability to breakage). Identifying such thresholds would provide invaluable insight for river management, especially for soil and water bioengineering techniques (Prugne et al., 2024).

A common practice in biogeomorphology for studying the interplay between channels and vegetation dynamics is to quantify rates of landform extension and sediment aggradation, along with vegetation patch expansion and community composition. To our knowledge, such studies are very rare for cold region rivers, but promoting such work would benefit our understanding on their biogeomorphological behavior. Moreover, the increasing accessibility of new technologies such as airborne devices equipped with LiDAR and multispectral sensors makes it increasingly faster and easier to conduct such measurements over large areas. Quantifying the volume of deposited sediment either during mechanical ice breakups or open-water floods within patches of different vegetation types would allow us to describe the biogeomorphological functions of plant communities in cold rivers, develop clear vegetation classification, and yields insights to inform good practice in river management.

4.7.3 Long-term monitoring

To identify and analyze more subtle ice-related effects such as ice abrasion and riparian ice or co-adjustment dynamics within a given reach, we believe that long-term monitoring of both the succession pathway of vegetation and the evolution of fluvial landforms is essential. It would allow to properly identify key species that drive the Fluvial Biogeomorphological Succession in cold rivers and define typical patterns of biogeomorphological trajectories constrained by ice dynamics. This knowledge could also be applied in practice to enhance river restoration planning (O'Briain et al., 2024). Combined with the previously described quantitative assessment, long-term monitoring of pioneer landforms construction would allow to understand how different ice forms and processes may influence the bioconstruction of these landforms and assess more precisely the rate and strength of co-adjustment dynamics. As described in Section 4.5, multiple ecogeomorphological patterns have been associated with ice dynamics and can also serve as proxies for determining ice dynamics

within reaches. For example, Boucher et al. 2009b) proposed that ice-scoured two-level riverbanks are maintained only when subjected to ice jams at least every 5 years, suggesting zones of high ice-jam intensity. However, there may be more subtle signatures of ice dynamics hidden in the spatial organization or temporal adjustment of the riverscapes. Sustained monitoring of spatial patterns and temporal changes in vegetation and landforms mosaics could lead to the identification of other typical patterns associated with ice and be used for preliminary assessment of rivers for which no data already exist.

4.7.4 Comparative studies

Prugne et al. (2025) compared two rivers with different ice-jam regimes, but it remains difficult in such a context to precisely identify notable differences arising from ice disturbances, as they were active in both systems. One approach would be to quantify ice contributions within river systems by comparing geomorphologically similar rivers with and without ice disturbances. The functional traits approach successfully allows this by simplifying vegetation composition within functionally identical groups of plants or functional metrics, resolving the problem associated with geographic species pools differing between regions (Bejarano et al., 2018; Diehl et al., 2017). It is proposed that plant functional responses to fluvial disturbances are limited to a narrow range of survival mechanisms against inundations, scouring and burial, making communities functionally similar across the globe from a biogeomorphological perspective (Corenblit et al., 2024b). Thus, international collaboration based on cross-regional comparisons could help isolate the role of ice dynamics in shaping the biogeomorphological template of rivers. Comparative reach-scale studies along latitudinal or altitudinal gradients, in geologically comparable but climatically distinct regions, could highlight key differences and help establish links between ice and river behavior.

4.7.5 Modeling integration

Numerical modelling integrating hydrogeomorphological processes with vegetation dynamics (taxonomical and functional) has been increasingly developed in the last decade (Bertoldi et al., 2014; Caponi et al., 2019; Solari et al., 2016). Despite the complexity of such models that integrate water structure (e.g., depth, velocity, direction, shear stress), sediment dynamics (e.g., erosion, transport, deposition) and vegetation response (e.g., recruitment, growth, uprooting, burial) and effects (stabilization, sediment trapping), results are continually refined and provide robust adequation when compared with real cases. Incorporating ice dynamics into such models could provide theoretical insights into how the frequency and magnitude of ice breakups affect the biogeomorphological dynamics of rivers. However, this remains a very challenging task, as complex interactions occur among ice, flow structure, and morphology. Mathematical equations have been developed to model the conditions needed for ice cover formation, breakup initiation and ice jam formation and release (Beltaos, 2007; Beltaos & Prowse, 2009), as well as the effects of breakups on water levels and associated shear stress (Beltaos, 1984). Future modelling efforts could aim to integrate and calibrate these equations as cause-and-effect relationships with hydrological modules in pre-existing hydrogeomorphological-vegetation models. Together, theoretical simulations exploring the effects of various ice parameters and applied models calibrated to real systems could yield hypotheses of interest and foster new questions to advance this field of research.

4.8 CONCLUDING REMARKS

This work proposed a broad discussion about the implications of ice dynamics on the biogeomorphological behavior of rivers, serving as a foundational step to bridge the gap between fluvial ice dynamics and the field of biogeomorphology. While the effects of ice dynamics on hydrology, geomorphology and ecology have been studied in the past, the body of work has been developed with little cross-disciplinary integration. Biogeomorphology, in contrast, offers tools that have proven useful to assess and predict the current and future state

of fluvial behaviors. The integration of ice dynamics conceptualized within the literature on biogeomorphology has led us to suggest that ice dynamics are more than just a physical disturbance that causes erosion and vegetation turnover, but rather a driver of co-adjustment dynamics that modulate vegetation feedback loops, successional trajectories, and landscape spatial organization. The current state of knowledge regarding this topic, however, is too sparse to allow us to develop robust conceptual models of fluvial ice dynamics, especially given that they encompass a wide range of forms and processes, leading to a diversity of possible outcomes. However, the hypotheses and reflections proposed in this work highlight promising research avenues for advancing our understanding of these disturbance regimes on fluvial biogeomorphological systems. We emphasize the need for long-term monitoring, cross-regional comparative studies, and the integration of ice into numerical models to deepen our understanding of the interactions among hydrogeomorphology, vegetation, and ice. Such new insights are not only of theoretical interest but hold critical implications for effective river management and restoration, especially as we seek to predict future river trajectories in a context of climate change.

4.9 AUTHOR CONTRIBUTIONS

Matthieu Prugne: Writing—review & editing, Writing—original draft, Visualization, Conceptualization. **Dov Corenblit**: Writing—review & editing. **Maxime Boivin**: Writing—review & editing. **Thomas Buffin-Bélanger** : Writing—review & editing.

CONCLUSION GÉNÉRALE

Cette thèse avait pour objectif principal de **définir le rôle des perturbations fluvioglacielles sur la biogéomorphologie des rivières de régions froides**. Pour ce faire, deux systèmes soumis à des régimes d'embâcle de glace et caractérisés par des styles fluviaux contrastés ont été comparés afin d'évaluer la variabilité des réponses selon le contexte hydrogéomorphologique. À l'aide d'approches multiscalaires et interdisciplinaires, les quatre chapitres présentés ont permis d'identifier des patrons et des mécanismes reliant les embâcles de glace aux ajustements biogéomorphologiques, à l'échelle du corridor fluvial et à l'échelle locale. Ces résultats illustrent le rôle que les embâcles de glace peuvent jouer sur l'évolution et les dynamiques d'ajustement des cours d'eau. Les différences de réponses entre les deux rivières à l'étude soulignent que les effets de la glace dépendent du contexte hydrogéomorphologique dans lequel ils se manifestent et rappellent l'importance de considérer chaque rivière comme un système complexe, façonné par l'interaction de multiples facteurs.

Consacré aux trajectoires hydrogéomorphologiques et de la végétation à l'échelle du corridor fluvial sur plusieurs décennies, le **premier chapitre** a révélé des patrons d'ajustements biogéomorphologiques attribuables aux perturbations par embâcle de glace. À une échelle plus fine, le **deuxième chapitre** a apporté un éclairage sur le rôle des régimes de perturbations par embâcle sur la composition des communautés riveraines, tout en montrant que les facteurs hydrogéomorphologiques demeurent les principaux déterminants. En complément, **le troisième chapitre** a transposé ces analyses au domaine de l'écologie fonctionnelle, mettant en évidence des guildes et des traits qui répondent aux régimes des embâcles de glace. Alors que ces trois premiers chapitres ont mis l'accent sur les effets structurants des embâcles de glace, le **quatrième chapitre** a permis d'intégrer ces nouvelles connaissances dans une revue de la littérature pour théoriser et conceptualiser le rôle joué par les embâcles de glace et d'autres processus fluvioglaciels sur le comportement biogéomorphologique des rivières.

Dans l'ensemble, cette thèse contribue au développement des connaissances sur l'écologie végétale riveraine des milieux froids et stimule l'intégration des dynamiques fluvioglacielles dans les cadres théoriques de la biogéomorphologie. L'approche descriptive et inductive adoptée dans ce projet a permis de proposer de multiples hypothèses sur les dynamiques d'interaction entre la végétation, l'hydrogéomorphologie et la glace, mais appelle également à de futures recherches pour tester ces hypothèses et approfondir notre compréhension des mécanismes sous-jacents aux patrons identifiés. De plus, il convient de noter que la caractérisation des processus fluvioglaciels, des communautés végétales et des dynamiques hydrogéomorphologiques constitue un défi et comporte des limites auxquelles nous avons été confrontés. Les prochaines sections présentent, par thématique, les grandes conclusions, limites et perspectives issues de cette thèse.

Les défis pour l'étude des processus fluvioglaciels

Les processus fluvioglaciels, par leurs effets sur les inondations et l'érosion, sont considérés par plusieurs comme des facteurs déterminants pour la structure et dynamique des rivières (Boucher, 2017b; Chassiot et al., 2020; Rokaya et al., 2018). Toutefois, ces processus demeurent sous-étudiés comparativement aux perturbations associées aux régimes des crues, et ce, particulièrement quant aux effets sur la végétation (Poulin et al., 2019). Dans le cas des embâcles de glace, malgré leurs effets morphogènes importants, la sous-représentation de ces évènements découle de plusieurs défis associés à leur caractérisation. Bien qu'il soit possible de combiner différentes sources d'information pour décrire un régime d'embâcle afin d'améliorer son estimation, comme ce fut le cas dans cette thèse, il est important de reconnaître les limites qui y sont associées. D'abord, les données historiques issues de journaux locaux ou de bases de données municipales et provinciales sont limitées quant à leur couverture spatiale et temporelle. Spatialement, les tronçons fluviaux sans risque d'inondation sont très peu, voire pas du tout, documentés. Temporellement, si les sites documentant des embâcles de glace peuvent fournir des informations riches sur la fréquence et l'amplitude des évènements, la quantité d'information exploitable dépend de l'année à laquelle les efforts d'observation ont été mis en place et de leur constance.

Pour déterminer des fréquences d'embâcles sur des sites où la documentation est limitée, l'approche dendrochronologique demeure prédominante et est largement employée (Lubiniecki et al., 2024). Elle reste toutefois limitée par des biais susceptibles de sous-représenter ou surreprésenter un régime. La sous-représentation peut être causée par la migration d'un cours d'eau, où l'érosion des berges entraîne le déracinement d'arbres potentiellement cicatrisés par des embâcles, ce qui emporte des individus qui auraient pu témoigner d'une année de perturbation. Inversement, des impacts autres que la glace sur les troncs d'arbres (p. ex., par des bois morts en transport) peuvent surreprésenter un régime d'embâcle en identifiant à tort une année de perturbation. Des erreurs de datation peuvent également survenir lors du comptage des cernes si les arbres échantillonnés présentent des cernes manquants ou des faux cernes. Dans le cadre de cette thèse, afin de réduire le risque de surreprésentation des évènements, deux critères ont été appliqués, soit (1) les arbres cicatrisés n'ont été récoltés que lorsque plusieurs individus présentaient des cicatrices à la même hauteur et (2) les années d'embâcles n'ont été confirmées que si un minimum de deux arbres affichait une cicatrice datée de cette même année. Bien que les erreurs associées aux faux cernes ou aux cernes manquants n'aient pas été prises en compte, nous estimons que la vaste couverture spatiale et temporelle de notre étude compense et réduit les biais potentiels liés à ces imprécisions. Toutefois, pour aller au-delà de cette compensation méthodologique et améliorer la précision de la datation dendrochronologique, une approche a récemment été développée par Lubiniecki et al. (2024). Cette méthode permet d'affiner la datation d'embâcles en dendrochronologie en comparant la séquence des largeurs de cernes sur les rondelles cicatrisées à une chronologie de référence établie à partir d'arbres sains et non impactés. Cette technique de datation croisée permet de détecter et de corriger les anomalies (faux cernes ou cernes manquants) causées par le stress lié à l'impact. Dans le cadre de futures recherches, nous recommandons d'appliquer systématiquement cette méthodologie afin que les études futures reposent sur une base méthodologique comparable.

Les résultats issus des trois premiers chapitres soutiennent malgré tout l'idée que les embâcles de glace constituent un régime de perturbations non négligeable, affectant à la fois les trajectoires d'ajustement des cours d'eau et la structure de leurs communautés végétales.

Malgré les biais associés à la caractérisation des régimes d'embâcle, la récurrence des patrons d'ajustements spatio-temporels au **Chapitre 1** et de la structure des communautés végétales aux **Chapitres 2 et 3** permet de renforcer la validité des résultats et de mettre en lumière plusieurs relations. Ces convergences attestent que les données analysées, malgré leurs limites méthodologiques, demeurent pertinentes pour caractériser les interactions entre les régimes de glace, la morphologie fluviale et les communautés végétales riveraines.

Ajustements biogéomorphologiques face aux perturbations par embâcle

Les ajustements biogéomorphologiques à l'échelle du corridor fluvial et pluridécennal ont été quantifiés dans le **Chapitre 1**, qui présente une approche géomatique basée sur la photo-interprétation d'images aériennes historiques couplée au régime de crue et au régime d'embâcle de glace. Bien que la quantification de l'érosion associée aux embâcles de glace ait été effectuée dans le passé (Vandermause et al., 2021), c'est à notre connaissance la première fois que les trajectoires hydrogéomorphologiques et de la végétation sur une période de plus de 50 ans sont explorées dans ce contexte. En combinant la caractérisation des régimes de crue et de glace à la quantification des changements spatio-temporels de la morphologie fluviale (largeur, sinuosité, érosion, déposition, migration) et de la succession végétale (changements de classes entre strates homogènes), nous avons mis en évidence des patrons récurrents de réponses biogéomorphologiques et distingué les effets propres aux perturbations glacielles de celles reliées aux crues. De plus, l'approche comparative incluant deux rivières contrastées (confinée et mobile) nous a offert à la fois une opportunité d'identifier des réponses biogéomorphologiques communes et divergentes, permettant ainsi d'apporter des nuances et d'approfondir notre compréhension du rôle des embâcles de glace sur l'évolution des cours d'eau.

Ces analyses de trajectoires ont révélé que les perturbations par embâcle de glace affectent avant tout la végétation en provoquant des renouvellements par destruction mécanique. Malgré le fait que des changements morphologiques tels qu'une migration latérale ou l'élargissement du chenal ont été identifiés au fil de plusieurs années d'embâcles,

ceux-ci demeuraient très localisés et n'avaient pas d'effets significatifs sur une période multidécennale. La variabilité du taux d'érosion à l'échelle des corridors fluviaux était plutôt comprise comme une réponse à la variation du régime de crue. Ces résultats suggèrent donc que, malgré les effets érosifs des embâcles, qui peuvent être très morphogènes, ces effets demeurent localisés et que les cours d'eau se réajustent rapidement entre deux évènements. Cependant, les résultats ont révélé que la végétation est systématiquement affectée par le passage d'un embâcle de glace, entraînant soit une régression des phases de succession, soit une limitation du taux de progression. Comme discuté dans le **Chapitre 4**, cet effet pourrait influencer indirectement les trajectoires d'ajustement en contrôlant la succession végétale et, par le fait même, les fonctions biogéomorphologiques des communautés riveraines. L'hypothèse émise dans ce dernier chapitre comme quoi les dynamiques de glace peuvent ralentir la construction d'unités biogéomorphologiques, sans toutefois l'inhiber, est supportée par l'analyse des trajectoires de succession biogéomorphologique, où malgré une présence d'embâcles de glace soutenue, plusieurs îles fluviales végétalisées se sont développées et stabilisées tout au long de la période d'étude dans la rivière Matapédia. Ces observations suggèrent donc que des boucles de rétroaction biogéomorphologiques sont présentes malgré le régime de perturbations liées à la glace.

Bien que ces analyses aient permis de décrire les ajustements hydrogéomorphologiques et végétaux dans un contexte fluvioglaciel, couverture temporelle et la nature des données utilisées limitent notre capacité à confirmer et quantifier les processus de co-ajustement entre la végétation et les rivières. Avec une décennie qui s'écoule entre chaque photographie, de nombreux effets de courte durée et localisés peuvent être non détectés, réduisant la précision avec laquelle nous pouvions mesurer les impacts biogéomorphologiques des embâcles de glace. Les relations entre le taux d'accumulation sédimentaire et la progression des stades de succession végétale, illustrées dans le **Chapitre 1**, suggèrent la présence de rétroactions biogéomorphologiques actives, sans toutefois permettre de déterminer si l'augmentation du taux d'accumulation résulte de la progression végétale ou si, à l'inverse, cette progression est favorisée par l'accumulation sédimentaire. Selon le cadre théorique de la biogéomorphologie et les études passées sur la co-construction des formes fluviales (Corenblit et al., 2007b;

Gurnell et al., 2012), nous pouvons malgré tout émettre l'hypothèse que la végétation agit comme ingénieur d'écosystème malgré les perturbations fluvioglacielles. De futures études sont toutefois nécessaires pour, d'une part, confirmer cette hypothèse et, d'autre part, quantifier les taux et la magnitude de ces interactions biogéomorphologiques. De plus, il est important de préciser que les deux cours d'eau à l'étude ne représentent pas l'ensemble des styles fluviaux et des contextes environnementaux des rivières de régions froides. Nos résultats, axés sur des rivières à galets avec une importante charge de fond en région montagneuse, offrent un premier exemple et peuvent participer à une réflexion sur la généralisation de ces processus, mais ne peuvent pas assumer le rôle d'une représentation globale transférable à toutes les rivières.

Ces limites n'enlèvent toutefois pas le caractère novateur de cette recherche qui apporte un éclairage sur la place du régime d'embâcle de glace comme facteur intégré aux systèmes fluviaux. Ce travail stimule le développement des connaissances sur la biogéomorphologie des rivières des régions froides et génère de nouveaux axes de recherche. Pour faire suite à ces découvertes, nous proposons que les recherches futures implantent des suivis long-termes à des échelles spatiales plus localisées (p. ex., tronçon et unité morphologique). Un éventail de technologies de pointe, telles que des drones équipés de capteurs LiDAR, est aujourd'hui largement accessible et permettrait de générer des données précises et en quantité suffisante pour concevoir des approches méthodologiques robustes, capables de préciser la nature des interactions entre les processus fluvioglaciels et les ajustements biogéomorphologiques. Plus la couverture temporelle est fréquente et longue, plus les chances de capturer des évènements fluvioglaciels et de déterminer leurs effets augmentent. Cette approche est d'autant plus pertinente dans l'idée que les processus fluvioglaciels ne se limitent pas qu'aux embâcles. Par exemple, des débâcles mécaniques plus modérées, qui ne résultent pas en la formation d'embâcles et ne s'élèvent pas au-dessus du niveau de plein bord, demeurent des évènements qui affectent le transport sédimentaire et les communautés riveraines. Les suivis à long terme et à haute fréquence permettraient donc de comprendre les mécanismes sous-jacents à la réponse biogéomorphologique des rivières face aux embâcles, mais aussi de découvrir d'autres processus d'importance qui peuvent influencer le comportement fluvial.

Le régime d'embâcle comme facteur structurant de la végétation

Malgré quelques études situant l'impact des glaces sur les communautés végétales riveraines, notre compréhension des interactions entre la glace et la végétation demeure peu développée (Poulin et al., 2019). Les **Chapitre 2 et 3** reposent sur l'étude taxonomique et fonctionnelle des communautés riveraines le long d'un gradient de régime de perturbations par embâcle de glace. Ces chapitres apportent un éclairage sur le rôle que jouent les régimes d'embâcle de glace dans la réponse des communautés végétales. Ils ont adopté une même approche de statistique multivariée pour mettre en relation les caractéristiques des communautés végétales avec les paramètres hydrogéomorphologiques et fluvioglaciels. Cette approche a permis de distinguer la part de variabilité expliquée par le contexte fluvial de celle attribuable au régime d'embâcle. Le **Chapitre 2** s'est concentré sur la composition taxonomique et les indices de diversité pour identifier les différences entre les deux rivières à l'étude ainsi que le long d'un gradient de perturbations. En complément, **le Chapitre 3** a exploité des valeurs de traits fonctionnels moyennés à la communauté et d'abondance de guildes fonctionnelles afin de mieux comprendre les mécanismes sous-jacents à la réponse des communautés face aux embâcles. Cette approche comparative, mettant en lumière des différences entre deux styles fluviaux contrastés et des sites soumis à des intensités variables d'embâcle, a permis de révéler des patrons taxonomiques et fonctionnels associés à différents niveaux de perturbation. De plus, l'étude révèle que les changements de composition et la sélection de traits induits par les embâcles varient d'une rivière à l'autre. Cette variabilité illustre le rôle fondamental des dynamiques hydrogéomorphologiques dans la modulation de la réponse de la végétation aux régimes de perturbation. Bien que ces résultats soient exclusivement consacrés à l'étude de la réponse de la végétation, ils constituent un fondement important d'un point de vue biogéomorphologique. Comme il est proposé dans la synthèse du **Chapitre 4**, la nature du comportement biogéomorphologique d'un milieu est fonction des espèces (et de leurs traits) présentes. Déterminer quelles influences ont les embâcles de glace sur la végétation est donc essentiel afin de pouvoir transposer ces connaissances à des

interprétations et des réflexions portant sur les potentielles rétroactions biogéomorphologiques à plus grande échelle.

Les analyses taxonomiques du **Chapitre 2** ont montré que la composition des communautés riveraines est davantage déterminée par les caractéristiques hydrogéomorphologiques que par les régimes d'embâcle de glace. Des différences significatives en termes de composition et d'abondance d'espèces ont été relevées entre les deux rivières. Notamment, les communautés liées aux stades pionniers de succession au sein de la rivière confinée étaient dominées par des espèces arbustives particulièrement adaptées aux perturbations mécaniques et physiologiques (p. ex., *Cornus sericea* et *Salix spp*.), alors que celles de la rivière mobile étaient dominées par le peuplier baumier (*Populus balsamifera*), une espèce arborescente pionnière des environnements fluviaux (Egger et al., 2015; González et al., 2018). Comme le montrent les analyses fonctionnelles du **Chapitre 3**, ces communautés se distinguent par un ensemble de traits fonctionnels qui reflètent les conditions environnementales de chaque rivière et correspondent aux trajectoires identifiées au **Chapitre 1**. L'absence de mobilité de la rivière Matapédia entraîne des écoulements concentrés dans le chenal qui applique une haute force de cisaillement sur l'ensemble de la largeur du chenal, filtrant les jeunes communautés en sélectionnant des traits de résistance tels qu'un enracinement profond, un taux de croissance rapide et une forte capacité à la propagation végétative. Inversement, la capacité d'ajustement spatial de la rivière Petite-Cascapédia résulte en des forces de cisaillement plus hétérogènes et localement moins importantes dû à la dissipation de l'énergie des écoulements en section sinueuse, permettant le recrutement et l'établissement d'arbres pionniers. En somme, les résultats ont mis en évidence les effets significatifs du confinement et de la migration latérale sur la composition taxonomique et fonctionnelle des communautés le long des deux corridors fluviaux. Ces observations illustrent le rôle du contexte hydrogéomorphologique dans la définition de la structure initiale des communautés, sur laquelle se superposent les perturbations fluvioglacielles.

Les analyses du gradient de perturbations ont révélé que la fréquence et l'amplitude des embâcles de glace expliquent significativement une portion de la variabilité quant à structure des communautés. Cet effet est toutefois modulé par le contexte hydrogéomorphologique, puisque les perturbations sévissant dans chaque cours d'eau n'affectent pas les mêmes communautés initialement définies par le contexte fluvial. Dans le cas de la rivière Matapédia, les sites sous des régimes d'embâcles intenses mettaient en évidence une plus grande abondance de traits d'évitement (*avoidance traits*), soit en faveur d'une flexibilité permettant aux plantes de se coucher sous le passage des glaces ou vers un cycle de vie court permettant aux plantes de ne pas subir ces perturbations. Associés à ces traits, ces sites présentaient une plus grande abondance de guildes de graminées et d'espèces bisannuelles. Dans le cas de la rivière Petite-Cascapédia, où les habitats au stade arbustif étaient principalement dominés par le peuplier, les sites les plus perturbés basculaient vers une abondance moindre de ces communautés, ce qui soutient l'idée que les peupliers sont des espèces particulièrement sensibles à l'abrasion glacielle (Smith & Pearce, 2000 b). De plus, les plaines alluviales boisées de ces sites se caractérisaient par une abondance d'espèces hygrophiles, notamment le frêne noir et la fougère-à-autruche. Cette composition floristique témoigne de l'influence des inondations par embâcle, qui favorisent le maintien de conditions humides en augmentant la fréquence des inondations. Si ce contraste souligne l'importance du contexte hydrogéomorphologique dans la diversité des réponses aux embâcles, les analyses taxonomiques et fonctionnelles ont néanmoins permis de dégager des similarités notables entre les deux rivières. Dans les deux cas, les régimes d'embâcles les plus sévères tendaient vers la sélection de traits associés à la propagation végétative, soulignant leurs effets à filtrer des espèces ayant la capacité de rapidement se régénérer ou se propager latéralement par des branches ou des tiges brisées. Cette réponse fonctionnelle est illustrée par l'expansion du cornouiller stolonifère qui gagnait en abondance au détriment des espèces de saules dans les zones fortement perturbées. Bien que les saules soient largement reconnus pour leurs adaptations aux contraintes fluviales (Edwards, 2024) et aient été documentés comme résistants aux contraintes de glaces (Karle, 2007; Poulin et al., 2019), nos résultats suggèrent que les embâcles exercent un filtrage sélectif au sein même des guildes d'espèces

tolérantes aux perturbations mécaniques. Cette distinction souligne la nécessité d'approfondir les connaissances sur le cornouiller stolonifère, dont la représentation dans la littérature scientifique demeure limitée.

Bien que ces analyses aient porté spécifiquement sur la réponse des communautés végétales plutôt que sur leurs fonctions biogéomorphologiques, elles constituent une base sur laquelle pourront s'appuyer de futures interprétations biogéomorphologiques. Comme présenté dans le **Chapitre 4**, la composition fonctionnelle d'une communauté comprend un ensemble de traits qui répondent à un contexte environnemental, mais qui peuvent aussi agir comme traits d'effet ou de rétroaction biogéomorphologiques (Corenblit et al., 2024b; Diehl et al., 2017). Puisque les **Chapitre 2 et 3** révèlent que les perturbations fluvioglacielles contribuent à la sélection et au maintien de guildes spécifiques, il est raisonnable d'émettre l'hypothèse qu'elles structurent également les fonctions biogéomorphologiques des communautés riveraines par la sélection de traits de rétroactions. Ce faisant, la transposition de ces observations à l'échelle du tronçon et du corridor fluvial suggère l'existence de trajectoires biogéomorphologiques indirectement influencées par le régime de glace, par l'entremise de la structure végétale que ce dernier impose.

Toutefois, la généralisation de ces mécanismes nécessite une certaine prudence. Si l'interprétation des résultats a permis d'identifier de possibles effets structurants du régime par embâcle sur la végétation riveraine, elle reste limitée par son approche descriptive reposant sur des techniques d'ordination. Afin de générer des inférences plus robustes, il aurait été recommandé d'employer des modèles de régression mixtes intégrant des facteurs aléatoires afin de prendre en compte la variabilité naturelle d'un site à l'autre. Or, le faible nombre de sites d'échantillonnage présents dans cette étude nous limite pour ce type d'approche. La significativité statistique des modèles d'analyse de redondance, couplée à la cohérence des résultats avec les mécanismes écologiques documentés dans la littérature, soutiennent toutefois la vraisemblance des patrons décrits. Ensuite, les analyses fonctionnelles reposaient sur des bases de données en ligne qui ne peuvent pas capturer la variabilité locale des traits fonctionnels, alors que nombreux d'entre eux sont plastiques et

peuvent varier en réponse aux stress locaux d'un environnement (Albert et al., 2010; Violle et al., 2012). Ainsi, nos résultats permettent de dégager des tendances adaptatives générales qui prédominent dans un contexte fluvioglaciel, mais ne rendent pas compte des effets locaux sur l'expression fonctionnelle de ces communautés.

L'identification des grandes différences observées entre les deux rivières à l'étude et le long d'un gradient de perturbations liées aux embâcles de glace contribue à approfondir nos connaissances sur l'écologie des plantes riveraines en région froide. D'un point de vue fondamental, cela implique que les réponses écologiques face à des perturbations fluvioglacielles ne peuvent être prises en compte sans tenir compte du contexte hydrogéomorphologique, qui demeure prédominant dans la structure des communautés riveraines. De plus, l'absence de corrélation entre les indices de richesse et de diversité et le régime de glace suggère que la réponse des communautés riveraines en régions froides repose davantage sur les stratégies fonctionnelles que sur la diversité taxonomique. Ce constat souligne l'importance de dépasser les simples métriques de richesse et de diversité spécifique pour étudier les effets des glaces sur la végétation riveraine. Dans une perspective où la restauration et la conservation des milieux fluviaux occupent une place grandissante dans nos sociétés avec une vision axée sur le maintien de services écosystémiques (Wohl et al., 2015), ces travaux apportent un éclairage sur les potentielles espèces ingénieurs de ces environnements. Ces chapitres ouvrent notamment la porte à de futures recherches en proposant une orientation vers une approche fonctionnelle afin de déterminer les réponses locales des communautés végétales face aux embâcles de glace. Nous pensons que des traits d'intérêt ou clés, tels que la flexibilité, la densité des tiges sur un individu, le taux de rejets, le taux de clonalité (mesuré avec une approche génétique), la hauteur ou la densité des individus dans une communauté, devraient être mesurés et comparés entre des milieux où il y a présence et absence de perturbations. Cette approche pourrait alors nuancer l'effet des glaces et affiner notre compréhension des mécanismes associant les communautés riveraines au régime fluvioglaciel.

La biogéomorphologie : Une science fondamentale et appliquée à approfondir

Basé sur une revue de littérature combinée aux résultats des trois premiers chapitres, le **Chapitre 4** expose différentes hypothèses quant aux possibles rôles des processus fluvioglaciels sur la biogéomorphologie fluviale, en passant de l'échelle de l'individu jusqu'au corridor fluvial. Soutenu par des exemples concrets issus des résultats précédents de cette thèse, il permet d'agréger l'ensemble des interprétations et réflexions dans un contexte biogéomorphologique et de discuter des effets possibles en cascade initiés par les embâcles de glace et d'autres processus. D'abord, il est proposé que le régime (fréquence et amplitude) de perturbations par les glaces puisse moduler l'expression des rétroactions biogéomorphologiques par la sélection de traits fonctionnels spécifiques. Puisque la sédimentation induite par la végétation est fonction de la structure des communautés (Bywater-Reyes et al., 2022a; Corenblit et al., 2024b) et que le régime d'embâcle influence la sélection de traits (**Chapitre 3**), il apparaît que ce filtrage écologique détermine en amont le potentiel ingénieur de la végétation, conditionnant ainsi les effets *bottom-up* depuis le trait fonctionnel jusqu'à l'unité biogéomorphologique. Ensuite, les trajectoires temporelles des processus de co-construction sont discutées, où la fréquence des perturbations mécaniques par la glace est présentée comme facteur de contrôle sur la succession biogéomorphologique fluviale. Il est suggéré que ces perturbations n'inhibent pas la construction biogéomorphologique des formes fluviales, mais qu'elles peuvent néanmoins interrompre et ralentir ce processus en augmentant la fréquence de réinitialisation de la végétation. Finalement, le **Chapitre 4** illustre les effets structurants de la glace sur l'organisation spatiale des morphologies et des communautés à l'échelle du corridor fluvial, pouvant conditionner la distribution des zones où des rétroactions biogéomorphologiques peuvent être initiées.

Tous ces éléments offrent une première illustration des dynamiques fluvioglacielles comme étant plus qu'un simple facteur d'érosion et de réinitialisation (*reset)* de la végétation. À la lumière de ces réflexions, nous suggérons que ces dynamiques exercent une influence structurante sur la trajectoire évolutive des rivières : elles agissent non seulement de manière directe sur les composantes hydrogéomorphologiques, mais aussi indirectement en dictant

l'organisation fonctionnelle des communautés végétales, modulant ainsi leur capacité à agir comme ingénieurs d'écosystème. Si les méthodologies employées dans cette thèse ne permettent pas de quantifier exhaustivement l'amplitude de ces interactions, elles posent néanmoins les bases nécessaires à leur compréhension et ouvrent la voie à de nombreuses perspectives de recherche. Considérant l'apport de la biogéomorphologie à la compréhension des hydrosystèmes (Gurnell & Bertoldi, 2024), nous pensons que des efforts doivent être déployés au Québec et dans les régions froides pour produire des connaissances interdisciplinaires entre biologistes et géomorphologues. Cette collaboration sera nécessaire afin d'appliquer, contextualiser et calibrer les cadres théoriques et modèles issues de la biogéomorphologie aux rivières de régions froides. Une intégration explicite du rôle de la glace dans ces modèles est essentielle pour rendre compte de toute la complexité des dynamiques d'ajustement propres à ces environnements. En parvenant à associer précisément différents processus fluvioglaciels aux formes et ajustements qu'ils engendrent, nous serons dès lors mieux outillés pour anticiper les futures trajectoires d'évolution des cours d'eau. Cette capacité prédictive s'avère d'autant plus importante dans un contexte de changements climatiques où plusieurs prédictions annoncent un changement des régimes fluvioglaciels, ce qui pourrait, par conséquent, redéfinir l'équilibre biogéomorphologique des rivières dans ces régions.

Bien que la biogéomorphologie demeure une science émergente dont les bases fondamentales sont encore en développement, elle commence toutefois à s'intégrer aux pratiques de gestion, offrant particulièrement des avantages pour la restauration de milieux hydriques (Johnson et al., 2020; O'Briain et al., 2024; Viles & Coombes, 2022). Notamment, l'édition 2026 de l'assemblée générale de l'Union Européenne des Géosciences (EGU2026) propose une session exclusivement axée sur l'intégration de la biogéomorphologie dans les pratiques de gestion et de restauration. La biogéomorphologie offre une approche qui permet non seulement de comprendre les paramètres optimaux favorisant la restauration des processus géomorphologiques et écologiques, mais aussi de mieux prédire et modéliser les trajectoires que prendront les systèmes restaurés. Pour reprendre les mots de O'Briain et al. (2024), « *l'accent actuellement mis sur l'écoulement et le transport sédimentaire, sans*

considérer adéquatement la végétation comme un agent structurant à part entière au-delà de son rôle de stabilisation, est trop restrictif pour une restauration durable ». Autrement dit, approfondir notre compréhension des interactions biogéomorphologiques et développer des modèles prédictifs intégrant les interactions plantes-rivières s'avère essentiel pour guider des projets de restauration durable des corridors fluviaux. Alors que des efforts grandissants sont déployés pour la création de tels modèles (Bertoldi et al., 2014; Caponi et al., 2019; Solari et al., 2016) et pour l'intégration d'une biogéomorphologie appliquée (Johnson et al., 2020; O'Briain et al., 2024; Viles & Coombes, 2022), les perturbations fluvioglacielles n'ont pas encore été considérées. Or, il s'agit d'une avenue prometteuse pour la gestion, la conservation et la restauration des rivières au Québec et dans les milieux où sévissent des perturbations par la glace.

En somme, nous souhaitons que cette thèse stimule l'essor de la recherche en biogéomorphologie au Québec afin d'affiner notre compréhension des systèmes fluviaux en régions froides. Le développement de ces connaissances nous apporterait non seulement une meilleure compréhension des dynamiques d'ajustement des rivières soumises aux processus fluvioglaciels, mais pourrait également servir d'outil à une meilleure gestion de nos cours d'eau.

ANNEXE I : CHAPTER 1 SUPPLEMENTARY MATERIALS

Table 13. Summary of the dendrochronological results, presenting both the total number of jams identified in each site (total jams) and the number of confirmed jams.

Site	Nb. of Samples	Mean tree age (year)	Confirmed jams	Average height (cm)
Matapédia				
1	6	52,67	3	148,33
2	14	93,57	2	104,29
3	2	29,00	0	92,50
4	8	88,50	3	149,50
5	5	67,00	4	181,00
6	11	63,82	5	119,73
7	3	76,67	1	136,00
8	6	30,00	1	111,67
9	15	52,13	1	96,73
10	14	69,36	4	121,50
Petite-Cascapédia				
1	4	26,25	1	40,00
2	5	33,60	2	82,00
3	4	37,50	1	127,50
4	16	119,44	2	199,69
5	5	47,00	2	112,20
6	11	73,36	5	113,64
7	4	45,25	0	75,00
8	2	28,00	1	71,00

Table 14. Summary of discharge characterization and ice jam analysis. QMmax, QMmean, and QMmin are descriptive statistics of the annual maximum discharge (m3/s) by period. The flood interval and jams indicate the number of events that occurred in the given period, followed by the calculated frequency (in bold). Missing years from the discharge database were not counted in the frequency calculation.

Matapédia						Petite-Cascapédia				
	1963-1974	1974-1985	1985-1993	1993-2004	2004-2016	1963-1975	1975-1986	1986-1992	1992-2004	2004-2016
Qmax	614	940	670	493.2	550.1	425	530	414	613.1	700
Qmean	483	471	431	353	408	245	318	249	300	392
Qmin	374	227	228	228	285	159	136	123	146.2	212
hq2	6 / **1.5**	7 / **0.6**	4 / **0.6**	4 / **0.4**	7 / **0.6**	5 / **0.4**	7 / **0.6**	4 / **0.7**	6 / **0.5**	6 / **0.8**
hq5	3 / **0.8**	4 / **0.4**	1 / **0.1**	0	3 / **0.3**	1 / **0.1**	4 / **0.4**	1 / **0.2**	3 / **0.3**	2 / **0.3**
hq10	1 / **0.25**	2 / **0.2**	1 / **0.1**	0	2 / **0.2**	0	1 / **0.1**	0	1 / **0.1**	2 / **0.3**
hq20	0	1 / **0.1**	1 / **0.1**	0	0	0	0	0	0	1 / **0.1**
hq50	0	1 / **0.1**	0	0	0	0	0	0	0	1 / **0.1**
jams	1 / **0.1**	2 / **0.2**	0	2 / **0.4**	7 / **0.6**	0	1 / **0.1**	0	1 / **0.1**	5 / **0.4**

Table 15. Descriptive table of mean width and mean area of subreaches.

	Matapédia		Petite-Cascapédia	
Sub-reach	Width (m)	Area (ha)	Width (m)	Area (ha)
1	149	9	70	6
2	138	13	96	8
3	114	12	131	15
4	143	15	78	18
5	130	13	69	9
6	110	11	71	8
7	113	11	57	8
8	90	9	64	7
9	102	10	63	7
10	94	9	62	6
11	85	9	62	8
12	99	10	72	10
13	76	8	72	8
14	83	8	74	8
15	98	10	54	6
16	82	8	80	6
17	93	9	91	5
18	86	9	-	-
19	57	6	-	-
20	66	7	-	-
21	91	9	-	-
22	88	9	-	-
23	68	7	-	-
24	93	9	-	-
25	90	9	-	-
26	78	8	-	-
27	82	8	-	-
28	69	7	-	-
29	64	6	-	-
30	54	5	-	-
31	43	4	-	-
32	62	6	-	-
33	64	7	-	-
34	60	4	-	-
35	66	3	-	-

Table 16. Surface area (ha) for each cover classes, rivers and years. WA = Water, BS = Barren surface, SV = Sparse Vegetation, DV = Dense vegetation

Year/Class	WA	BS	SV	DV	Forest	Anthropic
Matapédia						
1963	365	15	10	49	87	33
1974	335	25	11	71	98	16
1986	345	23	14	65	93	16
1993	344	17	13	69	102	11
2004	356	2	5	75	113	5
2016	349	15	12	58	117	6
Petite-Cascapédia						
1963	117	36	8	52	371	131
1975	108	21	13	69	372	132
1986	99	39	15	77	395	94
1992	111	18	15	68	412	93
2004	118	9	9	47	444	89
2016	105	32	17	43	443	75

ANNEXE II : CHAPTER 2 SUPPLEMENTARY MATERIALS

Table 17. List of the 115 species identified and used for this study in the Matapédia River and the Petite-Cascapédia River. Codes of the species are derived from the U.S. Department of Agriculture (USDA) Plants Database and codes for species identified at the genus level (n = 27) were coded with the three first letters of the genus followed by "sp". Abundance was calculated as the mean estimated cover ± 1 SE when present in each river. and the frequency of occurrences was measured as the number of plots where the species occurred divided by the total number of plots for each river.

Species	Code	Abundance (mean cover ± se)		Frequency of occurrence (%)	
		Matapédia	Petite-Cascapédia	Matapédia	Petite-Cascapédia
Abies balsamea	ABBA	25.2 ± 11.7	9.1 ± 2.8	4.5	9.9
Acer rubrum	ACRU		1.5 ± 0.5		2.5
Acer spicatum	ACSP2	27.1 ± 3.9	21 ± 8.5	8	12.3
Actaea rubra	ACRU2		1 ± NA		
Agrimonia striata	AGST	11.7 ± 6.7		3.4	
Agrostis sp.	AGRsp	44.2 ± 11.3	13.3 ± 8.3	12.5	3.7
Alnus incana	ALIN2	40.3 ± 10.5	14.6 ± 3.1	17	30.9
Amelanchier sp	AMEsp	17 ± 7.5	75 ± NA	5.7	1.2
Anemone canadensis	ANCA8	19.4 ± 5.8	32.7 ± 12.5	18.2	7.4
Angelica atropurpurea	ANAT	15 ± NA		1.1	
Apocynum androsaemifolium	APAN2	10.3 ± 6		6.8	
Apocynum cannabinum	APCA	19.5 ± 7		9.1	
Aralia nudicaulis	ARNU2		8.6 ± 5.6		6.2
Arctium lappa	ARLA3	5 ± 0	10 ± NA	2.3	1.2
Arisaema triphyllum	ARTR	11.9 ± 2.3	1 ± 0	9.1	2.5
Aster macrophyllus (Eurybia macrophylla)	EUMA27	8 ± 7	10 ± NA	2.3	1.2
Aster puniceus (Symphyotrichum puniceum)	SYPUP	5 ± 0	5.5 ± 4.5	2.3	2.5

Aster sp	ASTsp	4.1 ± 1.1	3 ± 2	9.1	2.5
Betula papyrifera	BEPA	18.3 ± 6.7	25 ± 0	3.4	2.5
Bromus sp	BROsp	5.2 ± 1.8	8.2 ± 3.6	4.5	16
Calamagrostis canadensis	CACA4	46 ± 17.8	17.5 ± 2.5	5.7	2.5
Carex sp	CARsp	17.7 ± 7	7 ± 3.4	15.9	8.6
Centaurea nigra	CENI2	13.4 ± 3.3	1.5 ± 0.5	17	2.5
Cirsium vulgare	CIVU	5 ± 0	1.2 ± 0.1	3.4	17.3
Convolvulus arvensis	COAR4	12.5 ± 5		12.5	
Cornus canadensis	COCA13	10 ± NA	5 ± NA	1.1	1.2
Cornus sericea	COSE16	41.5 ± 4.6	15.6 ± 3.7	52.3	46.9
Corylus cornuta	COCO6	34.2 ± 10.1		6.8	
Crataegus sp	CRAsp	50 ± 0		2.3	
Deschampsia sp	DEsp		12.8 ± 4.6		4.9
Dryas integrifolia	DRIN4		26.4 ± 14.8		6.2
Echium vulgare	ECVU		5 ± NA		
Elymus sp	ELYsp	5.3 ± 2.6	4 ± 1	3.4	3.7
Epipactis helleborine	EPHE	6.2 ± 1.7	3.2 ± 1.5	5.7	7.4
Equisetum arvense	EQAR	14.5 ± 3.4	26.9 ± 13	17	8.6
Equisetum sylvaticum	EQSY		8.8 ± 2.4		4.9
Erigeron sp	ERIsp	5 ± NA	1.1 ± 0.1	1.1	8.6
Eupatorium maculatum	EUMA9	21.5 ± 3.5	13.9 ± 6.5	55.7	11.1
Festuca sp	FESsp	11.2 ± 2.4	17.3 ± 5.6	4.5	18.5
Fragaria vesca	FRVE	12.8 ± 3.9	3.8 ± 2.2	10.2	7.4
Fragaria virginiana	FRVI	16.2 ± 4.9	22.8 ± 8	10.2	9.9
Fraxinus nigra	FRNI	42.3 ± 8.2	28.2 ± 5.3	22.7	29.6
Galium asprellum	GAAS2	5 ± NA	1 ± NA	1.1	1.2
Galium mollugo	GAMO	14.6 ± 2.5	28.1 ± 6.3	37.5	22.2
Galium palustre	GAPA3	5 ± 0	3.5 ± 1.5	4.5	2.5
Galium sp	GALsp		12.6 ± 3		24.7

Geum sp	GEUsp	1.3 ± 0.2	1 ± NA	8	1.2
Glyceria sp	GLYsp	10 ± NA	1 ± NA	1.1	1.2
Helianthus tuberosus	HETU		5 ± NA		1.2
Hieracium sp	HIEsp	1 ± 0	1.9 ± 0.5	3.4	13.6
Hypericum perforatum	HYPE	18.8 ± 8.1	1 ± NA	12.5	1.2
Impatiens capensis	IMCA	15 ± 4.5		5.7	
Iris versicolor	IRVE2	2.6 ± 1		5.7	
Larix laricina	LALA		5.4 ± 2		
Lathyrus latifolius	LALA4	5 ± NA		1.1	
Leucanthemum vulgare	LEVU	4.6 ± 1.7	3.7 ± 1.2	10.2	28.4
Lonicera sp	LONsp	10 ± 5	3 ± 2	2.3	2.5
Lotus corniculatus	LOCO6	2 ± NA	2 ± NA	1.1	1.2
Lycopus americanus	LYAM	10 ± 0		2.3	
Lysimachia ciliata	LYCI	1 ± NA	1 ± NA	1.1	1.2
Maianthemum canadense	MACA4	12.5 ± 2.5	3.2 ± 1	2.3	4.9
Maianthemum stellatum	MAST4	5.8 ± 4.8	5.4 ± 1.1	5.7	30.9
Matteuccia struthiopteris	MAST	51.2 ± 7.8	51.1 ± 7.9	29.5	38.3
Medicago lupulina	MELU		2.1 ± 0.6		9.9
Melilotus albus	MEOF	27.2 ± 9.7	23.3 ± 4.4	10.2	53.1
Mentha canadensis	MEAR4	7.3 ± 2.4	1.3 ± 0.3	11.4	3.7
Myrica gale	MYGA	35 ± 25		2.3	
Nabalus sp	NABsp	21.2 ± 6.9		9.1	
Oenothera biennis	OEBI	1 ± 0	3.4 ± 1	2.3	6.2
Onoclea sensibilis	ONSE	27.2 ± 5.8	1 ± NA	34.1	1.2
Osmunda claytoniana	OSCL2	25 ± NA		1.1	
Oxalis stricta	OXDI2	3 ± 1.2	5.2 ± 4	4.5	7.4
Phalaris arundinacea	PHAR3	25 ± 7.3	30.8 ± 10.9	14.8	13.6
Phegopteris connectilis	PHCO24		52.3 ± 25.2		
Phleum sp	PHLsp		9.2 ± 5.3		4.9

Picea mariana	PIMA	46 ± 14.5	22.8 ± 6.7	6.8	19.8
Plantago major	PLMA2	1 ± NA	1 ± 0	1.1	2.5
Poa sp	POAsp	16 ± 3.3	19.6 ± 4.1	35.2	44.4
Populus balsamifera	POBA2	35.6 ± 6.9	50.8 ± 4.8	19.3	77.8
Populus tremuloides	POTR5	16.2 ± 11.2	1 ± NA	4.5	1.2
Potentilla anserina	ARAN7	23.9 ± 12.8	1 ± NA	8	1.2
Prunella vulgaris	PRVU	10.6 ± 1.8	2.8 ± 0.4	11.4	18.5
Prunus pensylvanica	PRPEN	25.8 ± 4.7	5.3 ± 2.6	6.8	3.7
Pyrola asarifolia	PYAS	52.5 ± 37.5	6.1 ± 1.5	2.3	11.1
Pyrola elliptica	PYEL	47.5 ± 32.5	2 ± NA	2.3	1.2
Ranunculus acris	RAAC3	3.4 ± 1	4.2 ± 1.2	5.7	11.1
Rosa sp	ROSsp	11.5 ± 3.1	4 ± 1	15.9	4.9
Rubus idaeus	RUID	16.2 ± 5.3	7.6 ± 2.1	15.9	17.3
Rubus pubescens	RUPU	29.1 ± 4.6	31.7 ± 5	31.8	39.5
Rumex sp	RUMsp	1.5 ± 0.5		2.3	
Salix sp	SALsp	20.7 ± 3.4	11.9 ± 3	50	23.5
Sambucus canadensis	SANIC4	5 ± 0		2.3	
Scutellaria sp	SCUsp	5.3 ± 2.6	1.3 ± 0.3	3.4	3.7
Silene vulgaris	SIVU	5 ± NA	5.8 ± 1.1	1.1	35.8
Solanum dulcamara	SODU	10 ± NA		1.1	
Solidago sp	SOLsp	13.5 ± 4.4	13.5 ± 3.1	25	49.4
Sonchus sp	SONsp	5 ± NA	3.7 ± 1.3	1.1	3.7
Sorbus sp	SORsp	10 ± 5	1 ± NA	2.3	1.2
Stachys sp	STAsp		4.8 ± 2.2		7.4
Tanacetum vulgare	TAVU	6.5 ± 1.3		13.6	
Taraxacum officinale	TAOF	4 ± 1	2.2 ± 0.5	3.4	17.3
Taxus canadensis	TACA7	15 ± NA		1.1	
Thalictrum pubescens	THPU2	8.7 ± 1.3	1.7 ± 0.6	28.4	8.6
Thuja occidentalis	THOC2	25 ± 0	34.1 ± 9.7	2.3	17.3

Tiarella cordifolia	TICO	1 ± NA	1 ± NA	1.1	1.2
Toxicodendron radicans	TORA2	26.7 ± 11.1		6.8	
Trifolium pratense	TRPR2		4 ± 2.8		6.2
Trifolium repens	TRRE3		1.5 ± 0.5		2.5
Trillium cernuum	TRCE	3 ± 2		2.3	
Tussilago farfara	TUFA	12 ± 3	16.6 ± 2.3	19.3	66.7
Ulmus americana	ULAM	24.2 ± 7.8		6.8	
Valeriana officinalis	VAOF		1 ± 0		2.5
Viburnum opulus var. americanum	VIOPA2	24.5 ± 7	3 ± 0.9	9.1	7.4
Vicia cracca	VICR	10.3 ± 1.1	23.9 ± 4.3	40.9	61.7
Viola sp	VIOsp	5 ± 0	1 ± 0	2.3	4.9

Table 18. Pairwise PERMANOVA (adonis2) results comparing Hellinger-transformed species composition between all combinations of habitat–river groups. The table reports the proportion of explained variance (R^2), F-values, and Bonferroni-adjusted p-values (adj.p) for each pairwise comparison. All tests were based on Bray-Curtis's dissimilarity and 999 permutations. Mata - Matapédia River, PC - Petit-Cascapédia River

Group1	Group2	R2	F	adj.p
Mata.Floodplain	**PC.Floodplain**	0.117231	5,444757	0,001
Mata.Floodplain	**PC.Ecotone**	0,176067	11,11196	0,001
Mata.Floodplain	**Mata.Ecotone**	0,106447	7,505061	0,001
Mata.Floodplain	**Mata.Bar**	0,279165	14,71665	0,001
Mata.Floodplain	**PC.Bar**	0,247188	10,83567	0,001
PC.Floodplain	**PC.Ecotone**	0,112275	7,714987	0,001
PC.Floodplain	**Mata.Ecotone**	0,171643	14,919	0,001
PC.Floodplain	**Mata.Bar**	0,307678	20,88746	0,001
PC.Floodplain	**PC.Bar**	0,22624	12,28042	0,001
PC.Ecotone	**Mata.Ecotone**	0,134944	12,94754	0,001
PC.Ecotone	**Mata.Bar**	0,183659	13,04872	0,001
PC.Ecotone	**PC.Bar**	0,068157	3,876532	0,001
Mata.Ecotone	**Mata.Bar**	0,114228	8,898183	0,001
Mata.Ecotone	**PC.Bar**	0,140266	10,4416	0,001
Mata.Bar	**PC.Bar**	0,154358	7,118795	0,001

Table 19. Pairwise PERMANOVA (adonis2) results comparing presence-absence species composition between all combinations of habitat–river groups. The table reports the proportion of explained variance (R^2), F-values, and Bonferroni-adjusted p-values (adj.p) for each pairwise comparison. All tests were based on Jaccard's dissimilarity and 999 permutations. Mata - Matapédia River, PC - Petit-Cascapédia River

Group1	Group2	R2	F	adj.p
Mata.Floodplain	**PC.Floodplain**	0,130602	6,159086	0,001
Mata.Floodplain	**PC.Ecotone**	0,217149	14,42386	0,001
Mata.Floodplain	**Mata.Ecotone**	0,110531	7,828784	0,001
Mata.Floodplain	**Mata.Bar**	0,340743	19,64067	0,001
Mata.Floodplain	**PC.Bar**	0,285714	13,19997	0,001
PC.Floodplain	**PC.Ecotone**	0,12764	8,925278	0,001
PC.Floodplain	**Mata.Ecotone**	0,175971	15,37562	0,001
PC.Floodplain	**Mata.Bar**	0,344482	24,69908	0,001
PC.Floodplain	**PC.Bar**	0,24499	13,6284	0,001
PC.Ecotone	**Mata.Ecotone**	0,15045	14,69879	0,001
PC.Ecotone	**Mata.Bar**	0,231069	17,42941	0,001
PC.Ecotone	**PC.Bar**	0,085964	4,984583	0,001
Mata.Ecotone	**Mata.Bar**	0,133364	10,61823	0,001
Mata.Ecotone	**PC.Bar**	0,1699	13,09913	0,001
Mata.Bar	**PC.Bar**	0,197501	9,598164	0,001

Table 20. Pairwise Wilcoxon rank-sum test results comparing community richness, Shannon's diversity and Piélou's Evenness across River–Habitat combinations. Reported are the test statistic (W), raw p-values, and adjusted p-values (Benjamini–Hochberg correction) for each pairwise comparison. Mata - Matapédia River, PC - Petit-Cascapédia River

		Richness		Shannon		Evenness	
Group 1	**Group 2**	W	Adj. P-value	W	Adj. P-value	W	Adj. P-value
Mata.Floodplain	**PC.Floodplain**	86	0.002	152	0.148	398	0.000
Mata.Floodplain	**PC.Ecotone**	205.5	0.053	308	0.912	489	0.003
Mata.Floodplain	**Mata.Ecotone**	344	0.341	368	0.645	517	0.159
Mata.Floodplain	**Mata.Bar**	246	0.194	256	0.152	240	0.294
Mata.Floodplain	**PC.Bar**	237.5	0.008	255	0.002	161	0.804
PC.Floodplain	**PC.Ecotone**	700.5	0.004	573	0.254	339	0.089
PC.Floodplain	**Mata.Ecotone**	964	0.000	757	0.183	180	0.000
PC.Floodplain	**Mata.Bar**	547	0.000	500	0.000	121	0.001
PC.Floodplain	**PC.Bar**	451.5	0.000	437	0.000	92	0.003
PC.Ecotone	**Mata.Ecotone**	1032.5	0.215	863	0.888	525	0.003
PC.Ecotone	**Mata.Bar**	673.5	0.000	573	0.046	300	0.095
PC.Ecotone	**PC.Bar**	594	0.000	558	0.000	190	0.023
Mata.Ecotone	**Mata.Bar**	788	0.006	773	0.015	574	0.804
Mata.Ecotone	**PC.Bar**	730.5	0.000	727	0.000	349	0.294
Mata.Bar	**PC.Bar**	303	0.016	308	0.018	183	0.620

Table 21. Kendall's tau correlation matrix between community-aggregated metrics and ice-jam regime variables. Values underlined with asterisks shows significant p-values prior to post-hoc corrections (*pval < 0.05; **pval < 0.01, *pval < 0.001). Benjamini-Hochberg procedure was applied but adjusted p-values were all non-significant.

River and habitat	Ice jam frequency	Time since last ice jam	Average ice scars height
Matapédia Bar			
Evenness	-0.09	0.07	0.04
Shannon	0.16	-0.13	0.05
Richness	0.2	-0.14	0.08
Matapédia Ecotone			
Evenness	0.06	-0.07	-0.11
Shannon	0.01	-0.02	0.14
Richness	-0.01	0.01	0.19
Matapédia Floodplain			
Evenness	0.28	-0.28	-0.34
Shannon	-0.38*	0.34	0.25
Richness	-0.48*	0.44*	0.24
Petite-Cascapédia Bar			
Evenness	-0.18	0.06	-0.04
Shannon	0.18	-0.1	-0.08
Richness	0.23	-0.12	-0.08
Petite-Cascapédia Ecotone			
Evenness	0.01	-0.18	-0.09
Shannon	-0.13	0.03	0.04
Richness	-0.07	0.08	0.12
Petite-Cascapédia Floodplain			
Evenness	0.24	-0.16	0.03
Shannon	0.26	-0.25	-0.17
Richness	0.11	-0.11	-0.14

Table 22. Results of variation partitioning analysis on Hellinger-transformed plant community composition for the Matapédia and Petite-Cascapédia rivers. The three defined groups are: ice-jam regime variables ("Ice"), plot-scale hydrogeomorphological variables ("Plot"), and reach-scale hydrogeomorphological variables ("Reach"). Values represent the percentage of variance explained uniquely by each variable group (controlling for the others), along with F-statistics and associated p-values from permutation tests (rda with anova.cca).

	Matapédia			Petite-Cascapédia		
	%	**F**	**P**	**%**	**F**	**P**
Ice | Plot + Reach	2.4	2.17	0.001	4.7	3.19	0.001
Plot | Ice + Reach	12.1	4.04	0.001	13.4	4.23	0.001
Reach | Ice + Plot	2.5	2.25	0.001	2.1	1.67	0.003

Table 23. Results of partial redundancy analysis (partial RDA) assessing the contribution of ice regime variables (PC1_freq, Havg) to species composition (Hellinger-transformed) after accounting for reach-scale and plot-scale hydrogeomorphological variables in the Matapédia and Petite-Cascapédia rivers. Plant composition = f (ice regime | hydrogeomorphology).

Model diagnostics	**Matapédia**	**Petite-Cascapédia**
Raw R^2	4.1 %	6.2 %
Adjusted R^2	2.4 %	4.7 %
Overall model F (Pr)	F = 2.17, p = 0.001	F = 3.19, p = 0.001
Terms tested maginally		
PC1_freq	F = 1.83, p = 0.005	F = 2.24, p = 0.004
Havg	F = 2.53, p = 0.001	F = 4.32, p = 0.001
Axes	RDA1: F = 2.61, p = 0.002 RDA2: F = 1.73, p = 0.015	RDA1: F = 4.97, p = 0.001 RDA2: F = 1.42, p = 0.103

Table 24. Results of variation partitioning analysis on presence-absence plant community composition for the Matapédia and Petite-Cascapédia rivers. The three defined groups are: ice-jam regime variables ("Ice"), plot-scale hydrogeomorphological variables ("Plot"), and reach-scale hydrogeomorphological variables ("Reach"). Values represent the percentage of variance explained uniquely by each variable group (controlling for the others), along with F-statistics and associated p-values from permutation tests (cca with anova.cca).

	Matapédia			Petite-Cascapédia		
	%	**F**	**P**	**%**	**F**	**P**
Ice | Plot + Reach	1.4	1.60	0.001	3.3	2.05	0.001
Plot | Ice + Reach	10.4	2.34	0.001	8.0	1.91	0.001
Reach | Ice + Plot	1.6	1.48	0.003	2.7	1.77	0.001

Table 25. Results of partial canonical correspondence analysis (partial CCA) assessing the contribution of ice regime variables (PC1_freq, Havg) to species composition (presence-absence) after accounting for reach-scale and plot-scale hydrogeomorphological variables in the Matapédia and Petite-Cascapédia rivers. Plant composition = f (ice regime | hydrogeomorphology).

Model diagnostics	**Matapédia**	**Petite-Cascapédia**
Raw R^2	3.3 %	4.6 %
Adjusted R^2	1.4 %	2.6 %
Overall model F (Pr)	F = 1.60, p = 0.001	F = 2.05, p = 0.001
Terms tested maginally		
PC1_freq	F = 1.46, p = 0.024	F = 1.58, p = 0.007
Havg	F = 1.42, p = 0.022	F = 2.57, p = 0.001
Axes	RDA1: F = 1.86, p = 0.001 RDA2: F = 1.34, p = 1.000	RDA1: F = 2.62, p = 0.001 RDA2: F = 1.48, p = 1.000

ANNEXE III : CHAPTER 3 SUPPLEMENTARY MATERIALS

Table 26. Results of pairwise permutational multivariate analysis of variance (pairwise PERMANOVA) based on Bray–Curtis dissimilarities of riparian plant guild composition across habitat–river groups. Groups represent the interaction of river (Mata:Matapédia, PC:Petite-Cascapédia) and habitat type (Bar, Floodplain, Ecotone). Reported are the coefficient of determination (R^2), F statistic, and Bonferroni-adjusted p-values (adj. p) based on 999 permutations

Habitat1	Habitat2	R2	F	adj.p
Mata.Bar	Mata.Floodplain	0.412	26.631	0.001
Mata.Bar	Mata.Ecotone	0.168	13.931	0.001
Mata.Bar	PC.Bar	0.174	8.195	0.001
Mata.Bar	PC.Ecotone	0.254	19.771	0.001
Mata.Bar	PC.Floodplain	0.414	33.153	0.001
Mata.Floodplain	Mata.Ecotone	0.125	8.978	0.001
Mata.Floodplain	PC.Bar	0.316	15.254	0.001
Mata.Floodplain	PC.Ecotone	0.209	13.753	0.001
Mata.Floodplain	PC.Floodplain	0.095	4.310	0.004
Mata.Ecotone	PC.Bar	0.178	13.815	0.001
Mata.Ecotone	PC.Ecotone	0.168	16.758	0.001
Mata.Ecotone	PC.Floodplain	0.204	18.432	0.001
PC.Bar	PC.Ecotone	0.090	5.264	0.001
PC.Bar	PC.Floodplain	0.282	16.526	0.001
PC.Ecotone	PC.Floodplain	0.158	11.410	0.001

Table 27. Results of pairwise Wilcoxon rank–sum tests (two-sided Mann–Whitney U) comparing guild abundances within each habitat across rivers. For each guild, the Wilcoxon W statistic is reported along with the raw p-value and the false discovery rate–adjusted p-value (Benjamini–Hochberg correction).

Habitat	Guild	W statistic	p,value	adjusted p,value
Bar	DeeprClonal_tall_H	385.5	0.000	0.000
	SmallClonal_H	345.5	0.000	0.002
	Shallowr_R_S	322.5	0.001	0.015
	Clonal_R_T	126.5	0.001	0.002
	Fast_bi_H	149.5	0.008	0.034
Ecotone	Clonal_R_T	273.5	0.000	0.000
	TallSlow_bi_H	382.5	0.000	0.000
	FastClonal_R_S	1360.5	0.000	0.000
	DeeprClonal_tall_H	1247.5	0.001	0.004
	FastSmall_H	581.5	0.007	0.033
	Shallowr_R_S	1169.5	0.007	0.022
	FastClonal_F	1171	0.008	0.010
Floodplain	SmallClonal_H	91.5	0.001	0.007
	Clonal_G	120	0.007	0.027
	TallSlow_bi_H	161.5	0.023	0.043

Table 28. Results of pairwise permutational multivariate analysis of variance (pairwise PERMANOVA) based on Euclidean distances of community-weighted mean traits composition across habitat–river groups. Groups represent the interaction of river (Mata:Matapédia, PC:Petite-Cascapédia) and habitat type (Bar, Floodplain, Ecotone). Reported are the coefficient of determination (R^2), F statistic, and Bonferroni-adjusted p-values (adj. p) based on 999 permutations

Habitat1	Habitat2	R2	F	adj.p
Mata.Bar	Mata.Ecotone	0.111	8.598	0.001
Mata.Bar	Mata.Floodplain	0.27	14.086	0.001
Mata.Bar	PC.Bar	0.051	2.077	0.048
Mata.Bar	PC.Floodplain	0.286	18.828	0.001
Mata.Bar	PC.Ecotone	0.079	4.979	0.001
Mata.Ecotone	Mata.Floodplain	0.096	6.684	0.001
Mata.Ecotone	PC.Bar	0.117	8.47	0.001
Mata.Ecotone	PC.Floodplain	0.153	12.971	0.001
Mata.Ecotone	PC.Ecotone	0.113	10.579	0.001
Mata.Floodplain	PC.Bar	0.215	9.019	0.001
Mata.Floodplain	PC.Floodplain	0.076	3.364	0.001
Mata.Floodplain	PC.Ecotone	0.144	8.786	0.001
PC.Bar	PC.Floodplain	0.217	11.65	0.001
PC.Bar	PC.Ecotone	0.042	2.355	0.058
PC.Floodplain	PC.Ecotone	0.134	9.463	0.001

Table 29. Results of pairwise Wilcoxon rank–sum tests (two-sided Mann–Whitney U) comparing CWM within each habitat across rivers. For each trait, the Wilcoxon W statistic is reported along with the raw p-value and the false discovery rate–adjusted p-value (Benjamini–Hochberg correction). Only the significant results are shown. See methods for the definition of each trait abbreviation.

Habitat	Traits	statistic	p_raw	p_adj_bh
Bar	water_pref	371	0.000	0.000
	tree	133	0.005	0.007
	life_cyc_2_1	119	0.009	0.015
	life_cyc_3_1	288	0.020	0.035
Ecotone	water_pref	1544	0.000	0.000
	sla	1542	0.000	0.000
	tree	326.5	0.000	0.000
	raunkiaer_mc_1	1492.5	0.000	0.000
	life_cyc_2_1	345	0.000	0.000
	raunkiaer_mg_1	407.5	0.000	0.000
	shrub	1429.5	0.000	0.000
	life_cyc_3_1	1397	0.000	0.000
	max_height	430	0.000	0.000
	herb	505	0.001	0.001
	r_depth	473	0.000	0.002
	wa_1	475	0.000	0.004
	an_1	1274	0.001	0.005
	resprout_n_1	505.5	0.001	0.005
	fern	1188.5	0.005	0.006
	seed_wgt	1175	0.011	0.015
	ab_1	1177.5	0.010	0.015
	resprout_y_1	1255	0.001	0.017
	wi_1	577	0.006	0.022
	reprod_vp_1	1162	0.015	0.026
Floodplain	seed_wgt	355	0.001	0.002
	sla	351	0.001	0.003
	wa_1	95.5	0.002	0.010
	life_cyc_2_1	136	0.005	0.010
	herb	116	0.009	0.012
	life_cyc_3_1	314	0.006	0.012
	shrub	334	0.005	0.013
	grass	121.5	0.008	0.023

f_1	114	0.008	0.031

Table 30. Results of permutation tests (999 permutations) on individual RDA axes for each trait group (morphological, life-history, ecological) in the Matapédia and Petite-Cascapédia rivers. For each axis, the table reports the explained variance, F-statistic, and associated P-value from anova.cca(by = "axis") using the R package vegan (Oksanen et al., 2025), indicating which axes significantly explain variation in community-weighted means after conditioning on hydrogeomorphological covariates

River	Trait group	Axis	Variance	F	Pr(>F)
Matapédia	Morphological	RDA1	0,193	2,166	0.111
		RDA2	0,147	1,655	0.111
	Life-history	RDA1	0,574	3,323	**0.005**
		RDA2	0,184	1,065	0.388
	Ecological	RDA1	0,172	3,231	*0.076*
		RDA2	0,070	1,307	0.246
Petite-Cascapédia	Morphological	RDA1	0,475	5,121	**0.001**
		RDA2	0,105	1,131	0.323
	Life-history	RDA1	1,006	5,595	**0.001**
		RDA2	0,235	1,306	0.235
	Ecological	RDA1	0,269	5,434	**0.021**
		RDA2	0,047	0,945	0.361

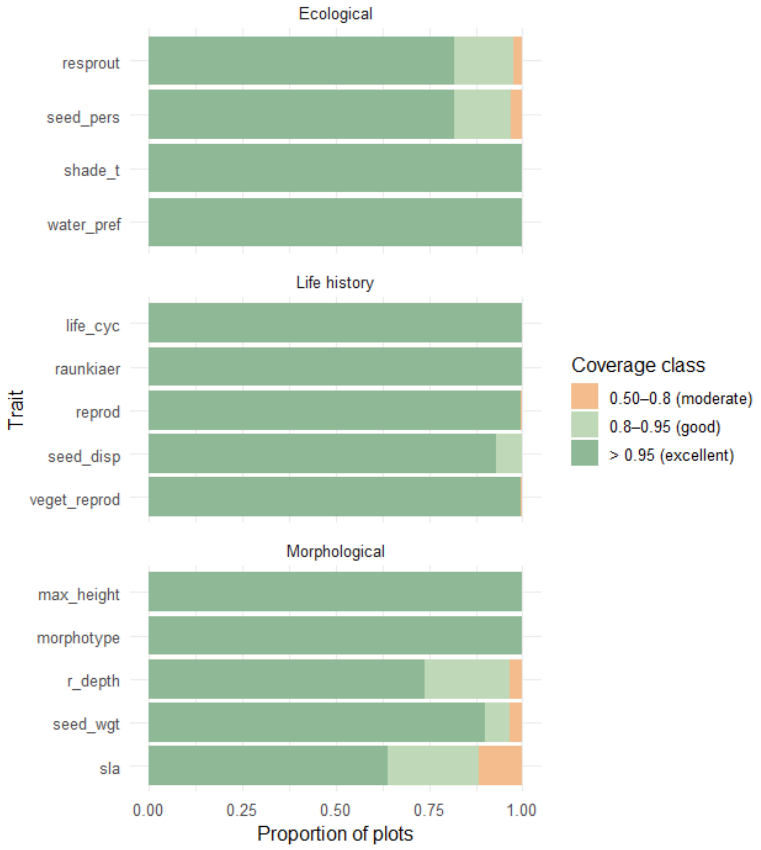


Figure 50. Proportion of plots with adequate trait coverage across the three trait groups (Morphological, Life history, Ecological). Bars represent the proportion of plots falling into different coverage classes: moderate (0.50–0.80), good (0.80–0.95), and excellent (>0.95). Traits are grouped by category, with coverage classes shown by color.

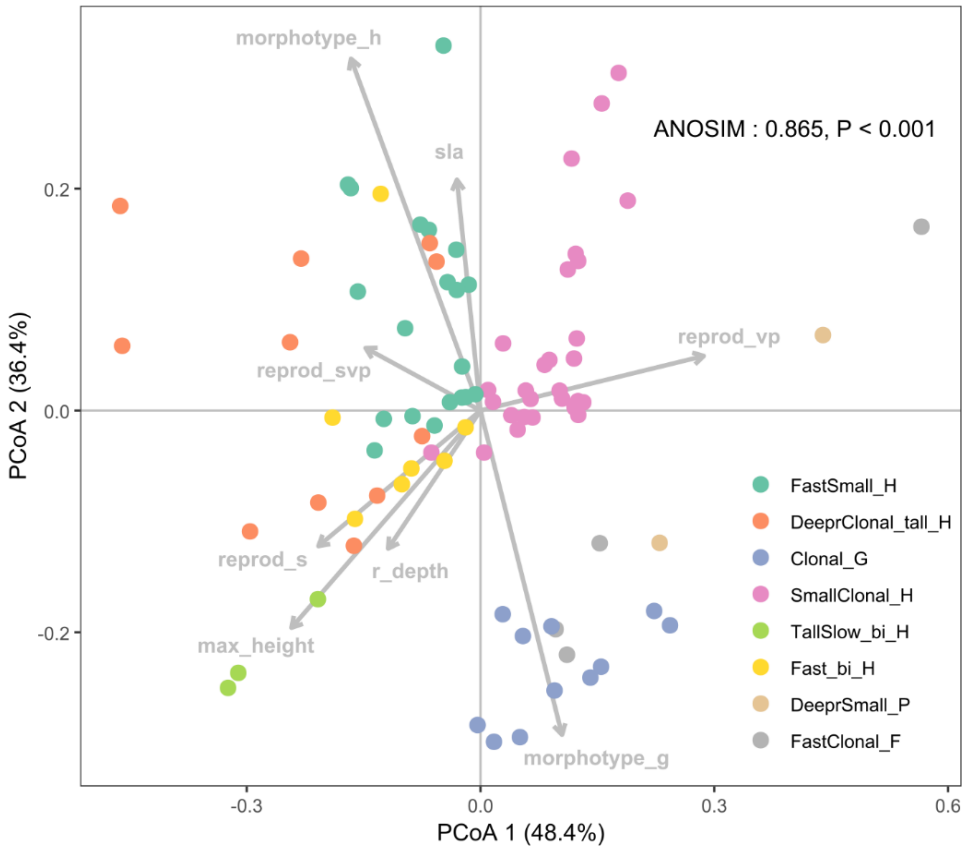


Figure 51. Principal coordinate analysis (PCoA) diagram of the 88 non-woody species based on a set of five functional traits (maximum height, specific leaf area, rooting depth, reproduction mode and morphotype), clustered into eight distinct functional guilds. Labels' colors correspond to distinct guilds and the plotted vectors with grey labels represent the significant traits after envfit().

ANNEXE IV : MEASUREMENTS OF SITE GEOMORPHOLOGICAL CHARACTERISTICS

Each site along the two studied rivers were geomorphologically characterised at the reach scale (~ 300 meters segments). Two-dimensional morphometric measures were taken from two set of Digital Elevation Models (2017 for Petite-Cascapédia; 2020 for Matapédia). Active channel and valley bottom polygons were drawn on each site to measure the bankfull width, the sinuosity index and confinement index. The sinuosity index follows the equation

$$SI = \frac{L_{thalweg}}{l}$$

where *SI* is the sinuosity index, $L_{thalweg}$ the length of the channel centerline (m) and l the length of a straight line between the upstream and downstream point of the reach (m). The confinement index follows the equation

$$CI = \frac{W_{channel}}{W_{valley}}$$

where *CI* is the confinement index, $W_{channel}$ the active channel width (m) and W_{valley} the valley bottom width (m). We also measured the average longitudinal slope of each site from the LiDAR elevations. Finally, the Unit Stream Power (USP) index was calculated for each site to have an aggregated metrics that could easily compare the different sites in term of both hydrology and geomorphology. The following formula was used to measure the USP:

$$USP = \frac{p_w g Q s}{W_{channel}}$$

where USP is the Unit Stream Power, p_w is the water density (1000 kg m^{-3}), g is the gravitational constant (9.81 m s^{-2}), Q is the bankfull level flood discharge Q_2 ($m^3 s^{-1}$) acquired from the *Centre d'expertise hydrique du Québec* (CEHQ) and s the longitudinal slope.

ANNEXE V : ICE-JAM DISTURBANCE REGIME GRADIENT

Following the detailed dendrochronological and historical data analysis outlined in Prugne et al. (2025), we calculated ice-jam frequencies using three distinct approaches. The first approach, termed '**Freq**' involved dividing the total number of recorded ice jams by the number of years since the oldest identified ice scar. This method has been used many times (Boucher et al., 2012; Lagadec et al., 2015; Morin et al., 2015) but can be biased as samples could be missing from trees being uprooted in the past. The second approach, 'Freq2008,' focused on the period of highest ice jam abundance, dividing the number of jams since 2008 by the 14-year span between 2008 and 2022. This method allows a better representation of the recent times by avoiding lost samples. Finally, 'Freq2008old' also considered jams since 2008 but divided this count by the total number of years since the oldest identified ice jam event to have a representation of disturbance frequency from the first known event. All these calculated frequencies yielded different values, which would change the rank order of frequencies between sites (Table 31).

To mitigate the bias of trends and patterns in ice jam frequencies from the selection of a specific frequency, we decided to combine them on a gradient using a Principal Component Analysis (Figure 52). The first axis of the PCA explained 68.4% of variation and resulted in a gradient of increasing frequencies from left (negative values) to right (positive values). We used this axis as a composite variable to represent the ice jam frequencies for each site in this study.

Table 31. Data showing the number of trees sampled in each study site (see study map for localisation), the number of individuals ice-jams identified from tree rings, the year of the most recent and oldest ice-jam event, and the frequency value resulting from the three different method (freq, freq2008, freq2008old) described above.

River site	Nb. Of trees	Identified jams	Most recent jam	Oldest jam	freq	freq2008	freq2008old
Mata1	16	7	2020	2014	0.33	0.02	0.64
Mata2	15	6	2018	1969	0.31	0.02	0.57
Mata3	3	4	2012	2011	0.25	0.02	0.29
Mata4	2	4	2010	2002	0.25	0.02	0.29
Mata5	7	8	2014	1977	0.18	0.01	0.27
Mata6	6	4	2016	2008	0.43	0.03	0.43
Mata7	14	4	2014	2007	0.29	0.02	0.36
P.-Casc.1	6	3	2021	2010	0.45	0.03	0.45
P.-Casc.2	5	2	2013	2011	0.27	0.02	0.3
P.-Casc.3	9	2	2018	2011	0.36	0.03	0.4
P.-Casc.4	10	5	2020	1993	0.18	0.01	0.54
P.-Casc.5	1	1	2018	2018	0.15	0.01	0.15
P.-Casc.6	4	4	2021	2008	0.31	0.02	0.31

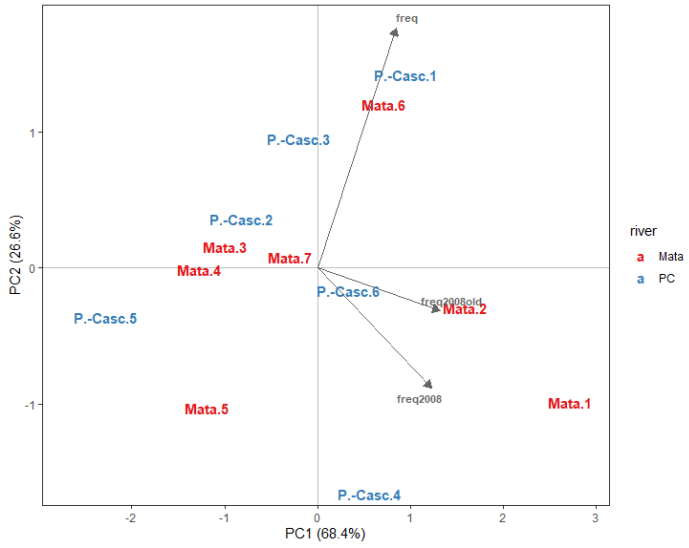


Figure 52. PCA with the three ways of measuring the ice jam frequencies. Numbers with different colors represent the site scores of the study sites across rivers (blue for Petite-Cascapédia and red for Matapédia)

ANNEXE VI : HABITAT CLASSIFICATION

To classify the plots into distinct habitats, we used geomorphological and vegetation data and conducted a cluster analysis on each river. We used median grain size (D50), depth of fine sediment and relative height from low flow as the geomorphological variables and the percentage cover of three vegetation strata (0-1m, 1-5m, +5m) recorded for each plot as vegetation variables. Prior to clustering, these variables were standardized by centering them to zero mean and scaling to unit variance. A dissimilarity matrix was then constructed from these standardized variables using Euclidean distances. Then, a hierarchical clustering with Ward's D2 linkage method was applied to the dissimilarity matrix and dendrograms (Figure 53) were generated for both rivers, with which we visually determined the optimal number of clusters.

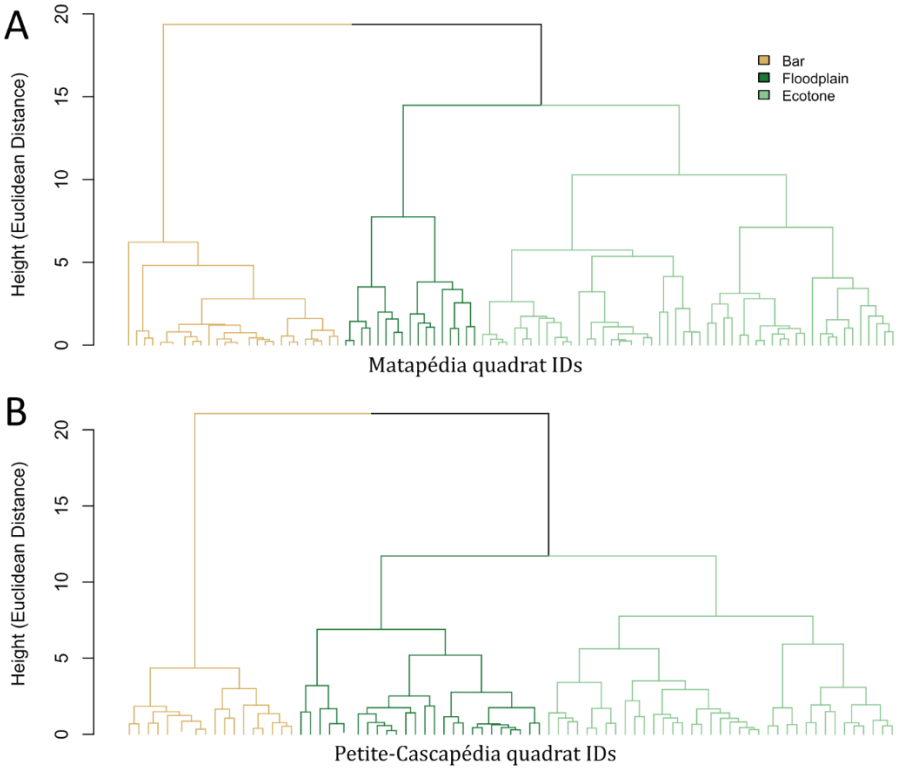


Figure 53. Dendrograms (A: Matapédia River; B: Petite-Cascapédia River) showing clusters based on geomorphological and vegetation strata cover variable.

Based on the interpretation of the clusters, we identified three distinct habitat types and calculated the mean ± SE of each parameter (Table 32). The first, referred to as **bar**, was characterized by the absence of fine sediment and a high median grain size. Vegetation cover in this habitat was dominated by non-woody species, with trees and shrubs occurring only rarely. We define the **ecotone** as the transitional zone between bar ecosystems (composed of highly pioneer communities) and the forested floodplain. This intermediate habitat was characterized by the presence of fine sediment, along with low adult tree abundance. It included a mix of fluvial landforms such as high benches, banks and newly formed (or rejuvenated) floodplain areas supporting dense and tall herbaceous vegetation, shrubs, and young trees under five meters in height. Lastly, the third habitat type named "floodplain" correspond to **forested floodplain**, which was dominated by a high canopy cover of trees exceeding five meters in height. These three habitats exhibit a clear geomorphological gradient (Figure 54), with increase in fine sediment depth and decrease in median size along the relative height and distance to low flow.

Table 32. Characteristics of sediment and vegetation cover in the defined habitats.

Habitat	Mean D50 (cm)	Mean fine sed. Depth (cm)	Tree cover (%)	Shrub cover (%)	Non-woody cover (%)
Bar	6.13 ± 0.42	1.70 ± 1.41	0.6 ± 0.2	10.8 ± 3.0	62.6 ± 5.3
Ecotone	0.25 ± 0.10	52.09 ± 4.14	24.2 ± 3.6	42.6 ± 4.1	90.9 ± 2.1
Floodplain	0.10 ± 0.00	85.50 ± 5.21	87.7 ± 3.8	40.8 ± 5.6	92.5 ± 2.9

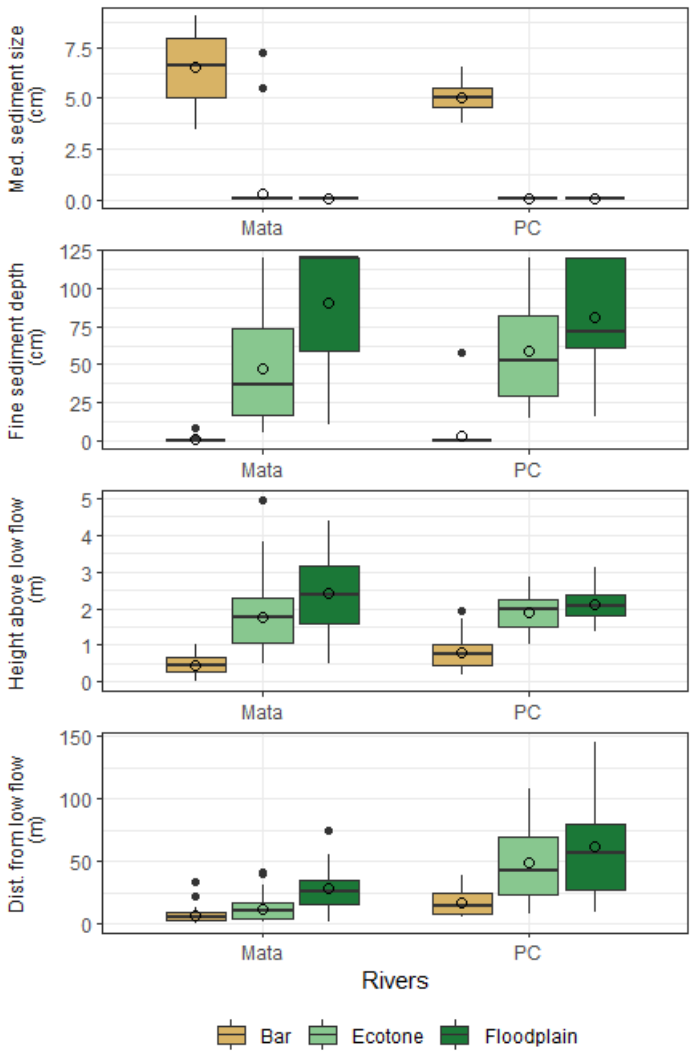


Figure 54. Geomorphological characteristics of plots in each defined habitat (bar, ecotone, floodplain) in each river (Mata = Matapédia, PC = Petite-Cascapédia). From top to bottom, the measured variables are the averaged pebble sediment size, the fine sediment depth, the relative height above the low flow water line and relative distance from the low flow water line. Top and bottom whiskers represent the maximum and minimum, respectively. The boxes limits represent the first and third quantiles and the horizontal black line represent the median. Empty circles are the mean of the samples.

ANNEXE VII : FUNCTIONAL TRAIT DATA

Functional traits values for each species identified in the study were retrieved principally through the TOPIC, TRY and USDA Plant databases, and missing values were retrieved from the following list of articles:

- Awada, T., Perry, M. E. L., & Schacht, W. H. (2003). Photosynthetic and growth responses of the C3 Bromus inermis and the C4 Andropogon gerardii to tree canopy cover. Canadian Journal of Plant Science, 83(3), 533-540. https://doi.org/10.4141/P02-129
- Brice, M.-H., Pellerin, S., & Poulin, M. (2016). Environmental filtering and spatial processes in urban riparian forests. Journal of Vegetation Science, 27(5), 1023-1035. https://doi.org/10.1111/jvs.12425
- Cascorbi, U. (2007). Integration of invasion ecology theories into the analysis of designed plant communities : A case study in Southern Germany. Landscape Ecology, 22(9), 1371-1381. https://doi.org/10.1007/s10980-007-9115-5
- Copeland, S. (2014). Abiotic conditions, biotic interactions, and species traits affect plant distribution across topographic microclimates in the Klamath-Siskiyou Mountains [Ph.D.]. https://www.proquest.com/docview/1618951783/abstract/729003BC12634E17PQ/1
- Danyagri, G., & Dang, Q.-L. (2014). Effects of elevated carbon dioxide concentration and soil temperature on the growth and biomass responses of mountain maple (Acer spicatum) seedlings to light availability. Journal of Plant Ecology, 7(6), 535-543. https://doi.org/10.1093/jpe/rtt061
- Fort, F., Jouany, C., & Cruz, P. (2013). Root and leaf functional trait relations in Poaceae species : Implications of differing resource-acquisition strategies. Journal of Plant Ecology, 6(3), 211-219. https://doi.org/10.1093/jpe/rts034
- Gratani, L., Crescente, M. F., Fabrini, G., & Varone, L. (2008). Growth pattern of Bidens cernua L. : Relationships between relative growth rate and its physiological and morphological components. Photosynthetica, 46(2), 179-184. https://doi.org/10.1007/s11099-008-0029-5
- Hibbs, D. E., & Fischer, B. C. (1979). Sexual and Vegetative Reproduction of Striped Maple (Acer pensylvanicum L.). Bulletin of the Torrey Botanical Club, 106(3), 222-227. https://doi.org/10.2307/2484558

- Jacques, M.-H., Lapointe, L., Rice, K., Montgomery, R. A., Stefanski, A., & Reich, P. B. (2015). Responses of two understory herbs, Maianthemum canadense and Eurybia macrophylla, to experimental forest warming : Early emergence is the key to enhanced reproductive output. American Journal of Botany, 102(10), 1610-1624. https://doi.org/10.3732/ajb.1500046
- Levačić, D., & Jelaska, S. D. (2022). Consistent Grime's CSR Strategy of Daisy Fleabane Erigeron annuus (L.) Pers. Despite Its High Morphological Variability—A Case Study from Zagreb and Medvednica Mt., Croatia. Diversity, 14(1), Article 1. https://doi.org/10.3390/d14010045
- Lillak, R. (Éd.). (2005). Integrating efficient grassland farming and biodiversity : Proceedings of the 13th International Occasional Symposium of the European Grassland Federation, Tartu, Estonia, 29 - 31 August 2005. European Grassland Federation.
- Mehrotra, P. (2004). ECOLOGICAL IMPLICATION OF PLANT TRAITS, STRATEGIES AND COMPETITIVE ABILITIES OF HERBS. Applied Ecology and Environmental Research, 2(2), 1-13. https://doi.org/10.15666/aeer/03001013
- O'Hara, J. P. M. (2008). TRAITS ASSOCIATED WITH COMPETITIVE ABILITIES OF 12 WETLAND SPECIES ALONG SUCCESSIONAL AND NUTRITIONAL GRADIENTS [Master]. Laurentian University.
- Pan, Y., Tang, S., Wei, C., & Li, X. (2017). Growth and photosynthetic responses of invasive Bidens frondosa to light and water availability : A comparison with invasive and native congeners. Weed Biology and Management, 17(1), 36-44. https://doi.org/10.1111/wbm.12114
- Piper, J. K. (1986). Germination and Growth of Bird-Dispersed Plants : Effects of Seed Size and Light on Seedling Vigor and Biomass Allocation. American Journal of Botany, 73(7), 959-965. https://doi.org/10.1002/j.1537-2197.1986.tb08539.x
- Sessa, E. B., & Givnish, T. J. (2014). Leaf form and photosynthetic physiology of ryopteris species distributed along light gradients in eastern North America. Functional Ecology, 28(1), 108-123. https://doi.org/10.1111/1365-2435.12150
- St. James, C., & Mallik, A. U. (2021). Functional Ecology of Forest, Heath, and Shrub Savannah Alternate States in Eastern Canada. Forests, 12(1), Article 1. https://doi.org/10.3390/f12010093
- Stutz, S., Mráz, P., Hinz, H. L., Müller-Schärer, H., & Schaffner, U. (2018). Biological invasion of oxeye daisy (Leucanthemum vulgare) in North America : Pre-adaptation, post-introduction evolution, or both? PLOS ONE, 13(1), e0190705. https://doi.org/10.1371/journal.pone.0190705
- Tumber-Dávila, S. (6073). Root Systems of Individual Plants Worldwide 2022. Harvard Forest Data Archive : HF426 (v.2). Environmental Data Initiative.
- Van Cleemput, E., Helsen, K., Feilhauer, H., Honnay, O., & Somers, B. (2021). Spectrally defined plant functional types adequately capture multidimensional trait variation in herbaceous communities. Ecological Indicators, 120, 106970. https://doi.org/10.1016/j.ecolind.2020.106970
- Ziska, L. H., Reeves III, J. B., & Blank, B. (2005). The impact of recent increases in atmospheric CO2 on biomass production and vegetative retention of Cheatgrass (Bromus tectorum) : Implications for fire disturbance. Global Change Biology, 11(8), 1325-1332. https://doi.org/10.1111/j.1365-2486.2005.00992.x

- Hawkins, S. M., Chappell, M., & Martin, M. T., Jr. (2013). Defining a Protocol for Vegetative Propagation of Baptisia, Eupatorium and Thermopsis. Journal of Environmental Horticulture, 31(3), 162-168. https://doi.org/10.24266/0738-2898.31.3.162
- Ministère du Gouvernement du Québec. Database on threatened or vulnerable plant species. Consulted on 05-06-2025. https://www.quebec.ca/agriculture-environnement-et-ressources-naturelles/flore/especes-floristiques-menacees-ou-vulnerables/liste-especes
- Krannitz, P. G. (1996). Reproductive ecology of Dryas integrifolia in the high Arctic semi-desert. Canadian Journal of Botany, 74(9), 1451-1460. https://doi.org/10.1139/b96-175
- Bliss, L. C. (1958). Seed Germination in Arctic and Alpine Species. ARCTIC, 11(3), Article 3. https://doi.org/10.14430/arctic3743

The Table 33 shows the final dataset used in Chapter 3 analyses. The name of the variables and their modalities go as follow:

- **Max_height** Max height reached by the species (m)
- **SLA** Specific leaf area (cm2/g)
- **R_depth** Root depth (cm)
- **Seed_wgt** Seed weights (g) of 1000 seeds
- **Morphotype** Morphotype (t : trees, s : shrubs, h : herbs, f : ferns, g : grasses, p : horsetails)
- **Raunkiaer** Raunkiaer life form (ch : chamaephyte, g : geophyte, h: hemicryptophyte, hel : helophyte, hyd : hydrophyte, mc : micro-nano-phanerophyte, mg : mega-meso-phanerophyte, t : therophyte)
- **Water_pref** Water preference (1 : Dry, 2: facultative dry, 3 : facultative generally, 4: Facultative humid, 5 : Humid)
- **Shade_t** Shade tolerance (i: intolerant, m: moderate, s: shade tolerant)
- **Life_cyc** Life cycle (1: annual, 2: biennal, 3: perennial)
- **Reprod** Reproduction strategy (s: seed only, svp: seed primarly but can reproduce vegetatively, vp: high vegetative reproduction)
- **Veget_reprod** Vegetative way of reproduction (ab: With aboveground organs, be: With belowground organs, f: by fragments, a : absent)

- **Seed_Disp** Seed dispersal vectors (an : animal, wa : water, wi : wind)
- **Seed_Pers** Seedbank persistance (a: absent, sp: Semi-persistent/1-2years, p: persistent/5+years)
- **Resprout** Resprout capabilities (y: yes, n:no)

Table 33. Values, by species, of the fourteen functional traits used in the Chapter 3 analyses.

species	Max_height	SLA	R_depth	Seed_wgt	Morphotype	raunkiaer	Water_pref	Shade_t	Life_cyc	Reprod	Veget_reprod	Seed_Disp	Seed_Pers	Resprout
Abies balsamea	25	148	151	8	t	mg	3	s	3	svp	ab	an, wi	sp	n
Acer pensylvanicum	10	565	71	37	t	mc	1	s	3	svp	ab	wi	sp	y
Acer rubrum	25	170	210	18	t	mg	3	m	3	svp	ab	wa, wi	sp	y
Acer spicatum	5	120	82	23	s	mc	3	s	3	svp	ab, be	wi	a	y
Actaea rubra	1	455	5	6	h	g	2	s	3	svp	be, ab	an	a	
Agrimonia striata	2	590		15	h	h	2	m	3	s	a	an		n
Agrostis sp	1	269	52	0	g	h	4	i	3	vp	ab, be	wi	p	n
Alnus incana	8	204	102	1	s	mg	4	i	3	vp	ab, be	wa, wi	a	y
Amelanchier sp	6	168	56	12	s	mc	1	m	3	vp	ab, be	an	p	y
Anemone canadensis	1	498	61	3	h	g	4	i	3	svp	ab, be	wi	a	y
Angelica atropurpurea	3			4	h	h	4	i	3	s	a	wi	a	n
Apocynum androsaemifolium	1	320	122	0	h	g	1	i	3	vp	be	wi	a	y
Apocynum cannabinum	1	102	30	1	h	g	3	i	3	vp	be	wi	sp	n
Aralia nudicaulis	0	523	25	7	h	g	2	s	3	vp	be	an	p	n
Arctium lappa	3	174		11	h	h	2	i	2	s	a	an	p	n
Arisaema triphyllum	1	636	20	33	h	g	3	s	3	svp	be	an	p	n
Aster macrophyllus (Eurybia macrophylla)	1	375	30	1	h	h	3	s	3	vp	ab, be	wi, an	a	n
Aster puniceus (Symphyotrichum puniceum)	2			0	h	h	4	i	3	vp	be, ab	wi		n
Aster sp	2	135	30	0	h	h	3	m	3	vp	ab, be	wi		n

Betula alleghaniensis	25	273	150	1	t	mg	3	m	3	svp	ab	wi	sp	y
Betula papyrifera	29	187	130	0	t	mg	2	i	3	svp	ab	wa, wi	sp	y
Bromus sp	1	180	60	4	g	h	1	i	3	s	a	an, wi, wa	sp	n
Calamagrostis canadensis	1	198	50	0	g	h	5	i	3	vp	be	wi, an	sp	n
Carex sp	1	168	67	2	g	h	3	m	3	vp	be	wa, wi, an	sp	y
Centaurea nigra	1	182		2	h	h	4	i	3	s	a	an, wi		y
Cirsium vulgare	2	138	130	3	h	h	3	i	2	s	a	an, wi	p	y
Convolvulus arvensis	2		224	18	h	h	1	i	3	vp	f, be	an, wa		y
Cornus canadensis	0	234	25	6	h	ch	3	s	3	vp	be	an	p	y
Cornus sericea	3	330	51	26	s	mc	4	i	3	vp	ab, be	an	a	y
Corylus cornuta	3	277	70	829	s	mc	2	s	3	vp	ab, be	an	a	y
Crataegus sp	8	223	269	43	s	mc	2	i	3	svp	f	an	a	y
Deschampsia sp	1	180	115	0	g	h	3	s	3	s	be	wi		y
Diervilla lonicera	1	314	41	0	s	mc	1	m	3	vp	be	an	p	y
Dryas integrifolia	0	65	10	0	h	ch	3	i	3	svp	ab	wi	a	y
Dryopteris sp	1	355	31		f	g	3	s	3	vp	be	wa, wi	sp	
Echium vulgare	1	135	75	3	h	h	1	i	2	s	a	an	a	y
Elymus sp	1	327	63	5	g	h	3	s	3	s	a	wa,wi,an		n
Epilobium ciliatum	1	394		0	h	h	4	i	3	s	a	wi		y
Epipactis helleborine	1	538		0	h	g	3	s	3	svp	be	wi	a	n
Equisetum arvense	1	191	235		p	g	3	m	3	vp	be	wa, wi	a	n
Equisetum sylvaticum	1		15		p	g	4	s	3	vp	be	wi	a	n
Erigeron sp	1	264	100	0	h	h	3	l	1	s	a	wi	sp	n
Eupatorium maculatum	2	246	20	0	h	h	5	i	3	s	a	wi, an	sp	n
Festuca sp	1	161	91	1	g	g	1	s	3	vp	be	wa, an, wi	sp	y
Fragaria vesca	0	205	3	0	h	h	2	s	3	vp	ab, be	an	p	n
Fragaria virginiana	0	167	3	0	h	h	2	m	3	vp	ab	an	p	n
Fraxinus nigra	27	236	100	55	t	mg	4	l	3	vp	ab, be	wi	p	y

Galium asprellum	2			1	h	h	4	s	3					n
Galium mollugo	2	348	50	1	h	h	3	m	3	svp	be	an	a	n
Galium palustre	1			1	h	h	5	m	3	svp	ab			n
Galium sp	1	415		1	h	h	3	m	3	svp	be	an	sp	n
Galium trifidum	1			1	h	h	2	m	3	svp			sp	n
Geum sp	1	328	35	1	h	h	3	s	3	vp	ab, be	an	p	n
Glyceria sp	1	316	71	0	g	h	5	i	3	svp	be	wi, wa, an	p	y
Helianthus tuberosus	2	200	130	4	h	h	4	m	3	svp	be	an		n
Hieracium sp	1		117	1	h	h	3	i	3	svp	ab, be	wi, wa, an	a	y
Hypericum perforatum	1	311	58	0	h	h	1	i	3	vp	f, be, ab	wa, wi, an	p	y
Impatiens capensis	1	909	36	7	h	t	4	s	1	s	a		a	n
Iris versicolor	1	150	10	15	h	g	5	i	3	vp	be	an	a	y
Larix laricina	25	83	180	2	t	mg	4	i	3	svp	ab, be	an, wi, wa	a	n
Lathyrus latifolius	3	161	15	40	h	g	4	i						n
Leucanthemum vulgare	1	158	20	1	h	h	3	m	3	svp	be	an, wi	p	n
Linnaea borealis	0	231	17	2	h	ch	2	m	3	vp	ab	an	a	n
Lonicera sp	3	245		4	s	mc	2	m	3	svp	ab	an	a	n
Lotus corniculatus	1	334	75	1	h	h	3	i	3	svp	be	wa, an	sp	n
Lycopus americanus	1	360	25	0	h	h	5	s	3	vp	ab	wa, an	sp	n
Lysimachia ciliata	1			1	h	h	4	s	3	svp	be	wa	sp	y
Maianthemum canadense	0	376	10	9	h	g	2	s	3	vp	be	an	a	n
Maianthemum stellatum	1		64	27	h	g	3	m	3	vp	be	an		
Matteuccia struthiopteris	2	272	15	0	f	g	3	s	3	vp	be	wi	sp	n
Medicago lupulina	1	295	75	2	h	t	2	i	2	s	a	an	p	n
Melilotus albus	3	186	156	3	h	h	1	i	2	s	a	wa, wi	p	n
Mentha canadensis	1	367	31	0	h	g	4	m	3	vp	be	wa	p	n
Moneses uniflora	0	437			h	h	2	s	3	svp	be	an		y
Myrica gale	2	145	35		s	mc	5	s	3			an, wa, wi		y

Nabalus sp	3			1	h	h	4	s	3	svp	be	wi		y
Oenothera biennis	2		55	0	h	h	1	i	2	s	a	an	p	n
Onoclea sensibilis	2	398	15	0	f	g	4	s	3	vp	be	wi	a	y
Osmunda claytoniana	2	351	30		f	g	5	s	3	vp	be	wi	a	n
Oxalis stricta	0			0	h	g	2	i	3	vp	f, be, ab		sp	y
Phalaris arundinacea	2	212	139	1	g	g	4	i	3	vp	f, be	wa, wi, an	p	n
Phegopteris connectilis	0				f	g	4	s	3	vp	be	wi		
Phleum sp	1	180	50	0	g	h	2	m	3	svp	ab, be	wi, an	sp	y
Picea mariana	30	59	99	1	t	mg	3	s	3	svp	ab	wi, wa, an	sp	n
Plantago major	0	206	80	0	h	h	3	m	3	svp	be	an	sp	n
Poa sp	1	213	62	0	g	h	2	m	3	svp	be	an, wi	p	y
Populus balsamifera	25	157	125	0	t	mg	4	i	3	vp	f, be, ab	wa, wi	a	y
Populus tremuloides	25	140	230	0	t	mg	3	i	3	vp	ab, be	wa, wi	a	y
Potentilla anserina	0	196	42	1	h	ch	4	s	3	vp	ab	an	sp	y
Prunella vulgaris	1	274	25	1	h	h	3	i	3	vp	ab	an, wa	sp	n
Prunus pensylvanica	12	202	50.8	44	t	mg	3	i	3	svp	ab, be	an	p	y
Pyrola asarifolia	0	192	18	0	h	h	1	s	3	vp	ab, be	wi	a	
Pyrola elliptica	0	300		0	h	h	2	s	3	vp	ab, be	wi	a	
Ranunculus acris	1	214	40		h	h	3	s	3	vp	ab	wa, an	sp	
Rosa sp	2		89	10	s	mc	3	m	3	vp	be	an	sp	y
Rubus idaeus	2	360	30	2	s	h	3	s	3	vp	ab, be	an	p	y
Rubus pubescens	0		32	3	h	h	4	m	3	vp	ab	an	p	y
Rumex sp	1		205	1	h	h	4	i	3	svp	be	an, wi, wa	p	y
Salix sp	5	155	39	0	s	mc	4	m	3	svp	f, ab, be	wa, wi	a	y
Sambucus canadensis	3	180	40	2	s	mc	4	i	3	svp	ab, be	an	p	y
Scutellaria sp	1			1	h	h	4	m	3	vp	ab, be	an, wa	a	
Silene vulgaris	1	230	100	1	h	h	1	i	3	svp	ab, be		p	
Solanum dulcamara	3	350		2	h	h	3	i	3	vp	ab, be	an	a	

Solidago sp	2	310	176	0	h	h	2	m	3	vp	ab, be	wi	sp	n
Sonchus sp	1	275	68	0	h	t	2	i	1	s	a	wa, an, wi	p	
Sorbus sp	13	172	120	3	s	mg	3	m	3	svp	ab	an	sp	y
Stachys sp	1	212	43	1	h	g	4	m	3	svp	be	an, wa		n
Tanacetum vulgare	1	235		0	h	h	2	i	3	vp	f, be	wa, an	sp	
Taraxacum officinale	1	455	140	1	h	h	2	m	3	svp	ab	wi	p	n
Taxus canadensis	2	112	61	26	s	ch	2	s	3	vp	ab	an, wi	p	y
Thalictrum pubescens	3	250		3	h	h	4	m	3	svp	be, ab	an	a	
Thuja occidentalis	18	54	90	2	t	mg	4	m	3	vp	ab	an, wi	sp	n
Tiarella cordifolia	0				h	h	4	s	3	vp	ab, be			
Toxicodendron radicans	1	512		16	s	mc	3	m	3	vp	f, be, ab	an	p	
Trifolium pratense	1	247	70	1	h	h	2	i	3	svp	be	an, wi	p	n
Trifolium repens	0	275	58	1	h	h	2	i	3	vp	ab	an, wi	p	n
Trillium cernuum	1	450		2	h	g	2	s	3	svp	be	an		
Tussilago farfara	0	186	10	0	h	g	2	i	3	vp	be	wi	a	y
Ulmus americana	35	125	300	5	t	mg	4	m	3	svp	ab, be	an, wa, wi	a	y
Vaccinium sp	0	137	35	0	s	ch	3	i	3	vp	ab	an	p	y
Valeriana officinalis	1	291	29	1	h	h	2	i	3	svp	be	wi	a	
Viburnum opulus	4	251	37	33	s	mc	4	i	3	svp	ab, be	an	a	n
Vicia cracca	2	275	36	14	h	h	1	m	3	svp	be	an	sp	n
Viola sp	0	533	10	1	h	h	2	s	3	vp	be	an	sp	n

RÉFÉRENCES BIBLIOGRAPHIQUES

Abgrall, C., Chauvat, M., Langlois, E., Hedde, M., Mouillot, D., Salmon, S., Winck, B., & Forey, E. (2017). Shifts and linkages of functional diversity between above- and below-ground compartments along a flooding gradient. *Functional Ecology*, *31*(2), 350-360. https://doi.org/10.1111/1365-2435.12718

Albert, C. H., Thuiller, W., Yoccoz, N. G., Soudant, A., Boucher, F., Saccone, P., & Lavorel, S. (2010). Intraspecific functional variability : Extent, structure and sources of variation. *Journal of Ecology*, *98*(3), 604-613. https://doi.org/10.1111/j.1365-2745.2010.01651.x

Allard, G. (2010). Dynamique fluvio-glacielle : Étude de cas d'une fosse-à-frasil, rivière Mitis, Bas-Saint-Laurent. *Mémoire de maîtrise. Université du Québec à Rimouski*.

Alvarez-Uria, P., & Körner, C. (2007). Low temperature limits of root growth in deciduous and evergreen temperate tree species. *Functional Ecology*, *21*(2), 211-218. https://doi.org/10.1111/j.1365-2435.2007.01231.x

Amlin, N. A., & Rood, S. B. (2001). Inundation Tolerances of Riparian Willows and Cottonwoods. *JAWRA Journal of the American Water Resources Association*, *37*(6), 1709-1720. https://doi.org/10.1111/j.1752-1688.2001.tb03671.x

Andersson, E., Nilsson, C., & Johansson, M. E. (2000). Plant dispersal in boreal rivers and its relation to the diversity of riparian flora. *Journal of Biogeography*, *27*(5), 1095-1106. https://doi.org/10.1046/j.1365-2699.2000.00481.x

Andreoli, A., Chiaradia, E. A., Cislaghi, A., Bischetti, G. B., & Comiti, F. (2020). Roots reinforcement by riparian trees in restored rivers. *Geomorphology*, *370*, 107389. https://doi.org/10.1016/j.geomorph.2020.107389

Aubin, I., Cardou, F., Boisvert-Marsh, L., Garnier, E., Strukelj, M., & Munson, A. D. (2020). Managing data locally to answer questions globally : The role of collaborative science in ecology. *Journal of Vegetation Science*, *31*(3), 509-517. https://doi.org/10.1111/jvs.12864

Balke, T., Bouma, T., Horstman, E., Webb, E., Erftemeijer, P., & Herman, P. (2011). Windows of opportunity : Thresholds to mangrove seedling establishment on tidal flats. *Marine Ecology Progress Series*, *440*, 1-9. https://doi.org/10.3354/meps09364

Bartušková, A., Filartiga, A. L., Herben, T., Qian, J., & Klimešová, J. (2021). Comparative analysis of root sprouting and its vigour in temperate herbs : Anatomical correlates and environmental predictors. *Annals of Botany*, *127*(7), 931-941. https://doi.org/10.1093/aob/mcab030

Bätz, N., Colombini, P., Cherubini, P., & Lane, S. N. (2016a). Groundwater controls on biogeomorphological succession and river channel morphodynamics : GROUNDWATER CONTROLS ON MORPHODYNAMICS. *Journal of Geophysical Research: Earth Surface*, *121*(10), 1763-1785. https://doi.org/10.1002/2016JF004009

Bätz, N., Colombini, P., Cherubini, P., & Lane, S. N. (2016b). Groundwater controls on biogeomorphological succession and river channel morphodynamics : GROUNDWATER CONTROLS ON MORPHODYNAMICS. *Journal of Geophysical Research: Earth Surface*, *121*(10), 1763-1785. https://doi.org/10.1002/2016JF004009

Beck, H. E., McVicar, T. R., Vergopolan, N., Berg, A., Lutsko, N. J., Dufour, A., Zeng, Z., Jiang, X., van Dijk, A. I. J. M., & Miralles, D. G. (2023). High-resolution (1 km) Köppen-Geiger maps for 1901–2099 based on constrained CMIP6 projections. *Scientific Data*, *10*(1), 724. https://doi.org/10.1038/s41597-023-02549-6

Bejarano, M. D., Nilsson, C., & Aguiar, F. C. (2018). Riparian plant guilds become simpler and most likely fewer following flow regulation. *Journal of Applied Ecology*, *55*(1), 365-376. https://doi.org/10.1111/1365-2664.12949

Beltaos, S. (1984). A conceptual model of river ice breakup. *Canadian Journal of Civil Engineering*, *11*(3), 516-529. https://doi.org/10.1139/l84-071

Beltaos, S. (2002). Effects of climate on mid-winter ice jams. *Hydrological Processes*, *16*(4), 789-804. https://doi.org/10.1002/hyp.370

Beltaos, S. (2003). Threshold between mechanical and thermal breakup of river ice cover. *Cold Regions Science and Technology*, *37*(1), 1-13. https://doi.org/10.1016/S0165-232X(03)00010-7

Beltaos, S. (2007). River ice breakup processes : Recent advances and future directions. *Canadian Journal of Civil Engineering*, *34*(6), 703-716. https://doi.org/10.1139/l06-021

Beltaos, S. (2008). Progress in the study and management of river ice jams. *Cold Regions Science and Technology*, *51*(1), 2-19. https://doi.org/10.1016/j.coldregions.2007.09.001

Beltaos, S. (2013). River ice formation. *Committee on River Ice Processes and the Environment Canadian Geophysical Union, Hydrology Section Edmonton*.

Beltaos, S. (2016). Extreme sediment pulses during ice breakup, Saint John River, Canada. *Cold Regions Science and Technology*, *128*, 38-46. https://doi.org/10.1016/j.coldregions.2016.05.005

Beltaos, S., & Burrell, B. C. (2010). Ice-jam model testing : Matapedia River case studies, 1994 and 1995. *Cold Regions Science and Technology*, *60*(1), 29-39. https://doi.org/10.1016/j.coldregions.2009.05.014

Beltaos, S., & Burrell, B. C. (2021). Effects of River-Ice Breakup on Sediment Transport and Implications to Stream Environments : A Review. *Water*, *13*(18), 2541. https://doi.org/10.3390/w13182541

Beltaos, S., & Prowse, T. (2009). River-ice hydrology in a shrinking cryosphere. *Hydrological Processes*, *23*(1), 122-144. https://doi.org/Bouche

Bergeron, N. E., Buffin-Bélanger, T., & Dubé, J. (2011). Conceptual model of river ice types and dynamics along sedimentary links : CONCEPTUAL MODEL OF RIVER ICE TYPES ALONG LINKS. *River Research and Applications*, *27*(9), 1159-1167. https://doi.org/10.1002/rra.1479

Bertoldi, W., & Gurnell, A. M. (2020). Physical engineering of an island-braided river by two riparian tree species : Evidence from aerial images and airborne lidar. *River Research and Applications*, rra.3657. https://doi.org/10.1002/rra.3657

Bertoldi, W., Siviglia, A., Tettamanti, S., Toffolon, M., Vetsch, D., & Francalanci, S. (2014). Modeling vegetation controls on fluvial morphological trajectories. *Geophysical Research Letters*, *41*(20), 7167-7175. https://doi.org/10.1002/2014GL061666

Boivin, M., Buffin-Bélanger, T., & Piégay, H. (2015). The raft of the Saint-Jean River, Gaspé (Québec, Canada) : A dynamic feature trapping most of the wood transported from the catchment. *Geomorphology*, *231*, 270-280. https://doi.org/10.1016/j.geomorph.2014.12.015

Boivin, M., Buffin-Bélanger, T., & Piégay, H. (2017). Interannual kinetics (2010–2013) of large wood in a river corridor exposed to a 50-year flood event and fluvial ice dynamics. *Geomorphology*, *279*, 59-73. https://doi.org/10.1016/j.geomorph.2016.07.010

Bollati, I. M., Pellegrini, L., Rinaldi, M., Duci, G., & Pelfini, M. (2014). Reach-scale morphological adjustments and stages of channel evolution : The case of the Trebbia River (northern Italy). *Geomorphology*, *221*, 176-186. https://doi.org/10.1016/j.geomorph.2014.06.007

Bonan, G. B. (1989). Environmental factors and ecological processes controlling vegetation patterns in boreal forests. *Landscape Ecology*, *3*(2), 111-130. https://doi.org/10.1007/BF00131174

Bornette, G., Tabacchi, E., Hupp, C., Puijalon, S., & Rostan, J. C. (2008). A model of plant strategies in fluvial hydrosystems. *Freshwater Biology*, *53*(8), 1692-1705. https://doi.org/10.1111/j.1365-2427.2008.01994.x

Boucher, É. (2017a). River Ice and Ice Jams. Dans *International Encyclopedia of Geography* (p. 1-8). John Wiley & Sons, Ltd. https://doi.org/10.1002/9781118786352.wbieg0512

Boucher, É. (2017b). River Ice and Ice Jams. Dans *International Encyclopedia of Geography* (p. 1-8). John Wiley & Sons, Ltd. https://doi.org/10.1002/9781118786352.wbieg0512

Boucher, É., Bégin, Y., & Arseneault, D. (2009a). Hydro-climatic analysis of mechanical breakups reconstructed from tree-rings, Necopastic watershed, northern Québec, Canada. *Journal of Hydrology*, *375*(3-4), 373-382. https://doi.org/10.1016/j.jhydrol.2009.06.027

Boucher, É., Bégin, Y., & Arseneault, D. (2009b). Impacts of recurring ice jams on channel geometry and geomorphology in a small high-boreal watershed. *Geomorphology*, *108*(3-4), 273-281. https://doi.org/10.1016/j.geomorph.2009.02.014

Boucher, E., Bégin, Y., Arseneault, D., & Ouarda, T. B. M. J. (2012). Long-Term and Large-Scale River-Ice Processes in Cold-Region Watersheds. Dans M. Church, P. M. Biron, & A. G. Roy (Éds.), *Gravel-Bed Rivers* (1re éd., p. 546-554). Wiley. https://doi.org/10.1002/9781119952497.ch39

Box, S. (2018). Impacts of Vegetation Growth on Reach-scale Flood Hydraulics in a Sand-bed River and the Implications for Vegetation-morphology Coevolution. *Graduate Student Theses, Dissertations, & Professional Papers*. https://scholarworks.umt.edu/etd/11144

Brazeiro, A. (2001). Relationship between species richness and morphodynamics in sandy beaches : What are the underlying factors? *Marine Ecology Progress Series*, *224*, 35-44. https://doi.org/10.3354/meps224035

Brockett, R. (2023). *Ostrich Fern Fiddlehead (Matteuccia struthiopteris L. Todaro) Cultivation : Controlled Environment Requirements and Growth Cycle Compression* [University of Guelph]. https://hdl.handle.net/10214/27720

Brown, J. H., Ernest, S. K. M., Parody, J. M., & Haskell, J. P. (2001). Regulation of diversity : Maintenance of species richness in changing environments. *Oecologia*, *126*(3), 321-332. https://doi.org/10.1007/s004420000536

Brown, R. L., Reilly, L. A. J., & Peet, R. K. (2016). Species Richness : Small Scale. Dans *eLS* (p. 1-9). John Wiley & Sons, Ltd. https://doi.org/10.1002/9780470015902.a0020488.pub2

Buffin-Belanger, T., Beaudoin, J.-F., Maltais, M., Laroche, S., & Tomety, Y. (2022). *Cartographie des zones inondables dans la MRC de Bonaventure. Volet 1—Analyse et cartographie des aléas. Rapport remis au Ministère des Affaires municipales et de l'habitation, décembre 2022, 68 pages et annexes.*

Buffin-Bélanger, T., Biron, P. M., Larocque, M., Demers, S., Olsen, T., Choné, G., Ouellet, M.-A., Cloutier, C.-A., Desjarlais, C., & Eyquem, J. (2015). Freedom space for rivers : An economically viable river management concept in a changing climate. *Geomorphology*, *251*, 137-148. https://doi.org/10.1016/j.geomorph.2015.05.013

Buffin-Bélanger, T., Lachapelle, F., Biron, P., & Boivin, M. (2024). Trajectoires et visées de l'hydrogéomorphologie au Québec. *Canadian Geographies / Géographies canadiennes*, *68*(2), 196-211. https://doi.org/10.1111/cag.12893

Burrell, B. C., Beltaos ,S., & and Turcotte, B. (2023). Effects of climate change on river-ice processes and ice jams. *International Journal of River Basin Management*, *21*(3), 421-441. https://doi.org/10.1080/15715124.2021.2007936

Bywater-Reyes, S., Diehl, R. M., Wilcox, A. C., Stella, J. C., & Kui, L. (2022a). A Green New Balance : Interactions among riparian vegetation plant traits and morphodynamics in alluvial rivers. *Earth Surface Processes and Landforms*, esp.5385. https://doi.org/10.1002/esp.5385

Bywater-Reyes, S., Diehl, R. M., Wilcox, A. C., Stella, J. C., & Kui, L. (2022b). A Green New Balance : Interactions among riparian vegetation plant traits and morphodynamics in alluvial rivers. *Earth Surface Processes and Landforms*, esp.5385. https://doi.org/10.1002/esp.5385

Bywater-Reyes, S., Wilcox, A. C., & Diehl, R. M. (2017). Multiscale influence of woody riparian vegetation on fluvial topography quantified with ground-based and airborne lidar. *J. Geophys. Res. Earth Surf.*, *122*, 1218-1235. https://doi.org/10.1002/2016JF004058

Camporeale, C., Perucca, E., Ridolfi, L., & Gurnell, A. M. (2013). Modeling the Interactions Between River Morphodynamics and Riparian Vegetation. *Reviews of Geophysics*, *51*(3), 379-414. https://doi.org/10.1002/rog.20014

Caponi, F., Koch, A., Bertoldi, W., Vetsch, D. F., & Siviglia, A. (2019). When Does Vegetation Establish on Gravel Bars? Observations and Modeling in the Alpine Rhine River. *Frontiers in Environmental Science*, *7*, 124. https://doi.org/10.3389/fenvs.2019.00124

Casanova, M. T. (2015). The seed bank as a mechanism for resilience and connectivity in a seasonal unregulated river. *Aquatic Botany*, *124*, 63-69. https://doi.org/10.1016/j.aquabot.2015.03.008

Catford, J. A., & Jansson, R. (2014). Drowned, buried and carried away : Effects of plant traits on the distribution of native and alien species in riparian ecosystems. *New Phytologist*, *204*(1), 19-36. https://doi.org/10.1111/nph.12951

Charles-Dominique, T., Edelin, C., & Bouchard, A. (2010). Architectural strategies of Cornus sericea, a native but invasive shrub of Southern Quebec, Canada, under an open or a closed canopy. *Annals of Botany*, *105*(2), 205-220. https://doi.org/10.1093/aob/mcp273

Chassiot, L., Lajeunesse, P., & Bernier, J.-F. (2020). Riverbank erosion in cold environments : Review and outlook. *Earth-Science Reviews*, *207*, 103231. https://doi.org/10.1016/j.earscirev.2020.103231

Chen, F., Chen, L., Zhang, W., Han, J., & Wang, J. (2019). Responses of channel morphology to flow-sediment variations after dam construction : A case study of the Shashi Reach, middle Yangtze River. *Hydrology Research*, *50*(5), 1359-1375. https://doi.org/10.2166/nh.2019.066

Choné, G., & Biron, P. M. (2016). Assessing the Relationship Between River Mobility and Habitat. *River Research and Applications*, *32*(4), 528-539. https://doi.org/10.1002/rra.2896

Church, M., & Ferguson, R. I. (2015). Morphodynamics : Rivers beyond steady state. *Water Resources Research*, *51*(4), 1883-1897. https://doi.org/10.1002/2014WR016862

Church, M., Uunila, L., & North, M. E. A. (2014). The Response of Riparian Vegetation to Flow Regulation Along Peace River, Alberta. Dans *The Regulation of Peace River* (p. 209-231). John Wiley & Sons, Ltd. https://doi.org/10.1002/9781118906170.ch9

Comiti, F., Cadol, D., & Wohl, E. (2009). Flow regimes, bed morphology, and flow resistance in self-formed step-pool channels. *Water Resources Research*, *45*(4). https://doi.org/10.1029/2008WR007259

Coombes, M. A. (2016). Biogeomorphology : Diverse, integrative and useful: Biogeomorphology: Diverse, Integrative and Useful. *Earth Surface Processes and Landforms*, *41*(15), 2296-2300. https://doi.org/10.1002/esp.4055

Corenblit, D., Baas, A., Balke, T., Bouma, T., Fromard, F., Garófano-Gómez, V., González, E., Gurnell, A. M., Hortobágyi, B., Julien, F., Kim, D., Lambs, L., Stallins, J. A., Steiger, J., Tabacchi, E., & Walcker, R. (2015). Engineer pioneer plants respond to and affect geomorphological constraints similarly along water-terrestrial interfaces world-wide : Biogeomorphological feedbacks along water-terrestrial interfaces. *Global Ecology and Biogeography*, *24*(12), 1363-1376. https://doi.org/10.1111/geb.12373

Corenblit, D., Garófano-Gómez, V., González, E., Hortobágyi, B., Julien, F., Lambs, L., Otto, T., Roussel, E., Steiger, J., Tabacchi, E., & Till-Bottraud, I. (2018). Niche construction within riparian corridors. Part II : The unexplored role of positive intraspecific interactions in Salicaceae species. *Geomorphology*, *305*, 112-122. https://doi.org/10.1016/j.geomorph.2017.09.016

Corenblit, D., Gurnell, A. M., Steiger, J., & Tabacchi, E. (2008). Reciprocal adjustments between landforms and living organisms : Extended geomorphological evolutionary insights. *CATENA*, *73*(3), 261-273. https://doi.org/10.1016/j.catena.2007.11.002

Corenblit, D., Mazal, L., Till-Bottraud, I., & Steiger, J. (2020a). Relier la biogéomorphologie fluviale à l'écologie évolutive : Un focus sur les arbres riverains pionniers. *Géomorphologie : relief, processus, environnement*, *26*(1), 55-72. https://doi.org/10.4000/geomorphologie.14127

Corenblit, D., Piégay, H., Arrignon, F., González-Sargas, E., Bonis, A., Davies, N. S., Ebengo, D. M., Garófano-Gómez, V., Gurnell, A. M., Henry, A. L., Hortobágyi, B., Martínez-Capel, F., Steiger, J., Tabacchi, E., Tooth, S., Vautier, F., & Walcker, R. (2024a). Interactions between vegetation and river morphodynamics. Part I : Research clarifications and challenges. *Earth-Science Reviews*, *253*, 104769. https://doi.org/10.1016/j.earscirev.2024.104769

Corenblit, D., Piégay, H., Arrignon, F., González-Sargas, E., Bonis, A., Ebengo, D. M., Garófano-Gómez, V., Gurnell, A. M., Henry, A. L., Hortobágyi, B., Martínez-Capel, F., Mazal, L., Steiger, J., Tabacchi, E., Tooth, S., Vautier, F., & Walcker, R. (2024b). Interactions between vegetation and river morphodynamics. Part II : Why is a functional trait framework important? *Earth-Science Reviews*, *253*, 104709. https://doi.org/10.1016/j.earscirev.2024.104709

Corenblit, D., Steiger, J., Charrier, G., Darrozes, J., Garófano-Gómez, V., Garreau, A., González, E., Gurnell, A. M., Hortobágyi, B., Julien, F., Lambs, L., Larrue, S., Otto, T., Roussel, E., Vautier, F., & Voldoire, O. (2016). *Populus nigra* L. establishment and fluvial landform construction : Biogeomorphological dynamics within a channelized river: Biogeomorphological Dynamics within a Channelized River. *Earth Surface Processes and Landforms*, *41*(9), 1276-1292. https://doi.org/10.1002/esp.3954

Corenblit, D., Steiger, J., Dufour, S., Liébault, F., & Piégay, H. (2024c). Chapter 13—Resilience and the biophysical science of rivers. Dans M. Thoms & I. Fuller (Éds.), *Resilience and Riverine Landscapes* (p. 269-286). Elsevier. https://doi.org/10.1016/B978-0-323-91716-2.00010-8

Corenblit, D., Steiger, J., González, E., Gurnell, A. M., Charrier, G., Darrozes, J., Dousseau, J., Julien, F., Lambs, L., Larrue, S., Roussel, E., Vautier, F., & Voldoire, O. (2014). The biogeomorphological life cycle of poplars during the fluvial biogeomorphological succession : A special focus on Populus nigra L. *Earth Surface Processes and Landforms*, *39*(4), 546-563. https://doi.org/10.1002/esp.3515

Corenblit, D., Steiger, J., Gurnell, A. M., Tabacchi, E., & Roques, L. (2009). Control of sediment dynamics by vegetation as a key function driving biogeomorphological succession within fluvial corridors. *Earth Surface Processes and Landforms*, *34*(13), 1790-1810. https://doi.org/10.1002/esp.1876

Corenblit, D., Steiger, J., Gurnell, A., & Tabacchi, E. (2007a). Darwinian origin of landforms. *Earth Surface Processes and Landforms*, *32*(13), 2070-2073. https://doi.org/10.1002/esp.1536

Corenblit, D., Steiger, J., & Tabacchi, E. (2010). Biogeomorphologic succession dynamics in a Mediterranean river system. *Ecography*, *33*(6), 1136-1148. https://doi.org/10.1111/j.1600-0587.2010.05894.x

Corenblit, D., Tabacchi, E., Steiger, J., & Gurnell, A. M. (2007b). Reciprocal interactions and adjustments between fluvial landforms and vegetation dynamics in river corridors : A review of complementary approaches. *Earth-Science Reviews*, *84*(1-2), 56-86. https://doi.org/10.1016/j.earscirev.2007.05.004

Corenblit, D., Vautier, F., González, E., & Steiger, J. (2020b). Formation and dynamics of vegetated fluvial landforms follow the biogeomorphological succession model in a channelized river. *Earth Surface Processes and Landforms*, esp.4863. https://doi.org/10.1002/esp.4863

Dahl, T. A., Gibson, S. A., & Webber, J. B. (2017). Using dendrochronology to identify historic ice jams. *Proc., CGU HS Committee on River Ice 736 Processes and the*

Environment 19th Workshop on the Hydraulics of Ice 737 Covered Rivers Whitehorse, 12.

Davis, L., Sumner, M., Stasolla, C., & Renault, S. (2014). Salinity-induced changes in the root development of a northern woody species, Cornus sericea. *Botany*, *92*(8), 597-606. https://doi.org/10.1139/cjb-2013-0272

De Bello, F., Botta-Dukát, Z., Lepš, J., & Fibich, P. (2021a). Towards a more balanced combination of multiple traits when computing functional differences between species. *Methods in Ecology and Evolution*, *12*(3), 443-448. https://doi.org/10.1111/2041-210X.13537

De Bello, F., Botta-Dukát, Z., Lepš, J., & Fibich, P. (2021b). Towards a more balanced combination of multiple traits when computing functional differences between species. *Methods in Ecology and Evolution*, *12*(3), 443-448. https://doi.org/10.1111/2041-210X.13537

De Munck, S., Gauthier, Y., Bernier, M., Chokmani, K., & Légaré, S. (2017). River predisposition to ice jams : A simplified geospatial model. *Natural Hazards and Earth System Sciences*, *17*(7), 1033-1045. https://doi.org/10.5194/nhess-17-1033-2017

Diehl, R. M., Merritt, D. M., Wilcox, A. C., & Scott, M. L. (2017). Applying Functional Traits to Ecogeomorphological Processes in Riparian Ecosystems. *BioScience*, *67*(8), 729-743. https://doi.org/10.1093/biosci/bix080

Dixon, M. D., & Turner, M. G. (2006). Simulated recruitment of riparian trees and shrubs under natural and regulated flow regimes on the Wisconsin River, USA. *River Research and Applications*, *22*(10), 1057-1083. https://doi.org/10.1002/rra.948

Dufour, S., Barsoum, N., Muller, E., & Piégay, H. (2007). Effects of channel confinement on pioneer woody vegetation structure, composition and diversity along the River Drôme (SE France). *Earth Surface Processes and Landforms*, *32*(8), 1244-1256. https://doi.org/10.1002/esp.1556

Dumitriu, D. (2020). Sediment flux during flood events along the Trotuș River channel : Hydrogeomorphological approach. *Journal of Soils and Sediments*, *20*(11), 4083-4102. https://doi.org/10.1007/s11368-020-02763-4

Edwards, P. J. (2024). Ecological traits of Saliceae and the species replacing them on the active floodplain. *River Research and Applications*, *40*(6), 988-1000. https://doi.org/10.1002/rra.4229

Edwards, P. J., Kollmann, J., Gurnell, A. M., Petts, G. E., Tockner, K., & Ward, J. V. (1999). A conceptual model of vegetation dynamics on gravel bars of a large Alpine

river. *Wetlands Ecology and Management*, *7*(3), 141-153. https://doi.org/10.1023/A:1008411311774

Egger, G., Politti, E., Lautsch, E., Benjankar, R., Gill, K. M., & Rood, S. B. (2015). Floodplain forest succession reveals fluvial processes : A hydrogeomorphological model for temperate riparian woodlands. *Journal of Environmental Management*, *161*, 72-82. https://doi.org/10.1016/j.jenvman.2015.06.018

Eichel, J., Corenblit, D., & Dikau, R. (2016). Conditions for feedbacks between geomorphological and vegetation dynamics on lateral moraine slopes : A biogeomorphological feedback window: CONDITIONS FOR BIOGEOMORPHOLOGICAL FEEDBACKS ON LATERAL MORAINE SLOPES. *Earth Surface Processes and Landforms*, *41*(3), 406-419. https://doi.org/10.1002/esp.3859

Elderd, B. D. (2003). The Impact of Changing Flow Regimes on Riparian Vegetation and the Riparian Species Mimulus guttatus. *Ecological Applications*, *13*(6), 1610-1625.

Engström, J., Jansson, R., Nilsson, C., & Weber, C. (2011). Effects of river ice on riparian vegetation : Ice and riparian vegetation. *Freshwater Biology*, *56*(6), 1095-1105. https://doi.org/10.1111/j.1365-2427.2010.02553.x

Ettema, R. (2002). Review of Alluvial-channel Responses to River Ice. *Journal of Cold Regions Engineering*, *16*(4), 191-217. https://doi.org/10.1061/(ASCE)0887-381X(2002)16:4(191)

Ettema, R., & Kempema, E. W. (2012). River-Ice Effects on Gravel-Bed Channels. Dans M. Church, P. M. Biron, & A. G. Roy (Éds.), *Gravel-Bed Rivers* (1re éd., p. 523-540). Wiley. https://doi.org/10.1002/9781119952497.ch37

Fei, S., Phillips, J., & Shouse, M. (2014). Biogeomorphological Impacts of Invasive Species. *Annual Review of Ecology, Evolution, and Systematics*, *45*(1), 69-87. https://doi.org/10.1146/annurev-ecolsys-120213-091928

Fischer, S., Greet, J., Walsh, C. J., & Catford, J. A. (2021). Flood disturbance affects morphology and reproduction of woody riparian plants. *Scientific Reports*, *11*, 16477. https://doi.org/10.1038/s41598-021-95543-0

Fraver, S., D'Amato, A. W., Reinikainen, M., Gill, K. G., & Palik, B. J. (2022). Stand dynamics and structure of old-growth Fraxinus nigra stands in northern Minnesota, USA. *Canadian Journal of Forest Research*, *52*(6), 910-919. https://doi.org/10.1139/cjfr-2021-0340

Fryirs, K. A. (2017). River sensitivity : A lost foundation concept in fluvial geomorphology: River sensitivity: A lost foundation concept in fluvial

geomorphology. *Earth Surface Processes and Landforms*, *42*(1), 55-70. https://doi.org/10.1002/esp.3940

Fryirs, K., & Brierley, G. (2022). Assemblages of geomorphological units : A building block approach to analysis and interpretation of river character, behaviour, condition and recovery. *Earth Surface Processes and Landforms*, *47*(1), 92-108. https://doi.org/10.1002/esp.5264

Funk, J. L., Larson, J. E., Ames, G. M., Butterfield, B. J., Cavender-Bares, J., Firn, J., Laughlin, D. C., Sutton-Grier, A. E., Williams, L., & Wright, J. (2017). Revisiting the Holy Grail : Using plant functional traits to understand ecological processes. *Biological Reviews*, *92*(2), 1156-1173. https://doi.org/10.1111/brv.12275

Garófano-Gómez, V., Arrignon, F., Vautier, F., Tabacchi, E., Allain, E., Bonis, A., Delmotte, S., González, E., Julien, F., Lambs, L., Martínez-Capel, F., Planty-Tabacchi, A.-M., Roussel, E., Steiger, J., Toumazet, J.-P., Till-Bottraud, I., Voldoire, O., Walcker, R., & Corenblit, D. (2022). Trait-based numerical modelling of feedbacks between river morphodynamics and riparian vegetation for sustainable river management in a changing climate. *EGU General Assembly Conference Abstracts*, EGU22-7443. https://doi.org/10.5194/egusphere-egu22-7443

Garófano-Gómez, V., Metz, M., Egger, G., Díaz-Redondo, M., Hortobágyi, B., Geerling, G., Corenblit, D., & Steiger, J. (2017). Vegetation succession processes and fluvial dynamics of a mobile temperate riparian ecosystem : The lower Allier River (France). *Géomorphologie : Relief, Processus, Environnement*, *23*(vol. 23-n° 3), Article 3. https://doi.org/10.4000/geomorphologie.11805

Geerling, G. W., Ragas, A. M. J., Leuven, R. S. E. W., van den Berg, J. H., Breedveld, M., Liefhebber, D., & Smits, A. J. M. (2006). Succession and Rejuvenation in Floodplains along the River Allier (France). *Hydrobiologia*, *565*(1), 71-86. https://doi.org/10.1007/s10750-005-1906-6

Gibert, A., Gray, E. F., Westoby, M., Wright, I. J., & Falster, D. S. (2016). On the link between functional traits and growth rate : Meta-analysis shows effects change with plant size, as predicted. *Journal of Ecology*, *104*(5), 1488-1503. https://doi.org/10.1111/1365-2745.12594

Gilvear, D., Francis, R., Willby, N., & Gurnell, A. (2007). 26 Gravel bars : A key habitat of gravel-bed rivers for vegetation. Dans *Developments in Earth Surface Processes* (Vol. 11, p. 677-700). Elsevier. https://doi.org/10.1016/S0928-2025(07)11154-8

González del Tánago, M., Bejarano, M. D., García de Jalón, D., & Schmidt, J. C. (2015). Biogeomorphological responses to flow regulation and fine sediment supply in Mediterranean streams (the Guadalete River, southern Spain). *Journal of Hydrology*, *528*, 751-762. https://doi.org/10.1016/j.jhydrol.2015.06.065

González, E., Martínez-Fernández, V., Shafroth, P. B., Sher, A. A., Henry, A. L., Garófano-Gómez, V., & Corenblit, D. (2018). Regeneration of *Salicaceae* riparian forests in the Northern Hemisphere : A new framework and management tool. *Journal of Environmental Management*, *218*, 374-387. https://doi.org/10.1016/j.jenvman.2018.04.069

González, E., Masip, A., & Tabacchi, E. (2016). Poplar plantations along regulated rivers may resemble riparian forests after abandonment : A comparison of passive restoration approaches. *Restoration Ecology*, *24*(4), 538-547. https://doi.org/10.1111/rec.12351

González, E., Shafroth, P. B., Lee, S. R., Leverich, G. T., Real De Asua, R., Sherry, R. A., Ostoja, S. M., & Orr, B. K. (2019a). Short-term geomorphological and riparian vegetation responses to a 40-year flood on a braided, dryland river. *Ecohydrology*, *12*(8), e2152. https://doi.org/10.1002/eco.2152

González, E., Shafroth, P. B., Lee, S. R., Leverich, G. T., Real De Asua, R., Sherry, R. A., Ostoja, S. M., & Orr, B. K. (2019b). Short-term geomorphological and riparian vegetation responses to a 40-year flood on a braided, dryland river. *Ecohydrology*, *12*(8). https://doi.org/10.1002/eco.2152

Götzenberger, L., de Bello, F., Bråthen, K. A., Davison, J., Dubuis, A., Guisan, A., Lepš, J., Lindborg, R., Moora, M., Pärtel, M., Pellissier, L., Pottier, J., Vittoz, P., Zobel, K., & Zobel, M. (2012). Ecological assembly rules in plant communities—Approaches, patterns and prospects. *Biological Reviews*, *87*(1), 111-127. https://doi.org/10.1111/j.1469-185X.2011.00187.x

Grams, P. E., Dean, D. J., Walker, A. E., Kasprak, A., & Schmidt, J. C. (2020). The roles of flood magnitude and duration in controlling channel width and complexity on the Green River in Canyonlands, Utah, USA. *Geomorphology*, *371*, 107438. https://doi.org/10.1016/j.geomorph.2020.107438

Graves, S., Piepho, H.-P., & with help from Sundar Dorai-Raj, L. S. (2024). *multcompView : Visualizations of paired comparisons* [Manual]. https://doi.org/10.32614/CRAN.package.multcompView

Gucker, C. (2012). *Cornus sericea. In : Fire Effects Information System, [Online]*. U.S. Department of Agriculture, Forest Service, Rocky Mountain Research Station, Fire Sciences Laboratory (Producer). Available: https://www.fs.usda.gov/database/feis/plants/shrub/corser/all.html [2025, August 7]

Gurnell, A., England, J., & Burgess-Gamble, L. (2019). Trees and wood : Working with natural river processes: Trees and Wood. *Water and Environment Journal*, *33*(3), 342-352. https://doi.org/10.1111/wej.12426

Gurnell, A. M., & Bertoldi, W. (2020). Extending the conceptual model of river island development to incorporate different tree species and environmental conditions. *River Research and Applications*, *36*(8), 1730-1747. https://doi.org/10.1002/rra.3691

Gurnell, A. M., & Bertoldi, W. (2022). The impact of plants on fine sediment storage within the active channels of gravel-bed rivers : A preliminary assessment. *Hydrological Processes*, *36*(7), e14637. https://doi.org/10.1002/hyp.14637

Gurnell, A. M., & Bertoldi, W. (2024). Plants and river morphodynamics : The emergence of fluvial biogeomorphology. *River Research and Applications*, *n/a*(n/a), 1-56. https://doi.org/10.1002/rra.4271

Gurnell, A. M., Bertoldi, W., & Corenblit, D. (2012). Changing river channels : The roles of hydrological processes, plants and pioneer fluvial landforms in humid temperate, mixed load, gravel bed rivers. *Earth-Science Reviews*, *111*(1-2), 129-141. https://doi.org/10.1016/j.earscirev.2011.11.005

Gurnell, A. M., Corenblit, D., García de Jalón, D., González del Tánago, M., Grabowski, R. C., O'Hare, M. T., & Szewczyk, M. (2016a). A Conceptual Model of Vegetation-hydrogeomorphology Interactions Within River Corridors : VEGETATION-HYDROGEOMORPHOLOGY INTERACTIONS. *River Research and Applications*, *32*(2), 142-163. https://doi.org/10.1002/rra.2928

Gurnell, A. M., Petts, G. E., Hannah, D. M., Smith, B. P. G., Edwards, P. J., Kollmann, J., Ward, J. V., & Tockner, K. (2001). *Riparian vegetation and island formation along the gravel-bed Fiume Tagliamento, Italy*. 32.

Gurnell, A. M., Rinaldi, M., Belletti, B., Bizzi, S., Blamauer, B., Braca, G., Buijse, A. D., Bussettini, M., Camenen, B., Comiti, F., Demarchi, L., García de Jalón, D., González del Tánago, M., Grabowski, R. C., Gunn, I. D. M., Habersack, H., Hendriks, D., Henshaw, A. J., Klösch, M., … Ziliani, L. (2016b). A multi-scale hierarchical framework for developing understanding of river behaviour to support river management. *Aquatic Sciences*, *78*(1), 1-16. https://doi.org/10.1007/s00027-015-0424-5

Hamelin, L.-E. (1979). The Bechevnik : A river bank feature from Siberia. *The Musk-Ox.*, *25*, 70-72.

Han, M., Brierley, G., Li, B., Li, Z., & Li, X. (2020). Impacts of flow regulation on geomorphological adjustment and riparian vegetation succession along an anabranching reach of the Upper Yellow River. *CATENA*, *190*, 104561. https://doi.org/10.1016/j.catena.2020.104561

Haussmann, N. S. (2011). Biogeomorphology : Understanding different research approaches. *Earth Surface Processes and Landforms*, *36*(1), 136-138. https://doi.org/10.1002/esp.2097

Helm, D. J., & Collins, W. B. (1997). Vegetation succession and disturbance on a boreal forest floodplain, Susitna River, Alaska. *Canadian Field Naturalist*, *111*, 553-566.

Hoppenreijs, J. H. T., Eckstein, R. L., & Lind, L. (2022). Pressures on Boreal Riparian Vegetation : A Literature Review. *Frontiers in Ecology and Evolution*, *9*, 806130. https://doi.org/10.3389/fevo.2021.806130

Hortobágyi, B., Corenblit, D., Vautier, F., Steiger, J., Roussel, E., Burkart, A., & Peiry, J.-L. (2017). A multi-scale approach of fluvial biogeomorphological dynamics using photogrammetry. *Journal of Environmental Management*, *202*, 348-362. https://doi.org/10.1016/j.jenvman.2016.08.069

Hugenholtz, C. H., Smith, D. G., & Livingston, J. M. (2009). Application of Floodplain Stratigraphy to Determine the Recurrence of Ice-Jam Flooding Along the Lower Peace and Athabasca Rivers, Alberta. *Canadian Water Resources Journal / Revue canadienne des ressources hydriques*, *34*(1), 79-94. https://doi.org/10.4296/cwrj3401079

Hupp, C. R., & Rinaldi, M. (2007). Riparian Vegetation Patterns in Relation to Fluvial Landforms and Channel Evolution Along Selected Rivers of Tuscany (Central Italy). *Annals of the Association of American Geographers*, *97*(1), 12-30. https://doi.org/10.1111/j.1467-8306.2007.00521.x

Janssen, P. (2025). The “guild” concept in riparian ecology : Use, limitations and prospects for improving the reproducibility and transferability of results. *Ecological Indicators*, *171*, 113152. https://doi.org/10.1016/j.ecolind.2025.113152

Janssen, P., Bisson-Gauthier, L., González-Sargas, E., Loiselle, A., Darveau, M., Bourgeois, B., & Poulin, M. (2024). How does the taxonomic and functional structure of plant communities differ between riverine and palustrine swamps? *Journal of Vegetation Science*, *35*(6), e13319. https://doi.org/10.1111/jvs.13319

Janssen, P., Piégay, H., & Evette, A. (2022). The taxonomic structure but not the functioning of riparian herbaceous communities varies with hydrological conditions on a large, highly regulated river : Evidence from a 2-year replicated study. *Ecohydrology*. https://doi.org/10.1002/eco.2405

Janssen, P., Stella, J. C., Piégay, H., Räpple, B., Pont, B., Faton, J.-M., Cornelissen, J. H. C., & Evette, A. (2020). Divergence of riparian forest composition and functional traits from natural succession along a degraded river with multiple stressor legacies.

Science of The Total Environment, *721*, 137730. https://doi.org/10.1016/j.scitotenv.2020.137730

Jansson, R., Zinko, U., Merritt, D. M., & Nilsson, C. (2005). Hydrochory increases riparian plant species richness : A comparison between a free-flowing and a regulated river: *Hydrochory and plant species richness*. *Journal of Ecology*, *93*(6), 1094-1103. https://doi.org/10.1111/j.1365-2745.2005.01057.x

Jautzy, T., Schmitt, L., & Rixhon, G. (2022). Historical geomorphological adjustments of an Upper Rhine sub-tributary over the two last centuries (Bruche River, France). *Géomorphologie : Relief, Processus, Environnement*, *28*(1), Article 1. https://doi.org/10.4000/geomorphologie.16661

Johnson, M. F., Thorne, C. R., Castro, J. M., Kondolf, G. M., Mazzacano, C. S., Rood, S. B., & Westbrook, C. (2020). Biomic river restoration : A new focus for river management. *River Research and Applications*, *36*(1), 3-12. https://doi.org/10.1002/rra.3529

Jolley, R. L., Lockaby, B. G., & Cavalcanti, G. G. (2010). Changes in riparian forest composition along a sedimentation rate gradient. *Plant Ecology*, *210*(2), 317-330. https://doi.org/10.1007/s11258-010-9759-0

Jones, L. S., & Schumm, S. A. (1999). Causes of Avulsion : An Overview. Dans *Fluvial Sedimentology VI* (p. 169-178). John Wiley & Sons, Ltd. https://doi.org/10.1002/9781444304213.ch13

Kalinin, V. G. (2008). Study of spatial distribution and occurrence frequency of ice jams in rivers of the Votkinsk reservoir catchment. *Russian Meteorology and Hydrology*, *33*(12), 819-822. https://doi.org/10.3103/S1068373908120091

Karle, K. F. (2003). *Evaluation of Bioengineered Stream Bank Stabilization in Alaska* (No. FHWA-AK-RD-03-03). Alaska Department of Transportation.

Karle, K. F. (2007). *The Effects of a Winter Ice Jam Event On Bioengineered Bank Stabilization Along The Kenai River* (No. FHWA-AK-RD-07-03). Alaska Department of Transportation.

Karrenberg, S., Blaser, S., Kollmann, J., Speck, T., & Edwards, P. J. (2003). Root anchorage of saplings and cuttings of woody pioneer species in a riparian environment. *Functional Ecology*, *17*(2), 170-177. https://doi.org/10.1046/j.1365-2435.2003.00709.x

Karrenberg, S., Edwards, P. J., & Kollmann, J. (2002). The life history of Salicaceae living in the active zone of floodplains. *Freshwater Biology*, *47*(4), 733-748. https://doi.org/10.1046/j.1365-2427.2002.00894.x

Kattge, J., Bönisch, G., Díaz, S., Lavorel, S., Prentice, I. C., Leadley, P., Tautenhahn, S., Werner, G. D. A., Aakala, T., Abedi, M., Acosta, A. T. R., Adamidis, G. C., Adamson, K., Aiba, M., Albert, C. H., Alcántara, J. M., Alcázar C, C., Aleixo, I., Ali, H., … Wirth, C. (2020). TRY plant trait database – enhanced coverage and open access. *Global Change Biology*, *26*(1), 119-188. https://doi.org/10.1111/gcb.14904

Kehr, J. M., Merritt, D. M., & Stromberg, J. C. (2014). Linkages between primary seed dispersal, hydrochory and flood timing in a semi-arid region river. *Journal of Vegetation Science*, *25*(1), 287-300. https://doi.org/10.1111/jvs.12061

Keita, N., Bourgeois, B., Evette, A., Tisserant, M., González, E., Breton, V., Goulet, C., & Poulin, M. (2021a). Growth Response of Cuttings to Drought and Intermittent Flooding for Three Salix Species and Implications for Riverbank Soil Bioengineering. *Environmental Management*, *67*(6), 1137-1144. https://doi.org/10.1007/s00267-021-01444-3

Keita, N., Bourgeois, B., Evette, A., Tisserant, M., González, E., Breton, V., Goulet, C., & Poulin, M. (2021b). Growth Response of Cuttings to Drought and Intermittent Flooding for Three Salix Species and Implications for Riverbank Soil Bioengineering. *Environmental Management*, *67*(6), 1137-1144. https://doi.org/10.1007/s00267-021-01444-3

Kenefick, C., Livesley, S., & Farrell, C. (2024). A systematic review of resprouting in woody plants and potential implications for the management of urban plantings. *Ecology and Evolution*, *14*(1), e10839. https://doi.org/10.1002/ece3.10839

Kim, D., & Kupfer, J. A. (2016). Tri-Variate Relationships among Vegetation, Soil, and Topography along Gradients of Fluvial Biogeomorphological Succession. *PLOS ONE*, *11*(9), e0163223. https://doi.org/10.1371/journal.pone.0163223

Kim, D., & Lee, K. (2022). Landforms as combined expressions of multiple reciprocally interacting species : Refining the ecosystem engineering concept. *Earth-Science Reviews*, *232*, 104152. https://doi.org/10.1016/j.earscirev.2022.104152

Kimiaghalam, N., Goharrokhi, M., Clark, S. P., & Ahmari, H. (2015). A comprehensive fluvial geomorphology study of riverbank erosion on the Red River in Winnipeg, Manitoba, Canada. *Journal of Hydrology*, *529*, 1488-1498. https://doi.org/10.1016/j.jhydrol.2015.08.033

Kindt, R., & Coe, R. (2005). *Tree diversity analysis. A manual and software for common statistical methods for ecological and biodiversity studies*. World Agroforestry Centre (ICRAF). http://www.worldagroforestry.org/output/tree-diversity-analysis

Klimešová, J., Martínková, J., & Ottaviani, G. (2018). Belowground plant functional ecology : Towards an integrated perspective. *Functional Ecology*, *32*(9), 2115-2126. https://doi.org/10.1111/1365-2435.13145

Kolerski, T., & Shen, H. T. (2015). Possible effects of the 1984 St. Clair River ice jam on bed changes. *Canadian Journal of Civil Engineering*, *42*(9), 696-703. https://doi.org/10.1139/cjce-2014-0275

Kondolf, G. M., Lisle, T. E., & Wolman, G. M. (2003). Bed Sediment Measurement. Dans *Tools in Fluvial Geomorphology* (p. 347-395). John Wiley & Sons, Ltd. https://doi.org/10.1002/0470868333.ch13

Kovachis, N., Burrell, B. C., Huokuna, M., Beltaos, S., Turcotte, B., & Jasek, M. (2017). Ice-jam flood delineation : Challenges and research needs. *Canadian Water Resources Journal / Revue Canadienne Des Ressources Hydriques*, *42*(3), 258-268. https://doi.org/10.1080/07011784.2017.1294998

Kozlowski, T. T., & Pallardy, S. G. (2002). Acclimation and Adaptive Responses of Woody Plants to Environmental Stresses. *The Botanical Review*, *68*(2), 270-334. https://doi.org/10.1663/0006-8101(2002)068%255B0270:AAAROW%255D2.0.CO;2

Kramer, N., & Wohl, E. (2014). Estimating fluvial wood discharge using time-lapse photography with varying sampling intervals. *Earth Surface Processes and Landforms*, *39*(6), 844-852. https://doi.org/10.1002/esp.3540

Krylenko, I., Alabyan, A., Aleksyuk, A., Belikov, V., Sazonov, A., Zavyalova, E., Pimanov, I., Potryasaev, S., & Zelentsov, V. (2020). Modeling Ice-Jam Floods in the Frameworks of an Intelligent System for River Monitoring. *Water Resources*, *47*(3), 387-398. https://doi.org/10.1134/S0097807820030069

Kui, L., Stella, J. C., Shafroth, P. B., House, P. K., & Wilcox, A. C. (2017). The long-term legacy of geomorphological and riparian vegetation feedbacks on the dammed Bill Williams River, Arizona, USA. *Ecohydrology*, *10*(4). https://doi.org/10.1002/eco.1839

Kyuka, T., Yamaguchi, S., Inoue, Y., Arnez Ferrel, K. R., Kon, H., & Shimizu, Y. (2021). Morphodynamic effects of vegetation life stage on experimental meandering channels. *Earth Surface Processes and Landforms*, esp.5051. https://doi.org/10.1002/esp.5051

Lagadec, A., Boucher, É., & Germain, D. (2015). Tree ring analysis of hydro-climatic thresholds that trigger ice jams on the Mistassini River, Quebec : Hydro-Climatic Thresholds Triggering River Ice Jams. *Hydrological Processes*, *29*(23), 4880-4890. https://doi.org/10.1002/hyp.10537

Laliberté, E., Legendre, P., & Shipley, B. (2014). *FD: measuring functional diversity from multiple traits, and other tools for functional ecology* [Manual].

Lallias-Tacon, S., Liébault, F., & Piégay, H. (2017). Use of airborne LiDAR and historical aerial photos for characterising the history of braided river floodplain morphology and vegetation responses. *CATENA*, *149*, 742-759. https://doi.org/10.1016/j.catena.2016.07.038

Larsen, A., Nardin, W., Lageweg, W. I., & Bätz, N. (2020). Biogeomorphology, quo vadis ? On processes, time, and space in biogeomorphology. *QUO VADIS*, *46*, 12.

Larsson, J., & Gustafsson, P. (2018). A case study in fitting area-proportional Euler diagrams with ellipses using eulerr. *Proceedings of International Workshop on Set Visualization and Reasoning*, *2116*, 84-91. https://cran.r-project.org/package=eulerr

Legendre, P., & Gallagher, E. D. (2001). Ecologically Meaningful Transformations for Ordination of Species Data. *Oecologia*, *129*(2), 271-280.

Legendre, P., & Legendre, L. (2012). *Numerical Ecology* (3e éd., Vol. 24). Elsevier. https://shop.elsevier.com/books/numerical-ecology/legendre/978-0-444-53868-0

Legras, G., Loiseau, N., Gaertner, J.-C., Poggiale, J.-C., & Gaertner-Mazouni, N. (2020). Assessing functional diversity : The influence of the number of the functional traits. *Theoretical Ecology*, *13*(1), 117-126. https://doi.org/10.1007/s12080-019-00433-x

Lepš, J., & de Bello, F. (2023). Differences in trait–environment relationships : Implications for community weighted means tests. *Journal of Ecology*, *111*(11), 2328-2341. https://doi.org/10.1111/1365-2745.14172

Li, X., He, D., Chen, G., Yang, J., Yang, Z., Guo, X. juan, Wang, C., Zhu, S., Huang, Y., Chen, H., Huang, G., Zhang, D., & Ye, C. (2022). Responses of leaf functional traits to different hydrological regimes and leaf economics spectrum in the water level fluctuation zone of Three Gorges Reservoir, China. *Frontiers in Plant Science*, *13*. https://doi.org/10.3389/fpls.2022.939452

Lienard, J., Florescu, I., & Strigul, N. (2015). An Appraisal of the Classic Forest Succession Paradigm with the Shade Tolerance Index. *PLOS ONE*, *10*(2), e0117138. https://doi.org/10.1371/journal.pone.0117138

Lind, L., & Nilsson, C. (2015). Vegetation patterns in small boreal streams relate to ice and winter floods. *Journal of Ecology*, *103*(2), 431-440. https://doi.org/10.1111/1365-2745.12355

Lind, L., Nilsson, C., Polvi, L. E., & Weber, C. (2014a). The role of ice dynamics in shaping vegetation in flowing waters : Ice dynamics and vegetation in flowing waters. *Biological Reviews*, *89*(4), 791-804. https://doi.org/10.1111/brv.12077

Lind, L., Nilsson, C., & Weber, C. (2014b). Effects of ice and floods on vegetation in streams in cold regions : Implications for climate change. *Ecology and Evolution*, *4*(21), 4173-4184. https://doi.org/10.1002/ece3.1283

Lindenschmidt, K.-E. (2020). Freeze-Up. Dans K.-E. Lindenschmidt (Éd.), *River Ice Processes and Ice Flood Forecasting : A Guide for Practitioners and Students* (p. 11-38). Springer International Publishing. https://doi.org/10.1007/978-3-030-28679-8_2

Liu, M., Wang, Z., Li, S., Lü, X., Wang, X., & Han, X. (2017). Changes in specific leaf area of dominant plants in temperate grasslands along a 2500-km transect in northern China. *Scientific Reports*, *7*(1), 10780. https://doi.org/10.1038/s41598-017-11133-z

Livingston, J. M., Smith, D. G., Froese, D. G., & Hugenholtz, C. H. (2009). Floodplain stratigraphy of the ice jam dominated middle Yukon River : A new approach to long-term flood frequency. *Hydrological Processes*, *23*(3), 357-371. https://doi.org/10.1002/hyp.7106

Looney, C. E., D'Amato, A. W., Fraver, S., Palik, B. J., & Frelich, L. E. (2018). Interspecific competition limits the realized niche of Fraxinus nigra along a waterlogging gradient. *Canadian Journal of Forest Research*, *48*(11), 1292-1301. https://doi.org/10.1139/cjfr-2018-0023

Lubiniecki, T., Laroque, C. P., & Lindenschmidt, K.-E. (2024). Identifying ice-jam flooding events through the application of dendrogeomorphological methods. *River Research and Applications*, *40*(2), 191-202. https://doi.org/10.1002/rra.4222

Lytle, D. A.,

Lytle, D. A., & Poff, N. L. (2004). Adaptation to natural flow regimes. *Trends in Ecology & Evolution*, *19*(2), 94-100. https://doi.org/10.1016/j.tree.2003.10.002

Madaeni, F., Lhissou, R., Chokmani, K., Raymond, S., & Gauthier, Y. (2020). Ice jam formation, breakup and prediction methods based on hydroclimatic data using artificial intelligence : A review. *Cold Regions Science and Technology*, *174*, 103032. https://doi.org/10.1016/j.coldregions.2020.103032

Maechler, M., Rousseeuw, P., Struyf, A., Hubert, M., & Hornik, K. (2025). *cluster : Cluster analysis basics and extensions* [Manual]. https://CRAN.R-project.org/package=cluster

Mahoney, J. M., & Rood, S. B. (1998a). Streamflow requirements for cottonwood seedling recruitment—An integrative model. *Wetlands*, *18*(4), 634-645. https://doi.org/10.1007/BF03161678

Mahoney, J. M., & Rood, S. B. (1998b). Streamflow requirements for cottonwood seedling recruitment—An integrative model. *Wetlands*, *18*(4), 634-645. https://doi.org/10.1007/BF03161678

Martínez-Fernández, V., Van Oorschot, M., De Smit, J., González del Tánago, M., & Buijse, A. D. (2018). Modelling feedbacks between geomorphologicaland riparian vegetation responses under climatechange in a Mediterranean context. *Earth Surface Processes and Landforms*, *43*, 1825-1835.

Masaki, T., Osumi, K., Takahashi, K., Hoshizaki, K., Matsune, K., & Suzuki, W. (2007). Effects of microenvironmental heterogeneity on the seed-to-seedling process and tree coexistence in a riparian forest. *Ecological Research*, *22*(5), 724-734. https://doi.org/10.1007/s11284-006-0308-1

Matte, R., Boivin, M., & Lavoie, C. (2022). Japanese knotweed increases soil erosion on riverbanks. *River Research and Applications*, *38*(3), 561-572. https://doi.org/10.1002/rra.3918

MELCCFP. (2025). *Atlas hydroclimatique du Québec méridional*.

Merritt, D. M., Nilsson, C., & Jansson, R. (2010). Consequences of propagule dispersal and river fragmentation for riparian plant community diversity and turnover. *Ecological Monographs*, *80*(4), 609-626. https://doi.org/10.1890/09-1533.1

Merritt, D. M., & Wohl, E. E. (2002). PROCESSES GOVERNING HYDROCHORY ALONG RIVERS : HYDRAULICS, HYDROLOGY, AND DISPERSAL PHENOLOGY. *Ecological Applications*, *12*(4), 1071-1087. https://doi.org/10.1890/1051-0761(2002)012%255B1071:PGHARH%255D2.0.CO;2

Micheli, E. R., Kirchner, J. W., & Larsen, E. W. (2004). Quantifying the effect of riparian forest versus agricultural vegetation on river meander migration rates, central Sacramento River, California, USA. *River Research and Applications*, *20*(5), 537-548. https://doi.org/10.1002/rra.756

Montakhab, A., Yusuf, B., Ghazali, A. H., & Mohamed, T. A. (2012). Flow and sediment transport in vegetated waterways : A review. *Reviews in Environmental Science and Bio/Technology*, *11*(3), 275-287. https://doi.org/10.1007/s11157-012-9266-y

Morin, S., Boucher, E., & Buffin-Belanger, T. (2015). The spatial variability of ice-jam bank morphologies along the Mistassini River (Quebec, Canada) : An indicator of

the ice-jam regime? *Natural Hazards*, *77*(3), 2117-2138. https://doi.org/10.1007/s11069-015-1693-y

Mossa, J., Chen, Y., Kondolf, G. M., & Walls, S. P. (2020). Channel and vegetation recovery from dredging of a large river in the Gulf coastal plain, USA. *Earth Surface Processes and Landforms*, *45*(9), 1926-1944. https://doi.org/10.1002/esp.4856

MRNF. (2018). Carte écoforestière originale et résultats du quatrième inventaire. *Ministère des ressources naturelles et des forêts. Données Québec.* https://www.donneesquebec.ca/recherche/dataset/resultats-d-inventaire-et-carte-ecoforestiere_4eme

Naiman, R. J., Décamps, H., & McClain, M. E. (2005). *Riparia : Ecology, conservation, and management of streamside communities*. Elsevier Academic.

Nakazawa, M. (2024). *fmsb : Functions for Medical Statistics Book with some Demographic Data* [Manual]. https://doi.org/10.32614/CRAN.package.fmsb

Nilsson, C., Brown, R. L., Jansson, R., & Merritt, D. M. (2010). The role of hydrochory in structuring riparian and wetland vegetation. *Biological Reviews*, no-no. https://doi.org/10.1111/j.1469-185X.2010.00129.x

Nilsson, C., Grelsson, G., Johansson, M., & Sperens, U. (1989). Patterns of Plant Species Richness Along Riverbanks. *Ecology*, *70*(1), 77-84. https://doi.org/10.2307/1938414

Nilsson, C., & Jansson, R. (1995). Floristic differences between riparian corridors of regulated and free-flowing boreal rivers. *Regulated Rivers: Research & Management*, *11*(1), 55-66. https://doi.org/10.1002/rrr.3450110106

Nilsson, C., Jansson, R., Kuglerová, L., Lind, L., & Ström, L. (2013). Boreal Riparian Vegetation Under Climate Change. *Ecosystems*, *16*(3), 401-410. https://doi.org/10.1007/s10021-012-9622-3

NRCS. (2019). PLANTS Database. *United States Department of Agriculture. Greensboro. NC.* https://plants.usda.gov

O'Briain, R., Corenblit, D., Garófano-Gómez, V., & O'Leary, C. (2024). Towards biogeomorphological river restoration : Vegetation as a critical driver of physical habitat. *River Research and Applications*, *40*(6), 1087-1105. https://doi.org/10.1002/rra.4288

Ochs, K., Egger, G., Kopecki, I., & Ferreira, T. (2019). Model-based reconstruction of the succession dynamics of a large river floodplain. *River Research and Applications*, *35*(7), 944-954. https://doi.org/10.1002/rra.3502

Oksanen, J., Simpson, G. L., Blanchet, F. G., Kindt, R., Legendre, P., Minchin, P. R., O'Hara, R. B., Solymos, P., Stevens, M. H. H., Szoecs, E., Wagner, H., Barbour, M., Bedward, M., Bolker, B., Borcard, D., Carvalho, G., Chirico, M., De Caceres, M., Durand, S., … Borman, T. (2025). *vegan : Community ecology package* [Manual]. https://doi.org/10.32614/CRAN.package.vegan

Paradis, E., & Schliep, K. (2019). ape 5.0 : An environment for modern phylogenetics and evolutionary analyses in R. *Bioinformatics (Oxford, England)*, *35*, 526-528. https://doi.org/10.1093/bioinformatics/bty633

Pasquale, N., Perona, P., Francis, R., & Burlando, P. (2014). Above-ground and below-ground Salix dynamics in response to river processes. *Hydrological Processes*, *28*(20), 5189-5203. https://doi.org/10.1002/hyp.9993

Peel, M. C., Finlayson, B. L., & McMahon, T. A. (2007). Updated world map of the Köppen-Geiger climate classification. *Hydrology and Earth System Sciences*, *11*(5), 1633-1644. https://doi.org/10.5194/hess-11-1633-2007

Pérez-Harguindeguy, N., Díaz, S., Garnier, E., Lavorel, S., Poorter, H., Jaureguiberry, P., Bret-Harte, M. S., Cornwell, W. K., Craine, J. M., Gurvich, D. E., Urcelay, C., Veneklaas, E. J., Reich, P. B., Poorter, L., Wright, I. J., Ray, P., Enrico, L., Pausas, J. G., Vos, A. C. de, … Cornelissen, J. H. C. (2013). New handbook for standardised measurement of plant functional traits worldwide. *Australian Journal of Botany*, *61*(3), 167-234. https://doi.org/10.1071/BT12225

Perucca, E., Camporeale, C., & Ridolfi, L. (2007). Significance of the riparian vegetation dynamics on meandering river morphodynamics. *Water Resources Research*, *43*(3). https://doi.org/10.1029/2006WR005234

Peters, D. L., Caissie, D., Monk, W. A., Rood, S. B., & St-Hilaire, A. (2016). An ecological perspective on floods in Canada. *Canadian Water Resources Journal / Revue Canadienne Des Ressources Hydriques*, *41*(1-2), 288-306. https://doi.org/10.1080/07011784.2015.1070694

Picco, L., Sitzia, T., Mao, L., Comiti, F., & Lenzi, M. A. (2016). Linking riparian woody communities and fluviomorphological characteristics in a regulated gravel-bed river (Piave River, Northern Italy) : RIPARIAN COMMUNITIES AND MORPHOLOGICAL CHARACTERISTICS IN GRAVEL-BED RIVER. *Ecohydrology*, *9*(1), 101-112. https://doi.org/10.1002/eco.1616

Pielech, R. (2021). Plant species richness in riparian forests : Comparison to other forest ecosystems, longitudinal patterns, role of rare species and topographic factors. *Forest Ecology and Management*, *496*, 119400. https://doi.org/10.1016/j.foreco.2021.119400

Pierce, A. R. (2002). Fiddlehead ferns (Matteucia struthiopteris) by Alan R Pierce. Dans *Tapping the Green Market* (1st éd.). Routledge.

Pinay, G., Clément, J. C., & Naiman, R. J. (2002). Basic Principles and Ecological Consequences of Changing Water Regimes on Nitrogen Cycling in Fluvial Systems. *Environmental Management*, *30*(4), 481-491. https://doi.org/10.1007/s00267-002-2736-1

Pittaro, M. G., Duchini, P. G., Guzatti, G. C., & Sbrissia, A. F. (2024). Unraveling the forage productivity puzzle : Comparing fast and slow-growing grasses. *PLOS ONE*, *19*(7), e0306692. https://doi.org/10.1371/journal.pone.0306692

Politti, E., Bertoldi, W., Gurnell, A., & Henshaw, A. (2018). Feedbacks between the riparian Salicaceae and hydrogeomorphological processes : A quantitative review. *Earth-Science Reviews*, *176*, 147-165. https://doi.org/10.1016/j.earscirev.2017.07.018

Polvi, L. E., & Sarneel, J. M. (2018). Ecosystem engineers in rivers : An introduction to how and where organisms create positive biogeomorphological feedbacks. *Wiley Interdisciplinary Reviews: Water*, *5*(2), e1271. https://doi.org/10.1002/wat2.1271

Posit team. (2025). *RStudio : Integrated Development Environment for R*. Posit Software, PBC. Boston, MA. http://www.posit.co/

Poulin, M., Evette, A., Tisserant, M., Keita, N., Breton, V., BIRON, P., RAYMOND, P., CHARBONNEAU, G., & FALARDEAU, I. (2019). Le génie végétal pour la protection des berges de cours d'eau au Québec : État des lieux et perspectives pour les Basses-terres du Saint-Laurent. *Sciences Eaux & Territoires*, *57*. https://doi.org/10.14758/SET-REVUE.2019.HS.06

Prowse, T. D. (2001). River-Ice Ecology. II : Biological Aspects. *Journal of Cold Regions Engineering*, *15*(1), 17-33. https://doi.org/10.1061/(ASCE)0887-381X(2001)15:1(17)

Prowse, T. D., & Culp, J. M. (2003). *Ice breakup : A neglected factor in river ecology*. *30*, 17.

Prugne, M., Corenblit, D., Boivin, M., & Buffin-Bélanger, T. (2025). Vegetation and channel adjustment trajectories in cold regions : The effects of ice disturbances in

two Gaspesian rivers. *Earth Surface Processes and Landforms*, *50*(5), e70051. https://doi.org/10.1002/esp.70051

Prugne, M., Corenblit, D., Boivin, M., Evette, A., & Buffin-Bélanger, T. (2024). Soil and water bioengineering in cold rivers : A biogeomorphological perspective. *Ecological Engineering*, *204*, 107261. https://doi.org/10.1016/j.ecoleng.2024.107261

Puijalon, S., Bouma, T. J., Douady, C. J., van Groenendael, J., Anten, N. P. R., Martel, E., & Bornette, G. (2011). Plant resistance to mechanical stress : Evidence of an avoidance–tolerance trade-off. *New Phytologist*, *191*(4), 1141-1149. https://doi.org/10.1111/j.1469-8137.2011.03763.x

Randall, C. (2015). *Survival & growth of sandbar willow, Salix interior, in bioengineering projects, and the implications for use in erosion control in Manitoba*. https://mspace.lib.umanitoba.ca/xmlui/handle/1993/30242

Reid, H. E., & Brierley, G. J. (2015). Assessing geomorphological sensitivity in relation to river capacity for adjustment. *Geomorphology*, *251*, 108-121. https://doi.org/10.1016/j.geomorph.2015.09.009

Rohli, R. V., Joyner, T. A., Reynolds, S. J., & Ballinger, T. J. (2015). Overlap of global Köppen–Geiger climates, biomes, and soil orders. *Physical Geography*, *36*(2), 158-175. https://doi.org/10.1080/02723646.2015.1016384

Rokaya, P., Budhathoki, S., & Lindenschmidt, K.-E. (2018). Ice-jam flood research : A scoping review. *Natural Hazards*, *94*(3), 1439-1457. https://doi.org/10.1007/s11069-018-3455-0

Rokaya, P., Lindenschmidt, K.-E., Pietroniro, A., & Clark, M. (2022). Modelling of ice jam floods under past and future climates : A review. *Journal of Hydrology X*, *15*, 100120. https://doi.org/10.1016/j.hydroa.2022.100120

Rood, S. B., Goater, L. A., Mahoney, J. M., Pearce, C. M., & Smith, D. G. (2007). Floods, fire, and ice : Disturbance ecology of riparian cottonwoods. *Canadian Journal of Botany*, *85*(11), 1019-1032. https://doi.org/10.1139/B07-073

Schenker, G., Lenz, A., Körner, C., & Hoch, G. (2014). Physiological minimum temperatures for root growth in seven common European broad-leaved tree species. *Tree Physiology*, *34*(3), 302-313. https://doi.org/10.1093/treephys/tpu003

Scorpio, V., & Comiti, F. (2024). Channel changes during and after extreme floods in two catchments of the Northern Apennines (Italy). *Geomorphology*, *463*, 109355. https://doi.org/10.1016/j.geomorph.2024.109355

Segura-Beltrán, F., & Sanchis-Ibor, C. (2013). Assessment of channel changes in a Mediterranean ephemeral stream since the early twentieth century. The Rambla de Cervera, eastern Spain. *Geomorphology*, *201*, 199-214. https://doi.org/10.1016/j.geomorph.2013.06.021

Serlet, A. J., Gurnell, A. M., Zolezzi, G., Wharton, G., Belleudy, P., & Jourdain, C. (2018). Biomorphodynamics of alternate bars in a channelized, regulated river : An integrated historical and modelling analysis: BIOMORPHODYNAMICS OF ALTERNATE BARS IN A CHANNELIZED, REGULATED RIVER. *Earth Surface Processes and Landforms*, *43*(9), 1739-1756. https://doi.org/10.1002/esp.4349

Shaw, J. D., Packee, Sr., E. C., & Ping, C.-L. (2001). Growth of balsam poplar and black cottonwood in Alaska in relation to landform and soil. *Canadian Journal of Forest Research*, *31*(10), 1793-1804. https://doi.org/10.1139/x01-119

Simon, A., Bennett, S. J., & Neary, V. S. (2004). Riparian vegetation and fluvial geomorphology : Problems and opportunities. Dans S. J. Bennett & A. Simon (Éds.), *Water Science and Application* (Vol. 8, p. 1-10). American Geophysical Union. https://doi.org/10.1029/008WSA01

Simon, A., & Collison, A. J. C. (2002). Quantifying the mechanical and hydrologic effects of riparian vegetation on streambank stability. *Earth Surface Processes and Landforms*, *27*(5), 527-546. https://doi.org/10.1002/esp.325

Sitzia, T., Picco, L., Ravazzolo, D., Comiti, F., Mao, L., & Lenzi, M. A. (2016). Relationships between woody vegetation and geomorphological patterns in three gravel-bed rivers with different intensities of anthropogenic disturbance. *Advances in Water Resources*, *93*, 193-204. https://doi.org/10.1016/j.advwatres.2015.11.016

Smith, D. G. (1979). Effects of channel enlargement by river ice processes on bankfull discharge in Alberta, Canada. *Water Resources Research*, *15*(2), 469-475. https://doi.org/10.1029/WR015i002p00469

Smith, D. G., & Pearce, C. M. (2000a). River ice and its role in limiting woodland development on a sandy braid-plain, Milk River, Montana. *Wetlands*, *20*(2), 232-250. https://doi.org/10.1672/0277-5212(2000)020%255B0232:RIAIRI%255D2.0.CO;2

Smith, D. G., & Pearce, C. M. (2000b). River ice and its role in limiting woodland development on a sandy braid-plain, Milk River, Montana. *Wetlands*, *20*(2), 232-250. https://doi.org/10.1672/0277-5212(2000)020%255B0232:RIAIRI%255D2.0.CO;2

Smith, D. G., & Pearce, C. M. (2002). Ice jam-caused fluvial gullies and scour holes on northern river flood plains. *Geomorphology*, *42*(1-2), 85-95. https://doi.org/10.1016/S0169-555X(01)00076-9

Smith, D. G., & Reynolds, D. M. (1983). Trees Scars to Determine the Frequency and Stage of High Magnitude River Ice Drives and Jams, Red Deer, Alberta. *Canadian Water Resources Journal / Revue canadienne des ressources hydriques*, *8*(3), 77-94. https://doi.org/10.4296/cwrj0803077

Smith, N. D., Cross, T. A., Dufficy, J. P., & Clough, S. R. (1989). Anatomy of an avulsion. *Sedimentology*, *36*(1), 1-23. https://doi.org/10.1111/j.1365-3091.1989.tb00817.x

Solari, L., Van Oorschot, M., Belletti, B., Hendriks, D., Rinaldi, M., & Vargas-Luna, A. (2016). Advances on Modelling Riparian Vegetation—Hydromorphology Interactions. *River Research and Applications*, *32*(2), 164-178. https://doi.org/10.1002/rra.2910

Souza, E. B., Junior, G. A. D., & Pott, A. (2019). SOIL SEED BANK IN PANTANAL RIPARIAN FOREST : PERSISTENCE, ABUNDANCE, FUNCTIONAL DIVERSITY AND COMPOSITION. *Oecologia Australis*, *23*(4). https://doi.org/10.4257/oeco.2019.2304.13

Steinberg, K. A., Eichhorst, K. D., & Rudgers, J. A. (2021). Flood regime alters the abiotic correlates of riparian vegetation. *Applied Vegetation Science*, *24*(2). https://doi.org/10.1111/avsc.12572

Stromberg, J. C., & Merritt, D. M. (2016). Riparian plant guilds of ephemeral, intermittent and perennial rivers. *Freshwater Biology*, *61*(8), 1259-1275. https://doi.org/10.1111/fwb.12686

Surian, N., Barban, M., Ziliani, L., Monegato, G., Bertoldi, W., & Comiti, F. (2015). Vegetation turnover in a braided river : Frequency and effectiveness of floods of different magnitude: VEGETATION TURNOVER IN A BRAIDED RIVER. *Earth Surface Processes and Landforms*, *40*(4), 542-558. https://doi.org/10.1002/esp.3660

Surmacz, B., Foremnik, K., & Pielech, R. (2024). Along the river : Longitudinal patterns of functional and taxonomic diversity of plants in riparian forests. *Journal of Vegetation Science*, *35*(1), e13225. https://doi.org/10.1111/jvs.13225

Suzuki, W., Osumi, K., Masaki, T., Takahashi, K., Daimaru, H., & Hoshizaki, K. (2002). Disturbance regimes and community structures of a riparian and an adjacent terrace stand in the Kanumazawa Riparian Research Forest, northern Japan. *Forest Ecology and Management*, *157*(1-3), 285-301. https://doi.org/10.1016/S0378-1127(00)00667-8

Tal, M., & Paola, C. (2010). Effects of vegetation on channel morphodynamics : Results and insights from laboratory experiments. *Earth Surface Processes and Landforms*, *35*(9), 1014-1028. https://doi.org/10.1002/esp.1908

Tardif, J., & Bergeron, Y. (1999). Population Dynamics of Fraxinus Nigra in Response to Flood-Level Variations, in Northwestern Quebec. *Ecological Monographs*, *69*(1), 107-125. https://doi.org/10.1890/0012-9615(1999)069%255B0107:PDOFNI%255D2.0.CO;2

Tardif, J. C., Kames, S., Nolin, A. F., & Bergeron, Y. (2021). Earlywood Vessels in Black Ash (Fraxinus nigra Marsh.) Trees Show Contrasting Sensitivity to Hydroclimate Variables According to Flood Exposure. *Frontiers in Plant Science*, *12*. https://doi.org/10.3389/fpls.2021.754596

Taylor, S. M. (2009, juin 14). *On the use of dendrochronology to analyse ice jam occurrences at a fluvial transition on the Ouelle River, Quebec* [Conference paper]. Proceedings of the 15th Workshop on River Ice, St. John's, Newfoundland and Labrador.

Tockner, K., Malard, F., & Ward, J. V. (2000). An extension of the flood pulse concept. *Hydrological Processes*, *14*(16-17), 2861-2883. https://doi.org/10.1002/1099-1085(200011/12)14:16/17%253C2861::AID-HYP124%253E3.0.CO;2-F

Tolkkinen, M. J., Heino, J., Ahonen, S. H. K., Lehosmaa, K., & Mykrä, H. (2020). Streams and riparian forests depend on each other : A review with a special focus on microbes. *Forest Ecology and Management*, *462*, 117962. https://doi.org/10.1016/j.foreco.2020.117962

Turcotte, B., Morse, B., Bergeron, N. E., & Roy, A. G. (2011a). Sediment transport in ice-affected rivers. *Journal of Hydrology*, *409*(1-2), 561-577. https://doi.org/10.1016/j.jhydrol.2011.08.009

Turcotte, B., Morse, B., Bergeron, N. E., & Roy, A. G. (2011b). Sediment transport in ice-affected rivers. *Journal of Hydrology*, *409*(1-2), 561-577. https://doi.org/10.1016/j.jhydrol.2011.08.009

Turcotte, B., Morse, B., & Pelchat, G. (2020). Impact of Climate Change on the Frequency of Dynamic Breakup Events and on the Risk of Ice-Jam Floods in Quebec, Canada. *Water*, *12*(10), 2891. https://doi.org/10.3390/w12102891

Uunila, L., & Church, M. (2014). Ice on Peace River : Effects on Bank Morphology and Riparian Vegetation. Dans M. Church (Éd.), *The Regulation of Peace River* (p. 115-140). John Wiley & Sons, Ltd. https://doi.org/10.1002/9781118906170.ch6

Uunila, L. S. (1999). *Effects of river ice on bank morphology and riparian vegetation : Peace River, Alberta* [University of British Columbia]. https://doi.org/10.14288/1.0089091

Vandermause, R., Harvey, M., Zevenbergen, L., & Ettema, R. (2021). River-ice effects on bank erosion along the middle segment of the Susitna river, Alaska. *Cold Regions Science and Technology*, *185*, 103239. https://doi.org/10.1016/j.coldregions.2021.103239

van Eck, W. H. J. M., Lenssen, J. P. M., van de Steeg, H. M., Blom, C. W. P. M., & de Kroon, H. (2006). Seasonal Dependent Effects of Flooding on Plant Species Survival and Zonation : A Comparative Study of 10 Terrestrial Grassland Species. *Hydrobiologia*, *565*(1), 59-69. https://doi.org/10.1007/s10750-005-1905-7

Vargas-Luna, A., Crosato, A., & Uijttewaal, W. S. J. (2015). Effects of vegetation on flow and sediment transport : Comparative analyses and validation of predicting models. *Earth Surface Processes and Landforms*, *40*(2), 157-176. https://doi.org/10.1002/esp.3633

Vautier, F., Corenblit, D., Hortobágyi, B., Fafournoux, L., & Steiger, J. (2016). Monitoring and reconstructing past biogeomorphological succession within fluvial corridors using stereophotogrammetry : Stereophotogrammetry: Monitoring Past Fluvial Biogeomorphological Succession. *Earth Surface Processes and Landforms*, *41*(10), 1448-1463. https://doi.org/10.1002/esp.3962

Viles, H. (2020). Biogeomorphology : Past, present and future. *Geomorphology*, *366*, 106809. https://doi.org/10.1016/j.geomorph.2019.06.022

Viles, H., & Coombes, M. (2022). Biogeomorphology in the Anthropocene : A hierarchical, traits-based approach. *Geomorphology*, *417*, 108446. https://doi.org/10.1016/j.geomorph.2022.108446

Violle, C., Enquist, B. J., McGill, B. J., Jiang, L., Albert, C. H., Hulshof, C., Jung, V., & Messier, J. (2012). The return of the variance : Intraspecific variability in community ecology. *Trends in Ecology & Evolution*, *27*(4), 244-252. https://doi.org/10.1016/j.tree.2011.11.014

Violle, C., Navas, M.-L., Vile, D., Kazakou, E., Fortunel, C., Hummel, I., & Garnier, E. (2007). Let the concept of trait be functional! *Oikos*, *116*(5), 882-892. https://doi.org/10.1111/j.0030-1299.2007.15559.x

Wan, X., Landhäusser, S. M., Zwiazek, J. J., & Lieffers, V. J. (1999). Root water flow and growth of aspen (Populus tremuloides) at low root temperatures. *Tree Physiology*, *19*(13), 879-884. https://doi.org/10.1093/treephys/19.13.879

Westerband, A. C., Funk, J. L., & Barton, K. E. (2021). Intraspecific trait variation in plants : A renewed focus on its role in ecological processes. *Annals of Botany*, *127*(4), 397-410. https://doi.org/10.1093/aob/mcab011

Westoby, M. (1998). A leaf-height-seed (LHS) plant ecology strategy scheme. *Plant and Soil*, *199*(2), 213-227. https://doi.org/10.1023/A:1004327224729

Wickham, H. (2016). *ggplot2 : Elegant graphics for data analysis*. Springer-Verlag New York. https://ggplot2.tidyverse.org

Williams, L., Reich, P., Capon, S. J., & Raulings, E. (2008). Soil seed banks of degraded riparian zones in southeastern Australia and their potential contribution to the restoration of understorey vegetation. *River Research and Applications*, *24*(7), 1002-1017. https://doi.org/10.1002/rra.1123

Wohl, E. E., & Merritt, D. M. (2001). Bedrock channel morphology. *GSA Bulletin*, *113*(9), 1205-1212. https://doi.org/10.1130/0016-7606(2001)113%253C1205:BCM%253E2.0.CO;2

Wohl, E., Lane, S. N., & Wilcox, A. C. (2015). The science and practice of river restoration. *Water Resources Research*, *51*(8), 5974-5997. https://doi.org/10.1002/2014WR016874

Yang, S., Bai, Y., & Xu, H. (2018). Experimental Analysis of River Evolution with Riparian Vegetation. *Water*, *10*(11), Article 11. https://doi.org/10.3390/w10111500

Yu, G.-A., Li, Z., Yang, H., Lu, J., Huang, H. Q., & Yi, Y. (2020). Effects of riparian plant roots on the unconsolidated bank stability of meandering channels in the Tarim River, China. *Geomorphology*, *351*, 106958. https://doi.org/10.1016/j.geomorph.2019.106958

Yumoto, M., Ogata, T., Matsuoka, N., & Matsumoto, E. (2006). Riverbank freeze-thaw erosion along a small mountain stream, Nikko volcanic area, central Japan. *Permafrost and Periglacial Processes*, *17*(4), 325-339. https://doi.org/10.1002/ppp.569

Zhong, Y., Favillier, A., Cánovas, J. A. B., Qie, J., Manchado, A. M.-T., Guillet, S., Huneau, F., Corona, C., & Stoffel, M. (2023). 250 years of flood frequency and discharge in an ungauged Corsican mountain catchment : A dendrogeomorphological reconstruction. *Science of The Total Environment*, *879*, 163138. https://doi.org/10.1016/j.scitotenv.2023.163138

Zhu, R., & Tsubaki, R. (2022). The role of riparian vegetation flexibility in a bio-hydro-morphodynamic simulation. *Earth Surface Processes and Landforms*, *47*(15), 3481-3496. https://doi.org/10.1002/esp.5469